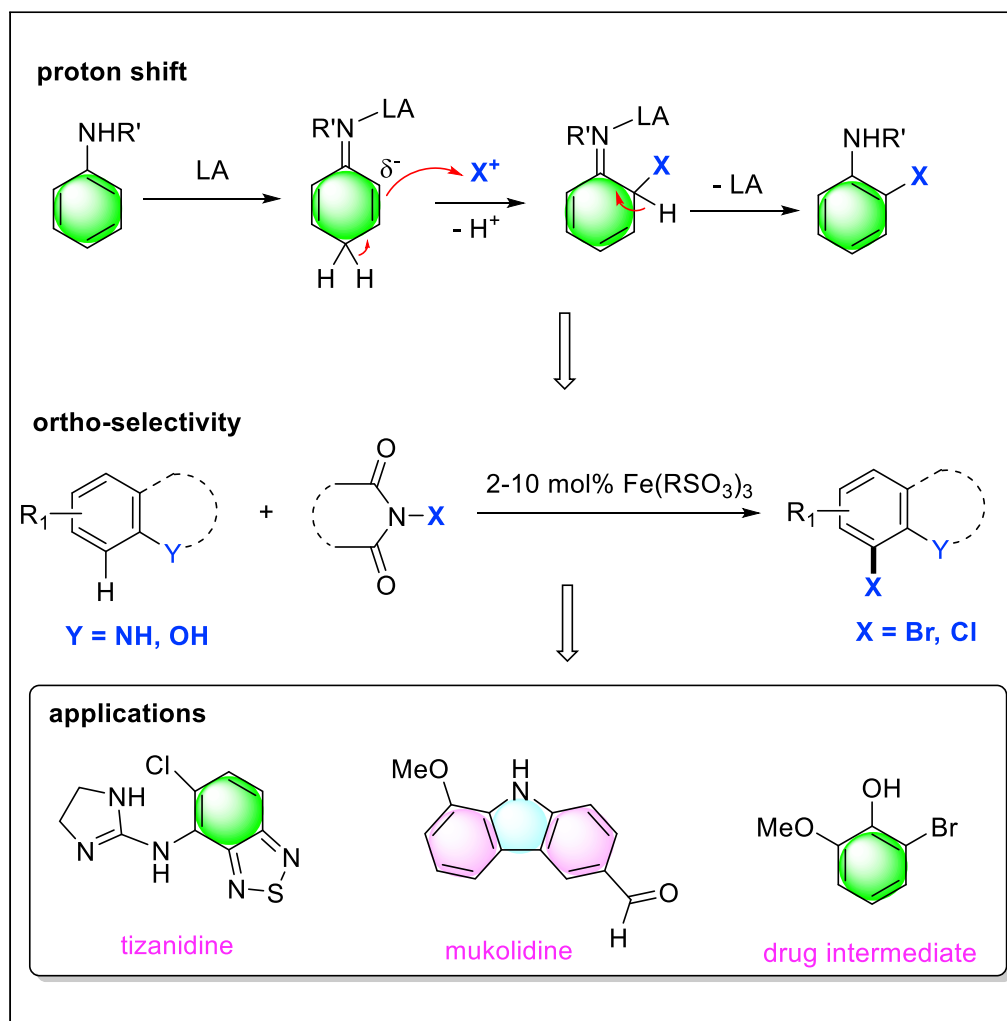# iScience

Article

Proton Transfer Can Govern Regioselectivity Assisted by Iron Catalysis

Yudong Li, Liyan Fu, Xiaolin Jiang, Dongmei Zhao, Hui-Fang Wang, Chungu Xia, Yuehui Li

wanghf@suda.edu.cn (H.-F.W.)
cgxia@licp.cas.cn (C.X.)
yhli@licp.cas.cn (Y.L.)

HIGHLIGHTS

Highly *ortho*-selective halogenations of anilines and carbazoles

Lewis acids being able to accelerate EAS reactions

Proton shift found to be crucial for the regioselectivity

Practical iron sulfonate catalysis being scaled up to 100 g

Article

Proton Transfer Can Govern Regioselectivity Assisted by Iron Catalysis

Yudong Li,[1,4,5] Liyan Fu,[1,5] Xiaolin Jiang,[1,3,5] Dongmei Zhao,[3] Hui-Fang Wang,[2,*] Chungu Xia,[1,*] and Yuehui Li[1,6,*]

SUMMARY

***Ortho*-selective aromatic C-H functionalization is frequently used in organic synthesis and chemical/pharmaceutical industries. However, this reaction relies heavily on the use of directing groups suffering from limited substrate scope and extra steps to put on and remove the directing/protecting groups. Herein we present the previously neglected concept that enables good to nearly complete selective *ortho* position. Proton transfer was utilized to tune the electron density on the aryl ring and determine the positional selectivity of electrophilic substitution. Consistently with deuteration experiments and DFT studies, this work demonstrates that acid-promoted proton transfer directs accelerated *ortho*-selective halogenation of NH/OH contained aromatic amines/phenols with excellent selectivity (>40 examples; up to 98:2 *ortho/para* selectivity). The application potential of this Fe-catalyzed method is demonstrated by the convenient synthesis of three alkaloids and tizanidine. This report raises the possibility that proton transfer could serve as the basis of developing new selective C-H functionalization reactions.**

INTRODUCTION

Undoubtedly, chemical structure determines reactivity. In addition, understanding how to activate substrate molecules benignly is fundamental in bioorganic chemistry, organic chemistry, and catalysis (Rudroff et al., 2018; Roduner, 2014; Bauer and Knölker, 2015). Electrophilic aromatic substitution reaction (S_EAr) is perhaps the most widely used reaction for aromatic C-H functionalization but often suffers from the production of mixture of positional isomers (Figure 1A) (Taylor, 1990). With catalysts and the directing group (DG), *ortho*-selective substitution is feasible via activation of the *ortho* C-H bond or by bringing the electrophile within close proximity of the *ortho* carbon (Figure 1B) (Wencel-Delord and Glorius, 2013; Engle et al., 2011; Wan et al., 2014; Wang and Ackermann, 2014; Song et al., 2015, 2020; Bedford et al., 2011; Xiong and Yeung, 2016). Accordingly, the chelation- or hydrogen bonding-assisted strategies have been successfully applied. However, these reactions require either high loading of transition metal catalysts or installation of specific directing groups, which till now precludes the general and practical application in organic synthesis and catalysis. Thus, no general strategy currently exists for highly *ortho*-selective C-H functionalization, especially considering the unbeneficial steric hindrance.

Herein, we describe the use of proton transfer assisted by iron(III) sulfonates under heating conditions as the general and convenient approach to *ortho*-halogenation of aromatic amines and phenols. Proton transfer occurs ubiquitously as the basic step in many biological and chemical transformations (Migliore et al., 2014; Markle et al., 2018). Moreover, proton transfer/shift commonly features in aromatic compounds such as phenols or aromatic amines (Bai et al., 2019; Chen and Sun, 2017). Specifically, proton transfer/shift is more often recognized as a kind of isomerization useful in organic synthesis. As a basic step, the influence of proton transfer (formal proton shift) in aromatic substitution reactions has never been carefully investigated. In this work, proton transfer as a powerful strategy is developed to be involved into determining selectivity, accelerating aromatic substitution reactions, and generating active intermediates favorable for *ortho*-halogenation of aryl amines and phenols (Figure 1C). This finding is notable providing a straightforward method to access valuable natural products and drug intermediates (Figure 1D). The application of this method is demonstrated by the convenient synthesis of tizanidine with up to 97% *ortho*-selectivity and scale-up to 100-g scale. This catalytic process involving proton shift/isomerization is backed by theoretical
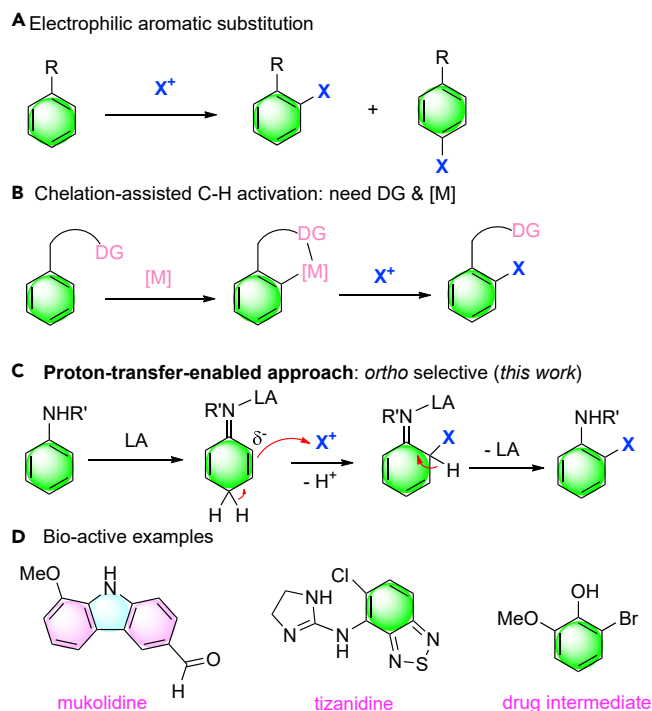
Figure 1. Selective C-H Functionalization

(A) Active site analysis of anilines in S_EAr reactions.

(B) Catalytic *ortho*-halogenations involving C-H activation.

(C) This work: $Fe(RSO_3)_3$-catalyzed *ortho*-halogenation via proton shift process.

(D) Bio-active compounds and drug intermediate requiring *ortho*-substitution.

and NMR studies and showcased the utility of Lewis acid altering the aromatic ring electronics and promoting *ortho*-halogenation.

RESULTS AND DISCUSSION

We take S_EAr reactions of N-H anilines as the model to explore the synthetic value of proton transfer strategy. It is well known that the advanced mechanism in chemistry textbooks involves the electrophilic attack and formation of a resonance-stabilized carbocation, and formation of the arenium ion is considered as the rate-determining step followed by deprotonation to restore aromaticity (Figure 2A). On the other hand, in the presence of Lewis acid or under heating conditions, partial dearomatization reactions might happen, including 1,3- or 1,5-proton shift via enamine isomerization procedures (*prototropic equilibria of anilines*) (Ma et al., 2017). Consequently, is it possible that higher electron density for *para* (species I) or *ortho* (species II) position could be achieved following such kind of isomerization? Is it possible to achieve higher reactivity for aromatic substitution under acidic conditions (e.g., Lewis acid)? Theoretically, the deprotonated anionic species III should be more nucleophilic compared with the neutral anilines. In contrary to the established notion of organic chemistry, this means in the presence of LA, more active species might be formed. Critically, proton shift in NH anilines needs to be first investigated.

Deuteration is an exchange reaction of proton with deuterium and is a straightforward method to test proton shift/transfer reactions. Initially, the deuteration reactions of N-Me aniline were carried out in the mixture of $SOCl_2/D_2O$ or $Fe(OTs)_3/D_2O$, which are useful methods to generate D^+ *in situ*. To our delight, for both reactions *ortho*- and *para*-deuterations were observed (40%–66% D ratios), which is consistent with electrophilic aromatic substitution-type reactivity for *ortho*- and *para*-sites (Scheme 1). When $SOCl_2$ or $Fe(OTs)_3$ was absent, no C-H deuteration was observed. Then, when N,N-dimethyl aniline is used, lower deuteration ratios (17%–33%) were obtained. This implies that the presence of N-H proton is involved for the promotion of H/D exchange process (reactions A/B versus C/D). Considering that N-H/D shift should occur rapidly, it is highly possible that deuteration could be promoted due to the proton transfer
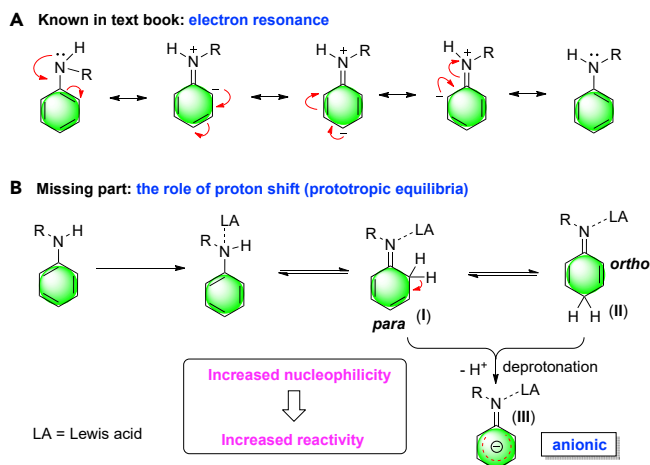
Figure 2. Analysis of the Positional Selectivity: Electron Resonance versus Proton Shift
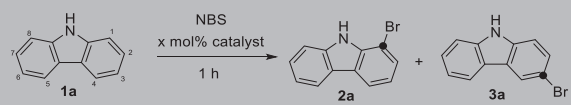
of N-D to the aryl ring. To prove this assumption, N-D-N-Me aniline (ca. 72% D by ^{1}H NMR) was prepared and treated under heating conditions in the presence of Fe(OTs)$_3$. *Ortho*-deuteration was observed (15% D), with trace of D-labeling at the *para*-position. Hence, we can make the claim that, in the presence of acids, proton shift could occur selectively between the N-H and C-H at *ortho/para*-positions.

At elevated temperature, quantitative D-labeling at *ortho*- and *para*-position was achieved for 2-phenyl aniline (Scheme 1F). Nevertheless, catalytic amounts of Lewis acid Fe(OTs)$_3$ (5 mol%) in D$_2$O could be used for the preparation of anilines with moderate D ratios at *ortho*- and *para*-positions. This is the first time such kind of Fe-promoted deuteration of sp^{2}C-H bond is noticed, which might be useful for the synthesis of deuterated drugs. In fact, such kind of proton shift in anilines is observed in gas phase chromotography studies (Raczyńska, et al., 2011), even though it is not well explored for the purpose of organic synthesis, such as deuteration or halogenation of sp^{2}C-H bonds.

Halogenation is a type of important reaction in electrophilic aromatic substitutions (S$_E$Ar) for preparation of aryl halides (Galabov et al., 2016; Anbarasan et al., 2011). Specifically, S$_E$Ar reactions of anilines/phenols are usually described in textbooks through resonance formalism to explain regioselectivity control,
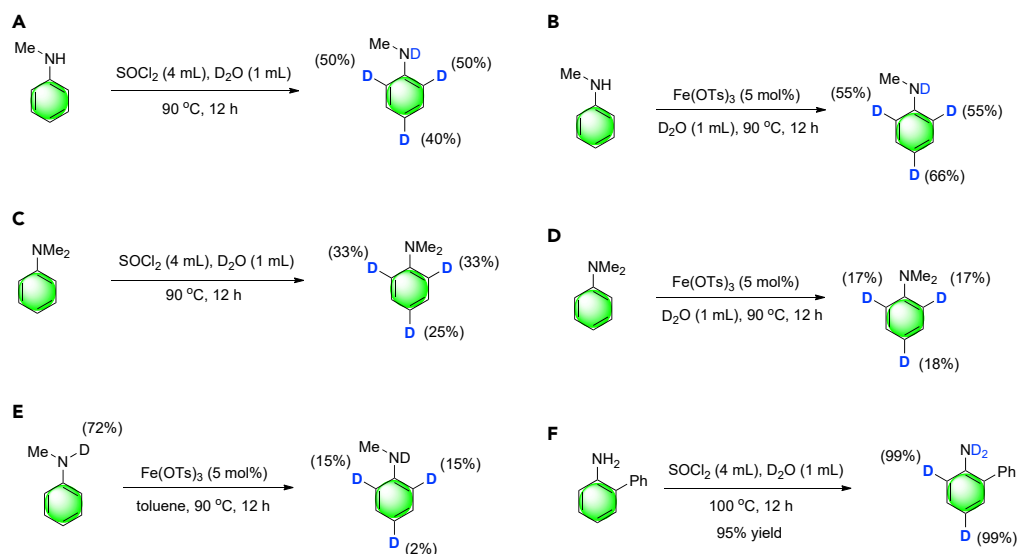
Scheme 1. Deuteration of Methyl Aniline Likely Promoted by N-H Proton Shift
OTs, tosylate.

Table 1. Fe(III)-Catalyzed Selective Bromination of Carbazole

Entry	T (°C)	x (mol%)	t (s)	Conv. (1a, %)	2a/3a[a]
1	25	–	300	18	3/97
2	25	2	300	15	5/95
3	90	–	45	42	23/77
4	90	2	45	99	97/3

Reaction conditions: **1a** (0.20 mmol), NBS (1.1 equiv.), benzene (10 mL).
[a]Yields and o/p ratios determined by GC using n-hexadecane as an internal standard.

which leads to mixture of *ortho-* and *para*-substituted products. Notably, we were taught to avoid the use of Lewis acids in S_EAr reaction for anilines due to LA-nitrogen interaction lowering the electron density on the aromatic ring. It was curious to see if the presence of LA could promote the S_EAr halogenation of aromatic amines/phenols. For this purpose, carbazole was chosen as the model substrate, since it has $C2$-symmetry with a 1:1 ratio of *ortho:para* carbon sites, acquiescent to positional selectivity studies. Specifically, we investigated the bromination of carbazole with N-bromosuccinimide (NBS) as the convenient and stable electrophilic bromide source. The reaction favored *para*-bromination without catalyst either at room temperature or 90°C (o/p = 3/97, 23/77; Table 1, entries 1, 3). Screening of various transition metal catalysts revealed that the use of palladium(II) or iron(III) triflates resulted in the formation of *ortho*-brominated isomer as the major product (Table S1, entries 2–6). Here, it is noteworthy to mention that other Lewis acids such as $CuCl_2$ and $FeCl_3$ have been applied for selective *para*-halogenation of anilines (Urones et al., 2013; Jin et al., 2011; Mostafa et al., 2017). Among the solvents screened, the use of nonpolar solvent is beneficial and the highest o/p ratio of 97/3 was obtained in benzene in the presence of 2 mol% of $Fe(OTf)_3$ (90% yield; Table 1, entry 4). Heating the reaction (>60°C) in the presence of $Fe(OTf)_3$ is necessary for *ortho*-selectivity, whereas *para*-bromination occurred at room temperature (o/p = 3/97; Table 1, entry 2). Notably, in the presence of 2 mol% of $Fe(OTf)_3$, the expected acceleration effect was observed and quantitative yield of *ortho* product was obtained in 45 s, which is much higher in the absence of catalyst (99% versus 42% yields; Table 1, entries 3 versus 4). Scaling up to 50 g of carbazole is also successful, with the efficiency retained (see the Supplemental Information). Such kind of promotion effect using Fe(III)-Lewis acid is striking and contrary to the description in chemistry textbook where the use of Lewis acid is claimed unsuitable for S_EAr reactions of anilines. Overall, the use of LA not only accelerated halogenation of aniline but also led to high *ortho*-selectivity control when using appropriate sulfonate anion of iron salts.

The attempt of bromination reaction of *N*-methylaniline using NBS in the absence of $Fe(OTs)_3$ catalyst afforded poor selectivity (o/m/p = 32/23/45) at 90°C. In contrast, when using catalyst $Fe(OTs)_3$, *ortho*-bromination was favored giving o/p as 66:34 with the *meta*-product not detected. Moreover, we considered that sulfonate anion has an effect in directing the *ortho* preference. Here, the sulfonates might be crucial for activation of the *ortho* positions. Specifically, the LA-assisted 1,n-shift of proton might make the *ortho*-position more nucleophilic leading to higher reactivity and *ortho*-selectivity. Accordingly, a plausible reaction mechanism for *ortho*-halogenation of N-H aryl amines is proposed (Figure 3). From the experimental results, it is apparent that heating is required for $Fe(OTf)_3$ to promote *ortho*-bromination to occur. This suggests that there is an energy barrier to overcome, which might correspond to isomerization of aryl amines. Formal 1,5-H shift via Fe-sulfonate promoted proton transfer might lead to species **II**, which is responsible for *ortho*-substitution. In fact, formal 1,n-H shift of N-H aniline derivatives is known and used to generate new resonance species for addition reaction (Bai et al., 2019). However, to the best of our knowledge, this strategy has never been applied for S_EAr reactions.

To rationalize such proposal and understand the origin of the regioselectivity, we used 1,8-di-deuterated carbazole with carbazole in competing reactions for kinetic isotope effect (KIE) study. The results gave an intermolecular KIE value of 1.0 implying that C-H bond cleavage is not involved in the rate-determining
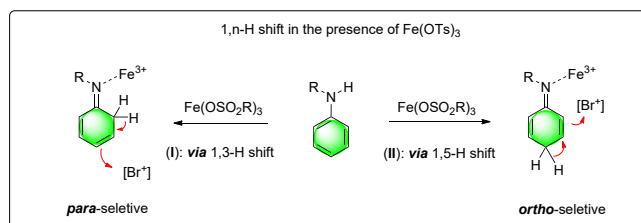
Figure 3. Proposed Mechanism for *Ortho*-Bromination Using Fe(OTs)₃ and NBS

step (Scheme 2). This result suggests that a mechanism similar to the classic S$_E$Ar is involved. Control experiments using N-chlorocarbazole revealed that intermolecular halogenation is involved rather than intramolecular halogen migration, which is also consistent with S$_E$Ar mechanism (see the Supplemental Information).

With respect to regioselectivity control using iron sulfonates, experiments showed that the presence of N-H in substrates is crucial for *ortho*-selectivity. Specifically, when N-methylcarbazole is used as substrate, *para*-selectivity was obtained under the optimal conditions (*o/p* = 5/95; see the Supplemental Information). Furthermore, the system was investigated by UV-vis and NMR spectroscopy. Monitoring the reaction under optimized conditions by UV-vis gave rise to a new signal, which corresponds to the distorted carbazole with lower planar aromaticity. In the ¹H NMR experiments, the interaction of NBS with carbazole caused the N-H signal to shift downfield by 0.2 ppm, which corresponds to hydrogen bonding interactions. In addition, the experiments using Al(OTf)₃ and NBS showed interaction to affect the methylene protons of NBS. For *metal*-carbazole interaction, a downfield shift of the N-H signal in ¹H NMR spectrum was only observed under heating conditions (>60°C), suggesting metal-N coordination (see the Supplemental Information).

Furthermore, DFT calculations were used to understand the plausibility of 1,3 and 1,5-H shift of carbazole and the reason behind the acceleration of the reaction rate with Fe(III) Lewis acids. In the proposed species **II** formed via 1,5-H shift, the *para*-position exists as methylene group and the favored selectivity to *ortho*-bromination might be attributed partially to the suppression of *para*-substitution reaction due to such kind of *para*-site blocking by proton. In DFT calculations, carbazole was chosen as substrate owing to the observed superior *ortho*-selectivity, whereas Fe(OMe)₃ was chosen as catalyst instead of Fe(OTs)₃ for computational efficiency. As shown in the potential energy surface (PES) of Figure 4, two carbazole molecules gather at the Fe(III) metal center by Fe-N coordination interaction (Fe-N bond distances are 2.24 and 2.41 Å) and hydrogen bonding between pyrrole NH group and OMe- group of sulfonate. As noticed during the reaction, the coordination of CZ to Fe(OMe)₃ would change the metal center d-d transition and thus change the color of solution. Besides, under heating conditions with the distortion of carbazole planar structure, the lone pair electrons of N atom is partially localized allowing for Fe(III)-N coordination (Chen et al., 1971).

Such combination process is exothermic with estimated interaction energy, around −16.0 kcal/mol. Then, the upper carbazole (CZ1) easily devotes the N-H proton to the *para*-position of the lower carbazole (CZ2) via **TS1** by overcoming a barrier, around 27.6 kcal/mol. To conquer such a barrier a temperature of nearly 400 K is necessary, which is in line with the experimental conditions. A protonated 6H-CZ2 in **MS1** is produced and would preferentially be brominated at the *ortho*-position by NBS subsequently. For comparison, the reaction profile for pyrrole proton transfer from CZ1 to the *ortho*-site of CZ2 was also shown in
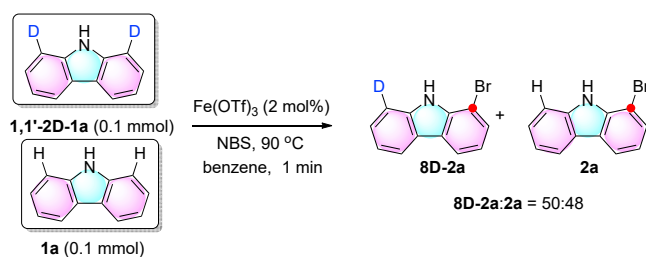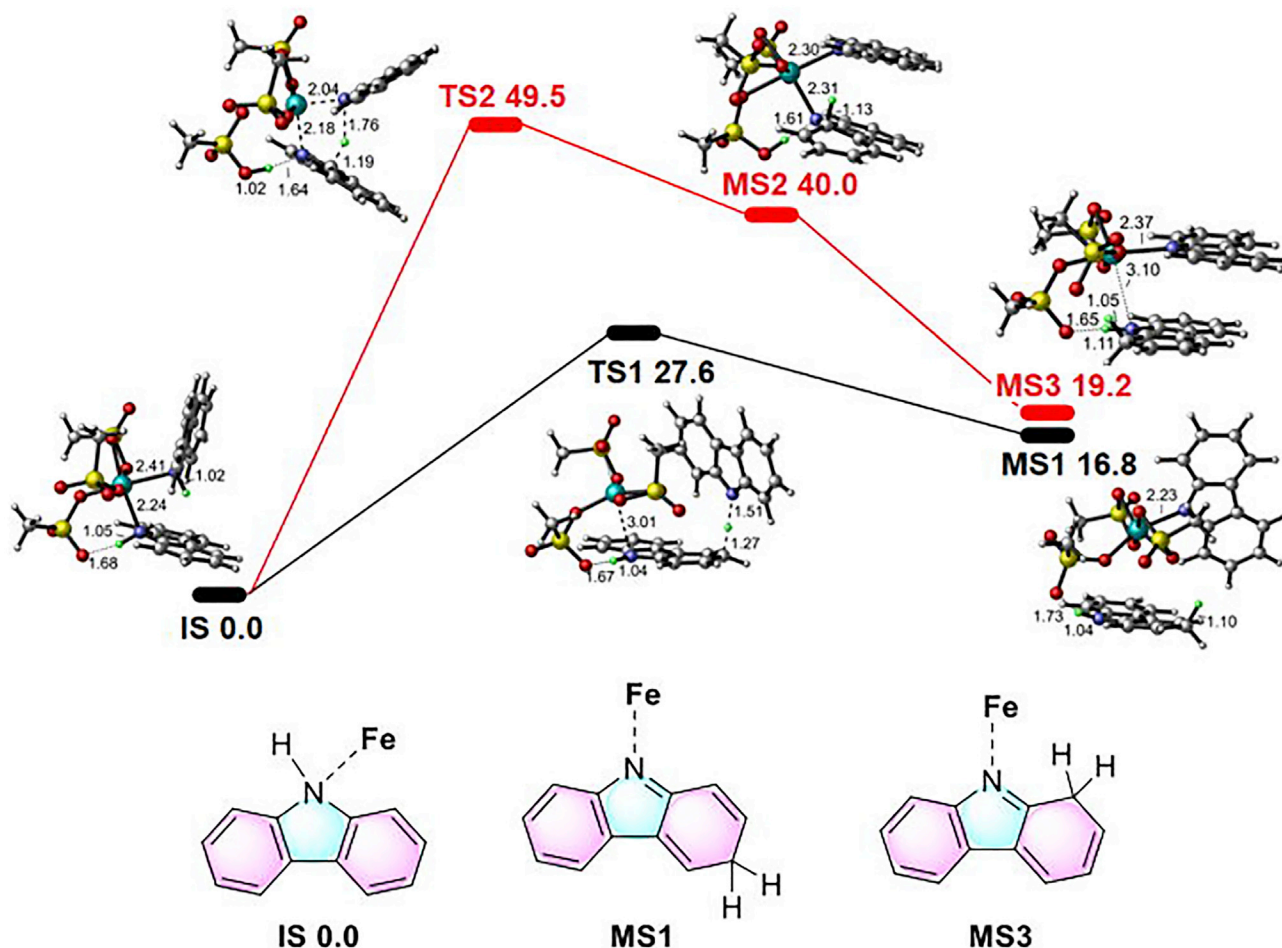

Scheme 2. KIE Study

Figure 4. PES of Fe(OMe)$_3$-Catalyzed Intermolecular Proton Transfer Reaction between Two Carbazoles

Fe, S, O, N, C, H (except pyrrole proton) are colored, respectively, by cyan, yellow, red, blue, gray, and white. The pyrrole proton is highlighted in green. Main distances are labeled including Fe-N bond and hydrogen bond in IS and MS states as well as the involved breaking/forming bond in TS. PES, potential energy surface.

Figure 4 (path via **TS2**). From **TS2** plot, CZ1 would transfer its pyrrole proton to the α-C (or α'-C) of CZ2 after the N-H bond of CZ2 breaks. The produced **MS2** is thermodynamically unstable and would favorably evolve into **MS3** in which a protonated 1H-CZ2 is formed. The rate-determining step of this process needs a very high energy barrier, around 49.5 kcal/mol. The calculated results indicate that the *para*-site of CZ2 would be favorably protonated by intermolecular proton transfer reaction via **TS1** in the presence of Fe(OMe)$_3$ and leave the *ortho*-site for subsequent bromination by NBS. All these combined interactions support the observed high *ortho*-bromination selectivity. The natural populations analyses on the deprotonated CZ1 coordinated to Fe(III) in both **MS1** and **MS3** shows that the *ortho*-site is more negative than the *para*-site. This is beneficial to the subsequent bromination at the *ortho*-position by NBS. Specifically, the deprotonation at *para*-position will render the aryl ring anionic and thus allow for accelerated electrophilic attack of Br/Cl atoms at the *ortho*-position.

Meanwhile, we believe that few weak interactions are involved including N-H…O=C hydrogen bonding and X…O=S halogen bonding (Cavallo et al., 2016; Beale et al., 2013) accompanied with metal…C=O interaction to make the halogen source close to the *ortho*-position. These cumulative effects with proton-transfer isomerization accelerate the reaction at the *ortho*-position significantly (45 s, 97% yield; Table 1, entry 4).

Halogenated anilines are important synthetic intermediates. For the chlorination of *N*-Me-aniline using different transition metal salts, iron sulfonates were found suitable catalyst. Specifically, when Fe(OTs)$_3$
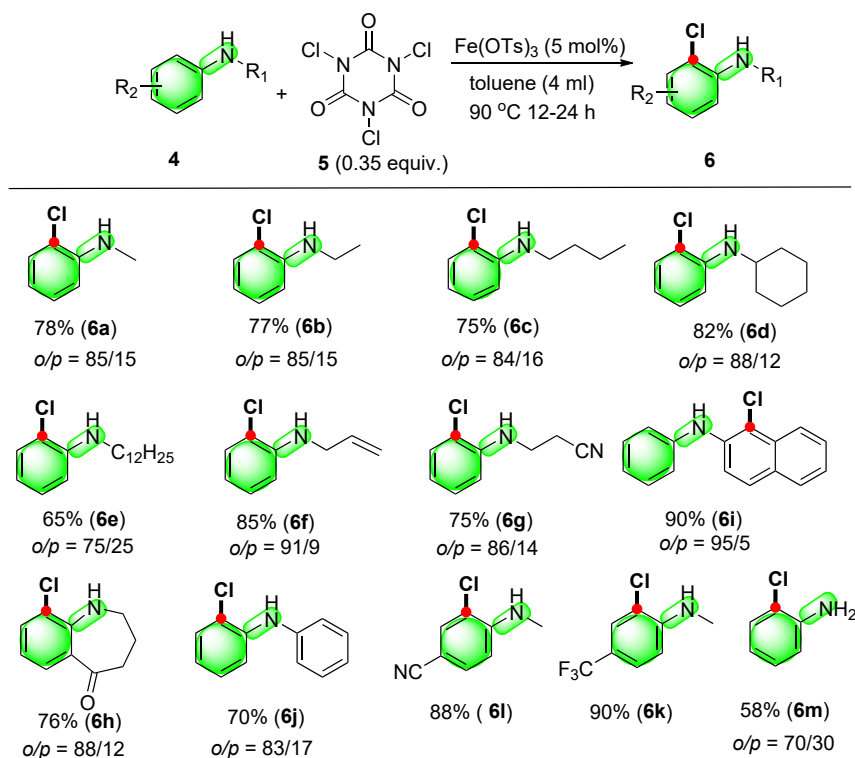
Scheme 3. Fe(OTs)₃-Catalyzed *ortho*-Chlorination of Anilines

[a]Reaction conditions: **4** (0.20 mmol), **5** (0.07 mmol), Fe(OTs)₃ (5 mol%), toluene (4 mL), 90 °C, 12–24 h; isolated yields.

(5 mol%) was used as the catalyst in the presence of chlorination reagent tri-chloroisocyanuric acid (**5**, 0.35 equiv.), high *ortho*-selectivity (*o/p* = 90/10) was obtained for the desired 2-chloro-*N*-methylaniline **6a** (78% yield; Scheme 3). In the absence of catalyst, bromination of *N*-methylaniline using NBS afforded no selectivity (*o/m/p* = 32/23/45) at 90°C. When using Fe(OTs)₃, *ortho*-bromination became the major pathway giving *o/p* as 66:34 with *meta*-product not detected. Under similar conditions, good to excellent *ortho*-selectivities were achieved for the substrates studied and the corresponding mono-chlorinated products were obtained in good to excellent yields (**6b-m**; 58%–90%). Unprecedented high regioselectivity (97%) was observed for the production of halogenated diaryl amine **6i** with 90% isolated yield. Notably, the reaction of aniline proceeded smoothly giving *o*-chloroaniline in 58% isolated yield.

Carbazoles are important molecules with their structural motif featuring in many bioactive and optically relevant compounds, and recently their selective catalytic transformation has attracted significant interests (Hirota et al., 2012; Ishikura et al., 2013; Uoyama et al., 2012; Ryan et al., 2018; Creutz et al., 2012). *To further elucidate the synthetic utility of such proton-transfer substitution strategy*, we examined the substrate scope of aromatic amines to synthesize different *ortho*-halogenated carbazole derivatives. The method is found to be suitable for bromination of a wide range of carbazoles with good to excellent yields obtained for *ortho*-brominated products (58%–83% isolated yields; Scheme 4). Interestingly, the bromination of 2-substituted carbazoles occurs on the more steric C-1 position with the corresponding products obtained in 68%–83% yields (**2g, 2i, 2k**). Moreover, epoxide groups can also be tolerated and the reaction of 4-(oxiran-2-ylmethoxy)-9H-carbazole provided product **2ac** in 66% yield. Notably, the N-H directing effect was observed for the reaction of benzofuran contained substrate **1ae**, and the desired mono-bromination product **2ae** was obtained in 65% yield, in sharp contrast to the reaction of **1ae** without catalyst producing complicated mixture of different halogenated products. Carprofen esters were smoothly transformed to the *ortho*-brominated esters in 75% and 74% yields, respectively (**2af, 2ag**). Meanwhile, with the success in bromination reactions, we progressed to investigate the chlorination of carbazoles using N-chlorosuccinimide (NCS). In general, similar results were obtained compared with the bromination reactions (Scheme 4). All used carbazole substrates were successfully *ortho*-chlorinated, for example, the reaction of 1-phenyl-9H-carbazole provided 1-chloro-8-phenylcarbazole product **2f** in 67% yield.
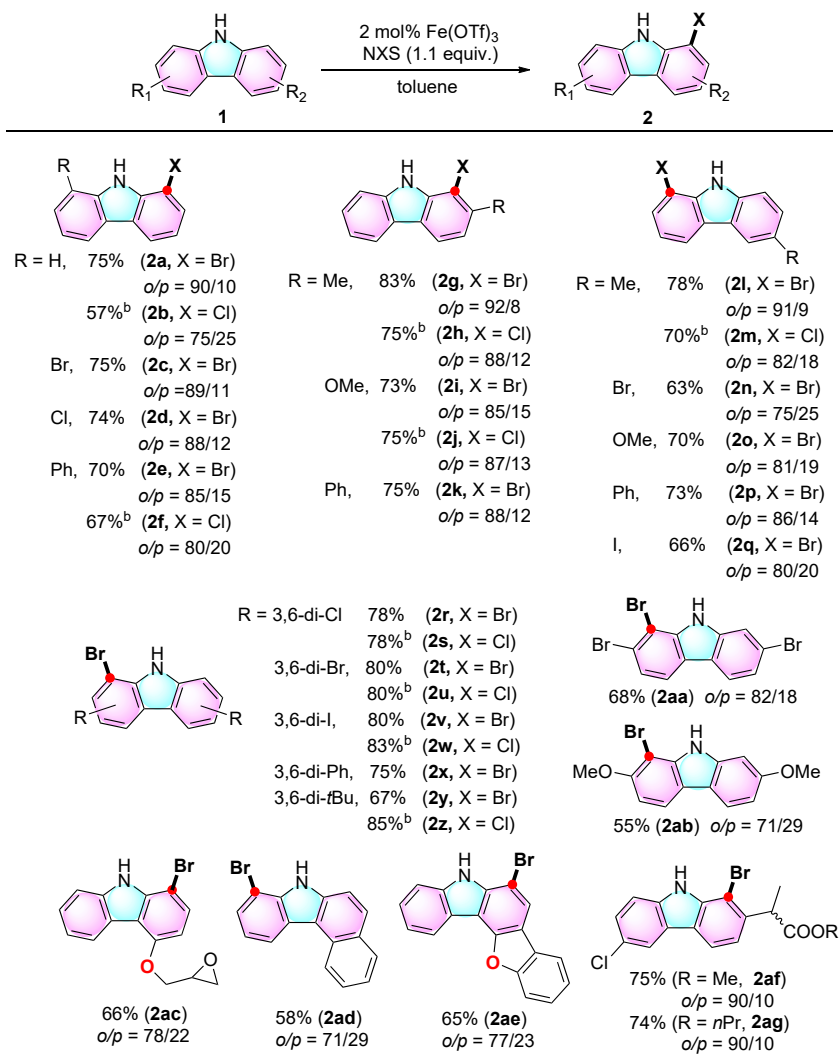
Scheme 4. Fe(OTf)₃-Catalyzed *ortho*-Halogenation of Carbazoles

[a]Reaction conditions: **1** (0.20 mmol), NBS (1.1 equiv.), Fe(OTf)$_3$ (2 mol%), toluene (10 mL), 1–6 h in the absence of light, 90 °C; isolated yields. [b]Reaction conditions: **1** (0.20 mmol), NCS (1.1 equiv.), Fe(OTf)$_3$ (10 mol%), toluene (10 mL), in dark, 110 °C; isolated yields.

To further demonstrate the application potential of this methodology, we choose to investigate total synthesis of natural products bearing carbazole moiety. First, we tested the versatile transformation of brominated carbazole **2a**, and the corresponding 1-substituted products bearing -NH$_2$, -CHO, -OMe, and -Ph were conveniently obtained in good yields (**7–10**, 65%–91%; Scheme 5).

Then, we applied this method for the synthesis of carbazole-type alkaloids, for which traditional methods suffer from complicated and/or inefficient multi-step procedures (Scheme 6). For example, starting from 1-bromo-6-methylcarbazole (**2l**), Clausenal was synthesized in 39% total yield in three steps: Fe-catalyzed *ortho*-bromination to **11**; Cu-catalyzed methoxylation to **12**, and oxidation by 2,3-Dichloro-5,6-dicyano-1,4-benzoquinone (DDQ) to Clausenal (Scheme 6A). This is in contrast to a recent report using iridium-based procedure for the synthesis of Clausenal through five steps with the total yield as 3% (Liyu and Sperry, 2017).

Meanwhile, total synthesis of natural product 1,8-dimethoxy-4-formylcarbazole **15** from carbazole **1a** was achieved in four steps with 33% total yield. Specifically, selective *ortho*-bromination of carbazole gave 1,8-dibromocarbazole **2c** in 64% yield (Scheme 6B). After methoxylation, 1,8-dimethoxycarbazole **13** was
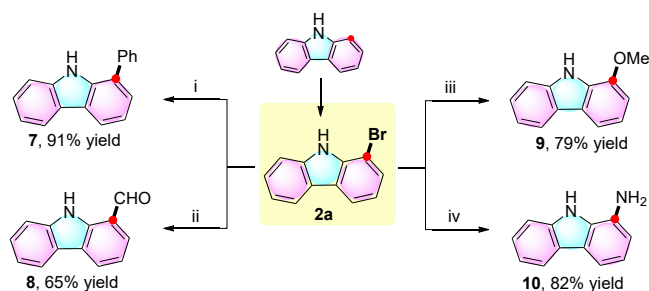
Scheme 5. Selective *ortho*-Functionalization of Anilines

[a]Reaction conditions: **2a** (0.5 mmol). (i) Phenylboronic acid (1.1 eq), K$_2$CO$_3$ (4 equiv.), PdCl$_2$(PPh$_3$)$_2$ (5 mol%), toluene/H$_2$O/ EtOH, 95 °C, 16 h. (ii) NaH, *n*BuLi, -78 °C, DMF. (iii) CuBr (2 equiv.), sodium methanolate (20 equiv.), DMF/MeOH, 120 °C, 3 h. (iv) CuI (0.2 equiv.), aqueous ammonia (5 equiv.), 2-carboxylic acid-quinoline-N-oxide (0.4 equiv.), K$_2$CO$_3$, DMSO, 80 °C, 24 h.

obtained in 82% yield. Bromination-formylation sequence gave the final product **15**. Meanwhile, Mukolidine was synthesized in three steps from 3-methylcarbazole **2l** in 52% total yield via 100-g scale Fe-catalyzed bromination reaction (Scheme 6C) (Schuster et al., 2014). Moreover, the method was also applied for the synthesis of tizanidine intermediate **6n** giving the product in 73% yield with an *o/p* ratio of 95:5 (Scheme 6D) (Xu et al., 2005).

At last, the *ortho*-chorination of phenols was also tested using this new methodology. To our delight, it is found that almost complete *ortho*-selectivity was achieved for phenol under optimal conditions (96:4 *ortho/para* ratio, 85% yield). In sharp contrast, without catalyst complicated products with oxidation side products were obtained. Hence, the substrate scope of phenols was investigated under the same conditions. All the substrates, including *ortho*-MeO phenol gave the desired products in good to excellent selectivity (64%–92% yields; Scheme 7).
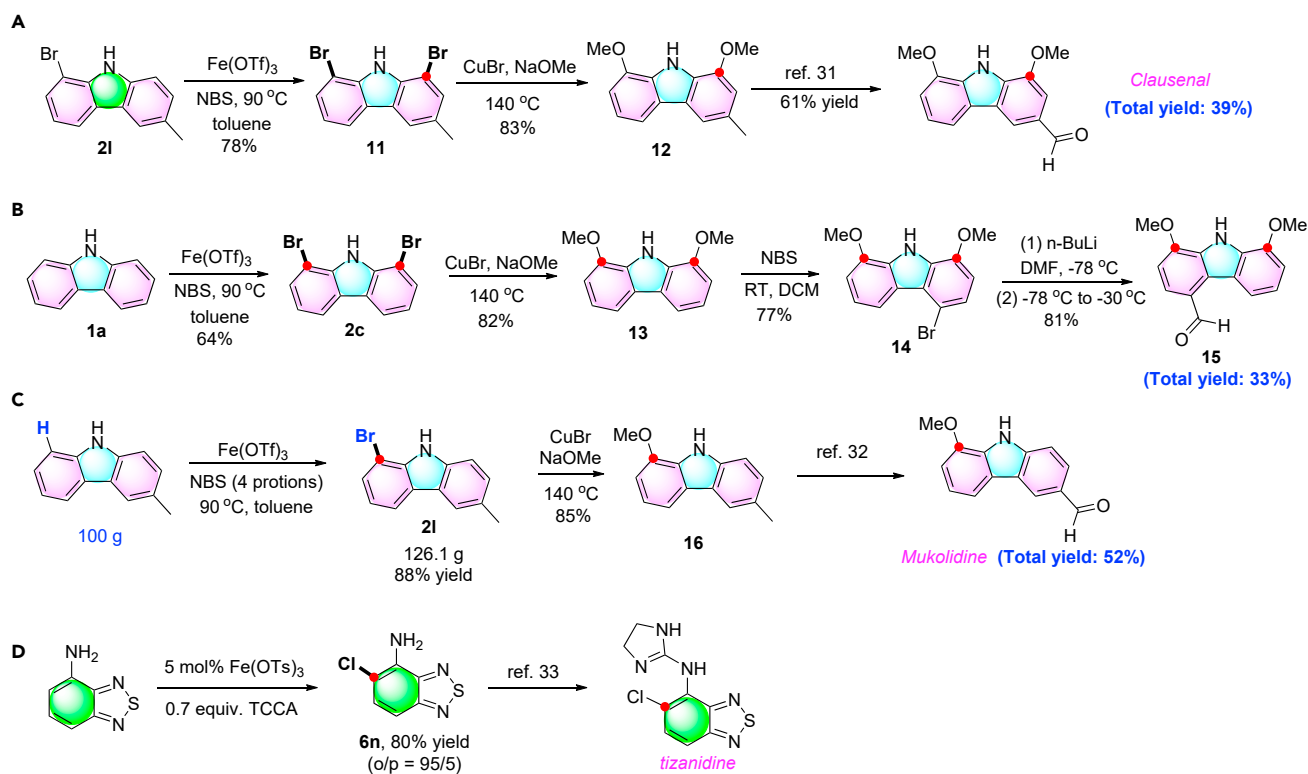
Scheme 6. Synthesis of Bio-active Natural Compounds
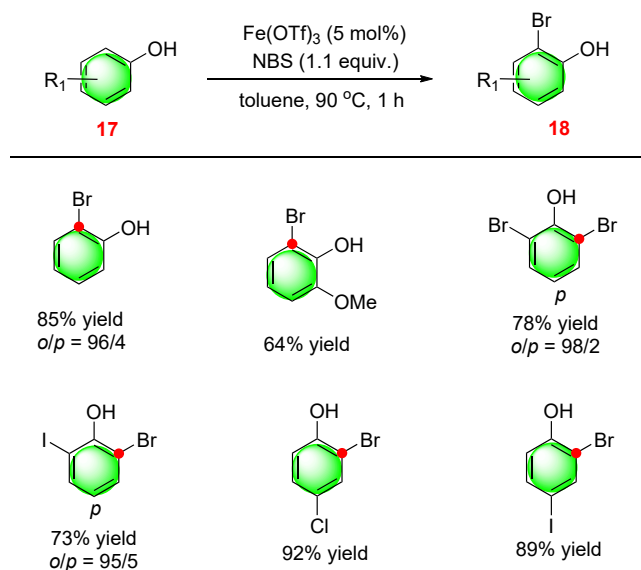
Scheme 7. Fe(OTf)₃-Catalyzed *ortho*-Bromination of Phenols

[a]Reaction conditions: **1** (0.50 mmol), NBS (1.1 equiv.), Fe(OTf)₃ (5 mol%), toluene (10 mL), 90 °C; GC yields.

Conclusions

In conclusion, we have revisited aromatic substitution of anilines and discovered proton shift process catalyzed by iron sulfonate catalysts favoring *ortho* substitution. We have developed a general site-selective deuteration and halogenation of aryl amines. Various non-N-protected anilines and carbazole-type heteroaryls were directly transformed to halogenated products in good to excellent selectivities and yields (>40 examples; 58%–90% yields). The practical application is demonstrated on 100-g scale reaction and convenient synthesis of alkaloids, and tizanidine intermediates. *Ortho*-halogenation of phenols was also achieved. Overall, this method is complementary to the traditional S$_E$Ar limited to *para*-halogenations. Mechanistic studies suggest that the *ortho*-regioselectivity promotion is likely controlled by 1,n-proton shift via Fe-N coordination. This strategy involving 1,n-proton shift in the presence of Lewis acids would serve the basis for other types of selective C-H functionalizations.

Limitations of the Study

This study systematically exploited proton shift process catalyzed by iron sulfonate catalysts for selective ortho substitutions. The methodology has wide range of substrates applicability, although this report is proof of concept for *ortho*-halogenations of aryl amines and phenols. Further studies are needed to apply 1,n-proton shift strategy in the presence of Lewis acids for other types of reactions.

METHODS

All methods can be found in the accompanying Transparent Methods supplemental file.

SUPPLEMENTAL INFORMATION

Supplemental Information can be found online at https://doi.org/10.1016/j.isci.2020.101214.

AUTHOR CONTRIBUTIONS

Y.L. and C.X. conceived, directed, and secured funding for the project. Y.L., L.F., and X.J. performed the experiments, analyzed the data, and prepared the supporting information. H.-F.W. performed DFT calculations. Y.L., D.Z., C.X., and H.-F.W. wrote the paper.

DECLARATION OF INTERESTS

The authors declare no competing interests.

REFERENCES

Anbarasan, P., Schareina, T., and Beller, M. (2011). Recent developments and perspectives in palladium-catalyzed cyanation of aryl halides: synthesis of benzonitriles. Chem. Soc. Rev. *40*, 5049–5067.

Bai, J.-F., Yasumoto, K., Kano, T., and Maruoka, K. (2019). Asymmetric synthesis of chiral 1,4-enynes through organocatalytic alkenylation of propargyl alcohols with trialkenylboroxines. Angew. Chem. Int. Ed. *58*, 8898–8901.

Bauer, I., and Knölker, H.-J. (2015). Iron catalysis in organic synthesis. Chem. Rev. *115*, 3170–3387.

Beale, T.M., Chudzinski, M.G., Sarwar, M.G., and Taylor, M.S. (2013). Halogen bonding in solution: thermodynamics and applications. Chem. Soc. Rev. *42*, 1667–1680.

Bedford, R.B., Haddow, M.F., Mitchell, C.J., and Webster, R.L. (2011). Mild C–H halogenation of anilides and the isolation of an unusual palladium(I)-palladium(II) species. Angew. Chem. Int. Ed. *50*, 5524–5527.

Cavallo, G., Metrangolo, P., Milani, R., Pilati, T., Priimagi, A., Resnati, G., and Terraneo, G. (2016). The halogen bond. Chem. Rev. *116*, 2478–2601.

Chen, M., and Sun, J. (2017). Catalytic asymmetric N-alkylation of indoles and carbazoles through 1,6-conjugate addition of aza-para-quinone methides. Angew. Chem. Int. Ed. *56*, 4583–4587.

Chen, H.J., Hakka, L.E., Hinman, R.L., Kresge, A.J., and Whipple, E.B. (1971). Basic strength of carbazole. Estimate of the nitrogen basicity of pyrrole and indole. J. Am. Chem. Soc. *93*, 5102–5107.

Creutz, S.E., Lotito, K.J., Fu, G.C., and Peters, J.C. (2012). Photoinduced Ullmann C–N coupling: demonstrating the viability of a radical pathway. Science *338*, 647–651.

Engle, K.M., Mei, T.-S., Wasa, M., and Yu, J.-Q. (2011). Weak coordination as a powerful means for developing broadly useful C-H functionalization reactions. Acc. Chem. Res. *45*, 788–802.

Galabov, B., Nalbantova, D., Schleyer, P.R., and Schaefer, H.F. (2016). Electrophilic aromatic substitution: new insights into an old class of reactions. Acc. Chem. Res. *49*, 1191–1199.

Hirota, T., Lee, J.K., St.John, P.C., Sawa, M., Iwaisako, K., Noguchi, T., Pongsawakul, P.Y.,

Sonntag, T., Welsh, D.K., Brenner, D.A., et al. (2012). Identification of small molecule activators of cryptochrome. Science *337*, 1094–1097.

Ishikura, M., Abe, T., Choshi, T., and Hibino, S. (2013). Simple indole alkaloids and those with a non-rearranged monoterpenoid unit. Nat. Prod. Rep. *30*, 694–752.

Jin, H., Huang, Z., Kuang, C., and Wang, X. (2011). Iron-catalyzed bromination of aryl azides by *N*-bromosuccinimide: efficient method for the synthesis of brominated aryl azides. Chin. Chem. Lett. *22*, 310–313.

Liyu, J., and Sperry, J. (2017). Synthesis of putative clausenal from carbazole using sequential C–H borylations. Tetrahedron Lett. *58*, 1699–1701.

Ma, G., Liu, G., Shen, S., Chai, Y., Yue, L., Zhao, S., and Pan, Y. (2017). Competitive benzyl cation transfer and proton transfer: collision-induced mass spectrometric fragmentation of protonated N,N-dibenzylaniline. J. Mass Spectrom. *52*, 197–203.

Markle, T.F., Darcy, J.W., and Mayer, J.M. (2018). A new strategy to efficiently cleave and form C-H bonds using proton-coupled electron transfer. Sci. Adv. *4*, eaat5776.

Migliore, A., Polizzi, N.F., Therien, M.J., and Beratan, D.N. (2014). Biochemistry and theory of proton-coupled electron transfer. Chem. Rev. *114*, 3381–3465.

Mostafa, M.A.B., Bowley, R.M., Racys, D.T., Henry, M.C., and Sutherland, A. (2017). Iron(III)-catalyzed chlorination of activated arenes. J. Org. Chem. *82*, 7529–7537.

Raczyńska, E.D., Stępniewski, T.M., and Kolczyńska, K. (2011). Consequence of one-electron oxidation and one-electron reduction for aniline. J. Mol. Model. *17*, 3229–3239.

Roduner, E. (2014). Understanding catalysis. Chem. Soc. Rev. *43*, 8226–8239.

Rudroff, F., Mihovilovic, M.D., Gröger, H., Snajdrova, R., Iding, H., and Bornscheuer, U.T. (2018). Opportunities and challenges for combining chemo- and biocatalysis. Nat. Catal. *1*, 12–22.

Ryan, M.C., Martinelli, J.R., and Stahl, S.S. (2018). Cu-catalyzed aerobic oxidative N–N coupling of carbazoles and diarylamines including selective

cross-coupling. J. Am. Chem. Soc. *140*, 9074–9077.

Schuster, C., Börger, C., Julich-Gruner, K.K., Hesse, R., Jäger, A., Kaufmann, G., Schmidt, A.W., and Knölker, H.-J. (2014). Synthesis of 2-hydroxy-7-methylcarbazole, glycozolicine, mukoline, mukolidine, sansoakamine, clausine-H, and clausine-K and structural revision of clausine-TY. Eur. J. Org. Chem. *2014*, 4741–4752.

Song, S., Sun, X., Li, X., Yuan, Y., and Jiao, N. (2015). Efficient and practical oxidative bromination and iodination of arenes and heteroarenes with DMSO and hydrogen halide: a mild protocol for late-stage functionalization. Org. Lett. *17*, 2886–2889.

Song, S., Li, X., Wei, J., Wang, W., Zhang, Y., Ai, L., Zhu, Y., Shi, X., Zhang, X., and Jiao, N. (2020). DMSO-catalysed late-stage chlorination of (hetero)arenes. Nat. Catal. *3*, 107–115.

Taylor, R. (1990). Electrophilic Aromatic Substitution (John Wiley & Sons).

Uoyama, H., Goushi, K., Shizu, K., Nomura, H., and Adachi, C. (2012). Highly efficient organic light-emitting diodes from delayed fluorescence. Nature *492*, 234–238.

Urones, B., Martínez, Á.M., Rodriguez, N., Arrayás, R.G., and Carretero, J.C. (2013). Copper-catalyzed *ortho*-halogenation of protected anilines. Chem. Commun. *49*, 11044–11046.

Wan, X., Ma, Z., Li, B., Zhang, K., Cao, S., Zhang, S., and Shi, Z. (2014). Highly selective C-H functionalization/halogenation of acetanilide. J. Am. Chem. Soc. *128*, 7416–7417.

Wang, L., and Ackermann, L. (2014). Ruthenium-catalyzed ortho-C-H halogenations of benzamides. Chem. Commun. *50*, 1083–1085.

Wencel-Delord, J., and Glorius, F. (2013). C-H bond activation enables the rapid construction and late-stage diversification of functional molecules. Nat. Chem. *5*, 369–375.

Xiong, X., and Yeung, Y.Y. (2016). Highly *ortho*-selective chlorination of anilines using a secondary ammonium salt organocatalyst. Angew. Chem. Int. Ed. *55*, 16101–16105.

Xu, J., Shen, Y., Xiang, L., and Deng, Y. (2005). Synthesis of tizanidine hydrochloride. Chin. J. Pharm. *36*, 593–596.

Supplemental Information

Proton Transfer Can Govern

Regioselectivity Assisted by Iron Catalysis

Yudong Li, Liyan Fu, Xiaolin Jiang, Dongmei Zhao, Hui-Fang Wang, Chungu Xia, and Yuehui Li

Supplemental Figures for NMR spectrums:

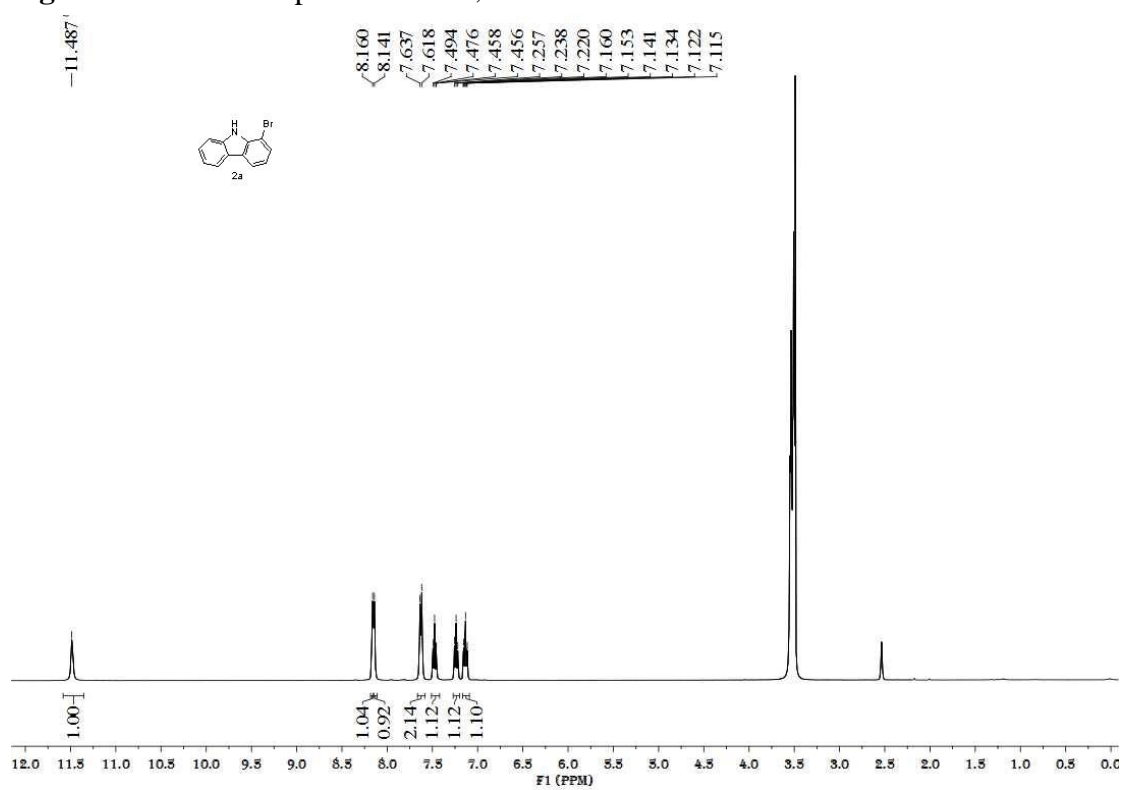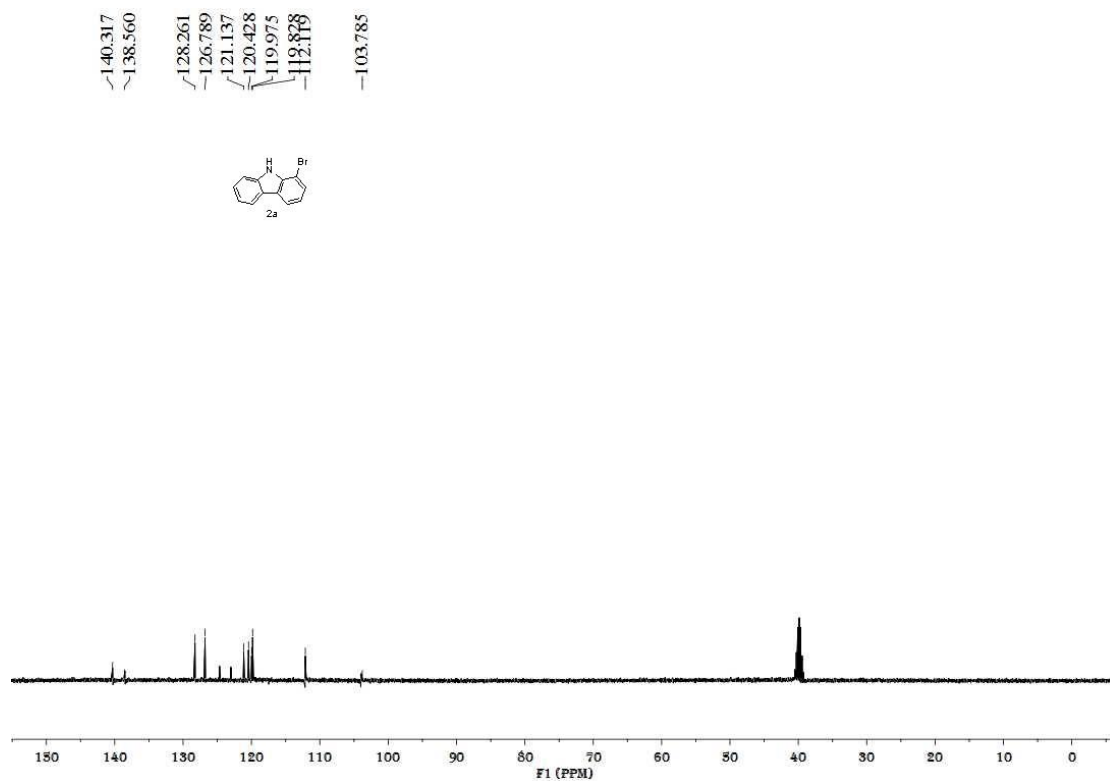**Figure S1**. ^{1}H NMR spectrum of **2a**, related to **Scheme 4**

Figure S2. ^{13}C NMR spectrum of **2a**, related to **Scheme 4**

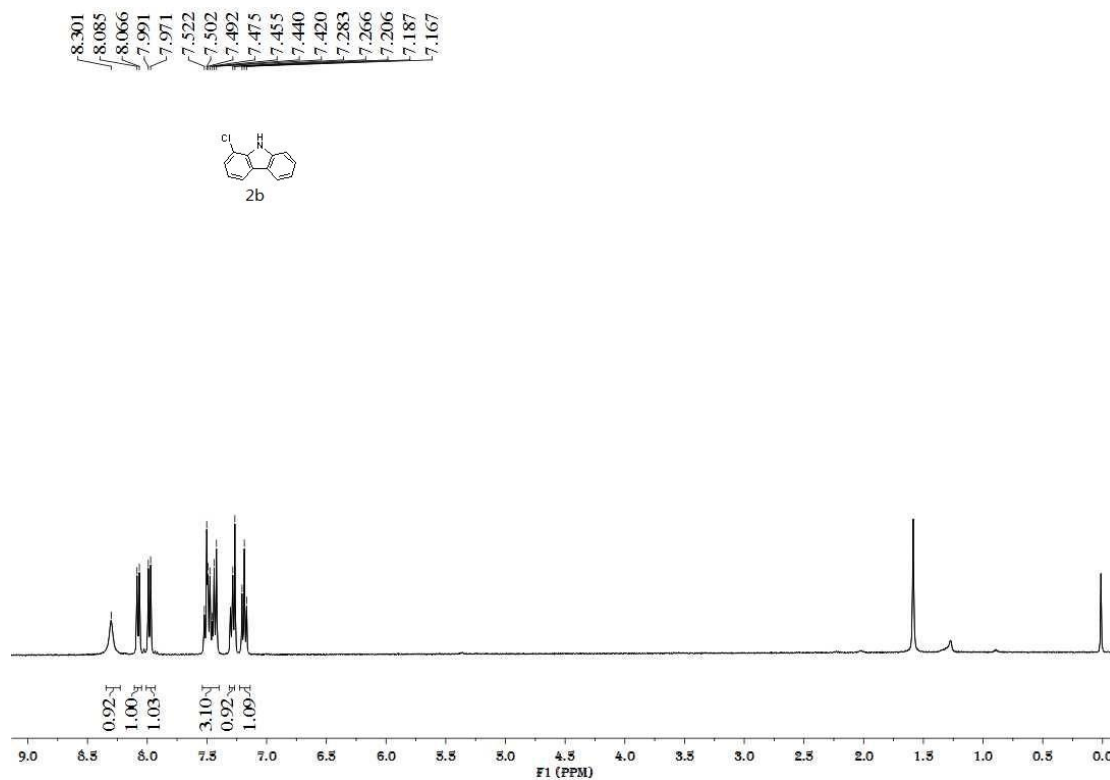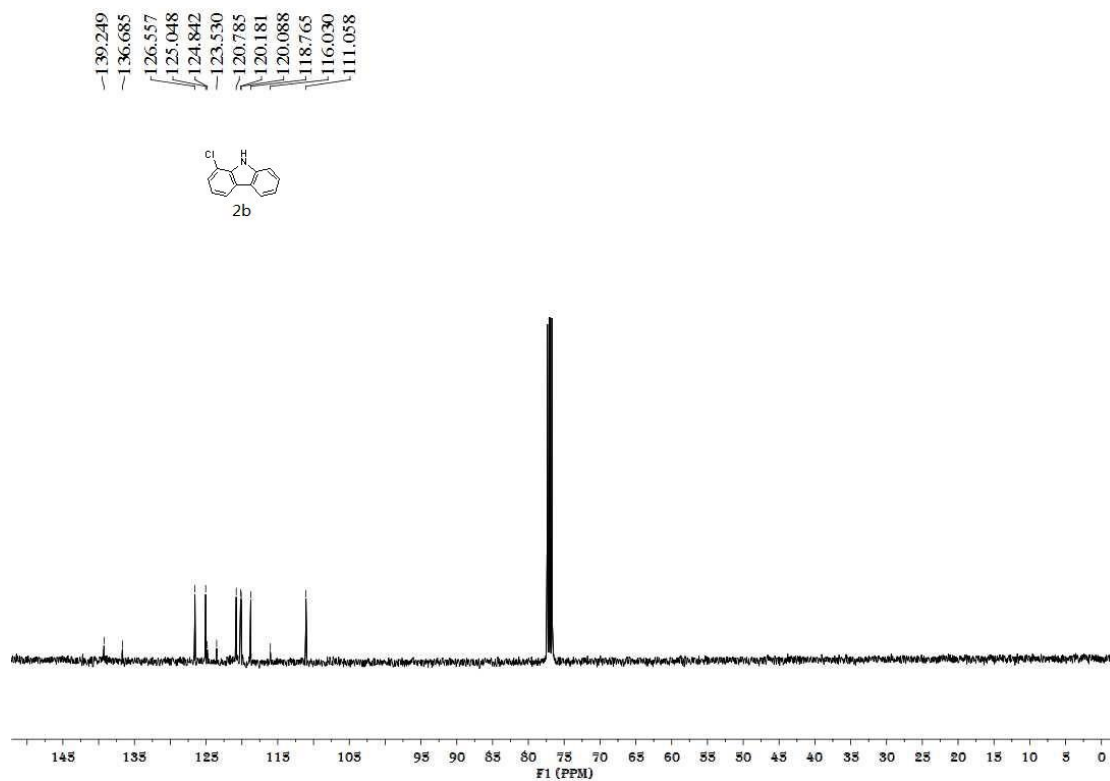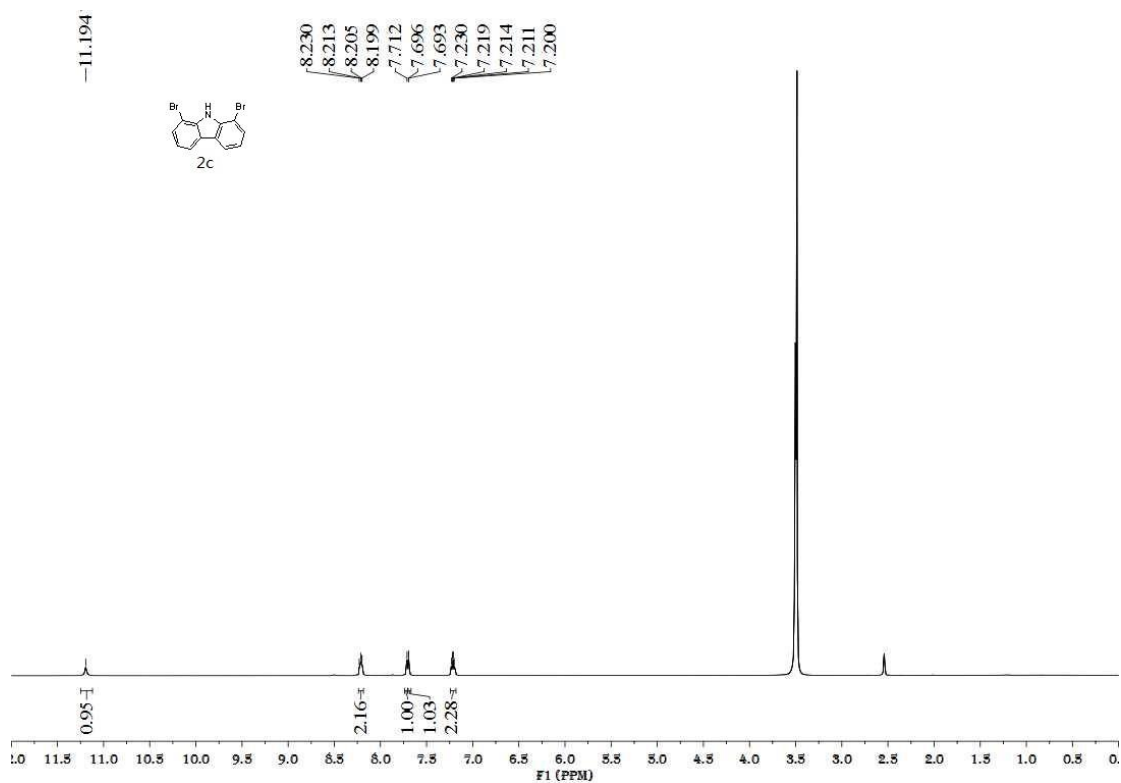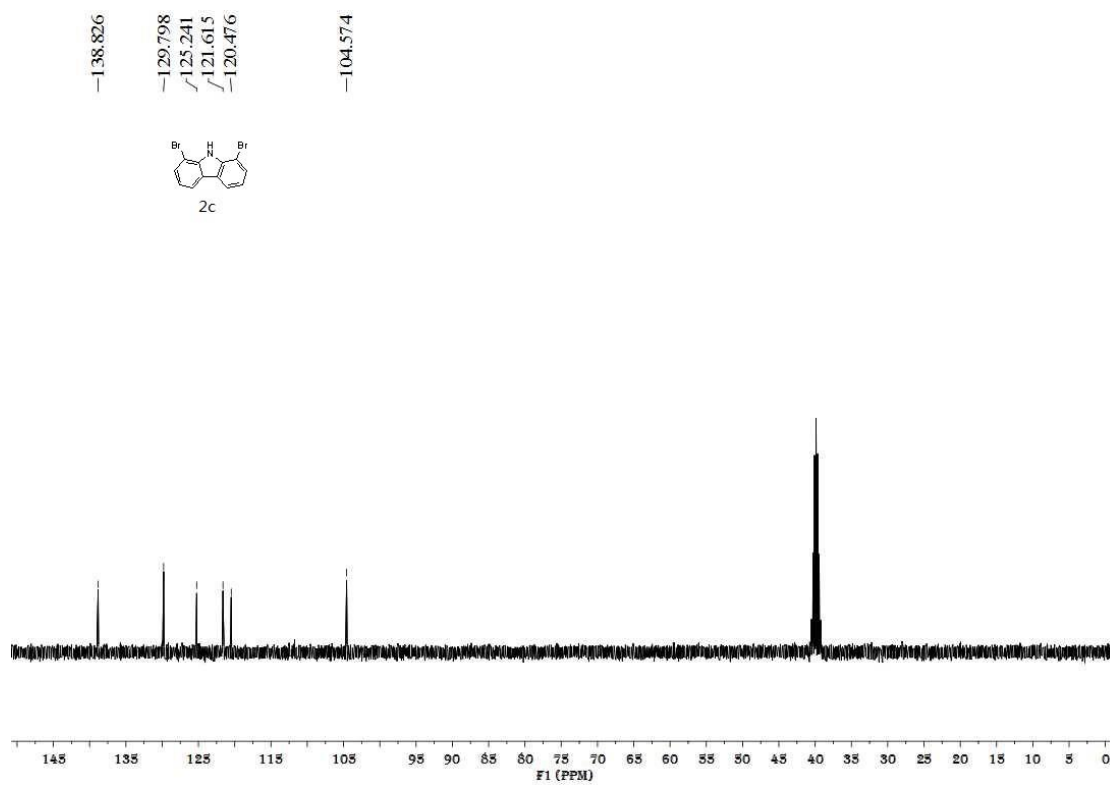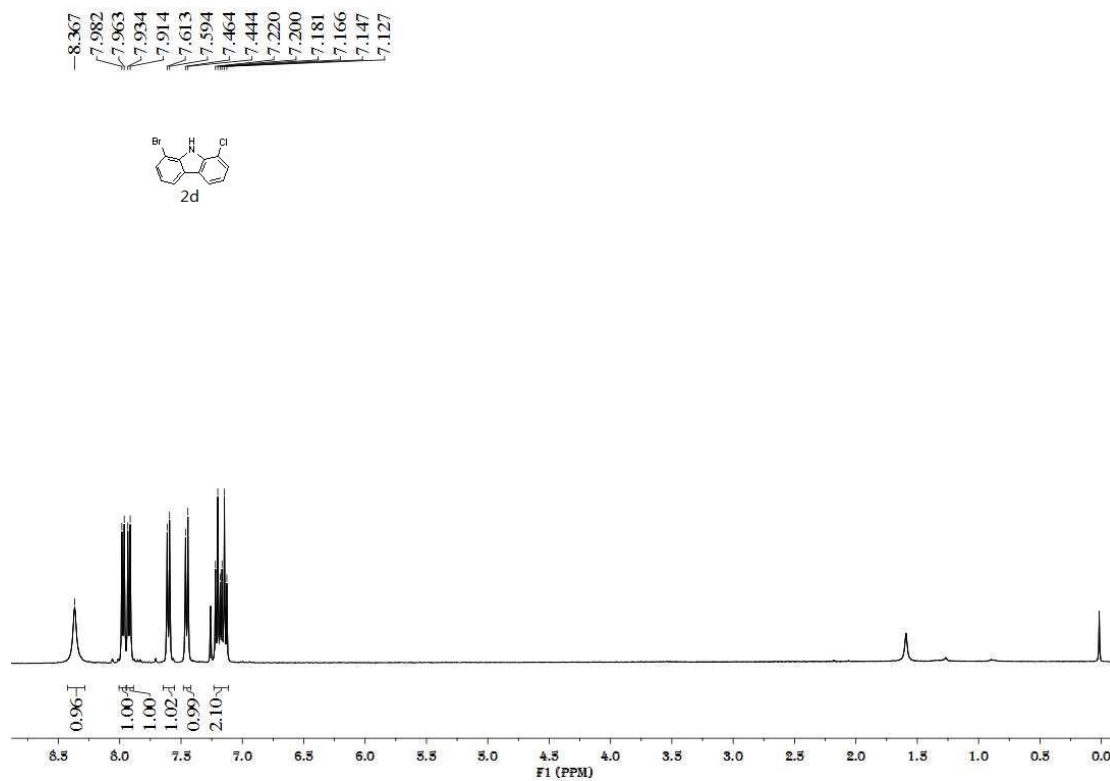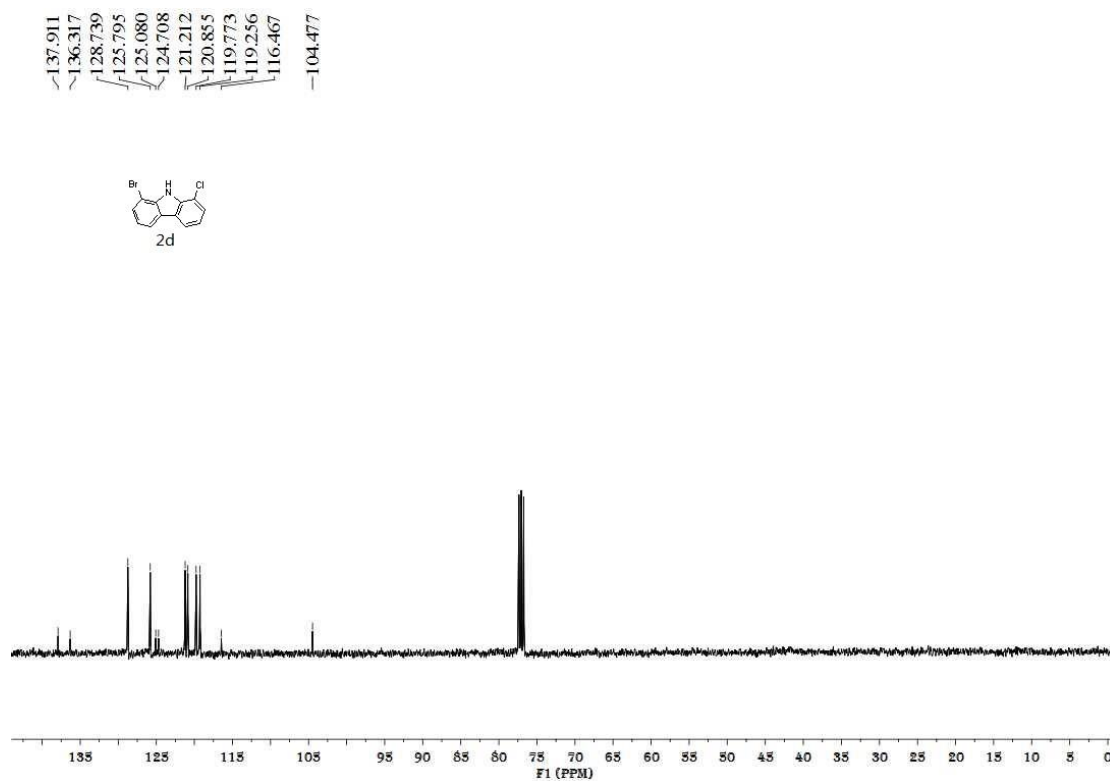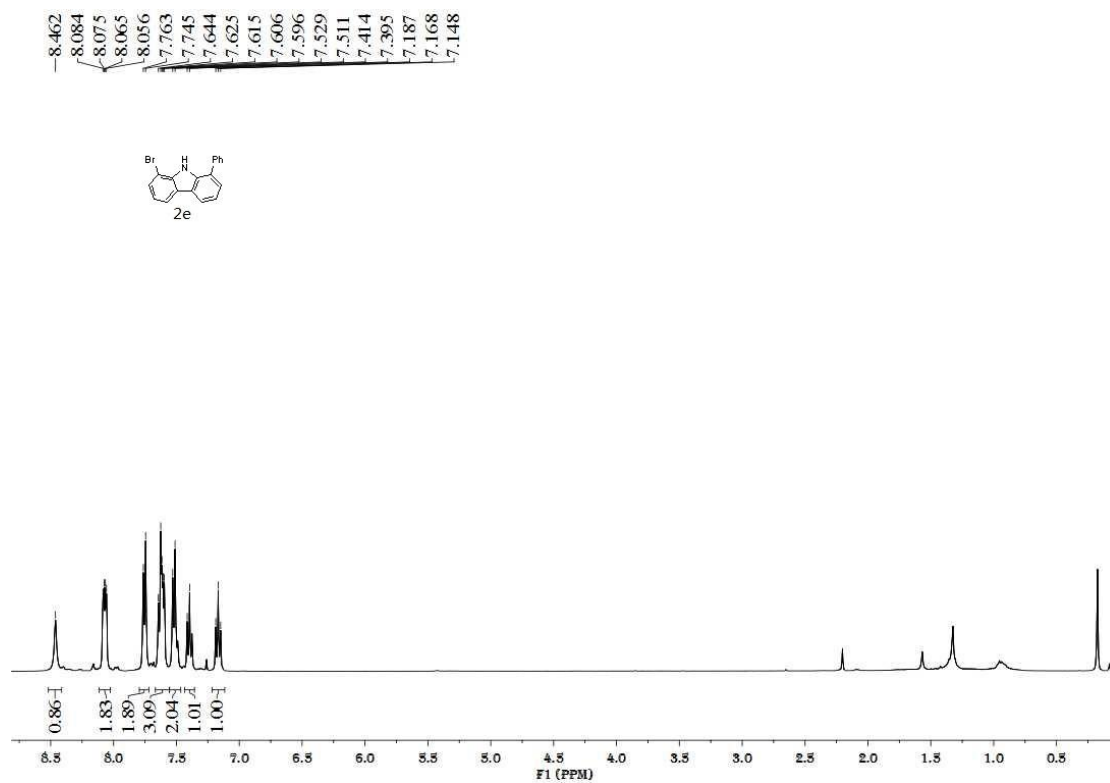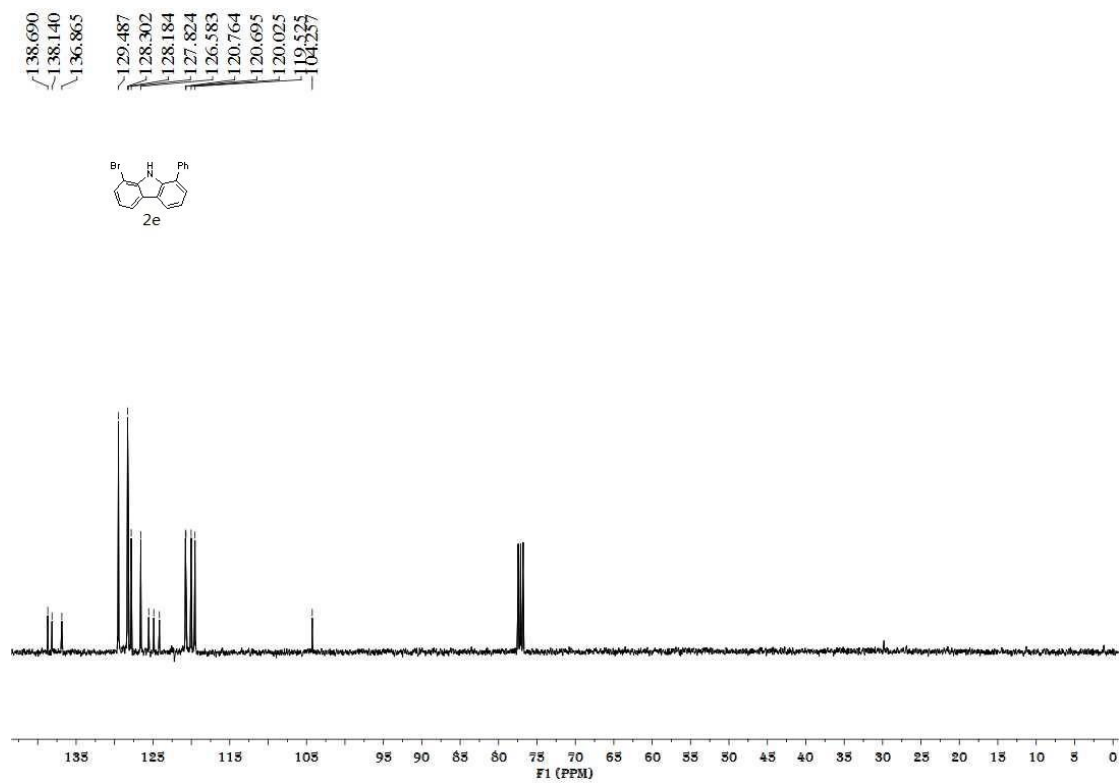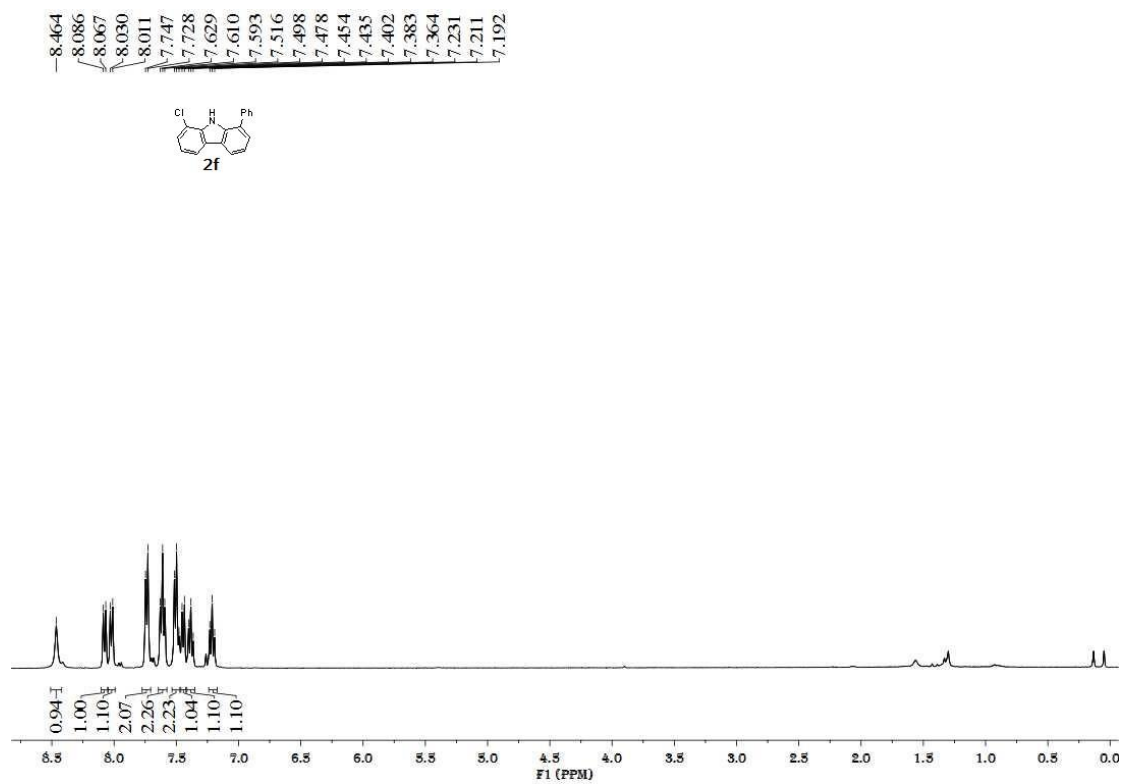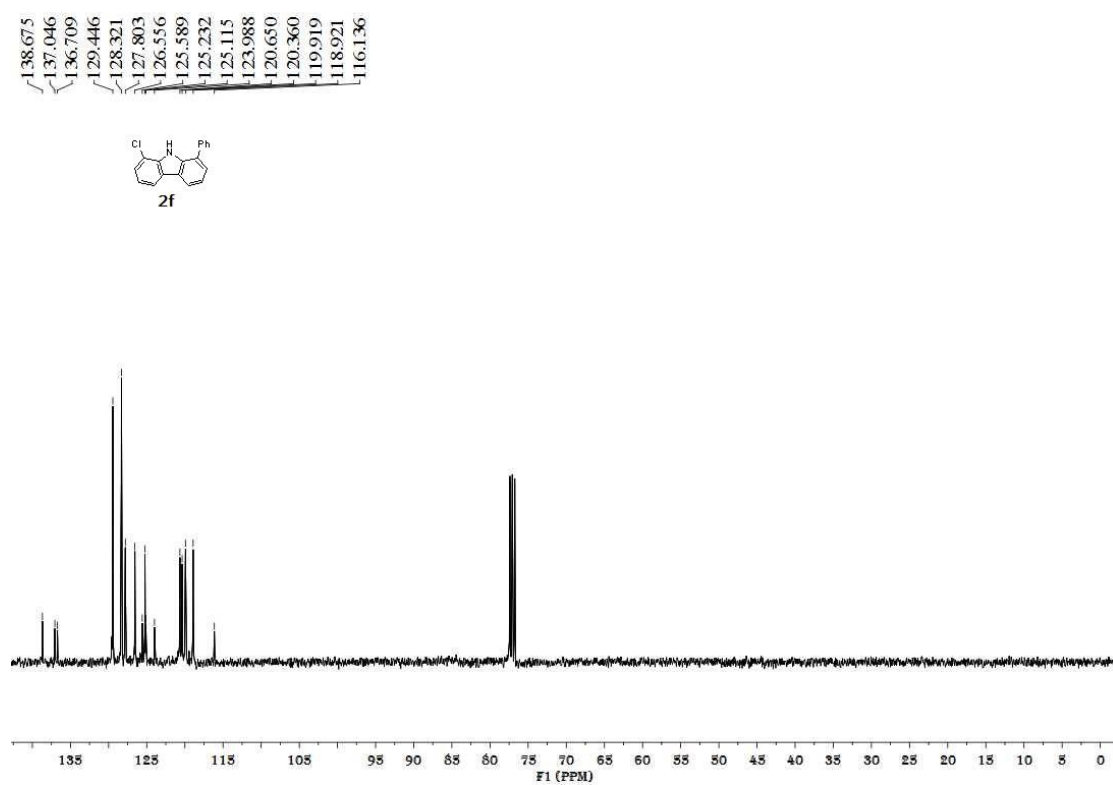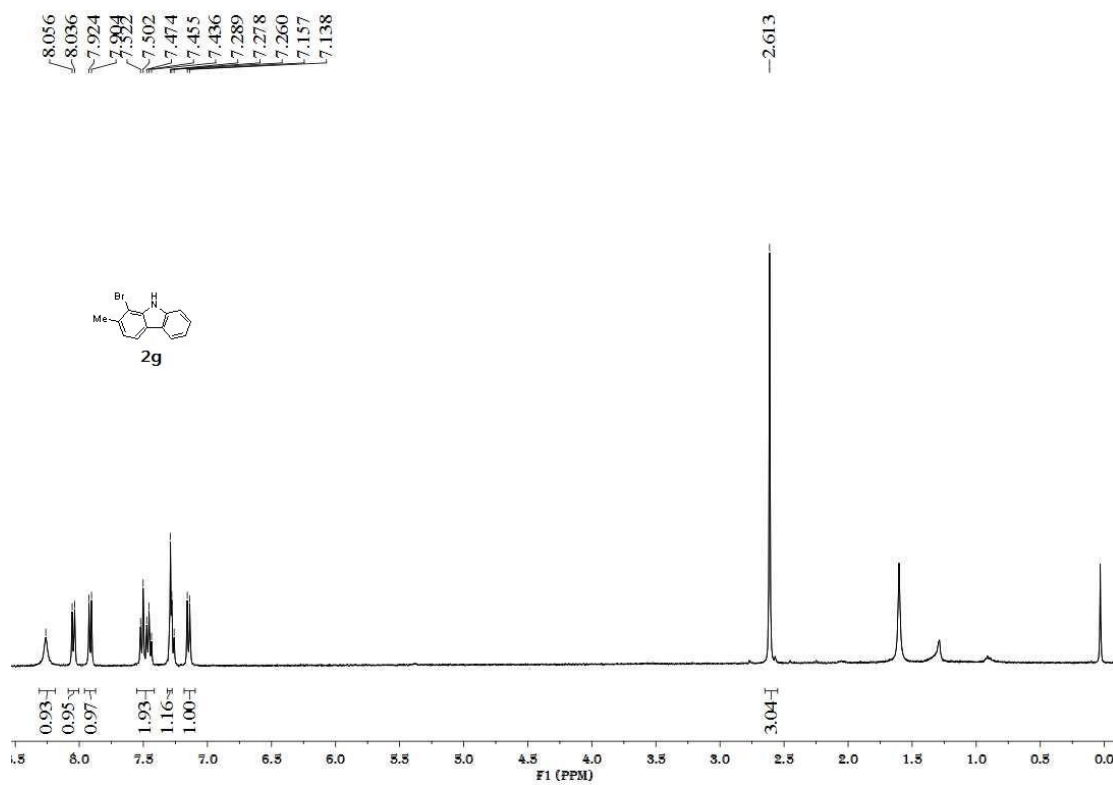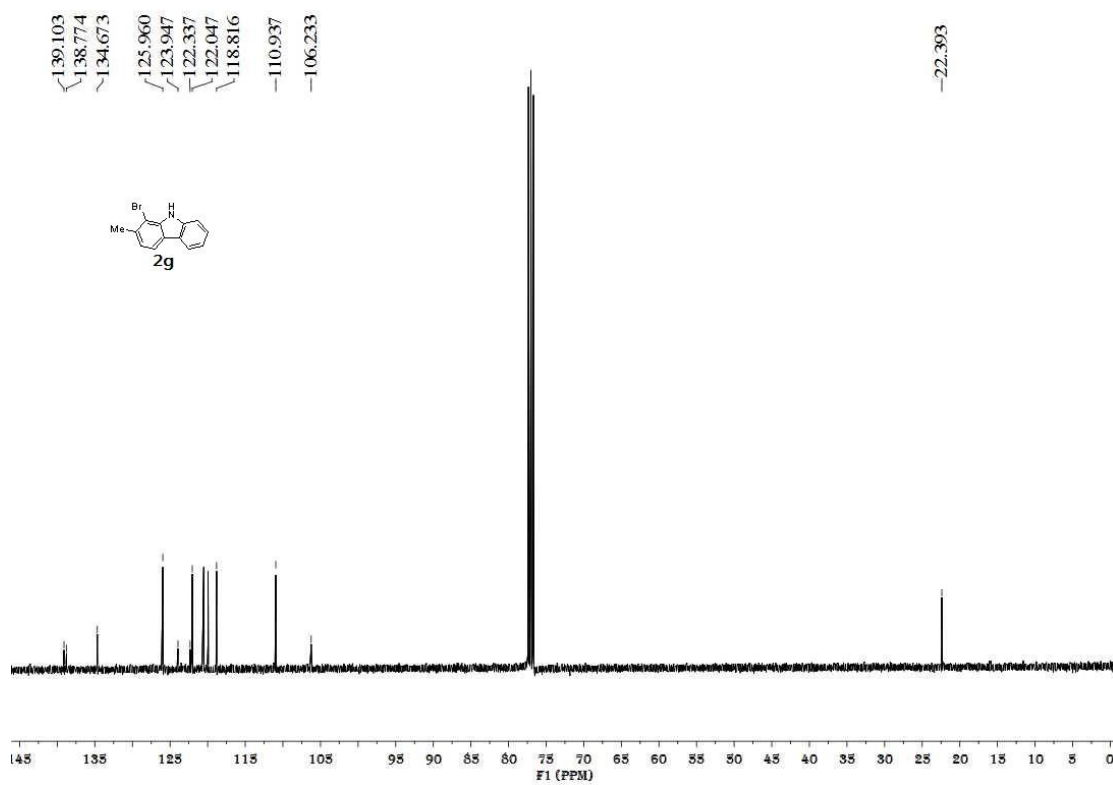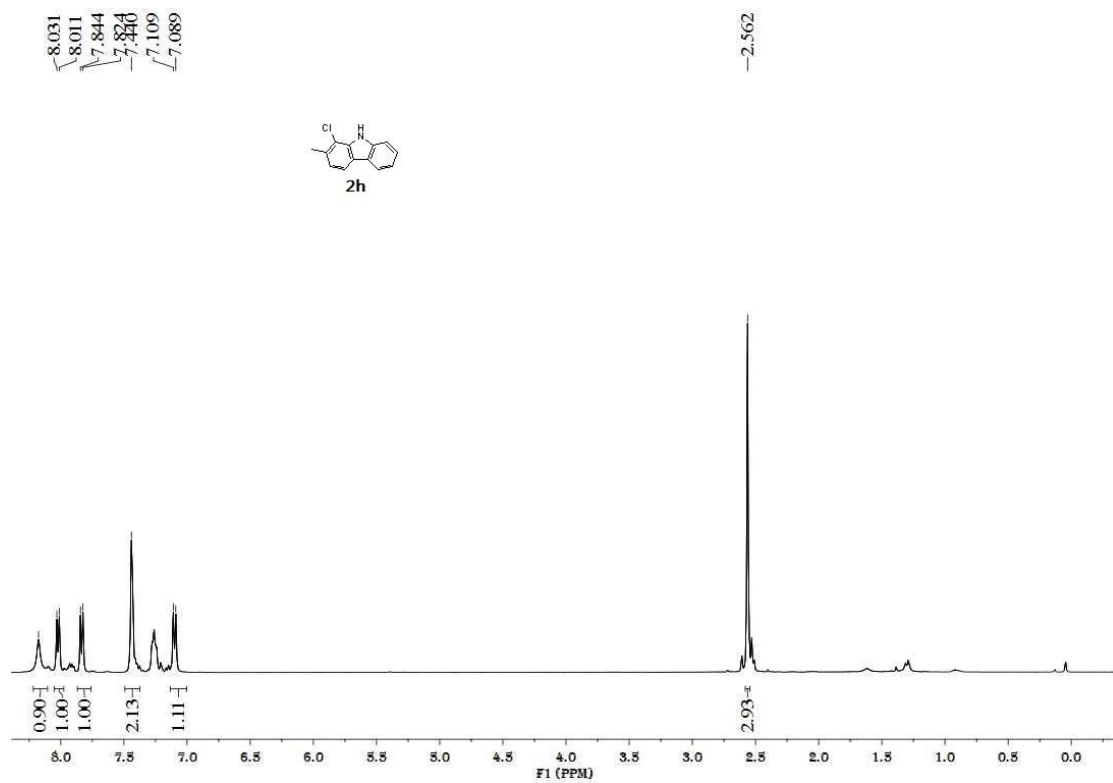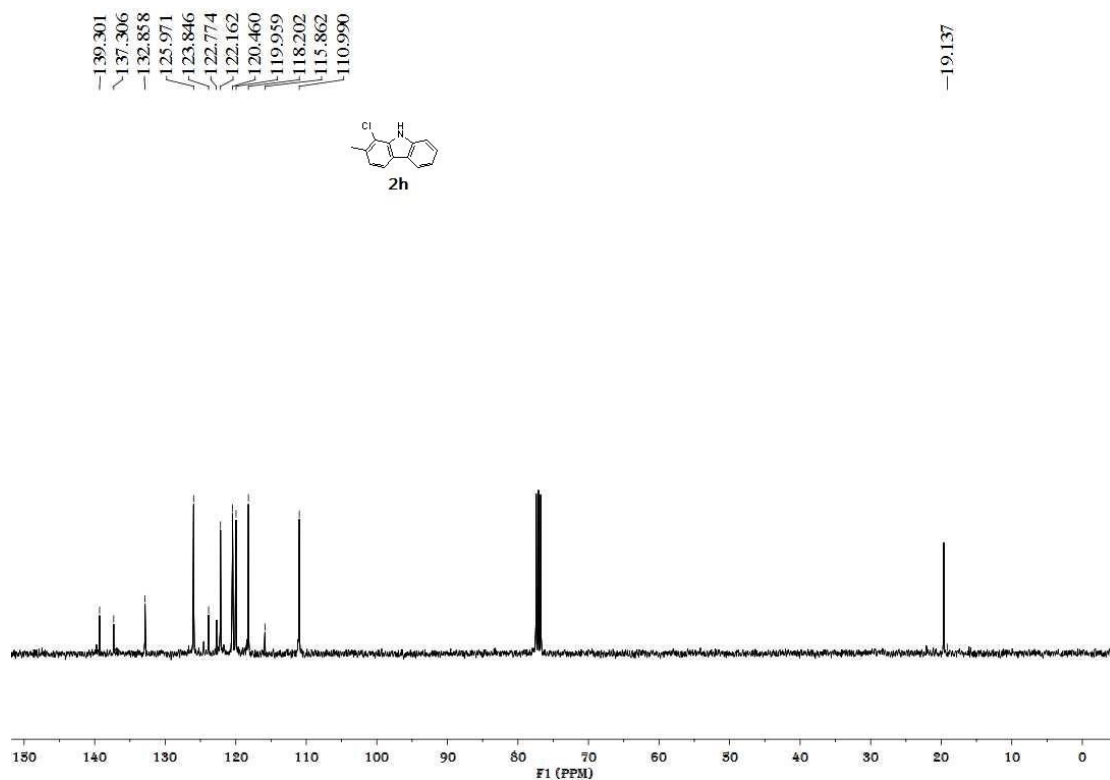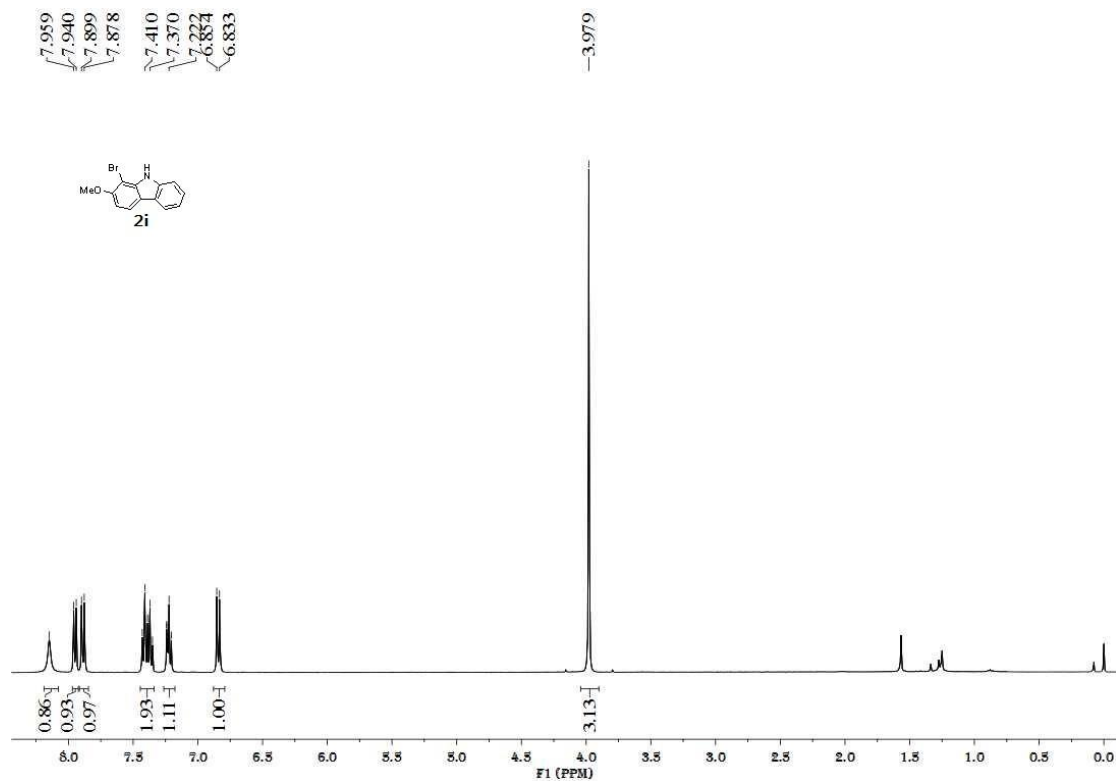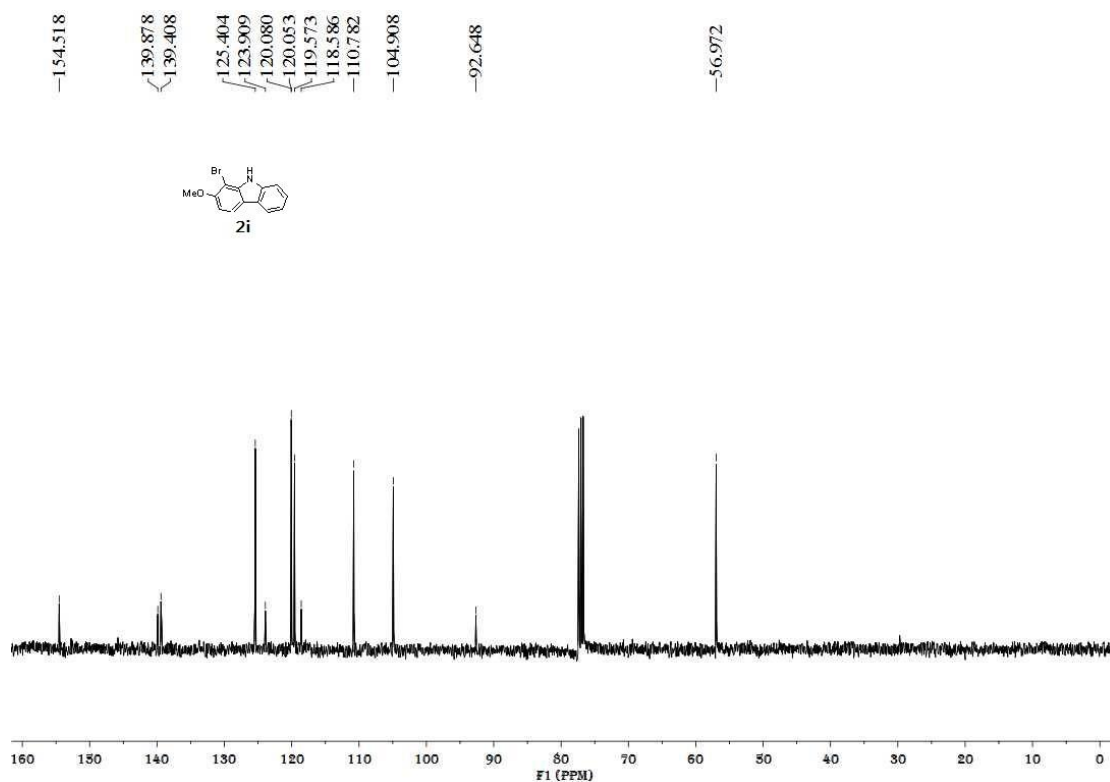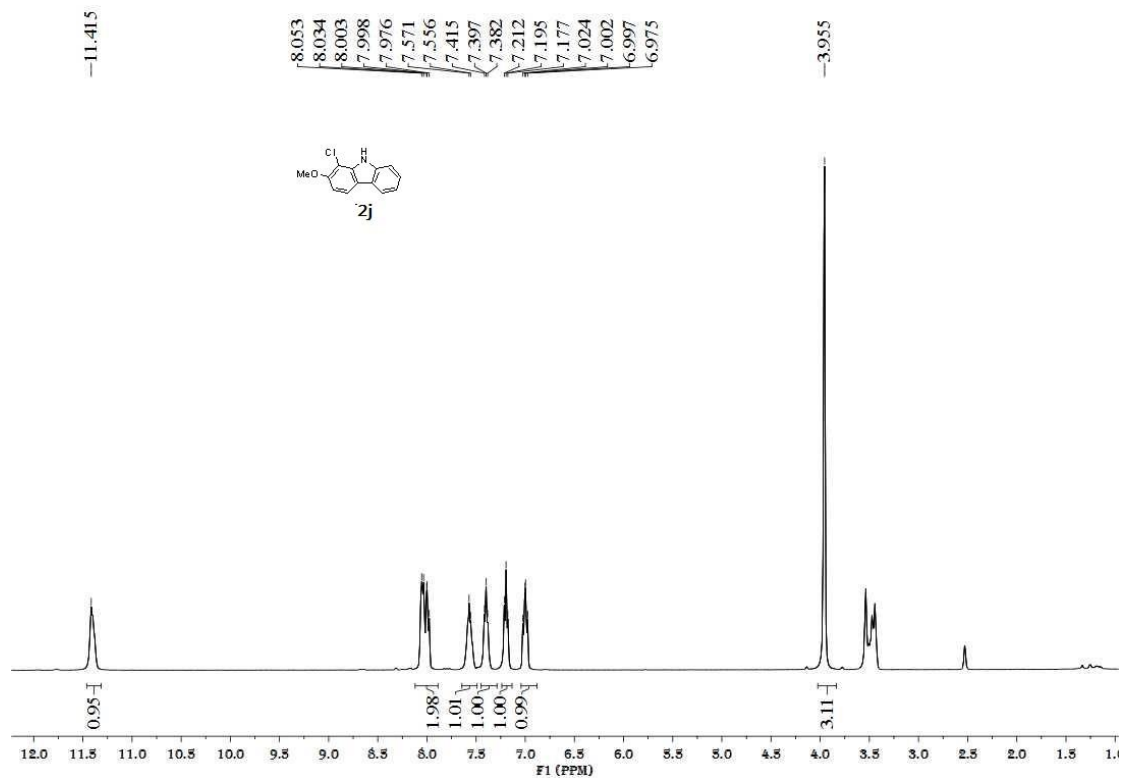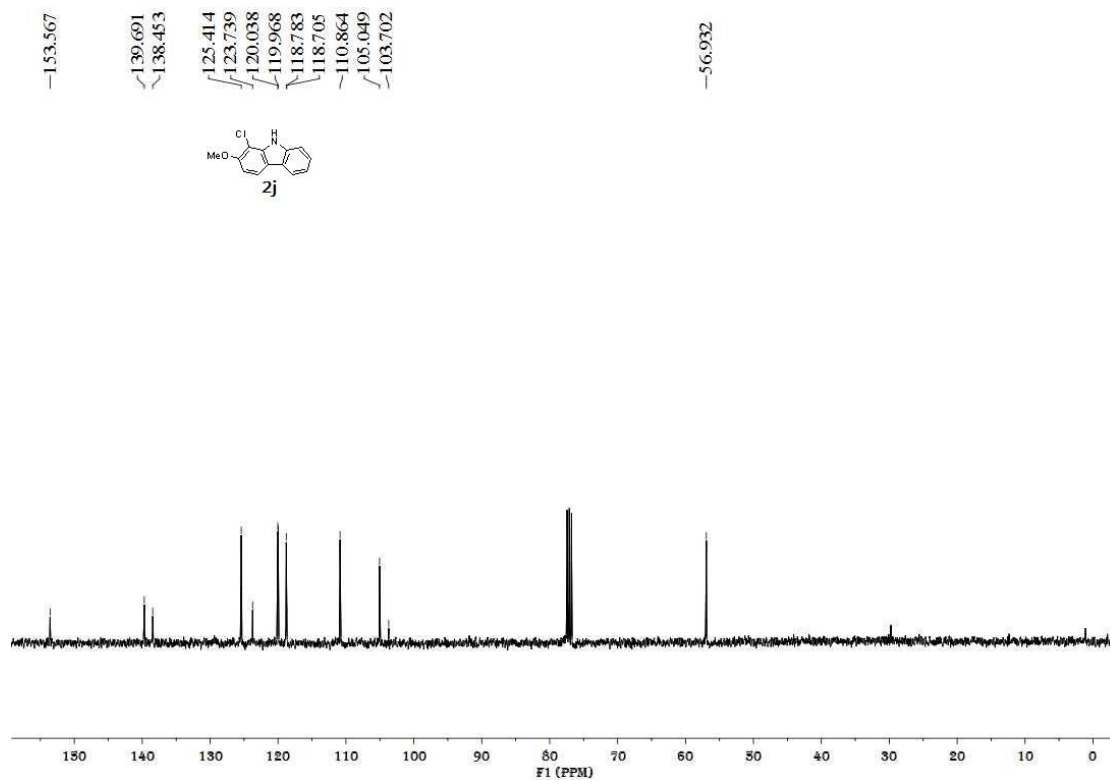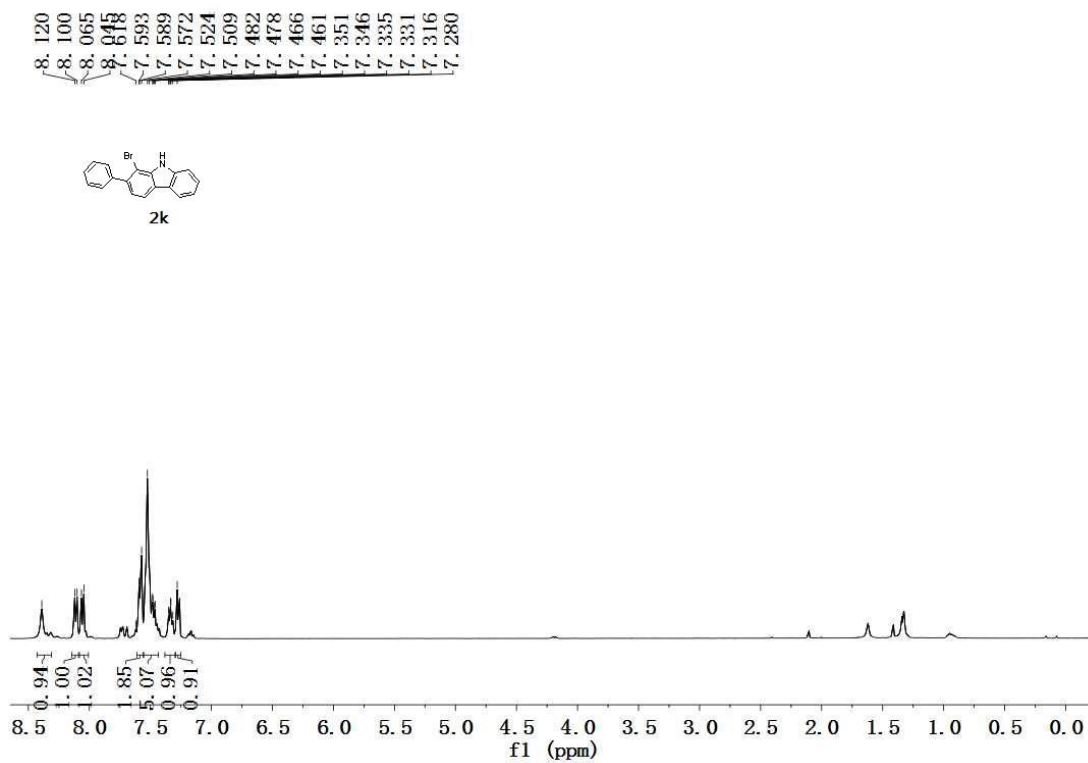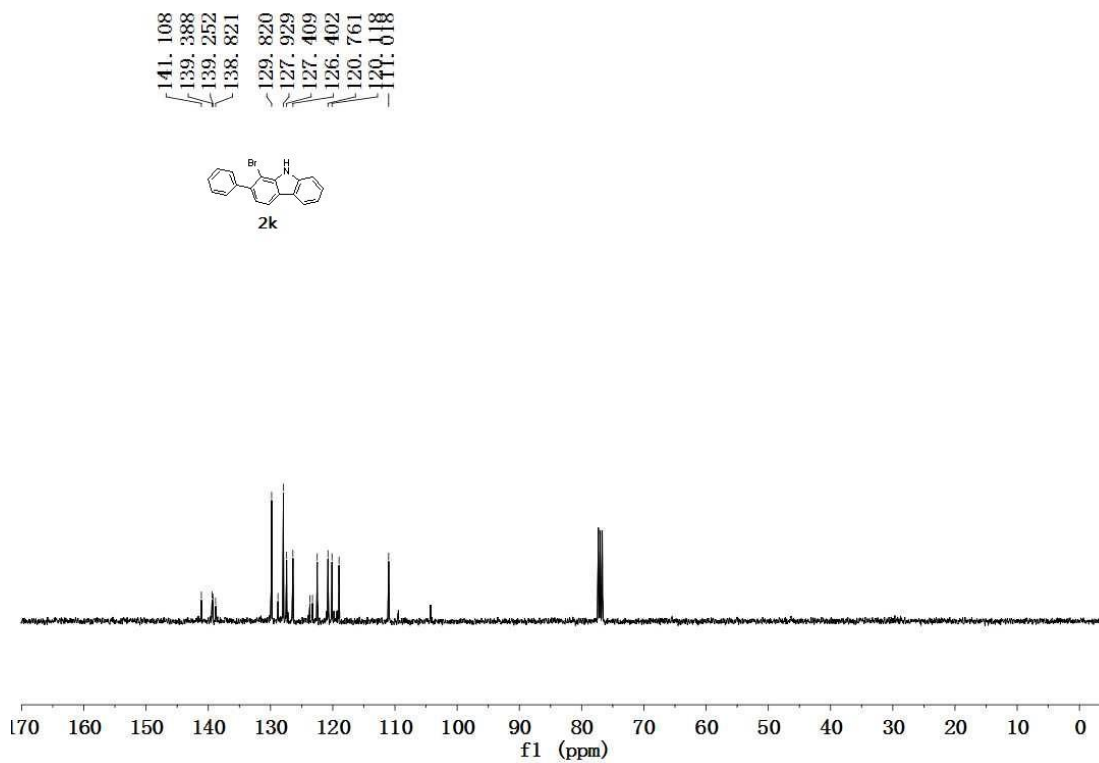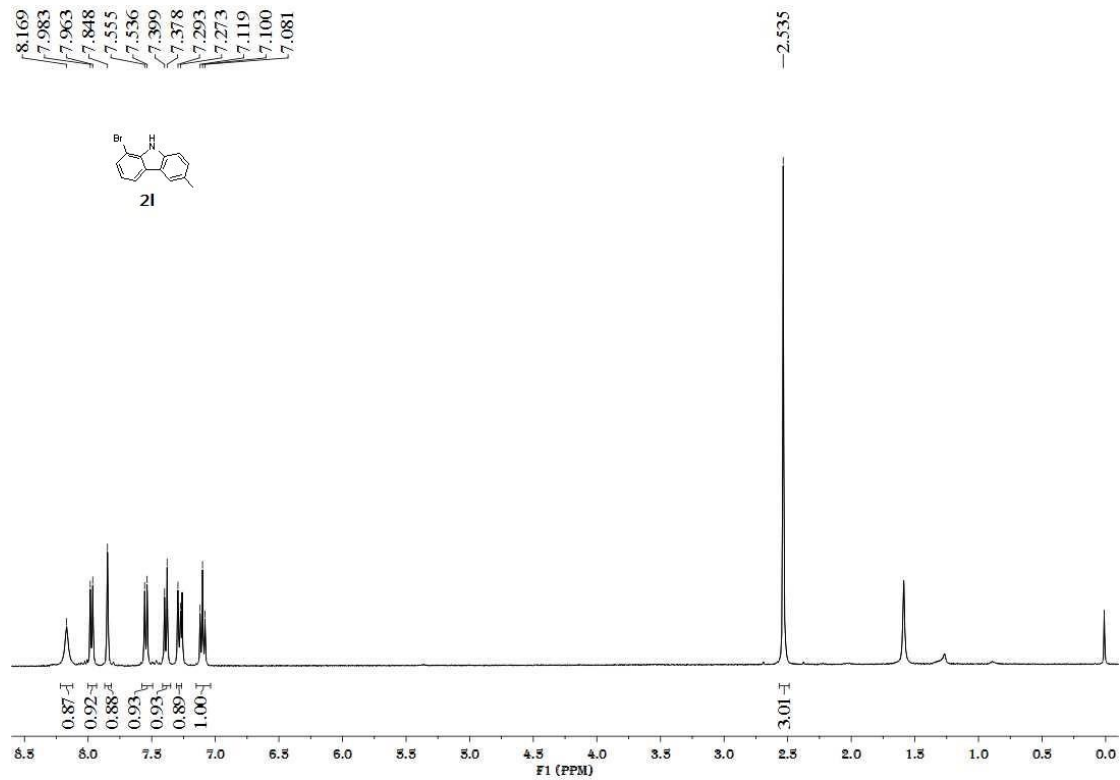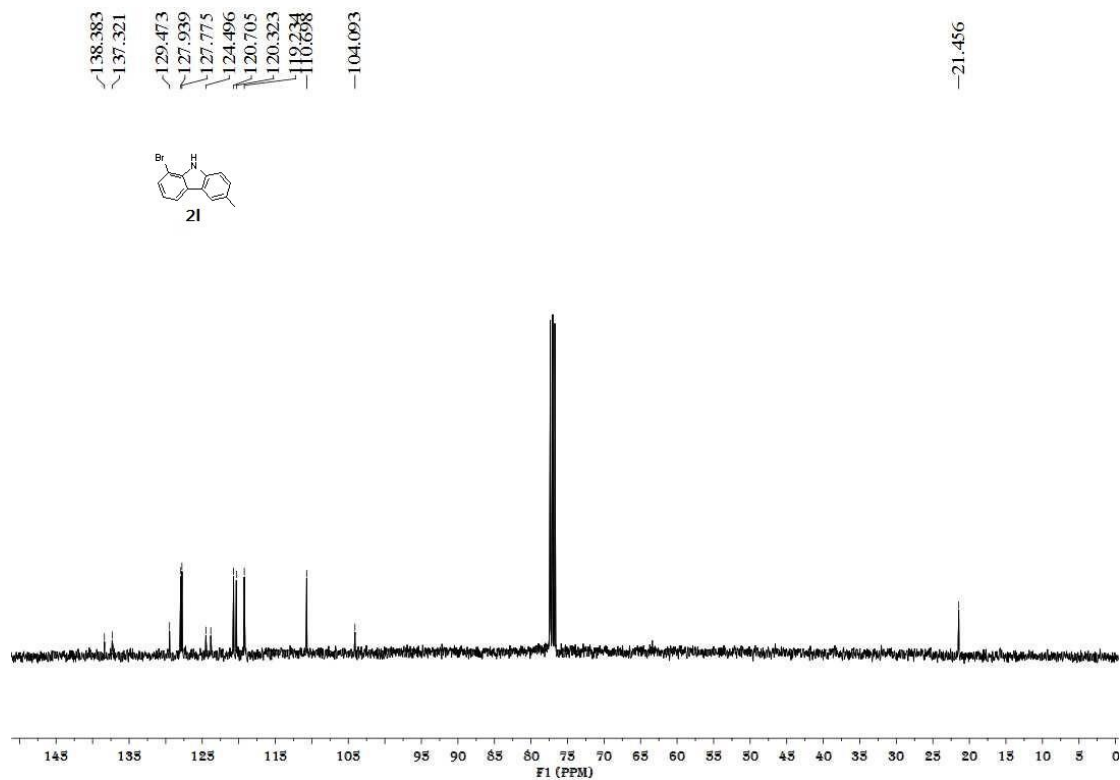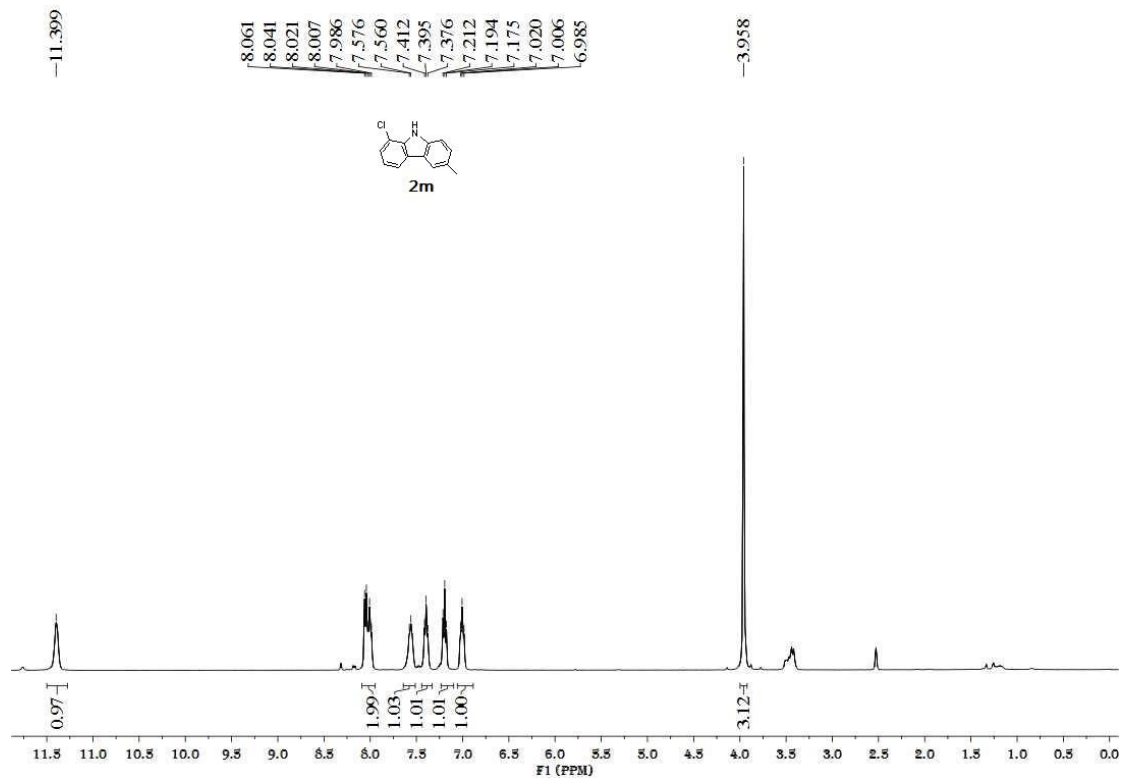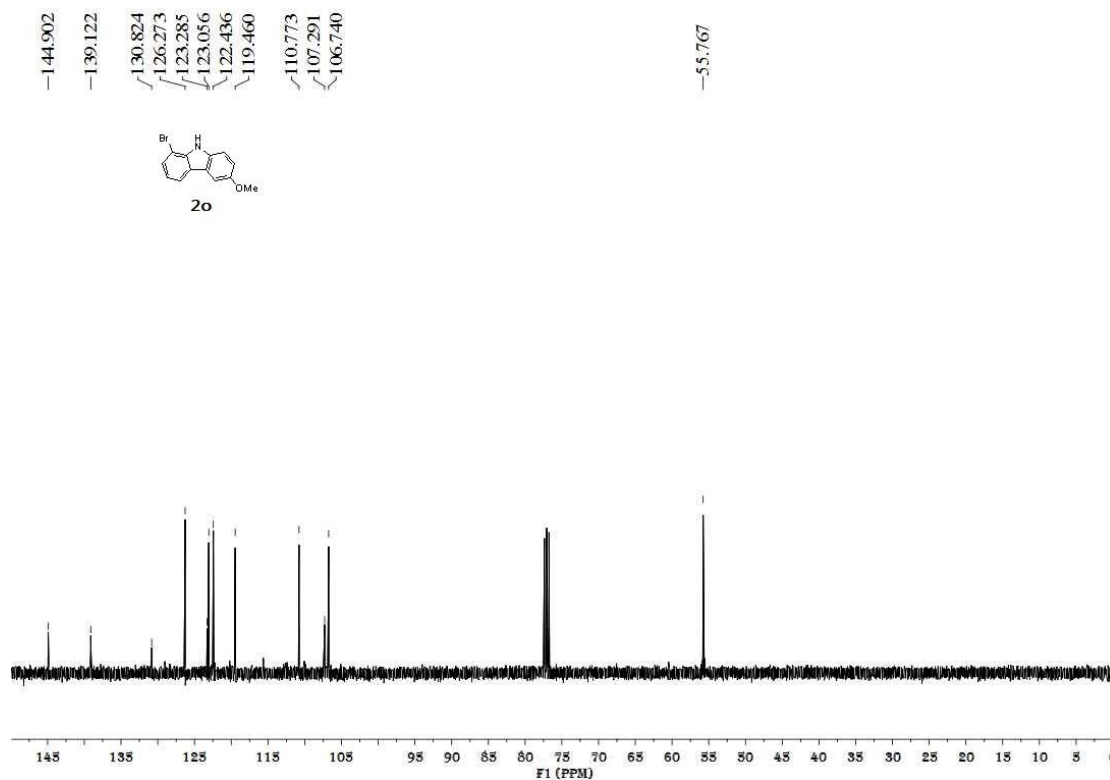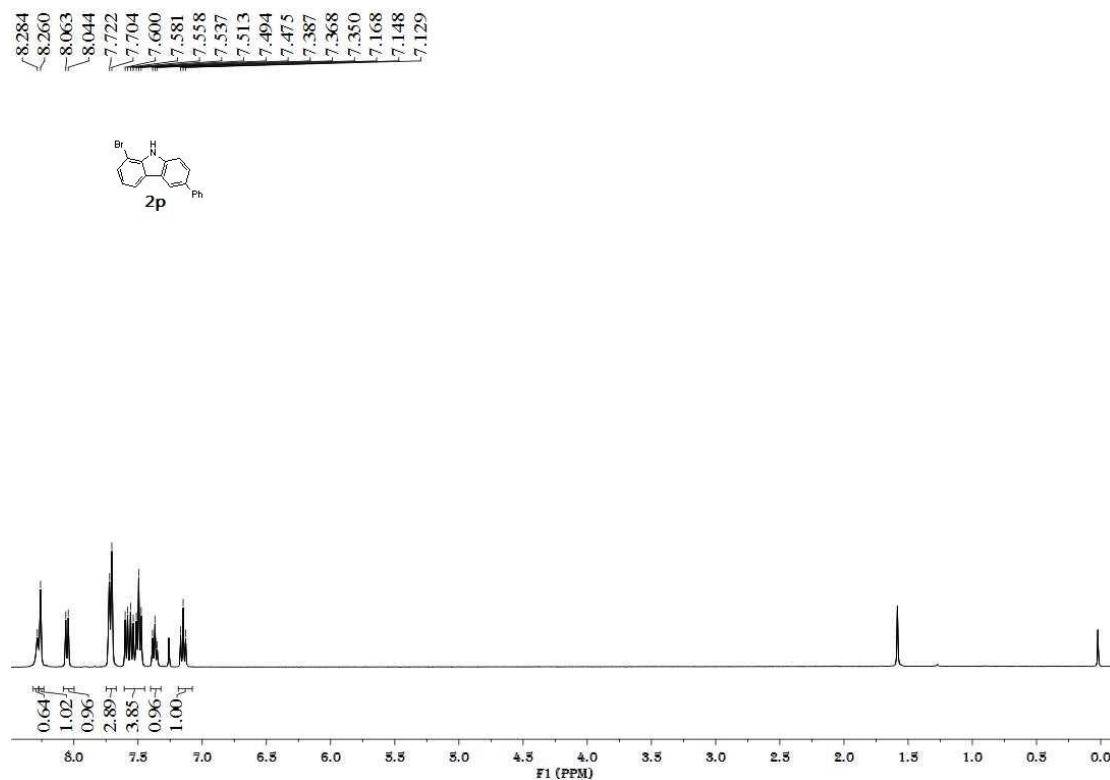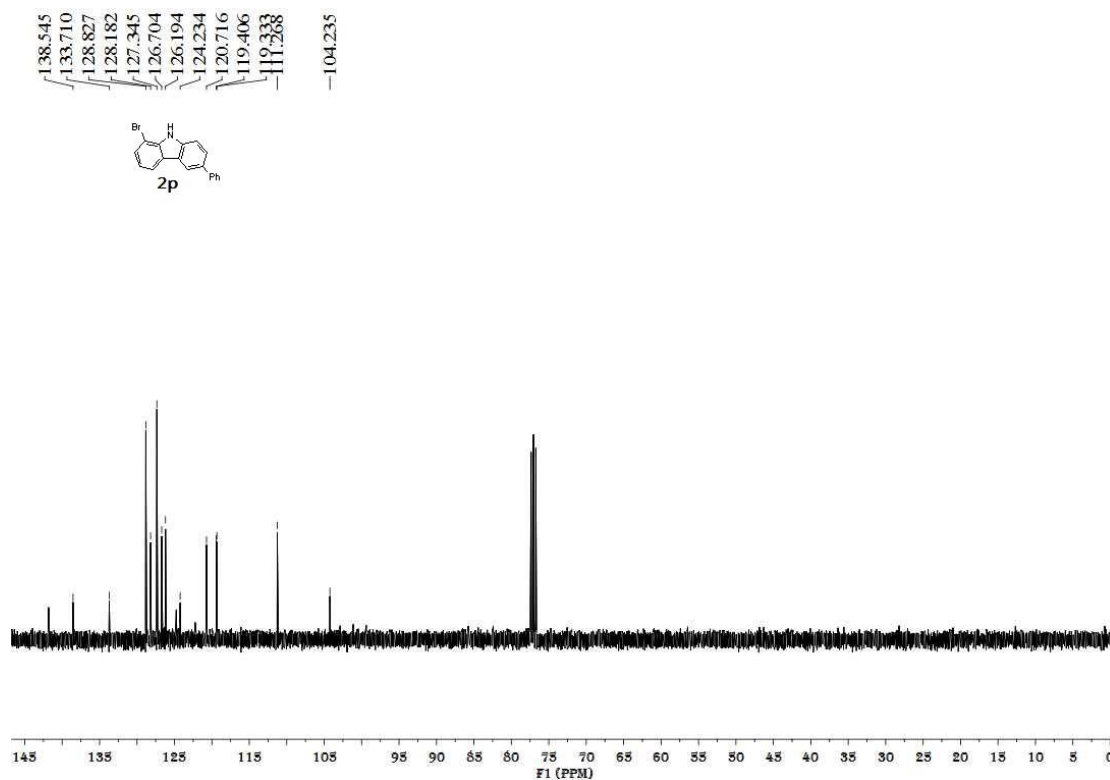**Figure S3**. ^{1}H NMR spectrum of **2b**, related to **Scheme 4**

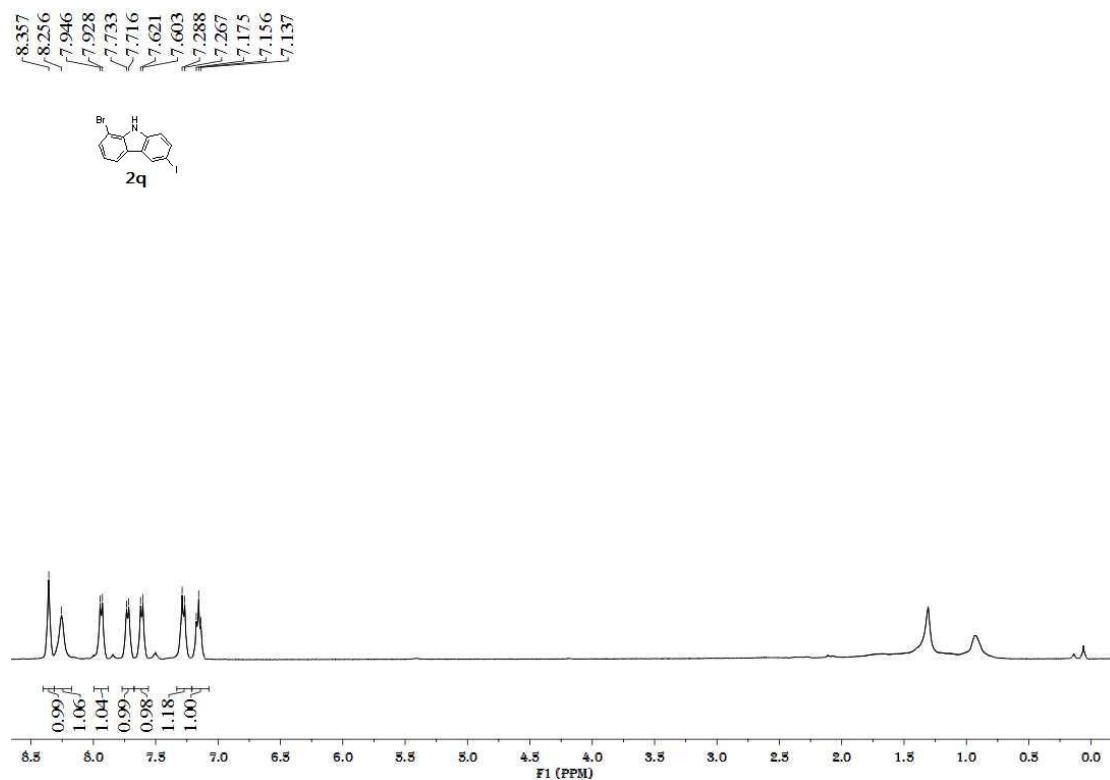**Figure S4**. ^{13}C NMR spectrum of **2b**, related to **Scheme 4**

Figure S5. ^{1}H NMR spectrum of **2c**, related to **Scheme 4**
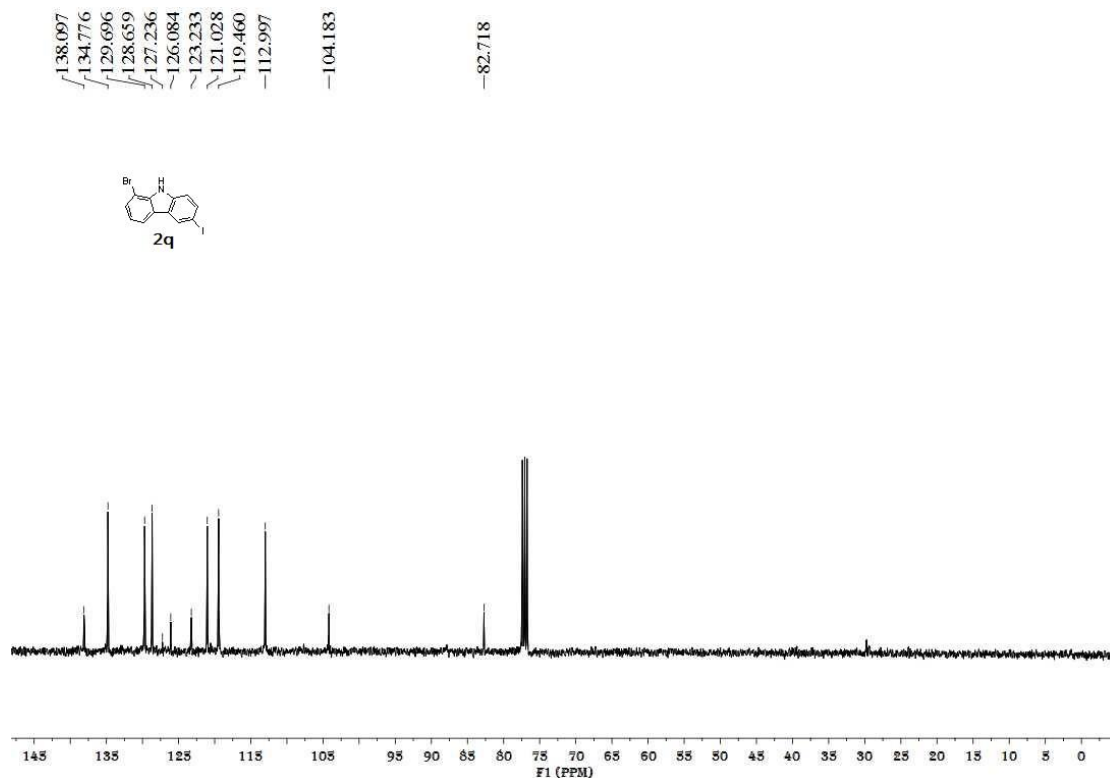

Figure S6. ^{13}C NMR spectrum of **2c**, related to **Scheme 4**

Figure S7. ^1H NMR spectrum of **2d**, related to **Scheme 4**

Figure S8. ^{13}C NMR spectrum of **2d**, related to **Scheme 4**

Figure S9. ^{1}H NMR spectrum of **2e**, related to **Scheme 4**

8.462
8.084
8.075
8.065
8.056
7.763
7.745
7.644
7.625
7.615
7.606
7.596
7.529
7.511
7.414
7.395
7.187
7.168
7.148

0.86
1.83
1.89
3.09
2.04
1.01
1.00

8.5 8.0 7.5 7.0 6.5 6.0 5.5 5.0 4.5 4.0 3.5 3.0 2.5 2.0 1.5 1.0 0.5
F1 (PPM)

Figure S10. ^{13}C NMR spectrum of **2e**, related to **Scheme 4**

Figure S11. ^{1}H NMR spectrum of **2f**, related to **Scheme 4**

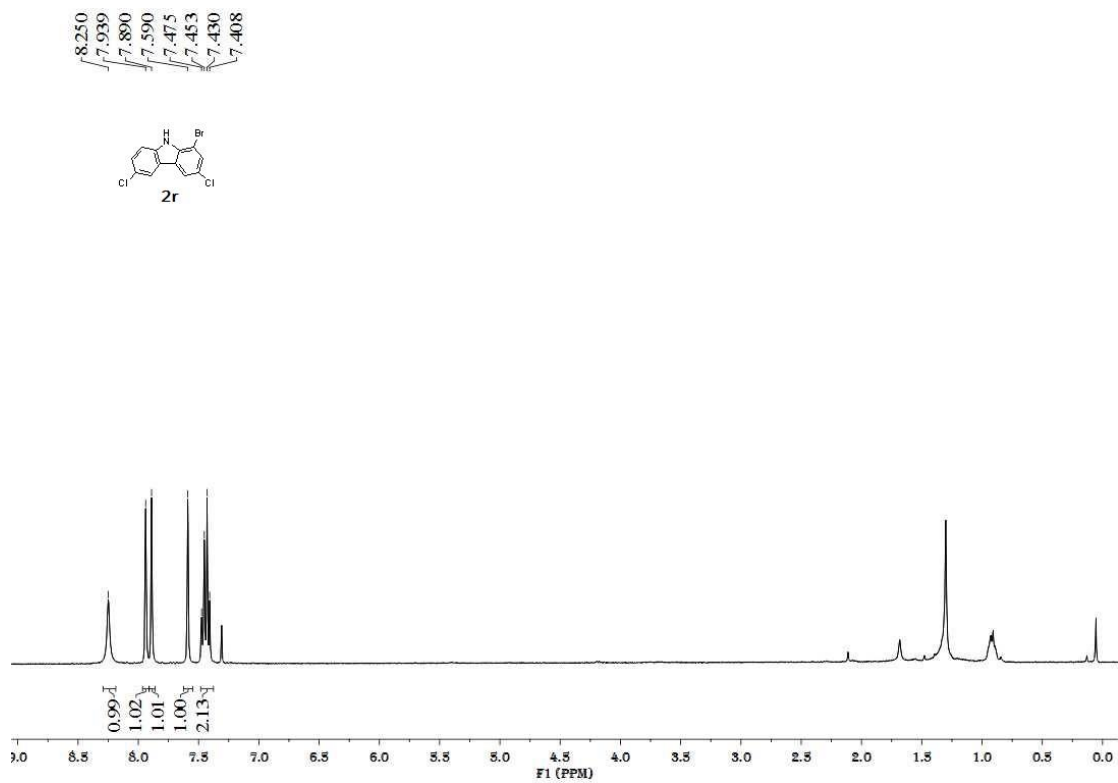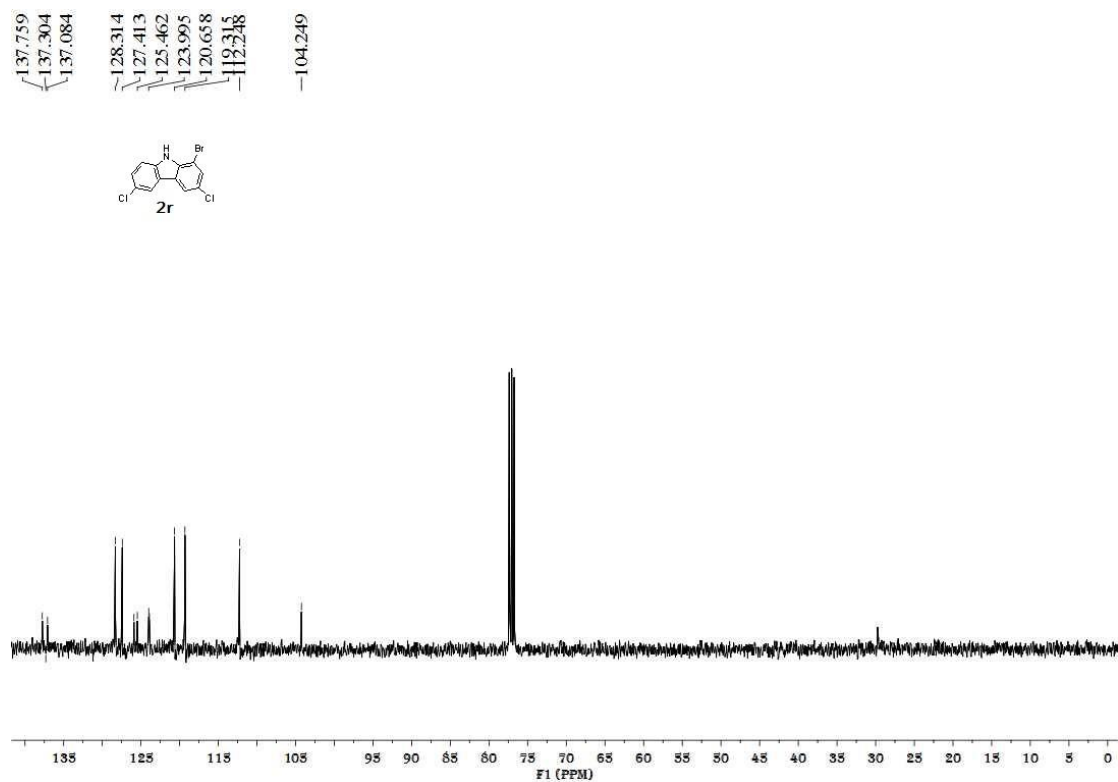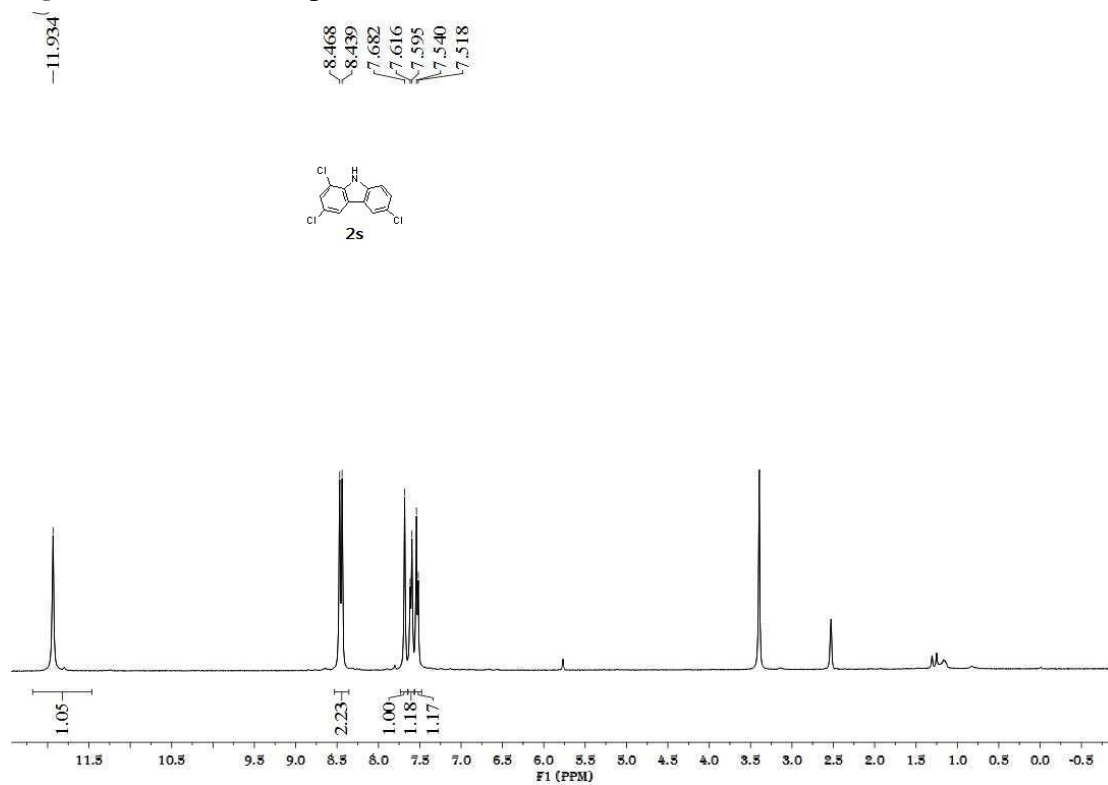Figure S12. ^{13}C NMR spectrum of **2f**, related to **Scheme 4**

13C NMR peaks: 138.675, 137.046, 136.709, 129.446, 128.321, 127.803, 126.556, 125.589, 125.232, 125.115, 123.988, 120.650, 120.360, 119.919, 118.921, 116.136

Structure label: **2f**

Figure S13. ¹H NMR spectrum of **2g**, related to **Scheme 4**

¹H NMR peaks: 8.056, 8.036, 7.924, 7.522, 7.502, 7.474, 7.455, 7.436, 7.289, 7.278, 7.260, 7.157, 7.138, 2.613

Structure label: **2g**

Integration values: 0.93, 0.95, 0.97, 1.93, 1.16, 1.00, 3.04

Figure S14. ^{13}C NMR spectrum of **2g**, related to **Scheme 4**

Figure S15. ^{1}H NMR spectrum of **2h**, related to **Scheme 4**

Figure S16. ^{13}C NMR spectrum of **2h**, related to **Scheme 4**

Figure S17. ^{1}H NMR spectrum of **2i**, related to **Scheme 4**

Figure S18. ^{13}C NMR spectrum of **2i**, related to **Scheme 4**

Figure S19. ^{1}H NMR spectrum of **2j**, related to **Scheme 4**

Figure S20. ^{13}C NMR spectrum of **2j**, related to **Scheme 4**

153.567
130.691
138.453
125.414
123.739
120.038
119.968
118.783
118.705
110.864
105.049
103.702
56.932

150 140 130 120 110 100 90 80 70 60 50 40 30 20 10 0
F1 (PPM)

Figure S21. ^{1}H NMR spectrum of **2k**, related to **Scheme 4**

8.120
8.100
8.065
8.045
8.018
7.593
7.589
7.572
7.524
7.509
7.482
7.478
7.466
7.461
7.351
7.346
7.335
7.331
7.316
7.280

0.94
1.00
1.02
1.85
5.07
0.96
0.91

8.5 8.0 7.5 7.0 6.5 6.0 5.5 5.0 4.5 4.0 3.5 3.0 2.5 2.0 1.5 1.0 0.5 0.0
f1 (ppm)

Figure S22. ^{13}C NMR spectrum of **2k**, related to **Scheme 4**

Figure S23. ^{1}H NMR spectrum of **2l**, related to **Scheme 4**

Figure S24. ^{13}C NMR spectrum of **2l**, related to **Scheme 4**

Figure S25. ^{1}H NMR spectrum of **2m**, related to **Scheme 4**

Figure S26. ^{13}C NMR spectrum of **2m**, related to **Scheme 4**
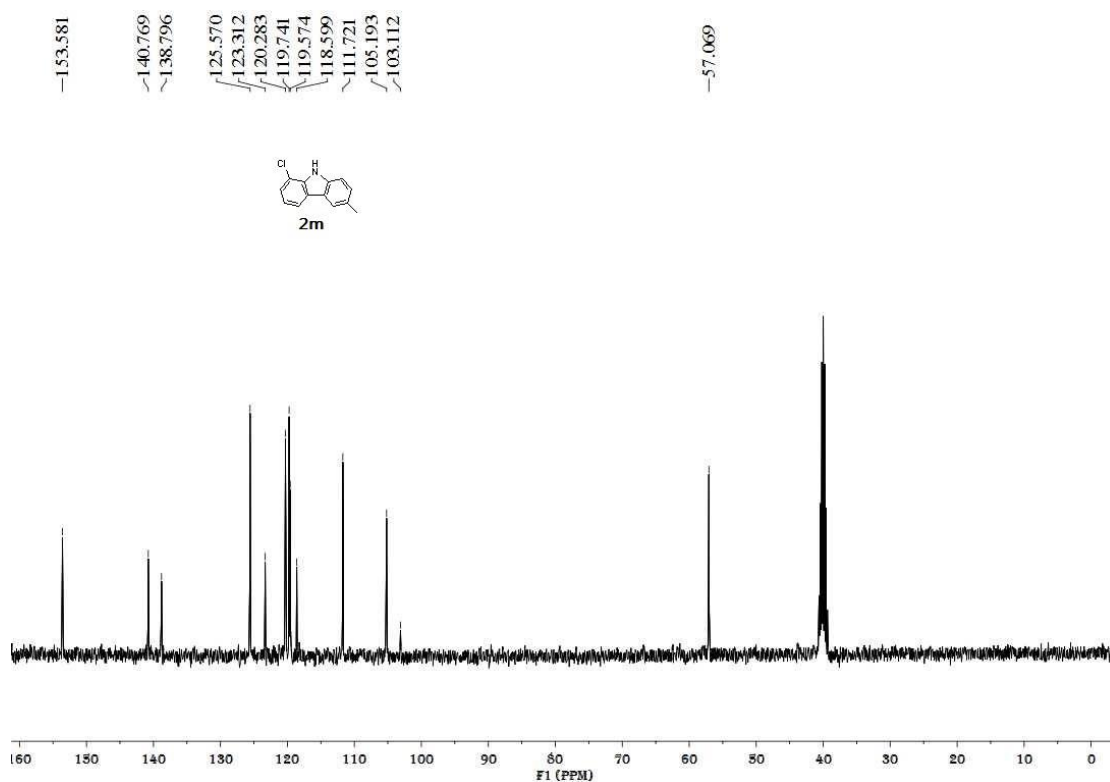
Figure S27. ^{1}H NMR spectrum of **2n**, related to **Scheme 4**
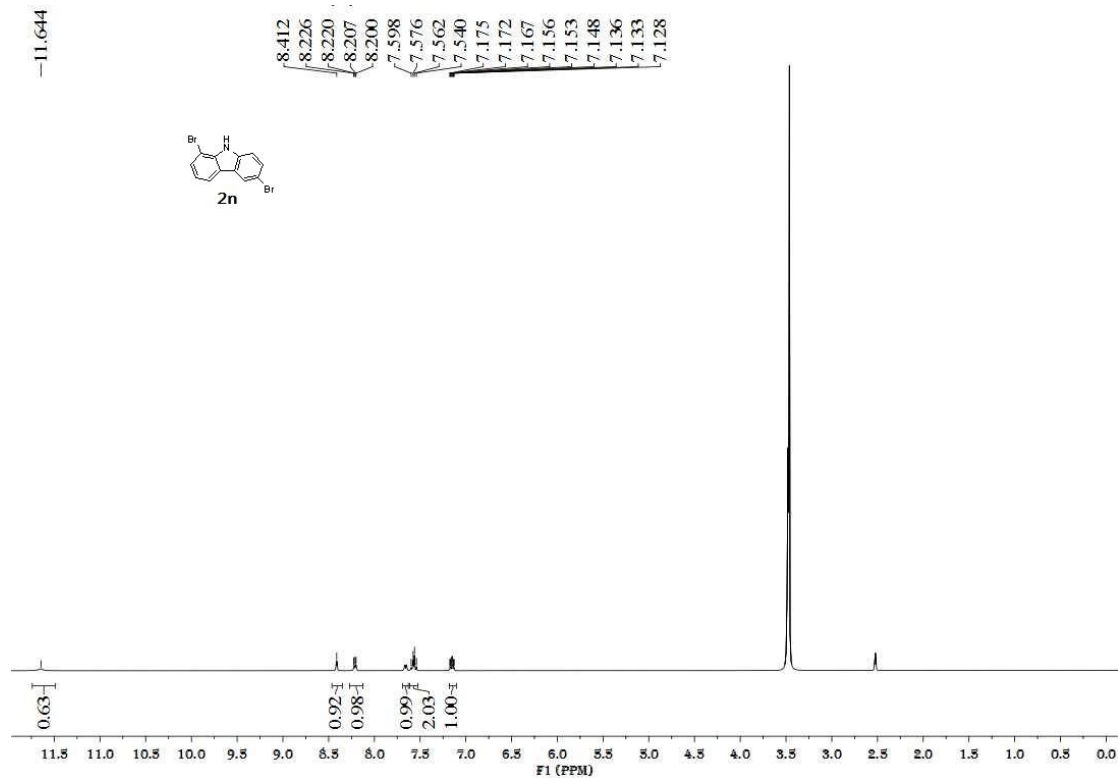
Figure S28. ^{13}C NMR spectrum of **2n**, related to **Scheme 4**
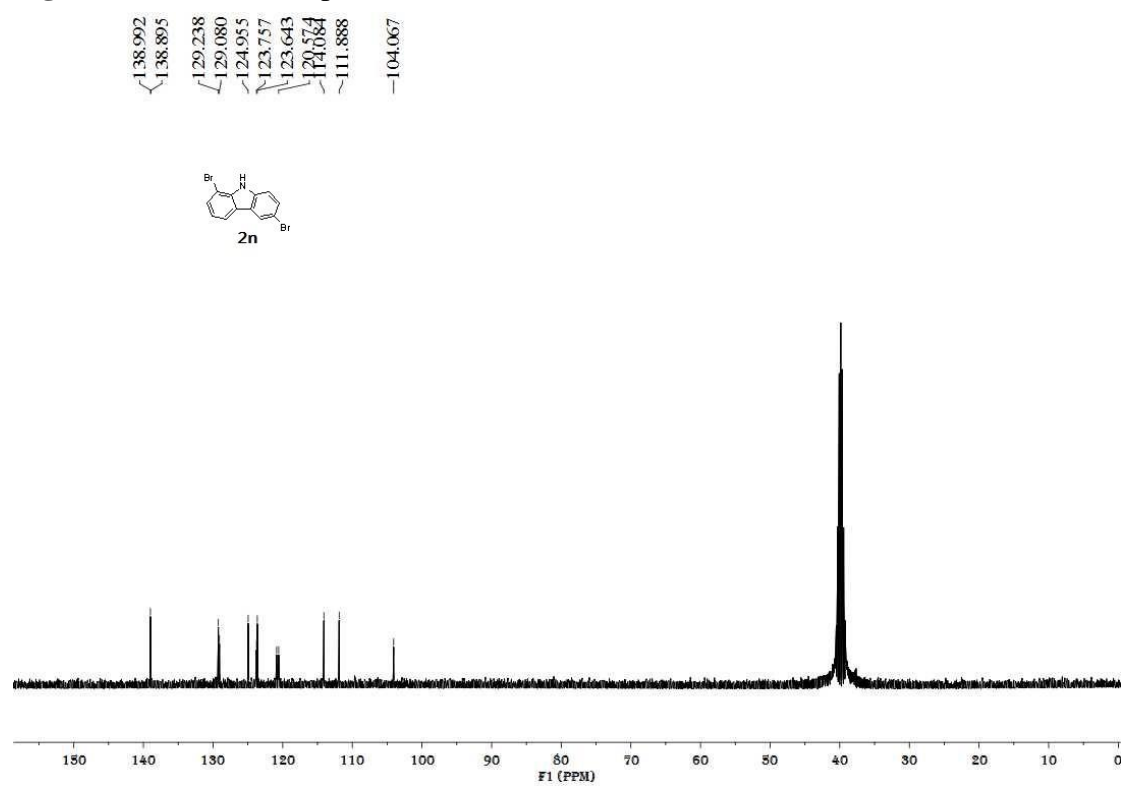
Figure S29. ^{1}H NMR spectrum of **2o**, related to **Scheme 4**

8.103, 8.083, 7.851, 7.628, 7.623, 7.469, 7.451, 7.433, 7.431, 7.365, 7.344, 7.282, 7.272, 7.260, 7.138, 7.132, 7.116, 7.110

3.980

2o
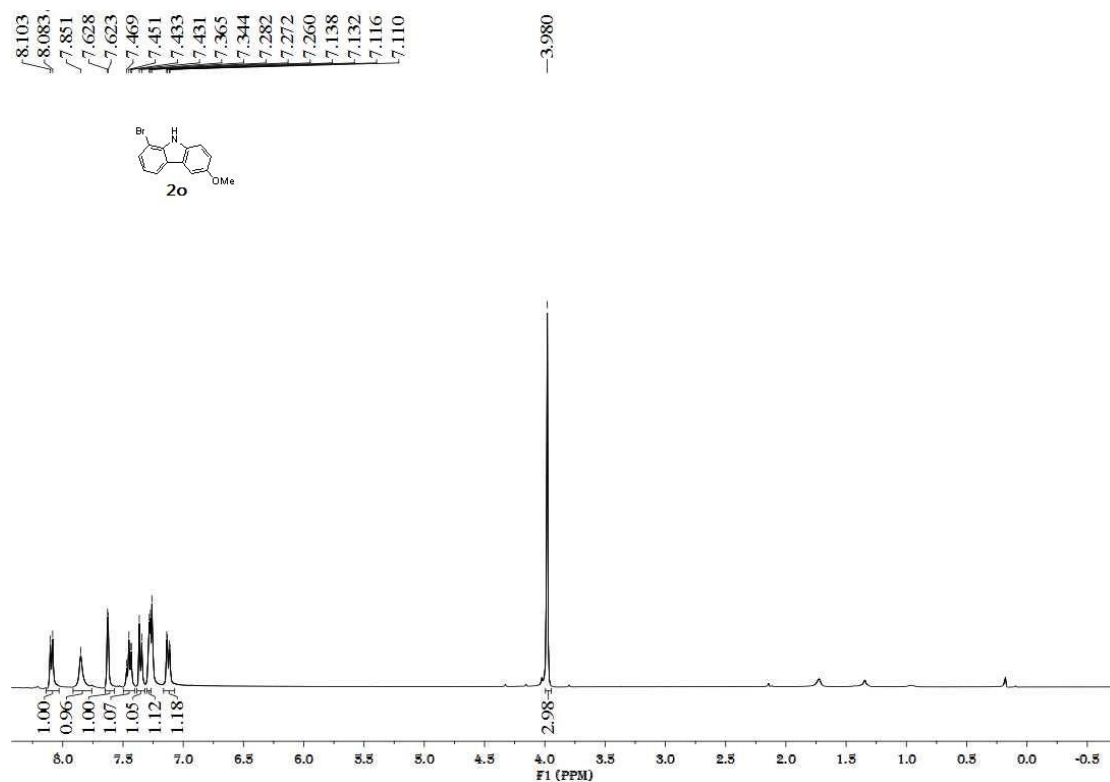
Figure S30. ^{13}C NMR spectrum of **2o**, related to **Scheme 4**

144.902, 139.122, 130.824, 126.273, 123.285, 123.056, 122.436, 119.460, 110.773, 107.291, 106.740
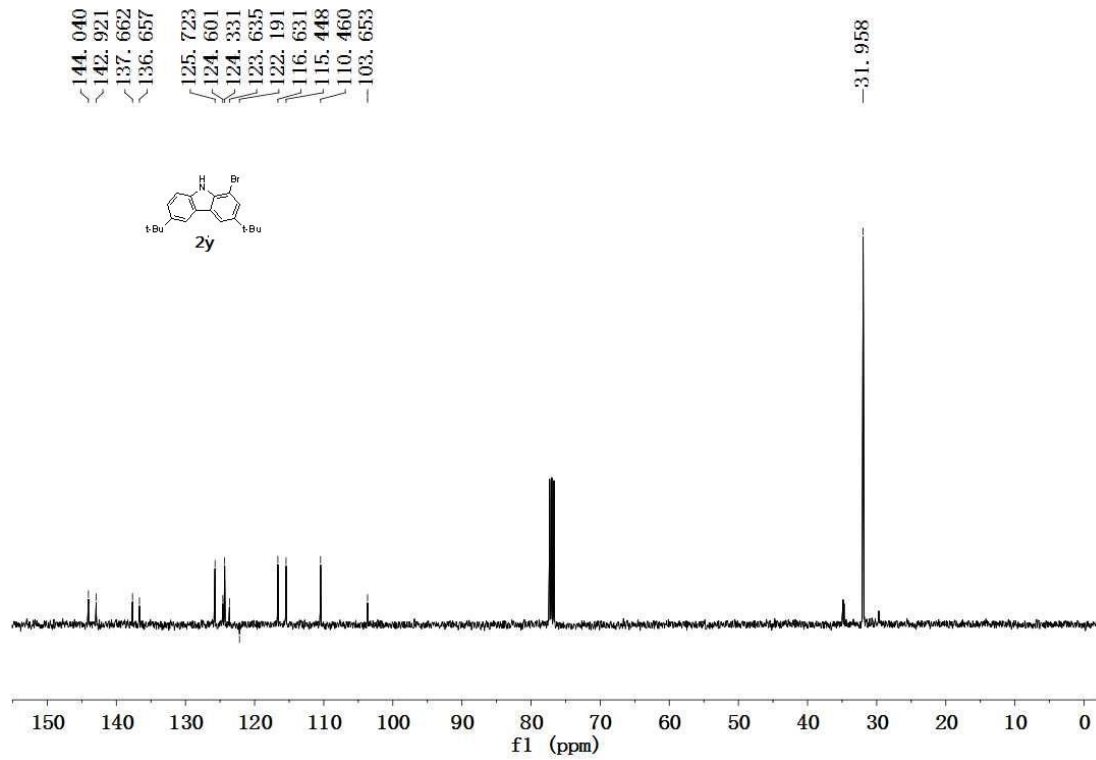
55.767

2o

Figure S31. ^{1}H NMR spectrum of **2p**, related to **Scheme 4**

Figure S32. ^{13}C NMR spectrum of **2p**, related to **Scheme 4**

Figure S33. ^{1}H NMR spectrum of **2q**, related to **Scheme 4**

8.357
8.256
7.946
7.928
7.733
7.716
7.621
7.603
7.288
7.267
7.175
7.156
7.137

2q

0.99
1.06
1.04
0.99
0.98
1.18
1.00

Figure S34. ^{13}C NMR spectrum of **2q**, related to **Scheme 4**

138.097
134.776
129.696
128.659
127.236
126.084
123.233
121.028
119.460
112.997
104.183
82.718

2q

Figure S35. ^{1}H NMR spectrum of **2r**, related to **Scheme 4**

Figure S36. ^{13}C NMR spectrum of **2r**, related to **Scheme 4**

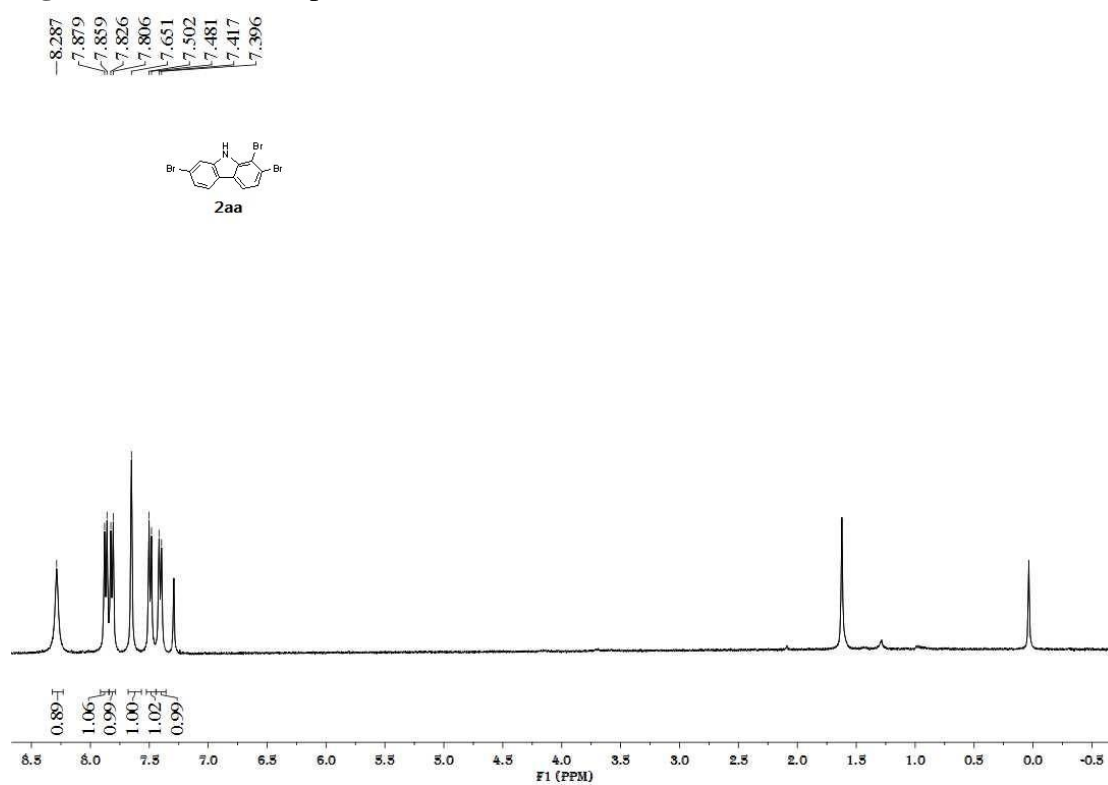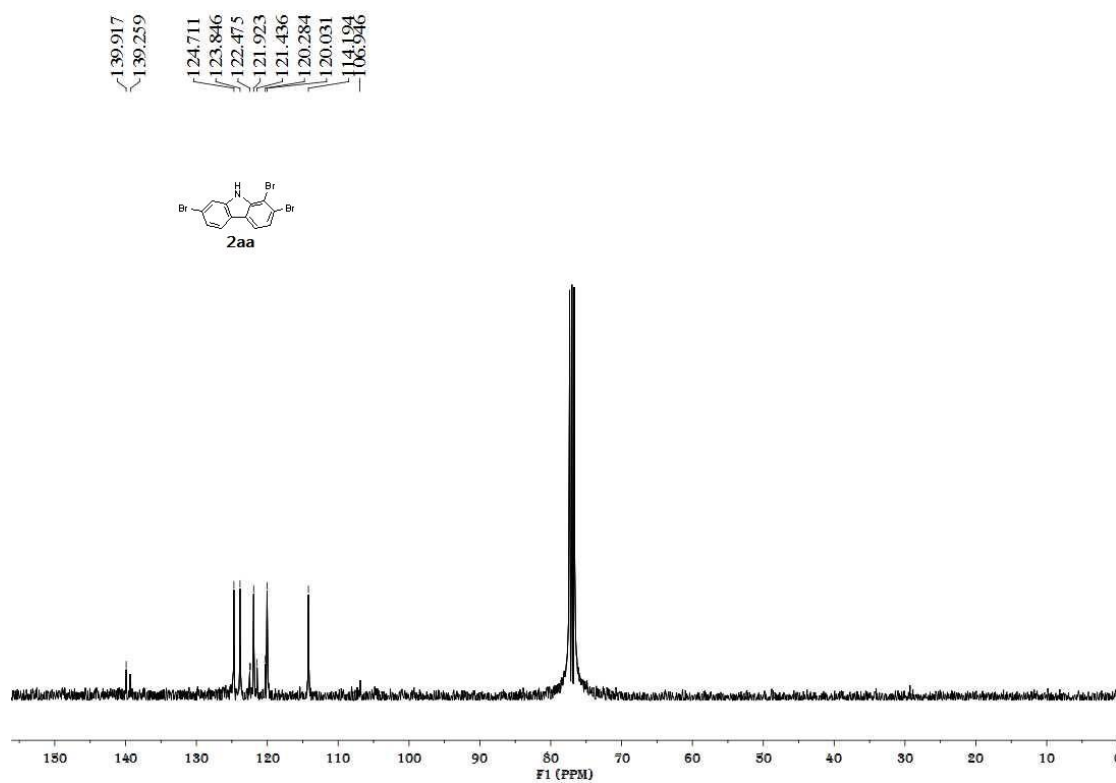**Figure S37**. ^{1}H NMR spectrum of **2s**, related to **Scheme 4**

Figure S38. ^{13}C NMR spectrum of **2s**, related to **Scheme 4**
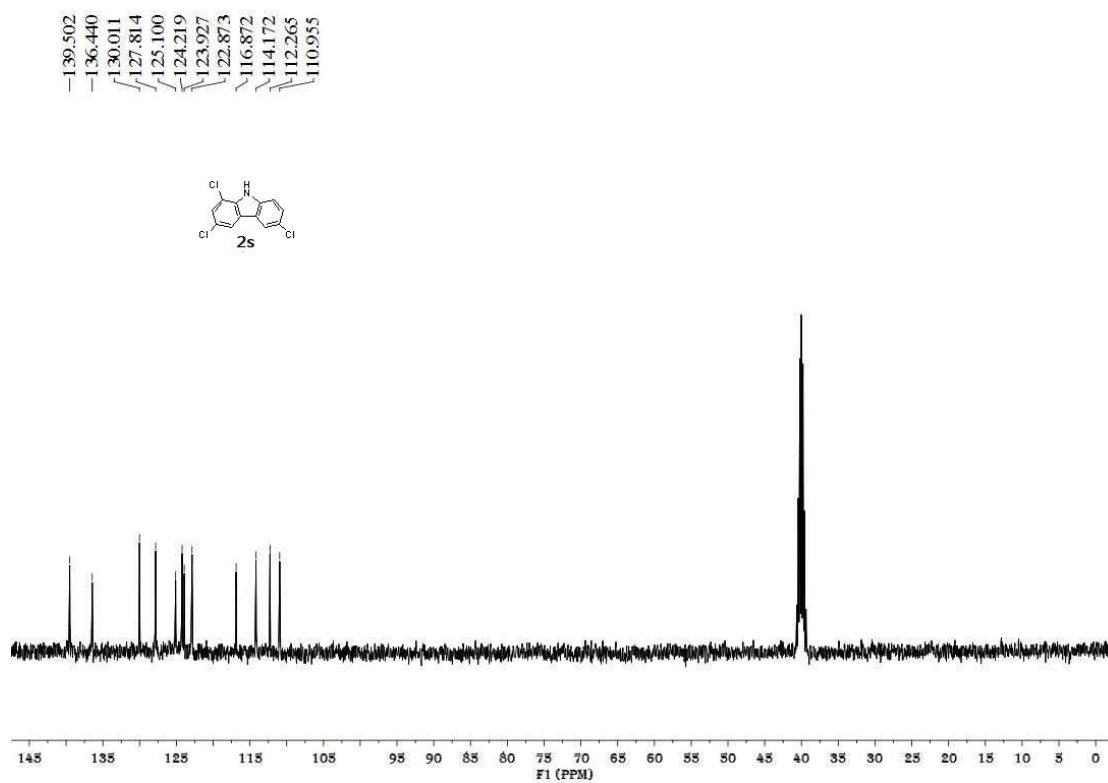
Figure S39. ^{1}H NMR spectrum of **2t**, related to **Scheme 4**
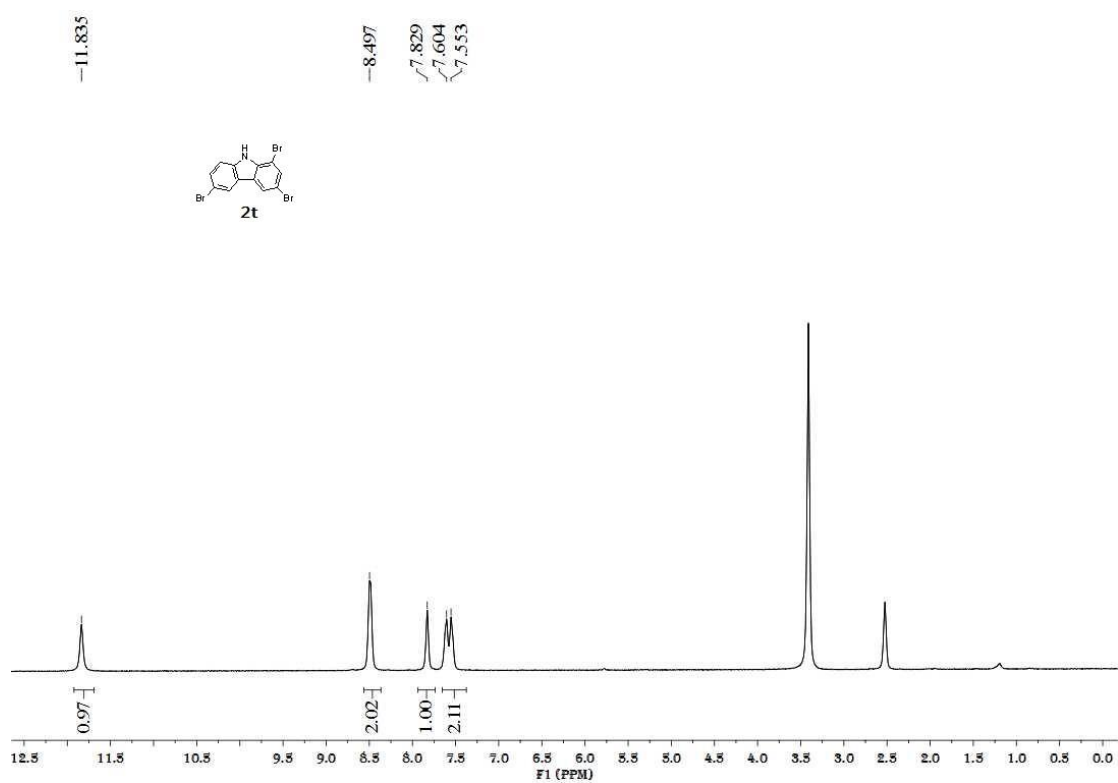
Figure S40. ^{13}C NMR spectrum of **2t**, related to **Scheme 4**
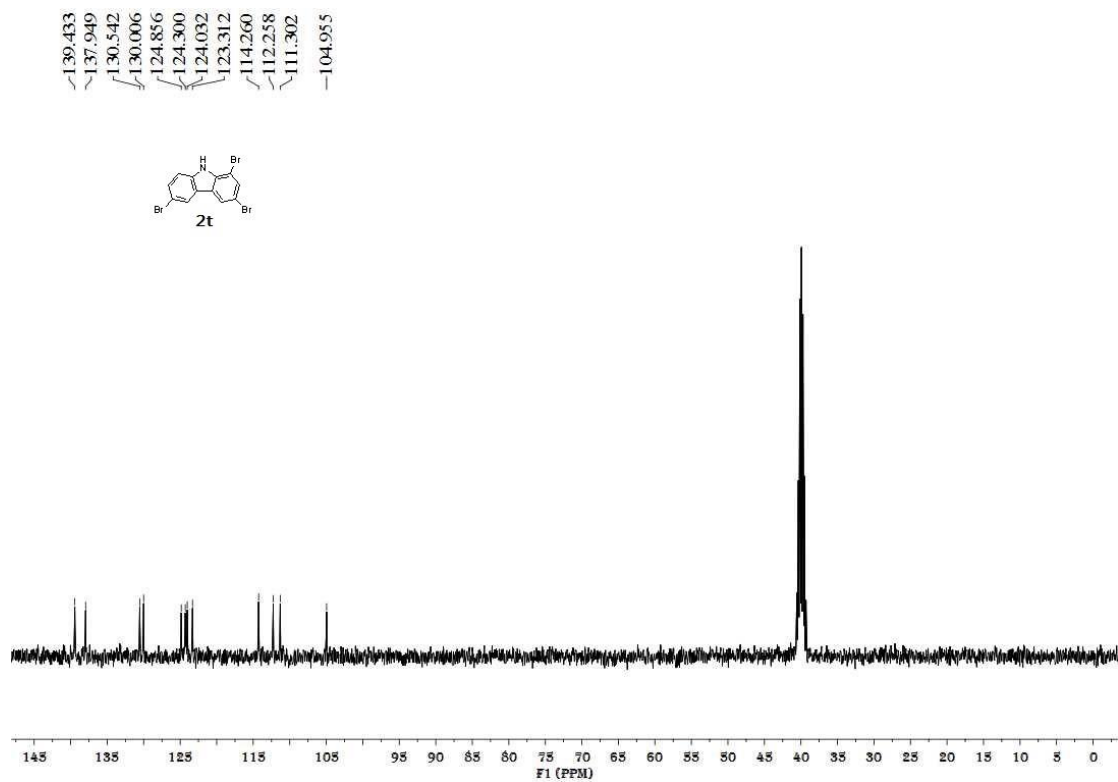
Figure S41. ^{1}H NMR spectrum of **2u**, related to **Scheme 4**
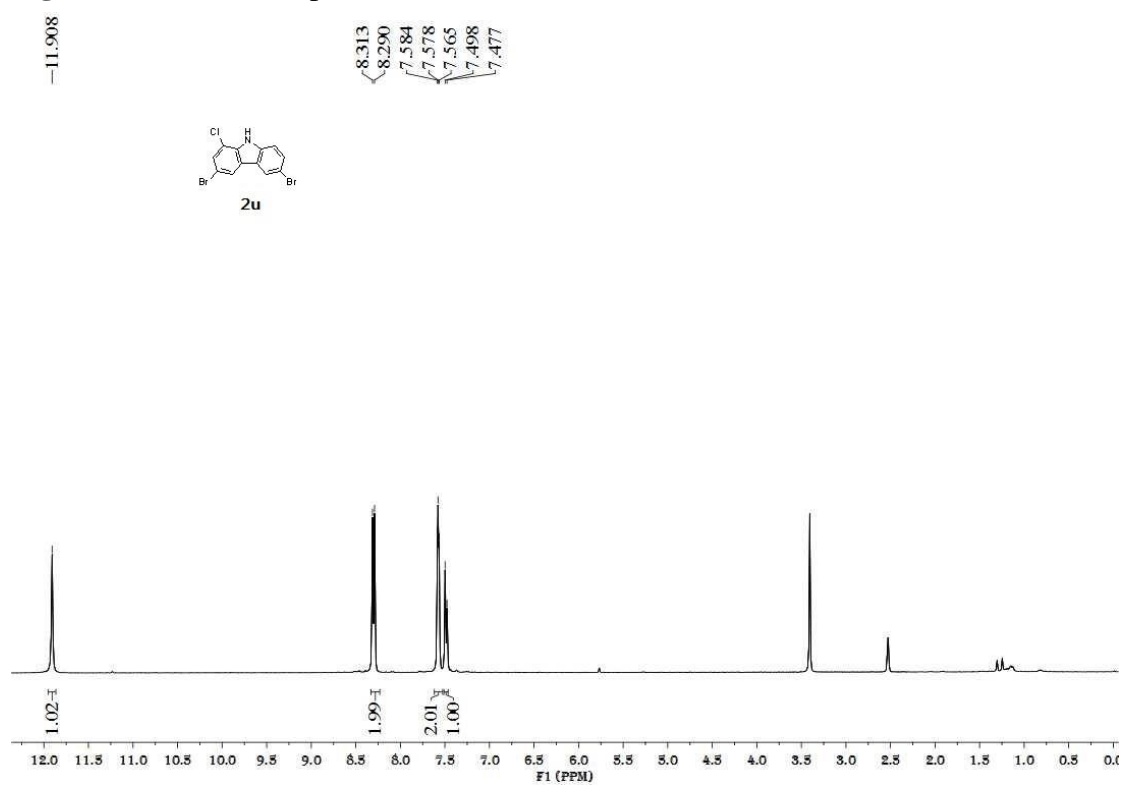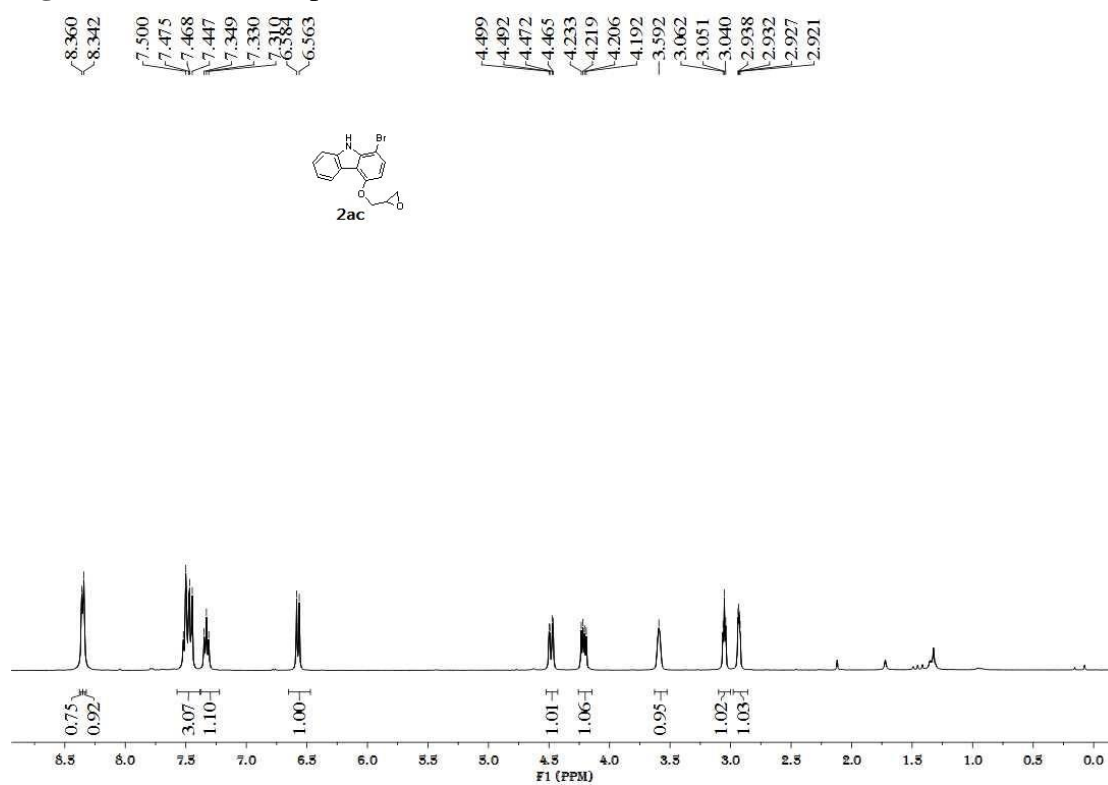

Figure S42. ^{13}C NMR spectrum of **2u**, related to **Scheme 4**
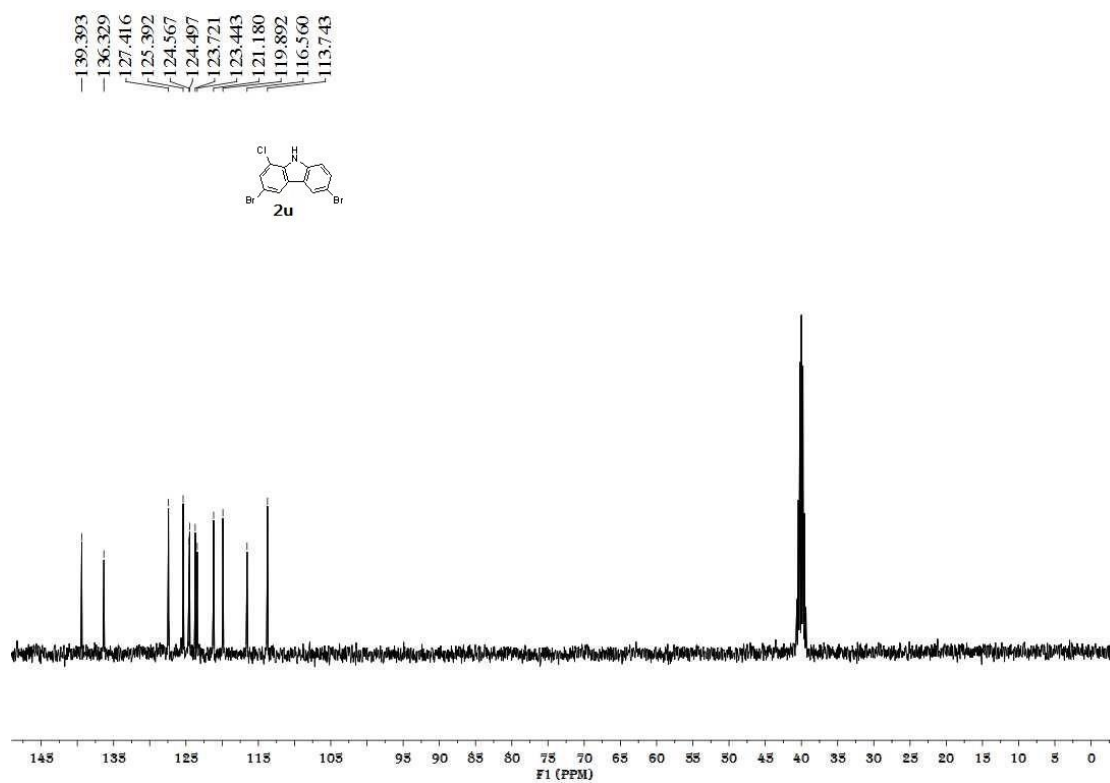
Figure S43. ^{1}H NMR spectrum of **2v**, related to **Scheme 4**
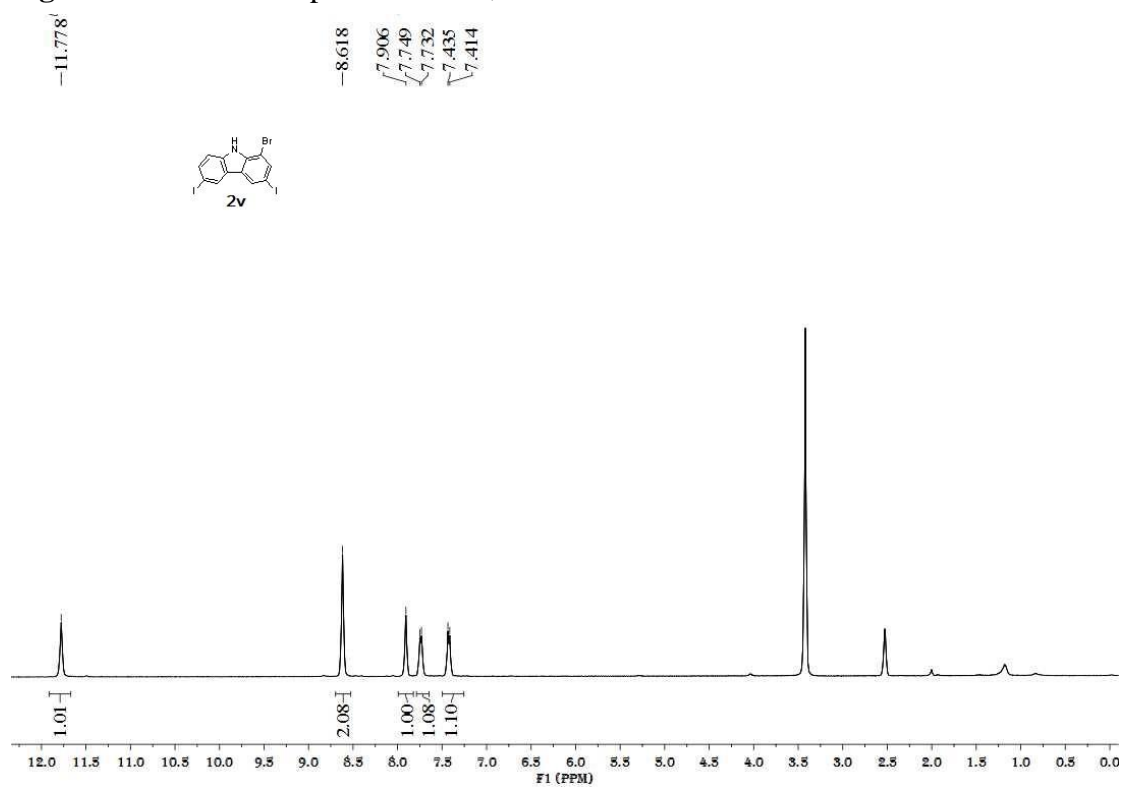
Figure S44. ^{13}C NMR spectrum of **2v**, related to **Scheme 4**
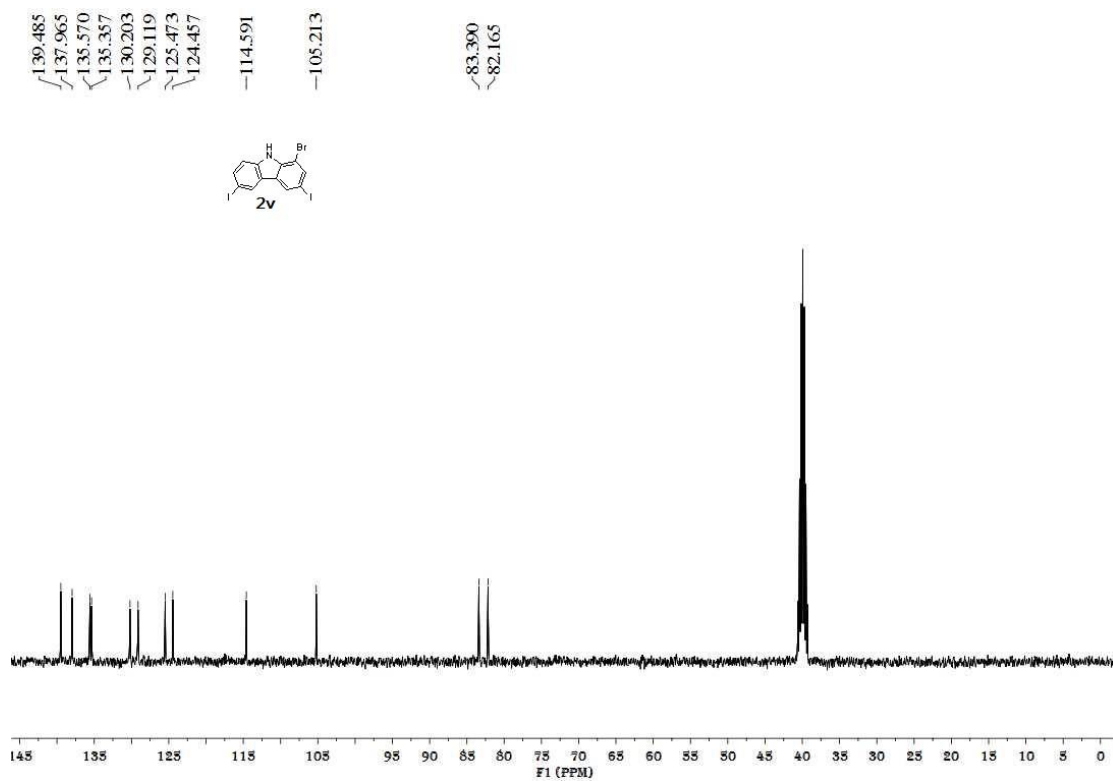
Figure S45. ¹H NMR spectrum of **2w**, related to **Scheme 4**
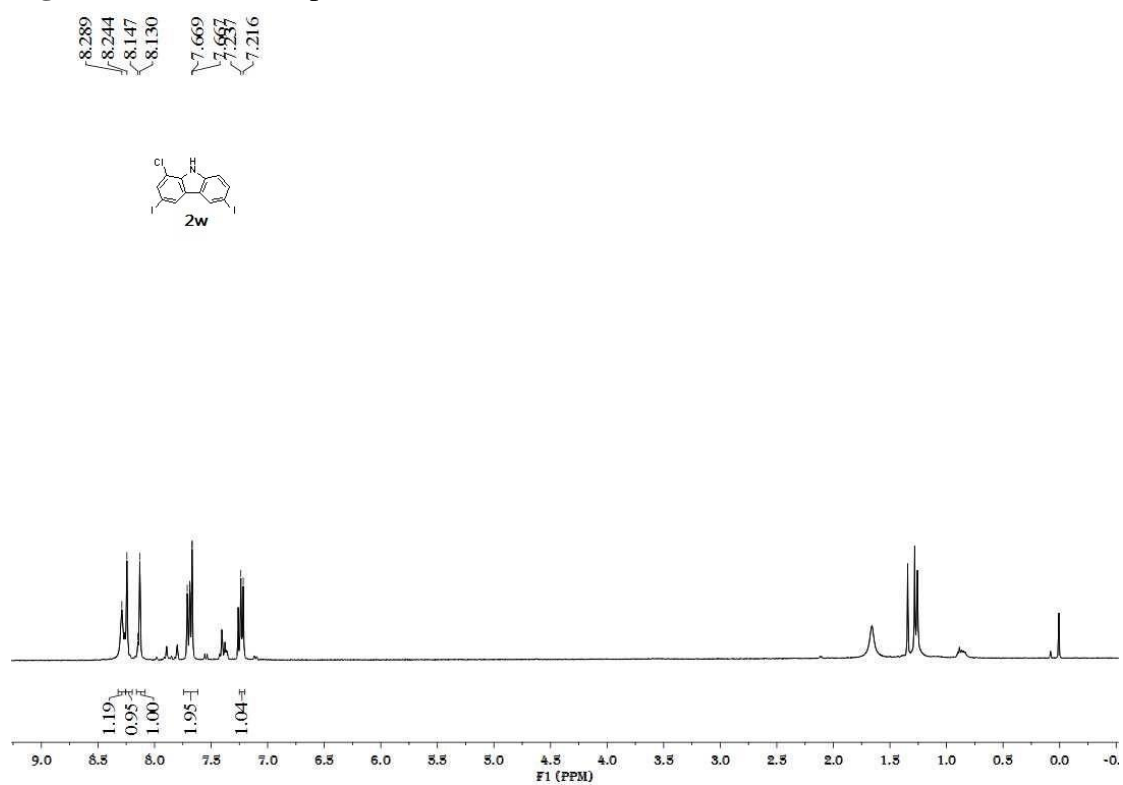
Figure S46. ¹³C NMR spectrum of **2w**, related to **Scheme 4**
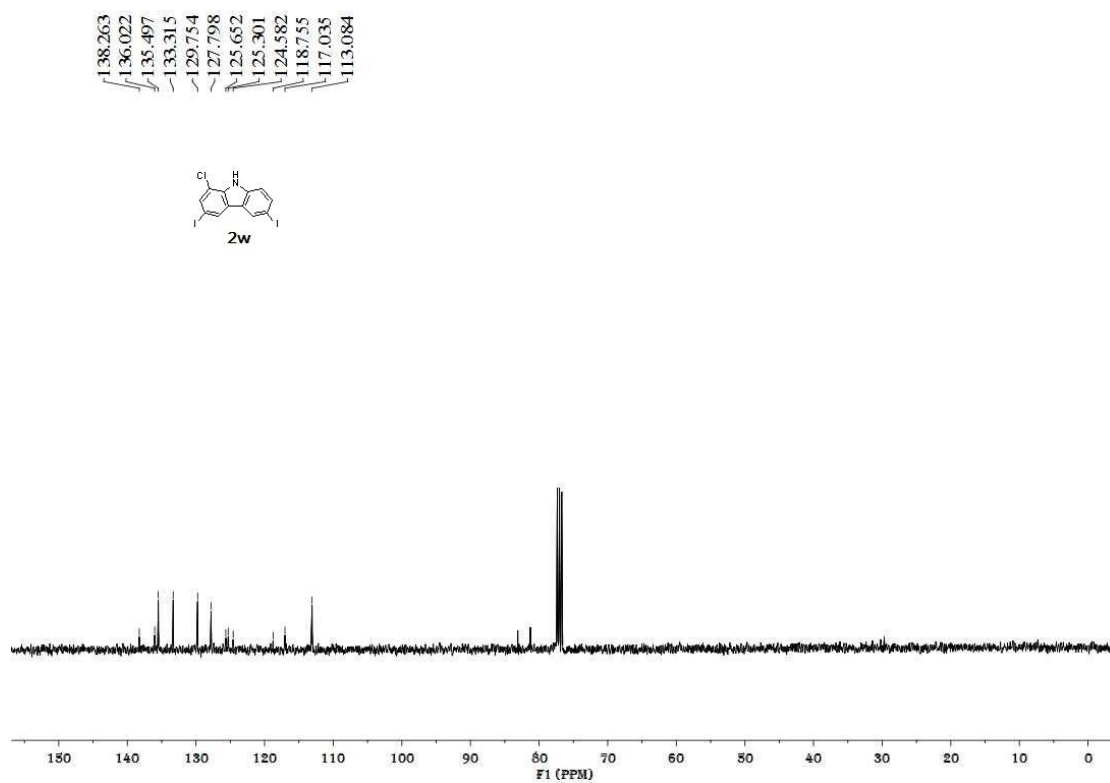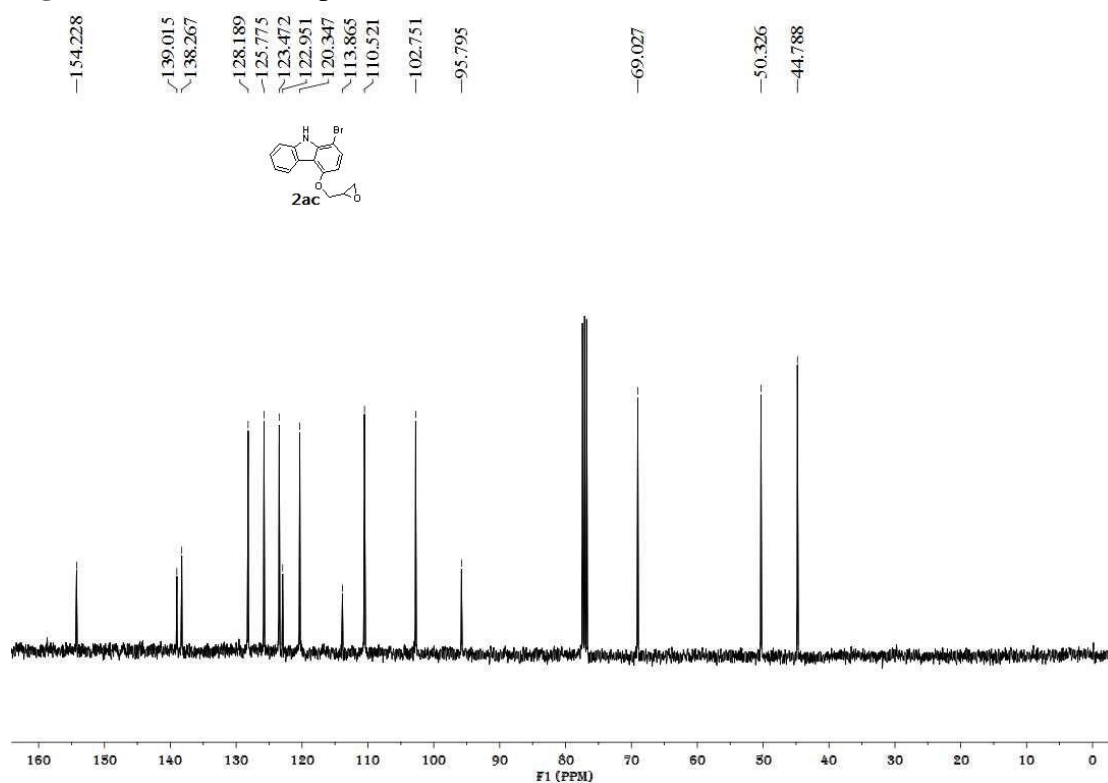
Figure S47. ^{1}H NMR spectrum of **2x**, related to **Scheme 4**
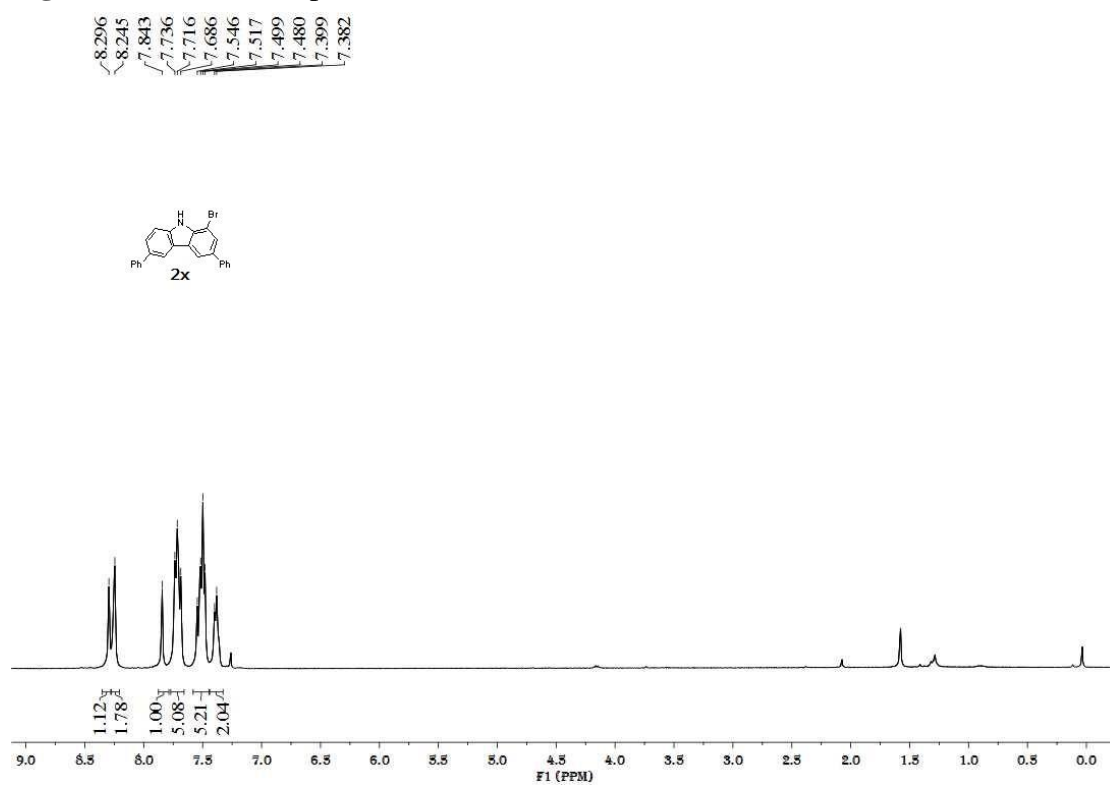
Figure S48. ^{13}C NMR spectrum of **2x**, related to **Scheme 4**
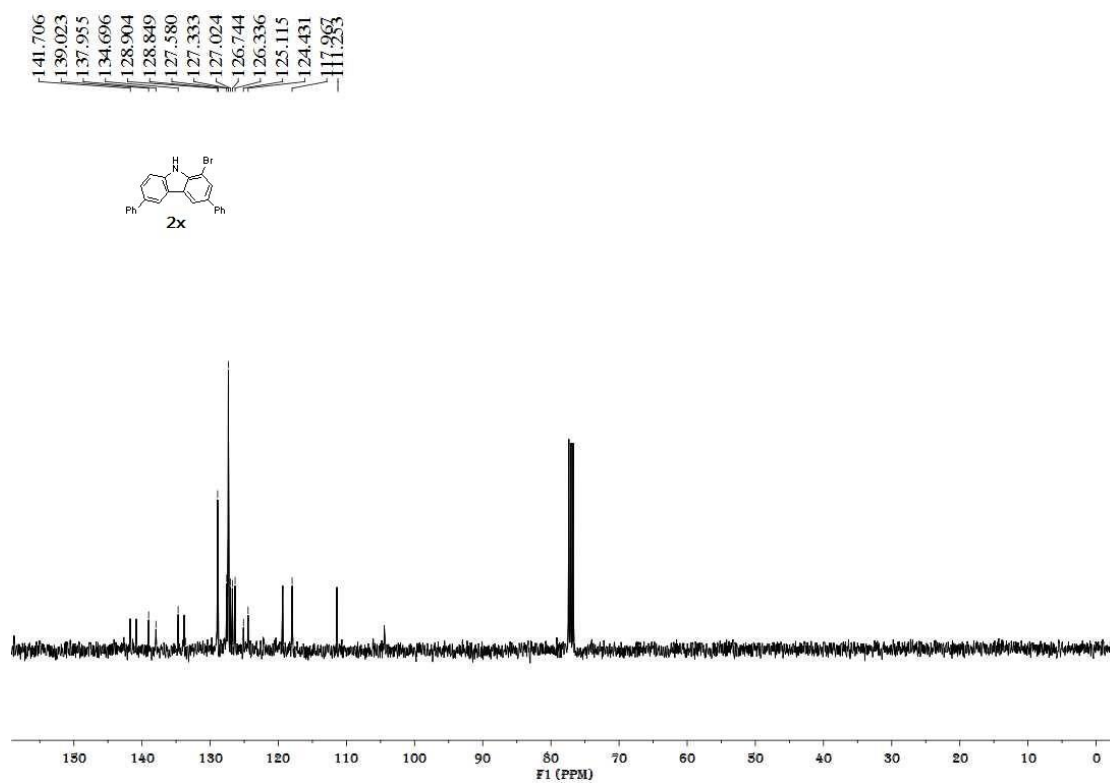
Figure S49. ^{1}H NMR spectrum of **2y**, related to **Scheme 4**
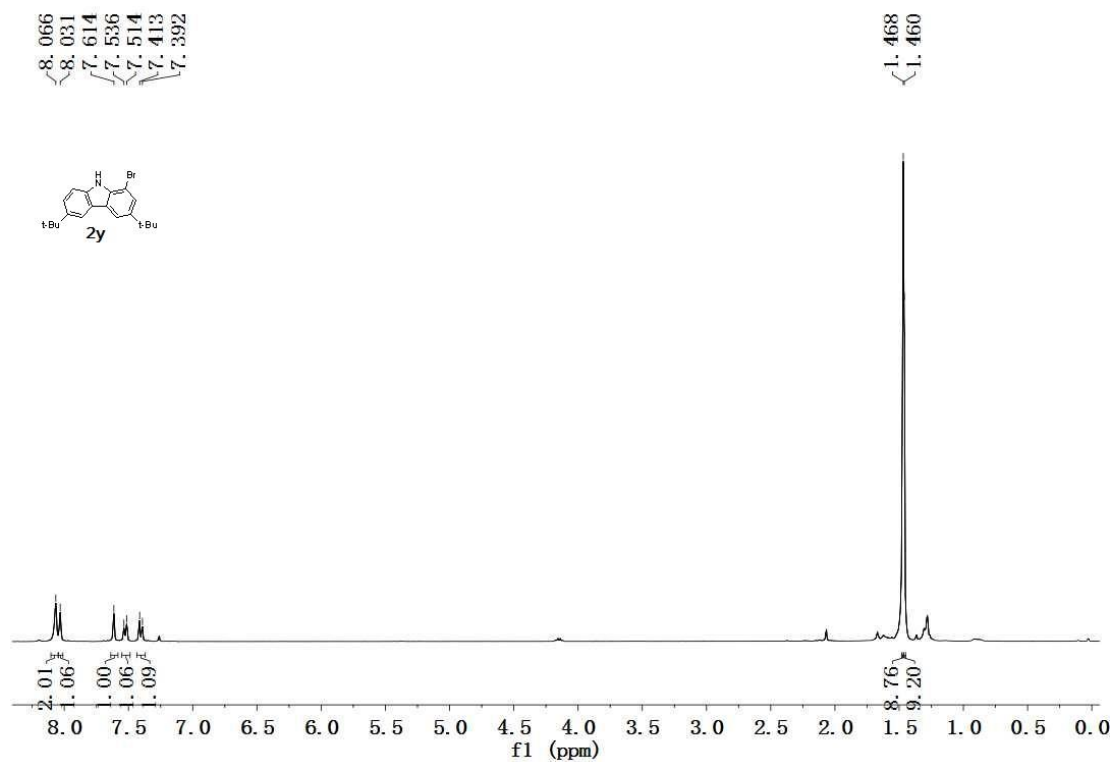
Figure S50. ^{13}C NMR spectrum of **2y**, related to **Scheme 4**

Figure S51. ^{1}H NMR spectrum of **2z**, related to **Scheme 4**
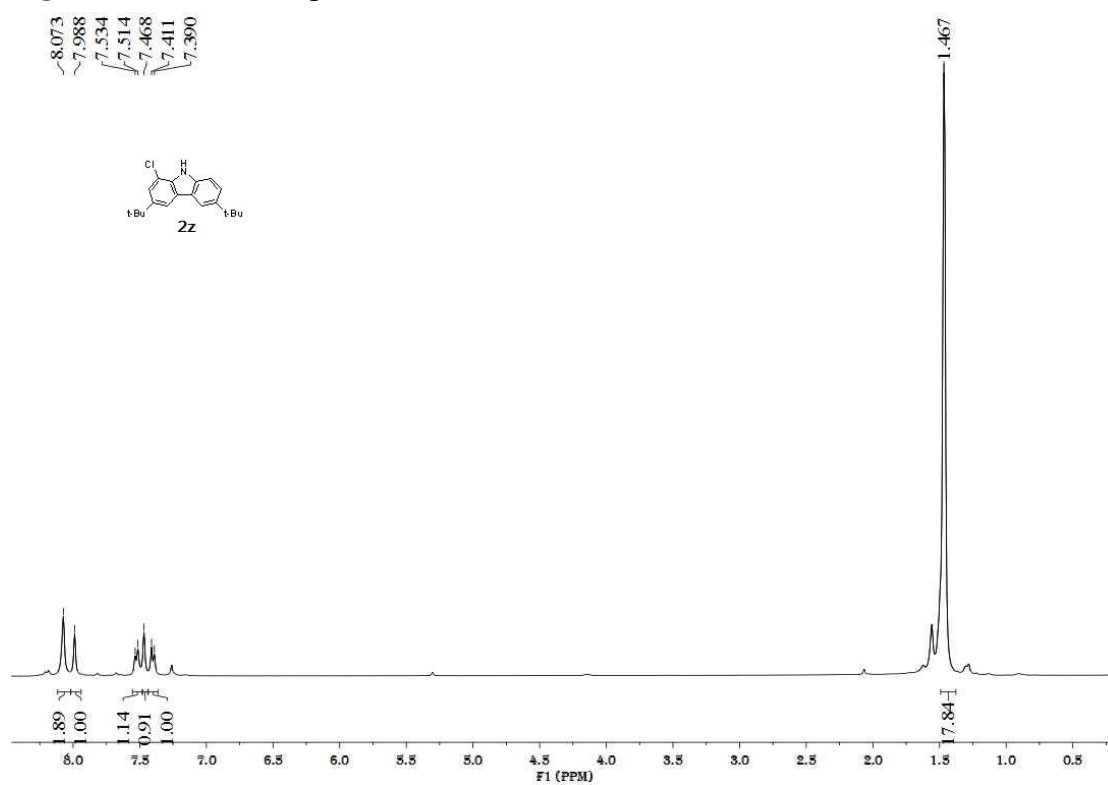
Figure S52. ^{13}C NMR spectrum of **2z**, related to **Scheme 4**
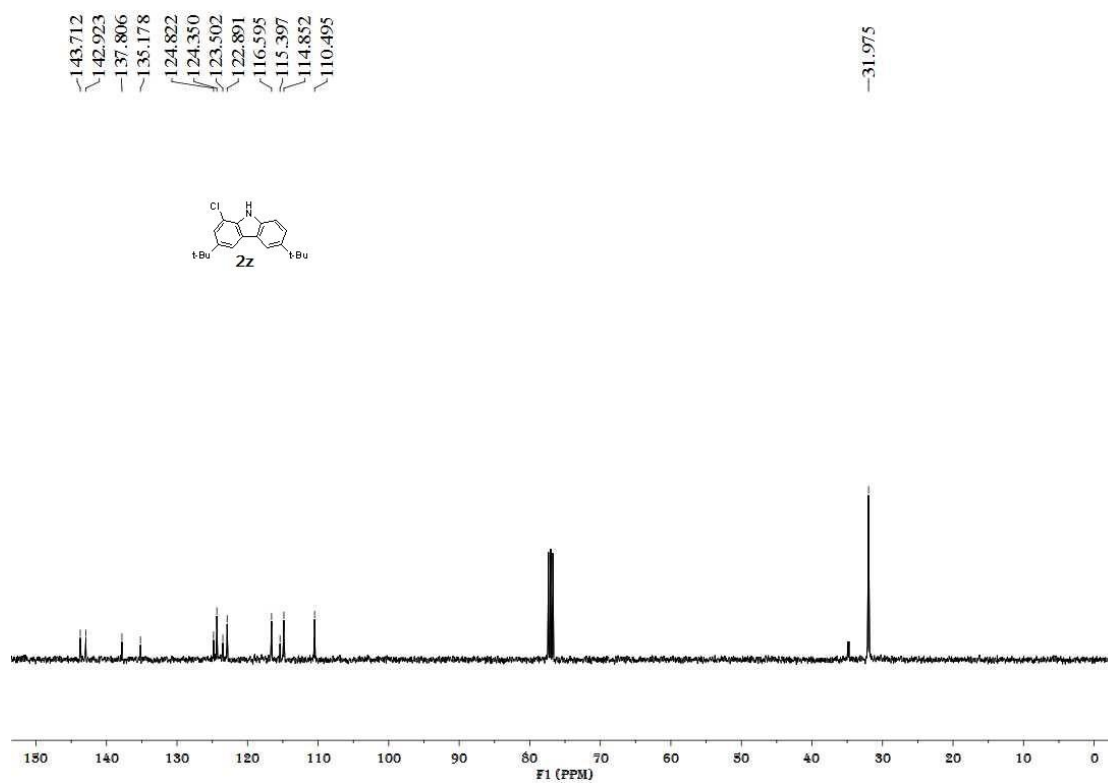
Figure S53. ^{1}H NMR spectrum of **2aa**, related to **Scheme 4**

Figure S54. ^{13}C NMR spectrum of **2aa**, related to **Scheme 4**

Figure S55. ^{1}H NMR spectrum of **2ab**, related to **Scheme 4**
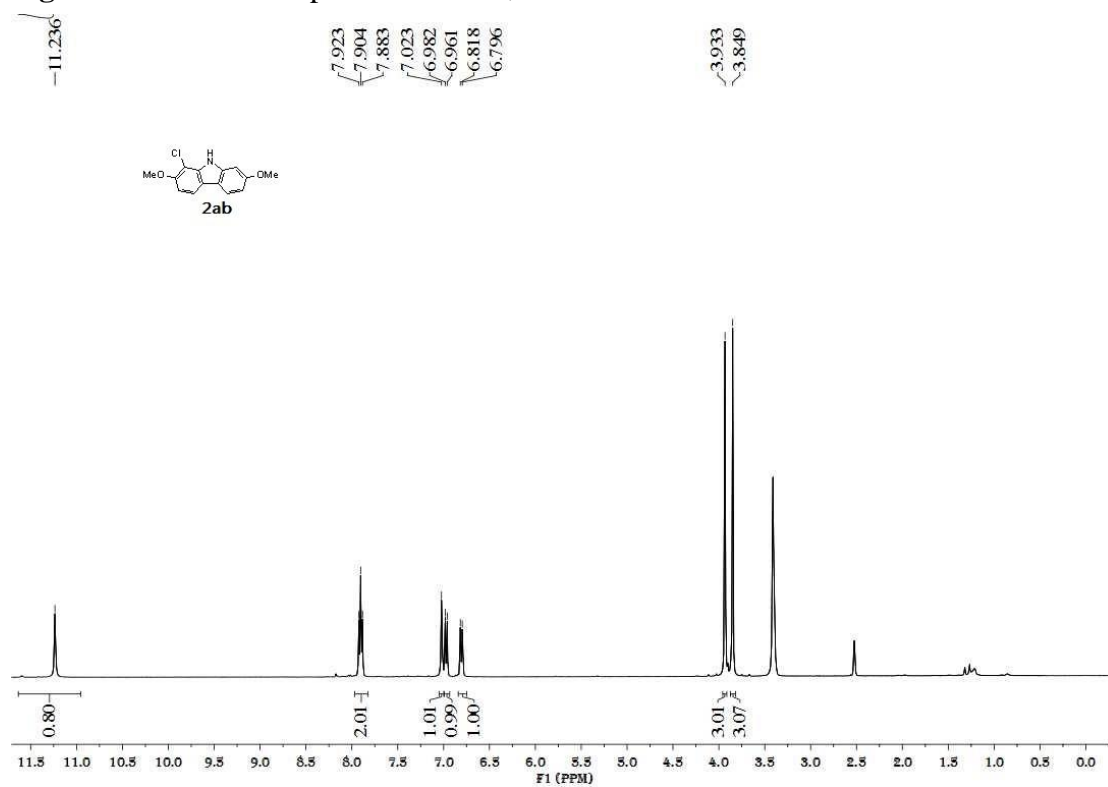
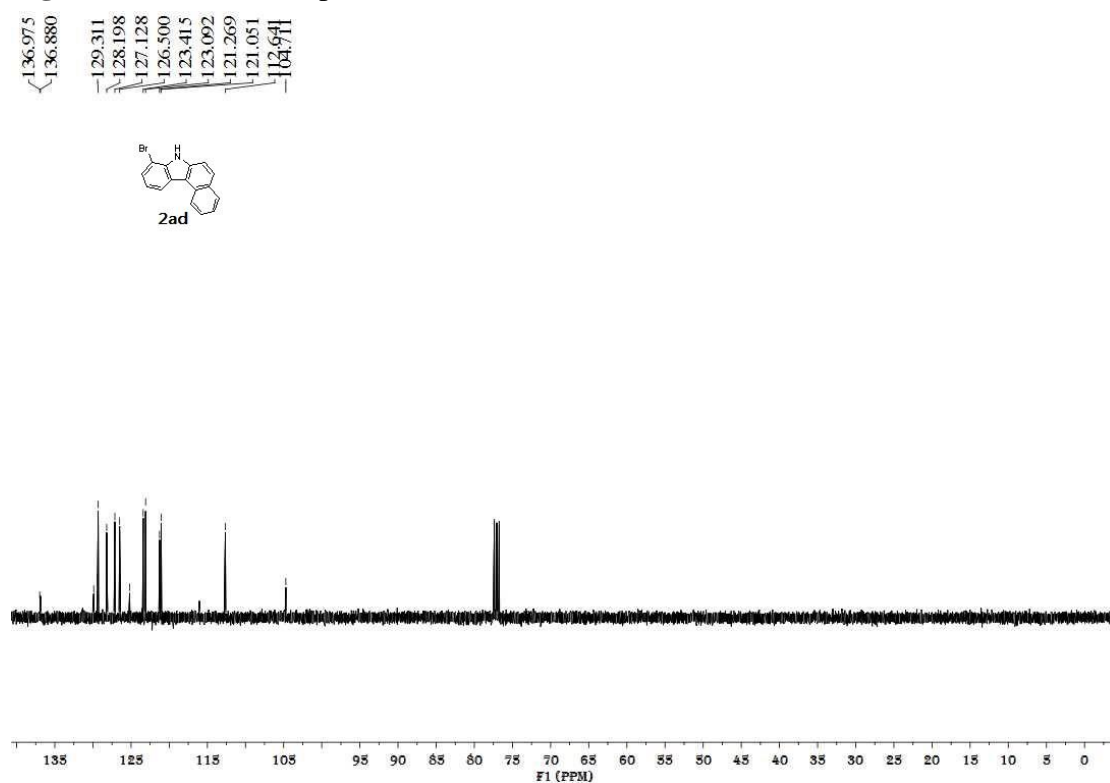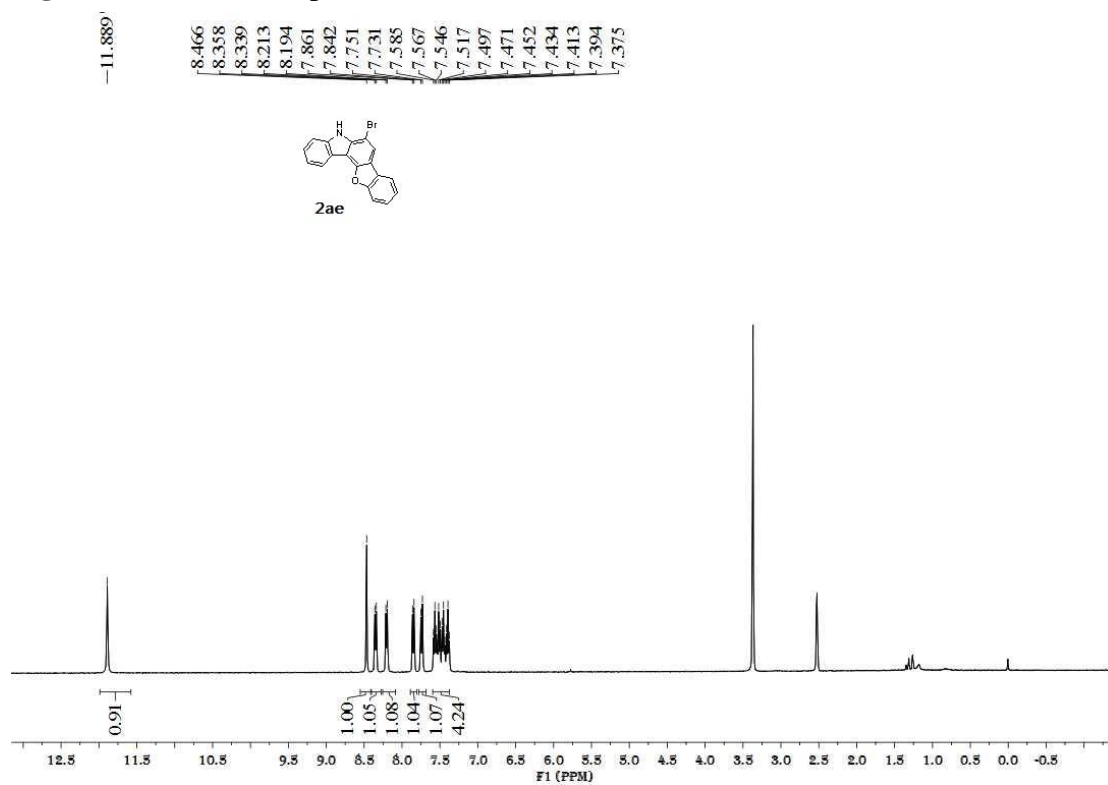**Figure S56**. ^{13}C NMR spectrum of **2ab**, related to **Scheme 4**
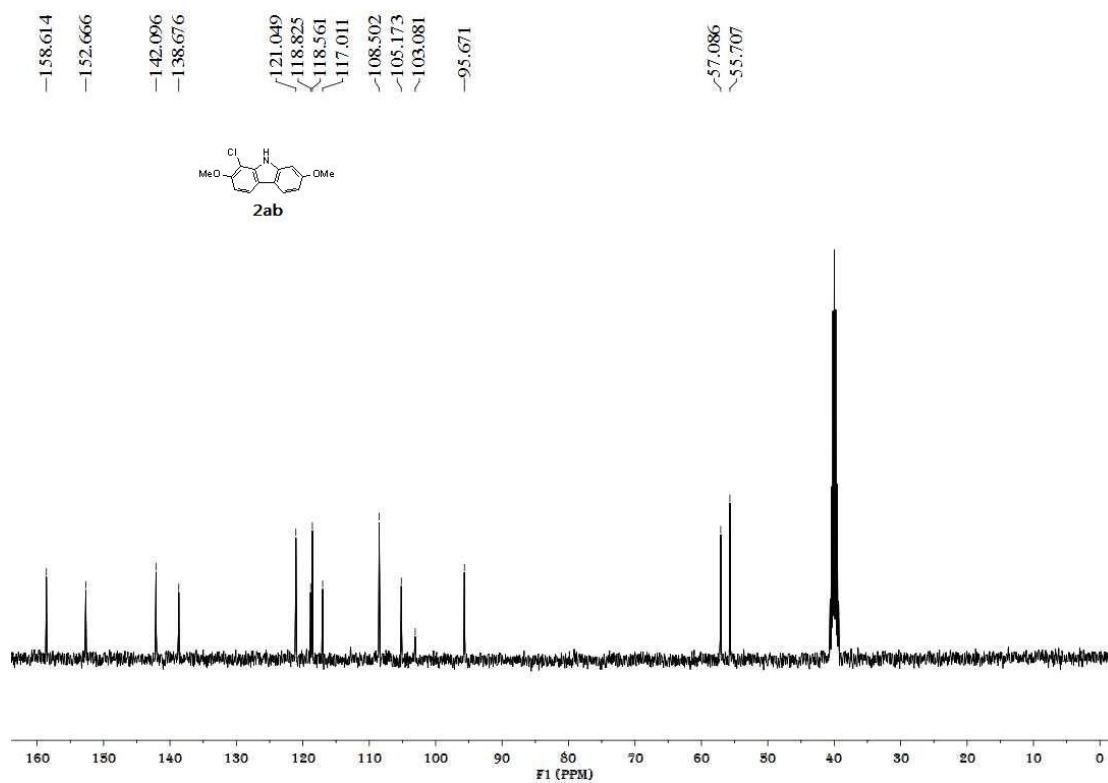
Figure S57. ^{1}H NMR spectrum of **2ac**, related to **Scheme 4**

Figure S58. ^{13}C NMR spectrum of **2ac**, related to **Scheme 4**

Figure S59. ^{1}H NMR spectrum of **2ad**, related to **Scheme 4**
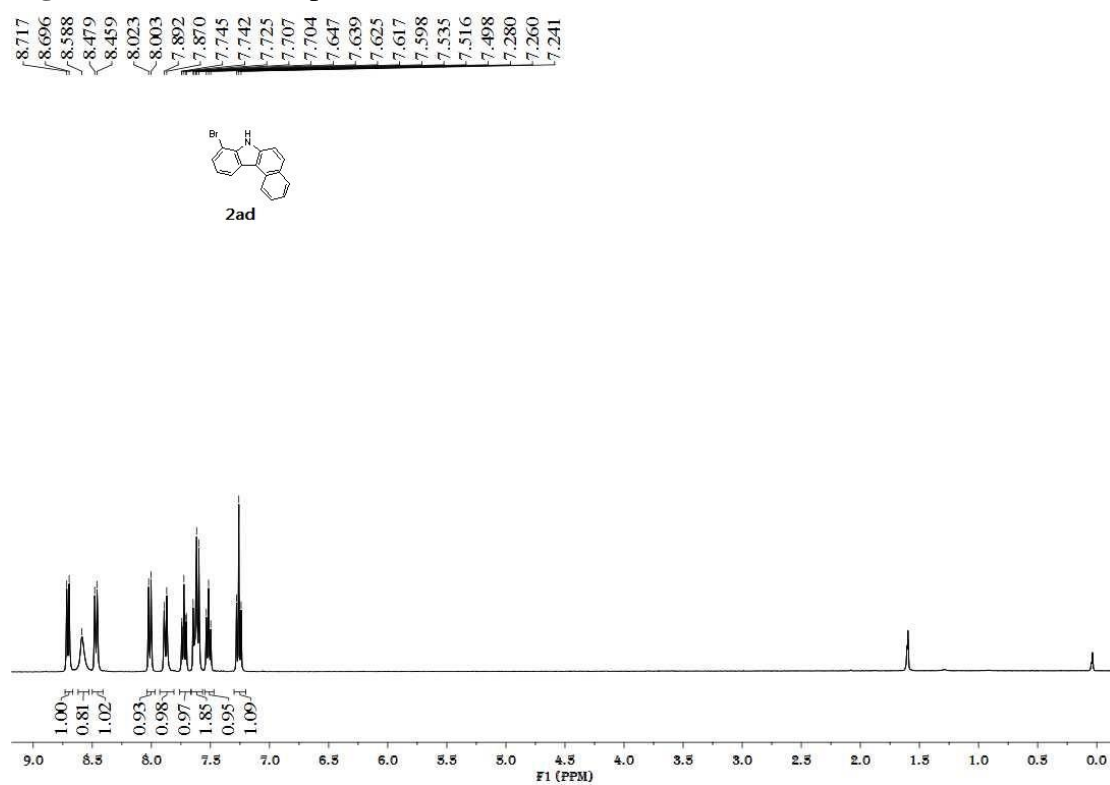
Figure S60. ^{13}C NMR spectrum of **2ad**, related to **Scheme 4**

Figure S61. ^{1}H NMR spectrum of **2ae**, related to **Scheme 4**
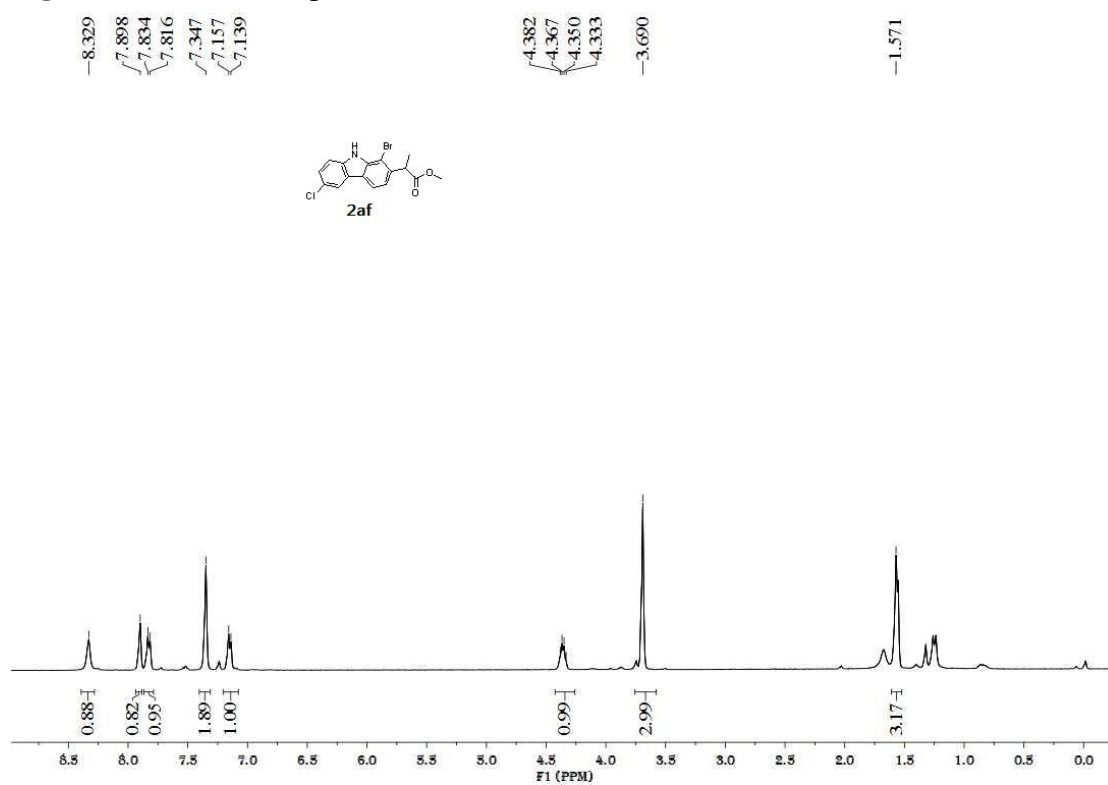

Figure S62. ^{13}C NMR spectrum of **2ae**, related to **Scheme 4**
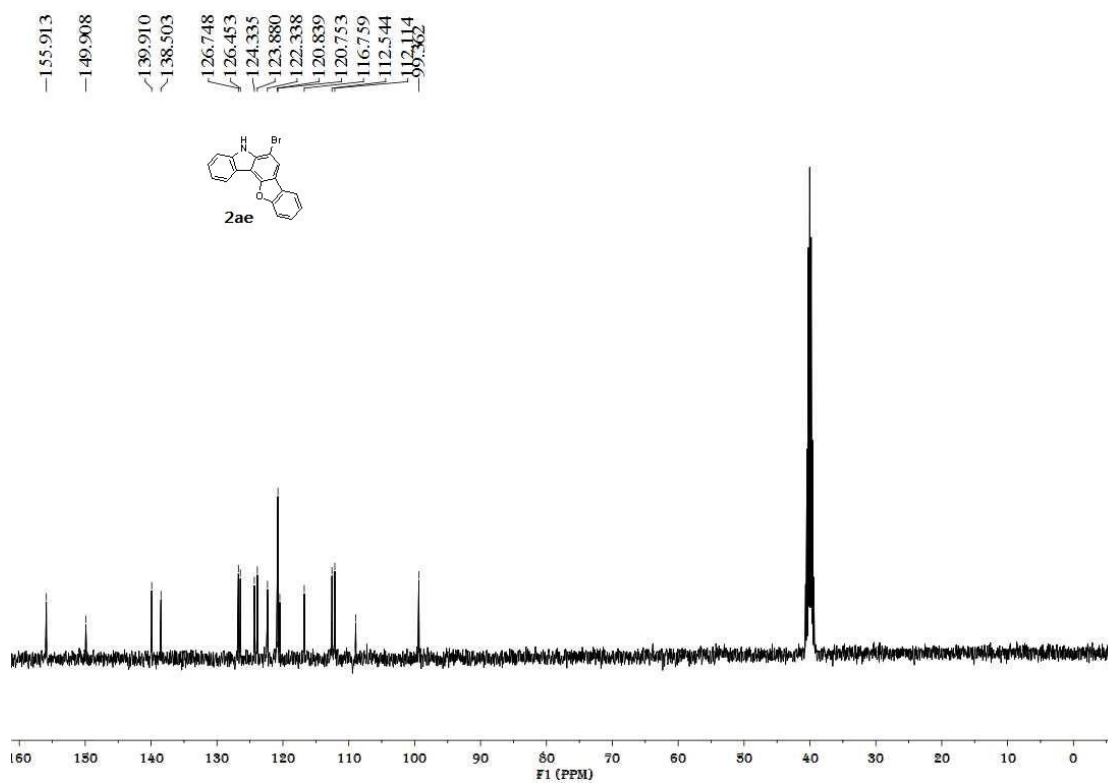
Figure S63. ¹H NMR spectrum of **2af**, related to **Scheme 4**

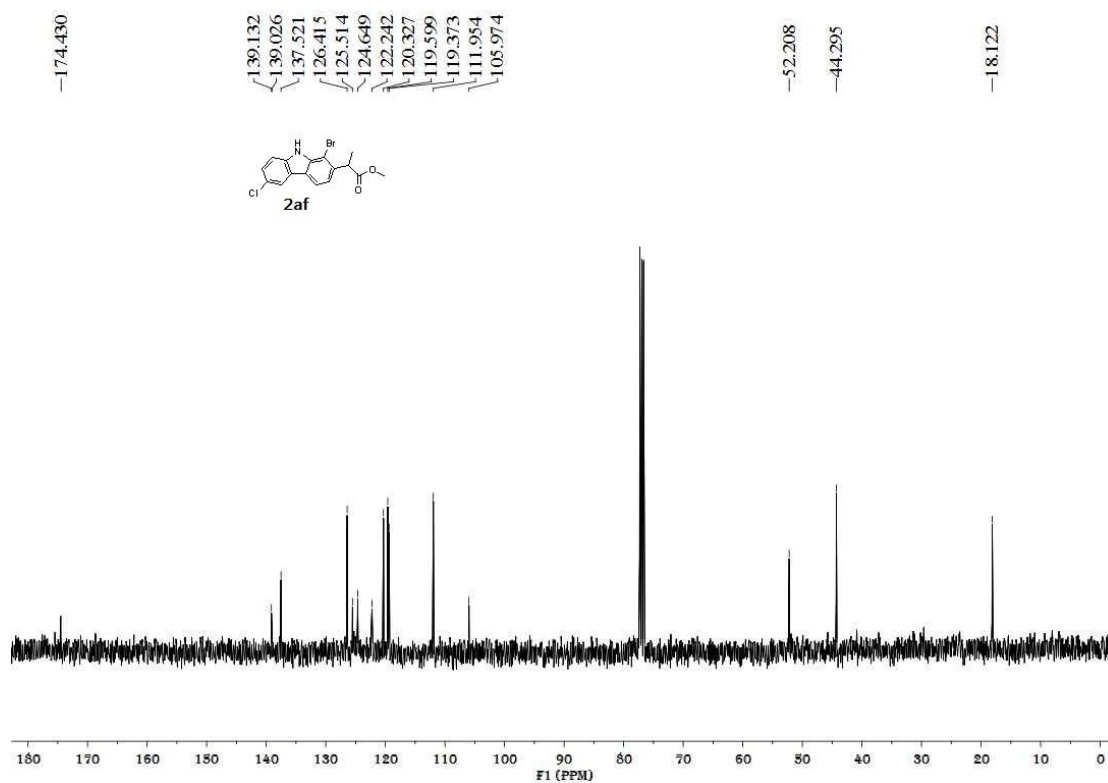**Figure S64**. ¹³C NMR spectrum of **2af**, related to **Scheme 4**

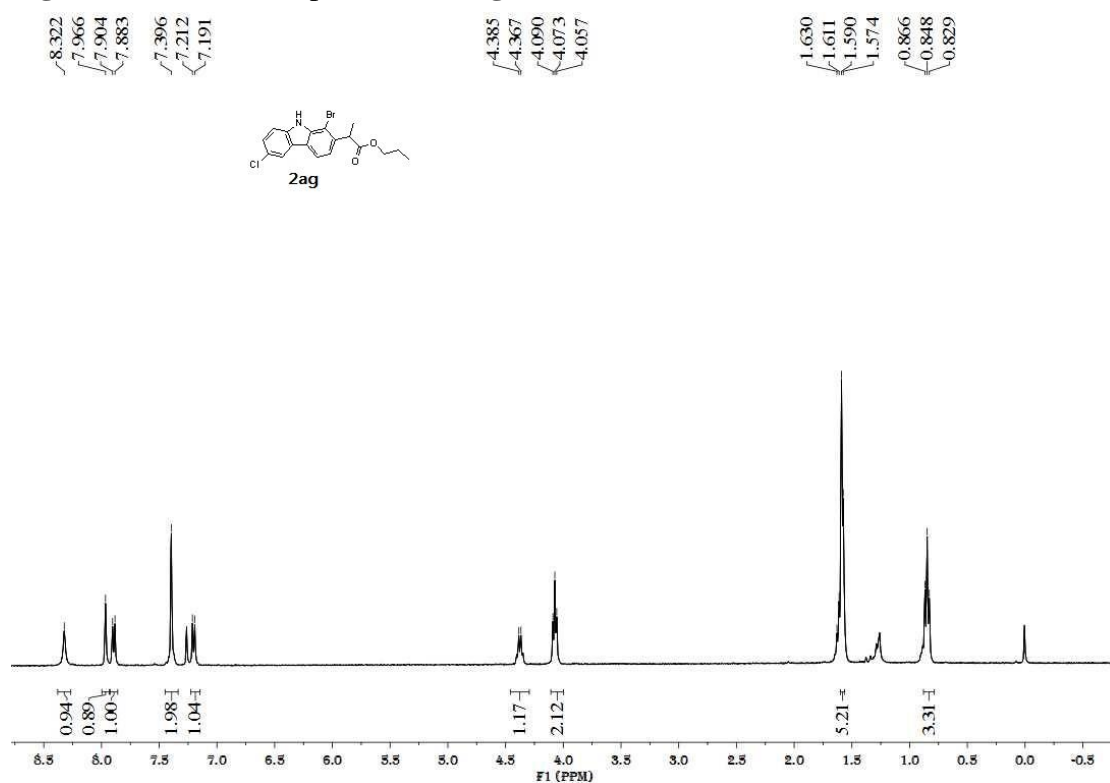**Figure S65**. ^{1}H NMR spectrum of **2ag**, related to **Scheme 4**

Figure S66. ^{13}C NMR spectrum of **2ag**, related to **Scheme 4**
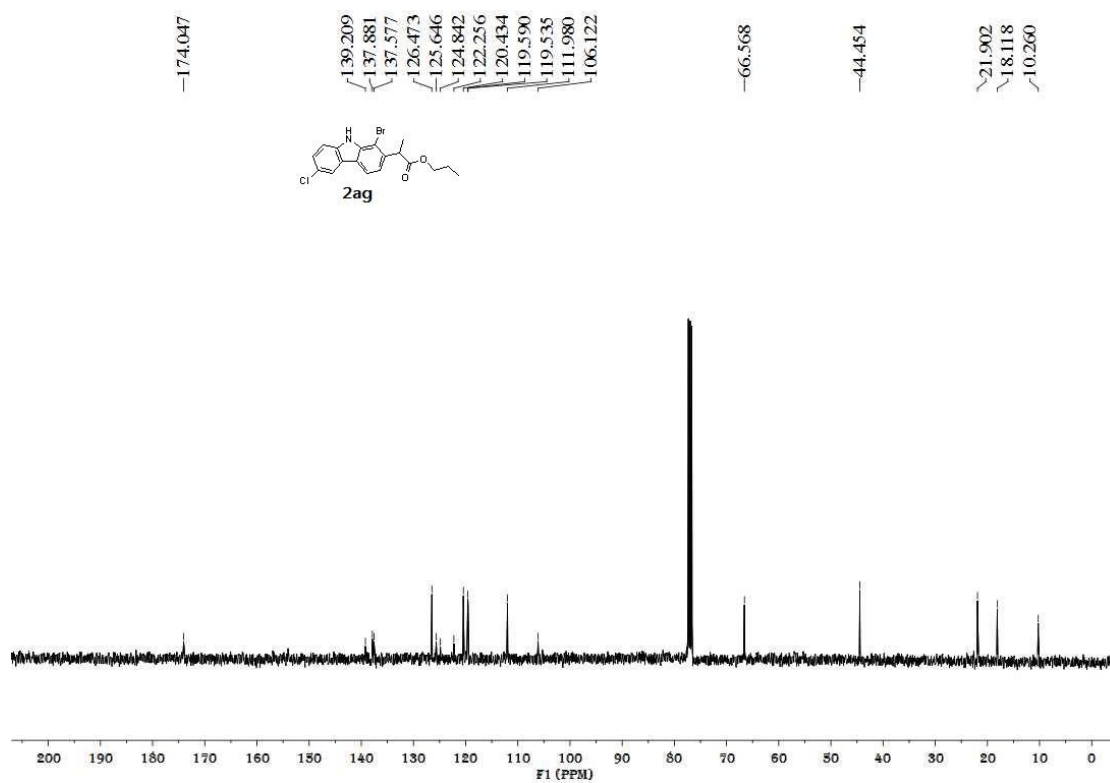
Figure S67. ^{1}H NMR spectrum of **6a**, related to **Scheme 3**

7.329
7.308
7.258
7.255
7.236
7.219
7.216
6.724
6.705
6.686
6.684

4.404

2.969
2.956

1.00
0.99
2.00
0.92
3.16

8.5 8.0 7.5 7.0 6.5 6.0 5.5 5.0 4.5 4.0 3.5 3.0 2.5 2.0 1.5 1.0 0.5 0.0
F1 (PPM)
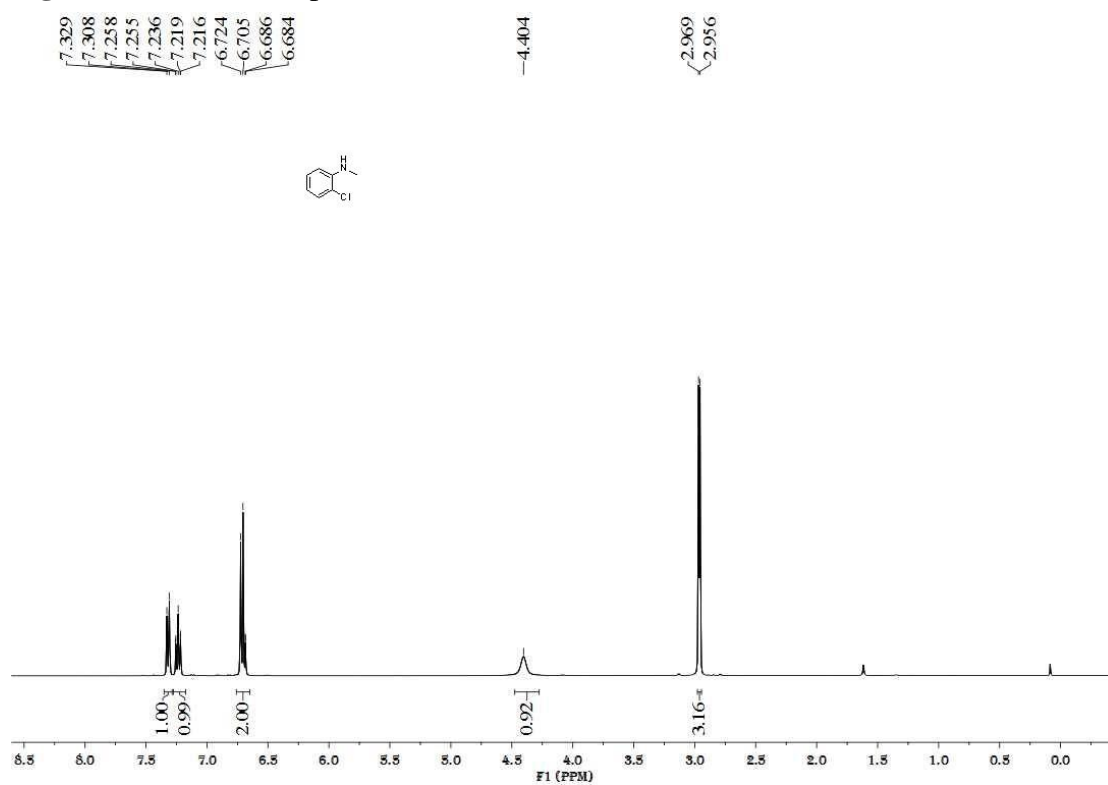
Figure S68. ^{13}C NMR spectrum of **6a**, related to **Scheme 3**

145.039

128.972
127.851

119.071
117.023

110.638

30.384

150 140 130 120 110 100 90 80 70 60 50 40 30 20 10 0
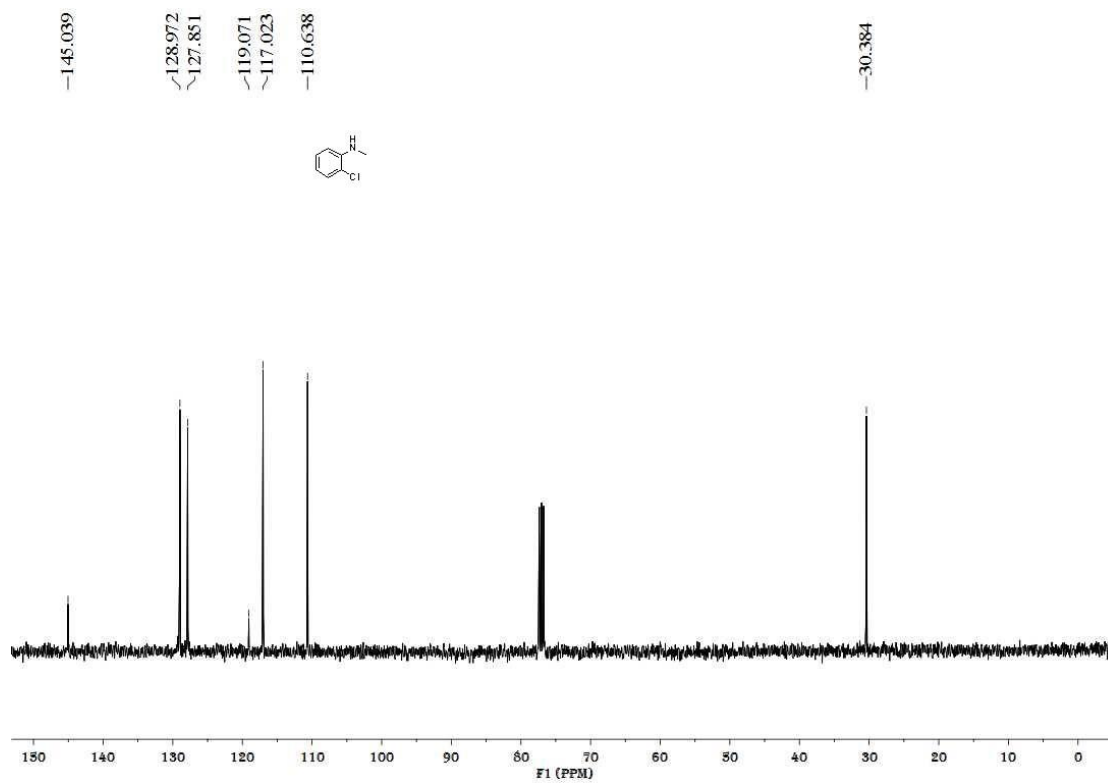F1 (PPM)

S35

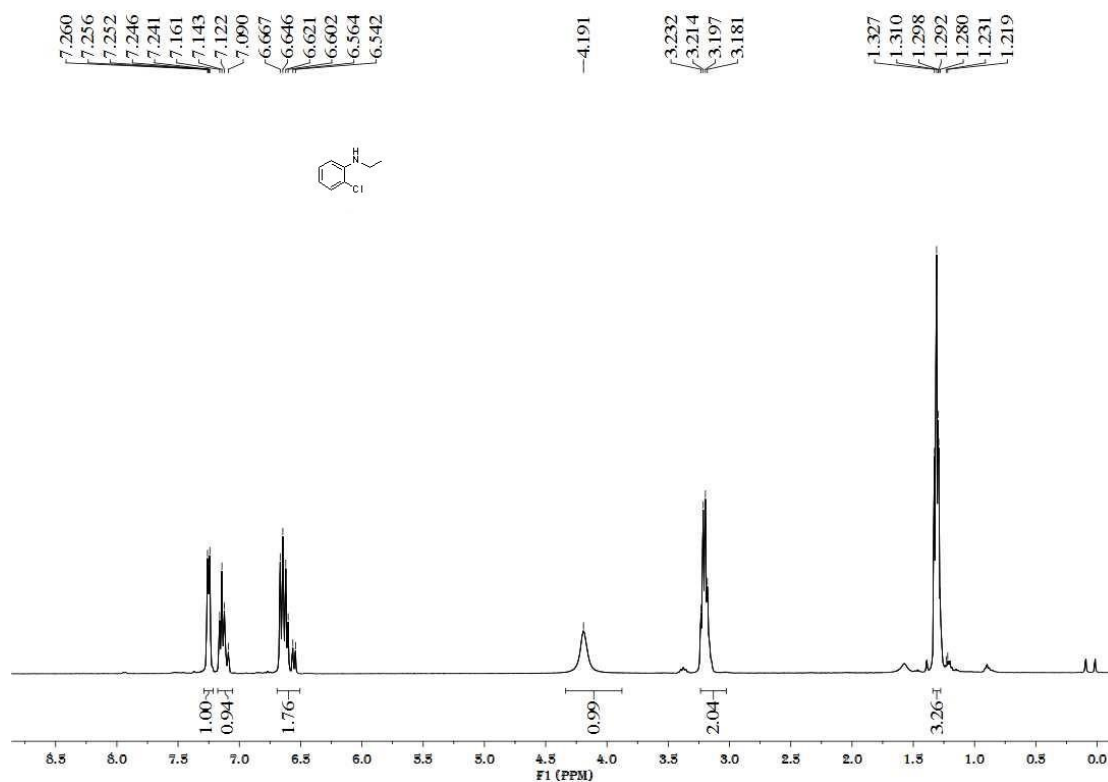**Figure S69**. ^{1}H NMR spectrum of **6b**, related to **Scheme 3**

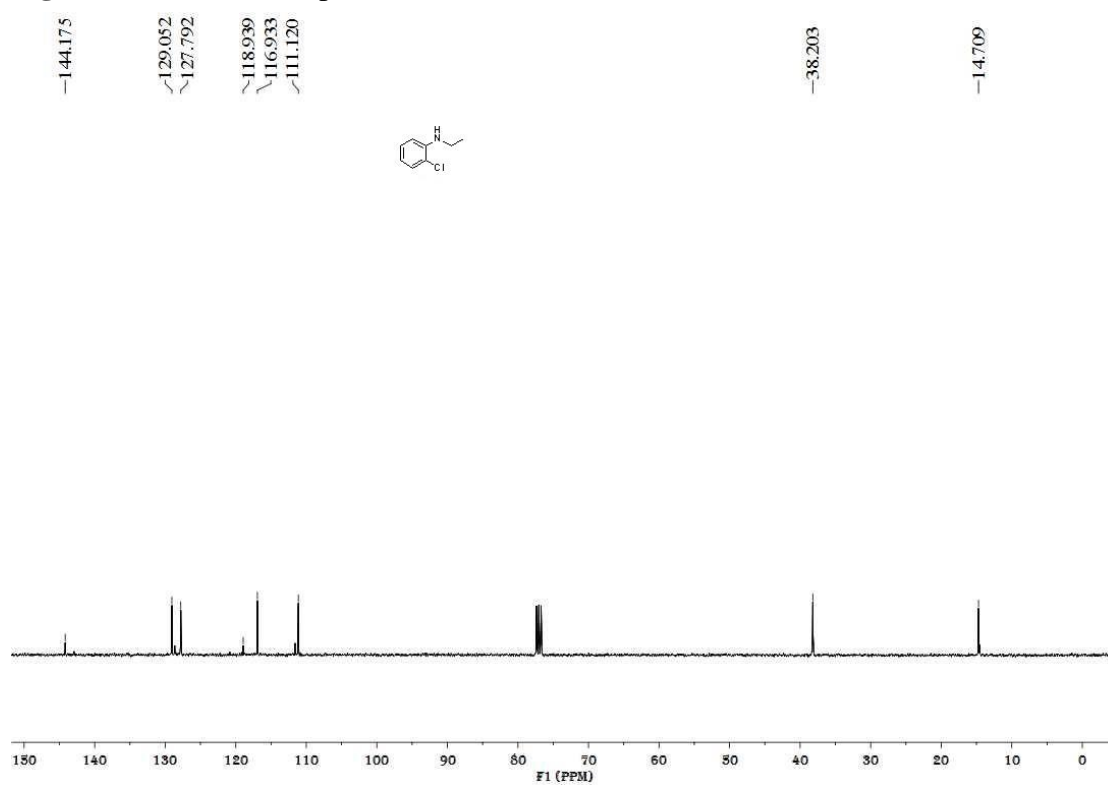**Figure S70**. ^{13}C NMR spectrum of **6b**, related to **Scheme 3**

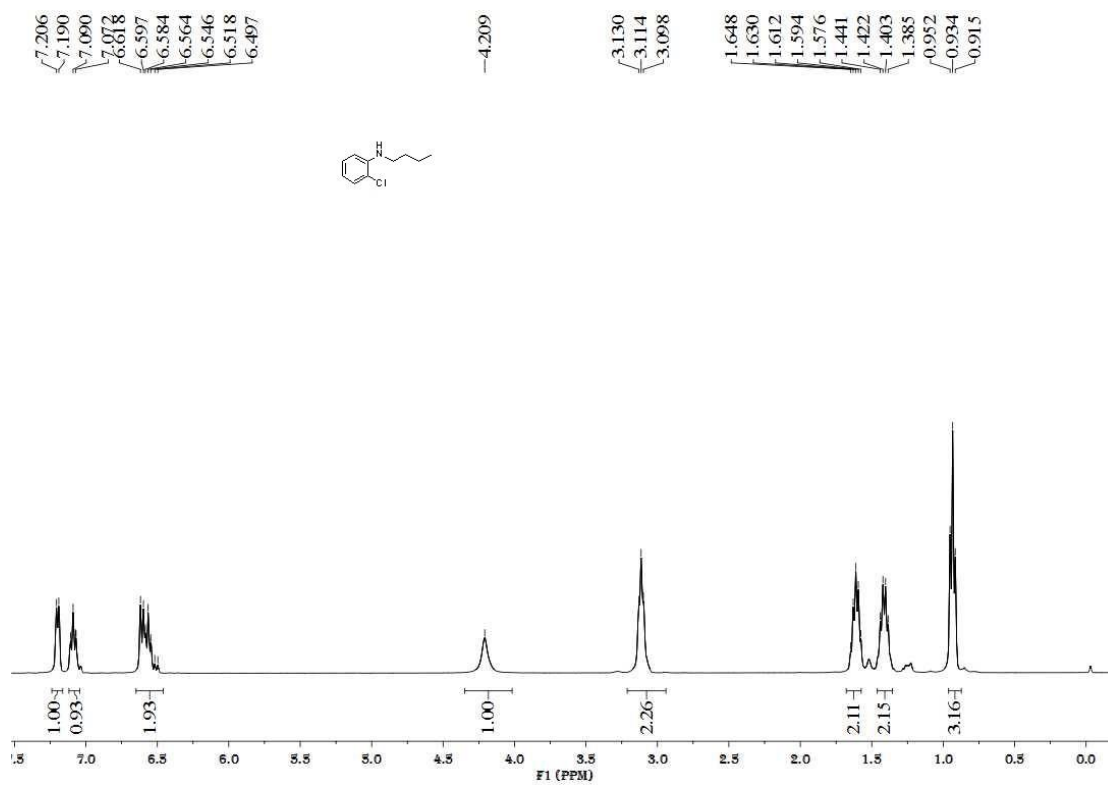**Figure S71**. ¹H NMR spectrum of **6c**, related to **Scheme 3**

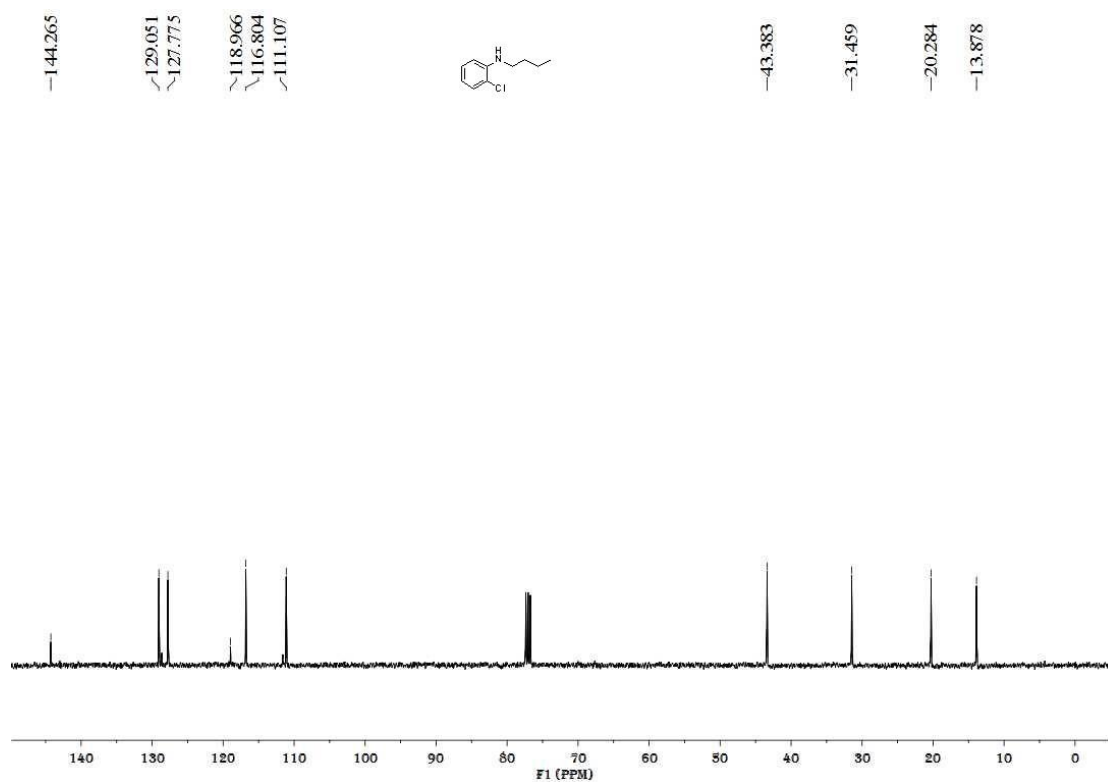**Figure S72**. ¹³C NMR spectrum of **6c**, related to **Scheme 3**

Figure S73. ¹H NMR spectrum of **6d**, related to **Scheme 3**

Figure S74. ¹³C NMR spectrum of **6d**, related to **Scheme 3**

Figure S75. ^{1}H NMR spectrum of **6e**, related to **Scheme 3**

7.307
7.304
7.288
7.208
7.188
7.169
6.716
6.695
6.682
6.663
6.644

4.310

3.205

1.335
0.966
0.951
0.934

1.00
0.91
1.78
0.88
2.07
2.09
18.31
3.25

8.0 7.5 7.0 6.5 6.0 5.5 5.0 4.5 4.0 3.5 3.0 2.5 2.0 1.5 1.0 0.5 0.0
F1 (PPM)

Figure S76. ^{13}C NMR spectrum of **6e**, related to **Scheme 3**

144.240

129.034
127.756

118.945
116.777
111.089

43.698

31.933
29.651
29.608
29.426
29.353
29.213
27.129
22.701
14.110

145 135 125 115 105 95 90 85 80 75 70 65 60 55 50 45 40 35 30 25 20 15 10 5 0
F1 (PPM)

Figure S77. [^1]H NMR spectrum of **6f**, related to **Scheme 3**

Figure S78. [^13]C NMR spectrum of **6f**, related to **Scheme 3**

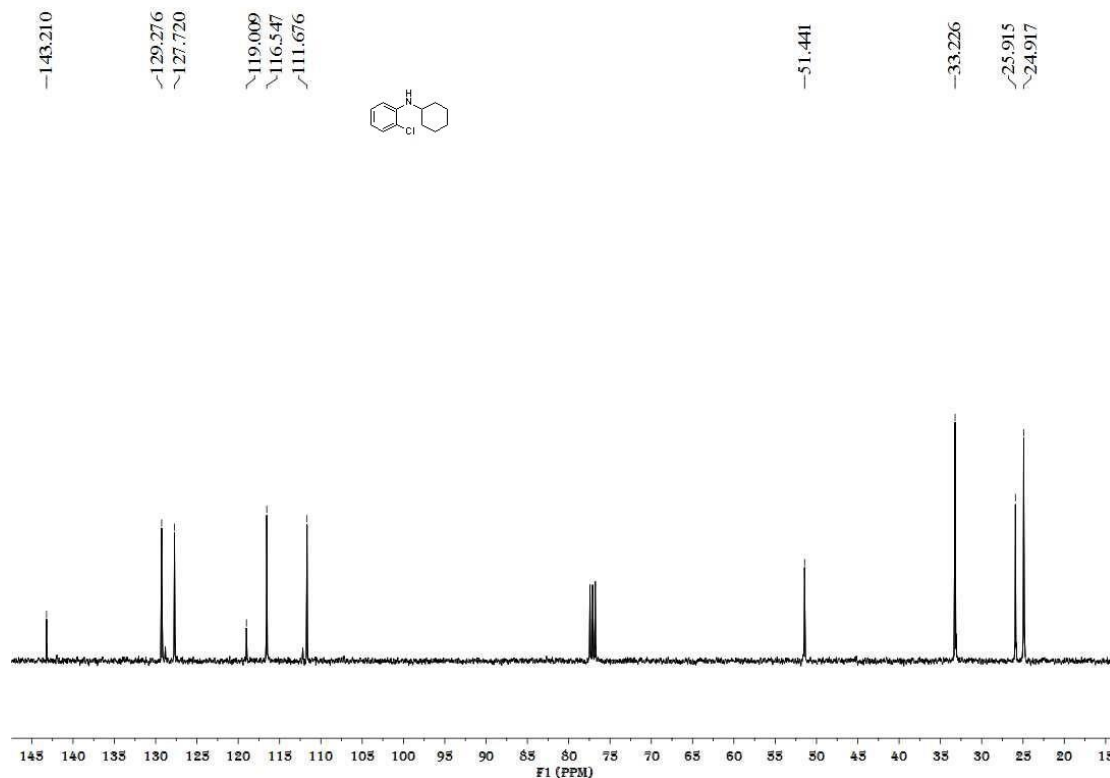**Figure S79**. ^{1}H NMR spectrum of **6g**, related to **Scheme 3**

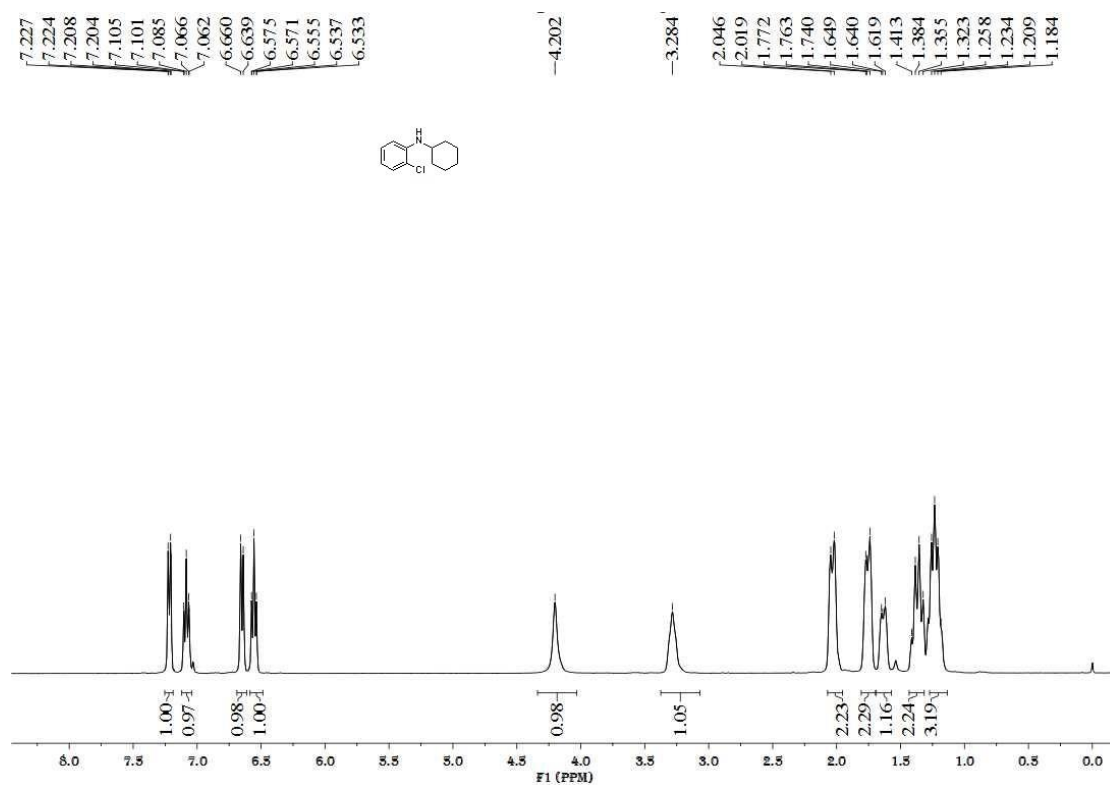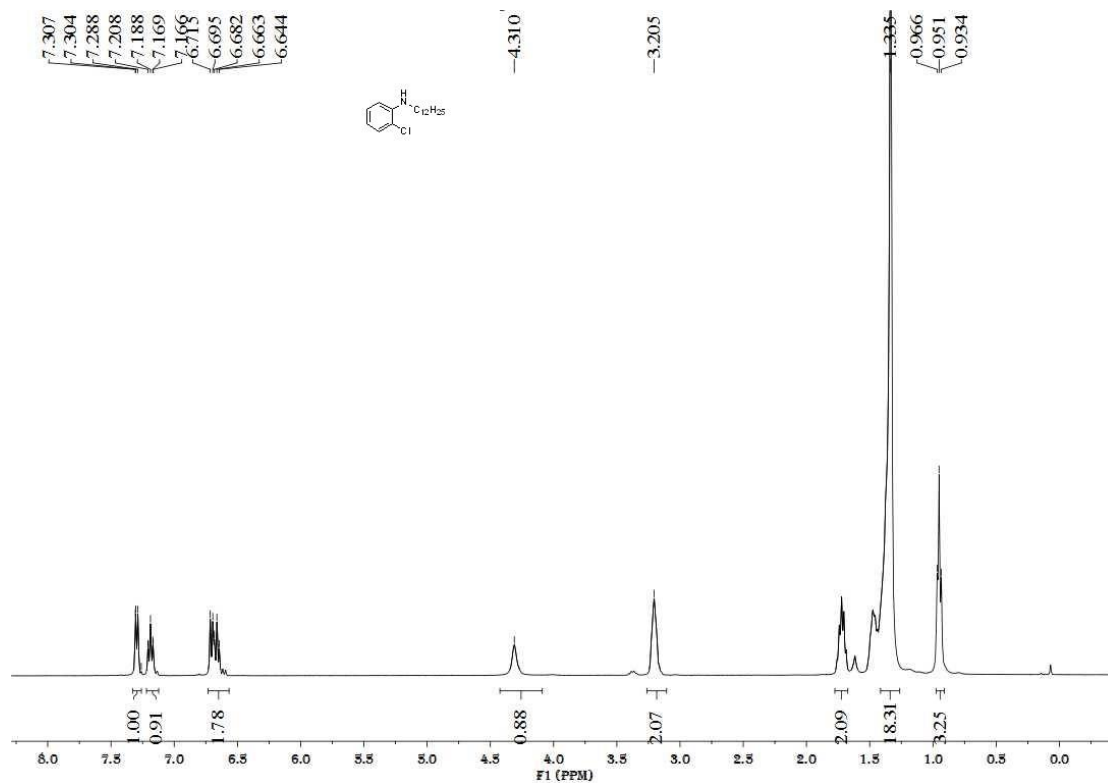**Figure S80**. ^{13}C NMR spectrum of **6g**, related to **Scheme 3**

Figure S81. ^{1}H NMR spectrum of **6j**, related to **Scheme 3**

Figure S82. ^{13}C NMR spectrum of **6j**, related to **Scheme 3**
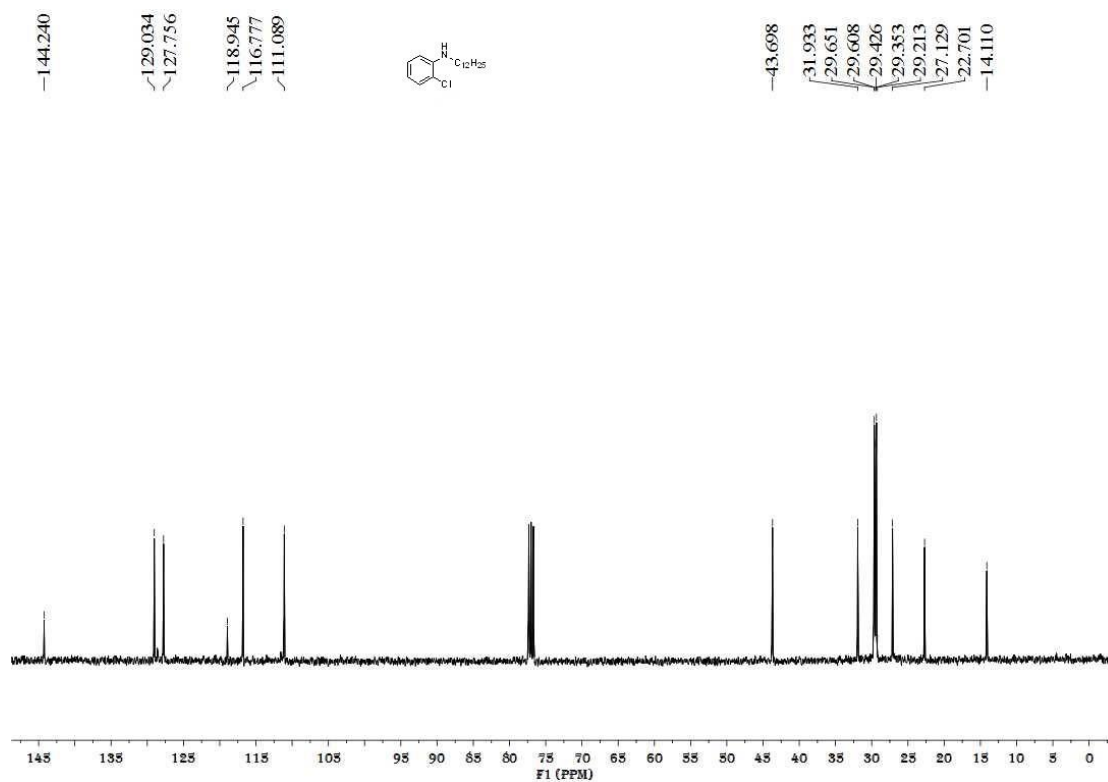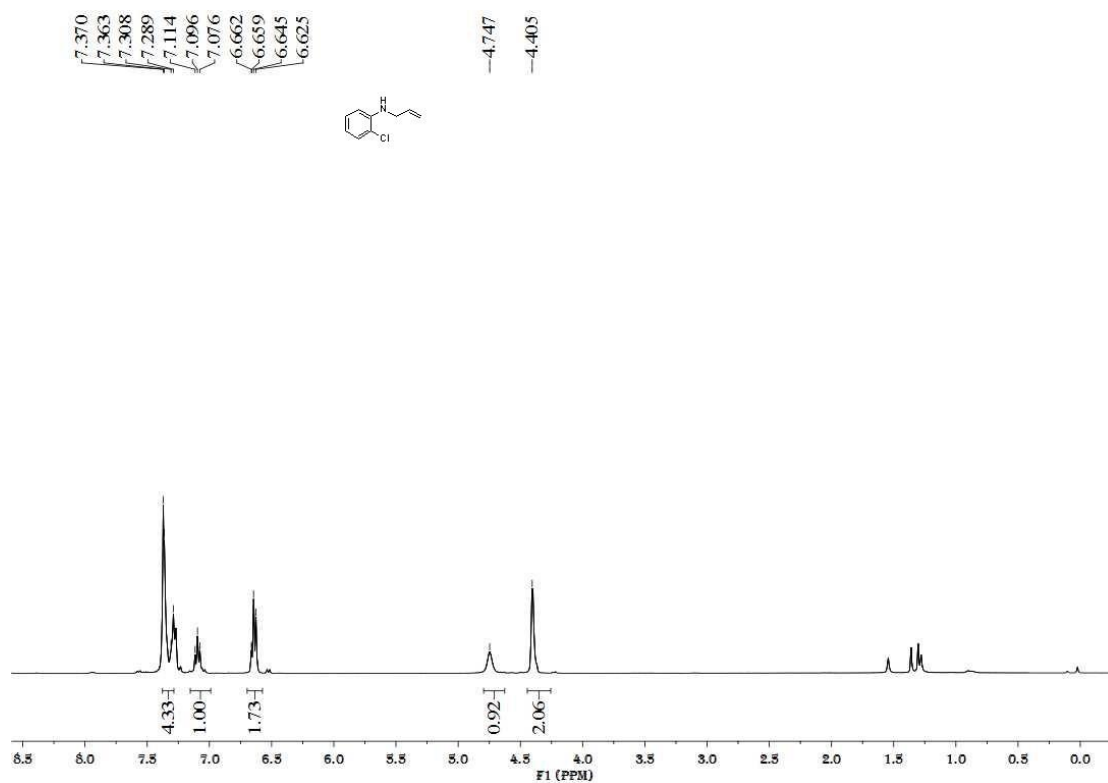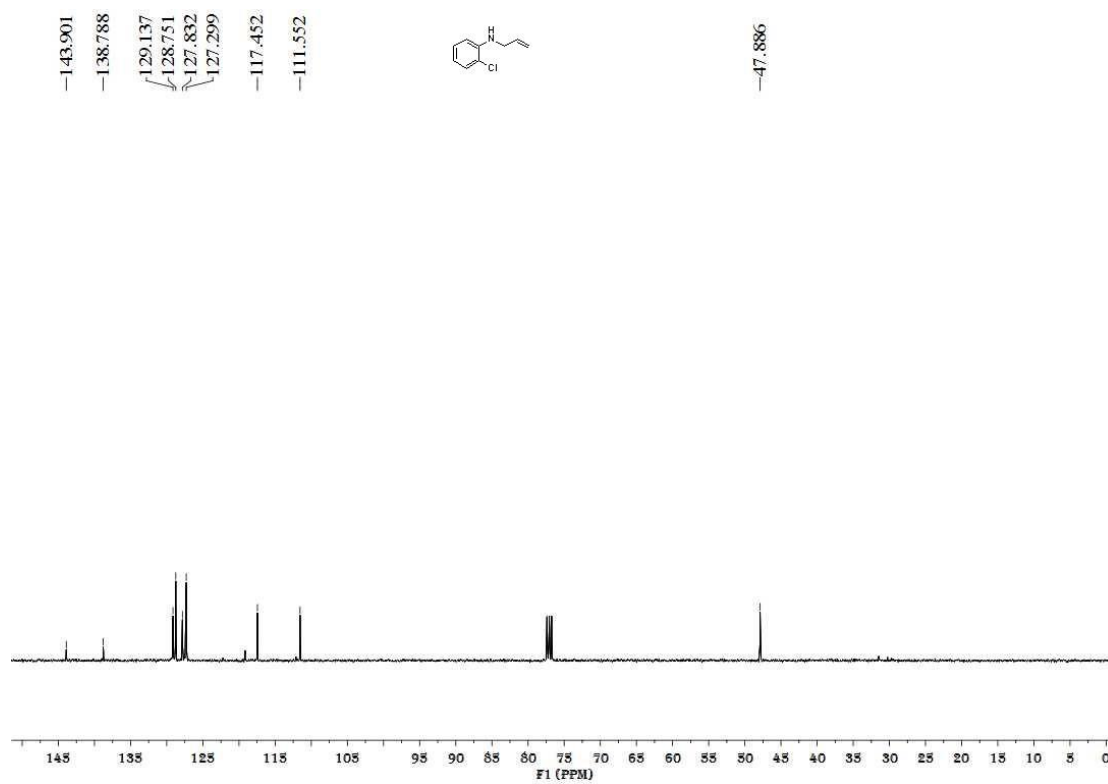
Figure S83. ^{1}H NMR spectrum of **6i**, related to **Scheme 3**

8.110
8.089
7.695
7.675
7.581
7.559
7.515
7.496
7.464
7.442
7.316
7.296
7.278
7.146
7.126
7.027
6.373

0.92
1.00
0.98
1.93
2.81
1.92
0.97
0.89

9.5 9.0 8.5 8.0 7.5 7.0 6.5 6.0 5.5 5.0 4.5 4.0 3.5 3.0 2.5 2.0 1.5 1.0 0.5 0.0 -0.

F1 (PPM)

Figure S84. ^{13}C NMR spectrum of **6i**, related to **Scheme 3**

141.702
137.907
131.870
129.518
129.389
128.132
127.506
127.409
123.716
122.937
122.857
120.291
117.291
115.105

145 135 125 115 105 95 90 85 80 75 70 65 60 55 50 45 40 35 30 25 20 15 10 5 0

F1 (PPM)

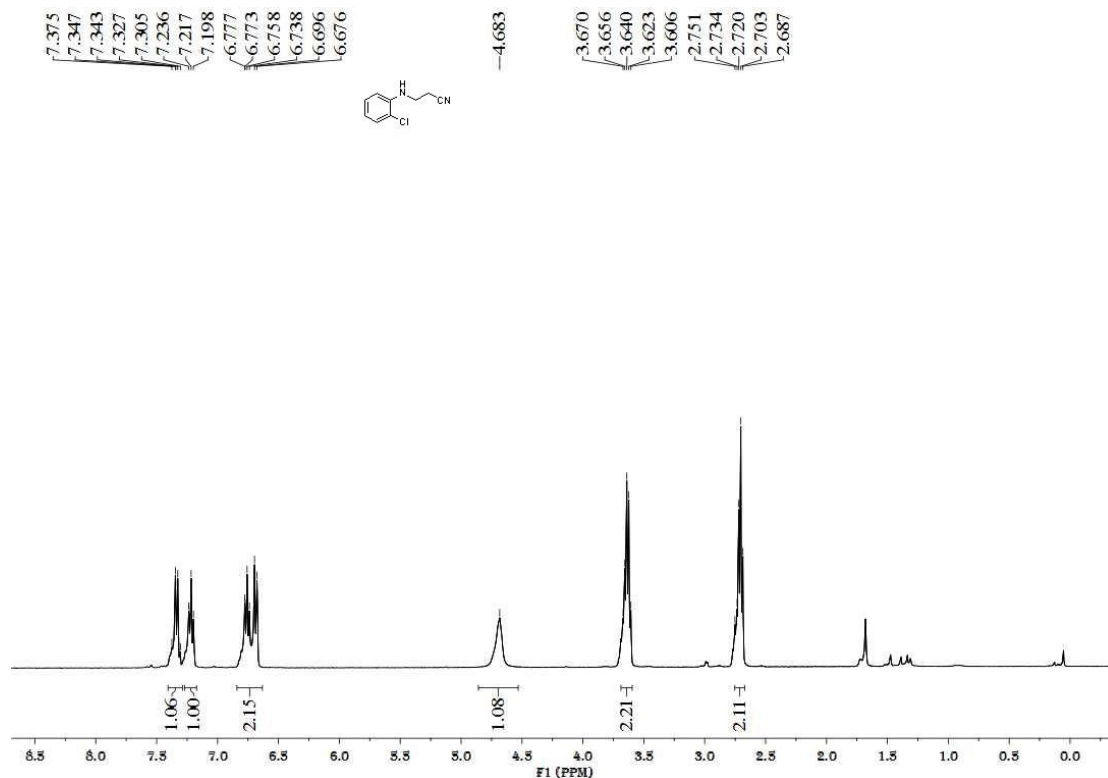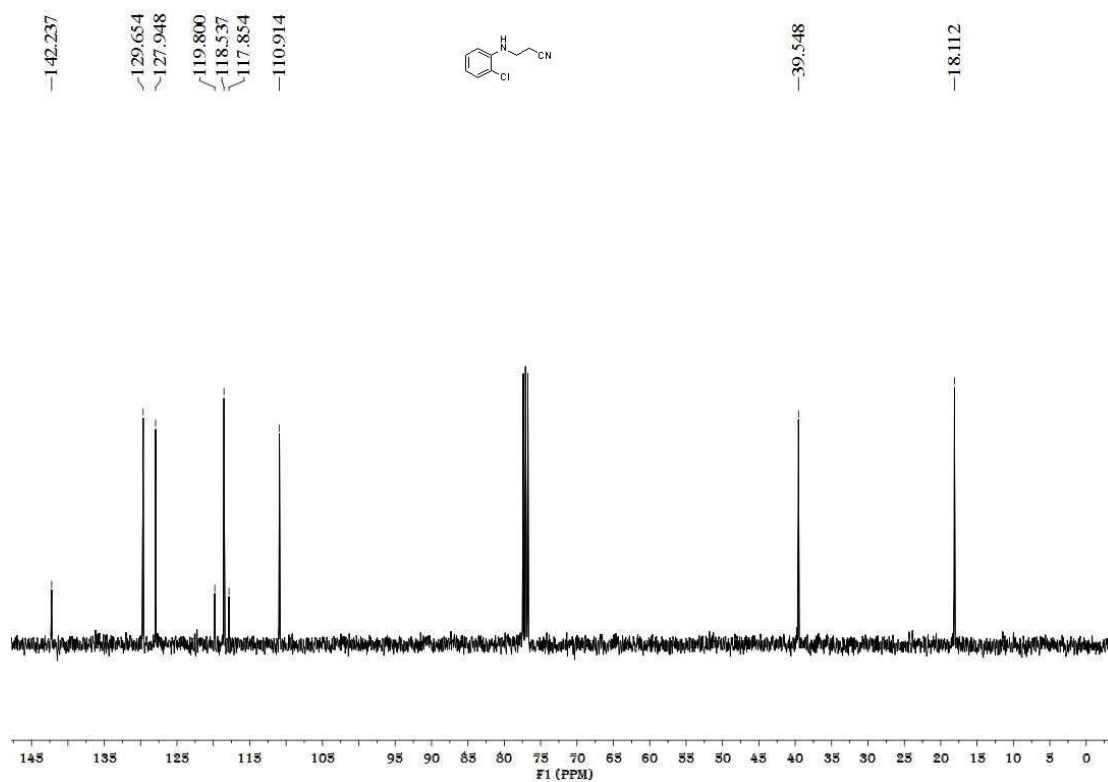**Figure S85**. ^{1}H NMR spectrum of **6h**, related to **Scheme 3**

Figure S86. ^{13}C NMR spectrum of **6h**, related to **Scheme 3**

Figure S87. ^{1}H NMR spectrum of **6k**, related to **Scheme 3**

Figure S88. ^{13}C NMR spectrum of **6k**, related to **Scheme 3**

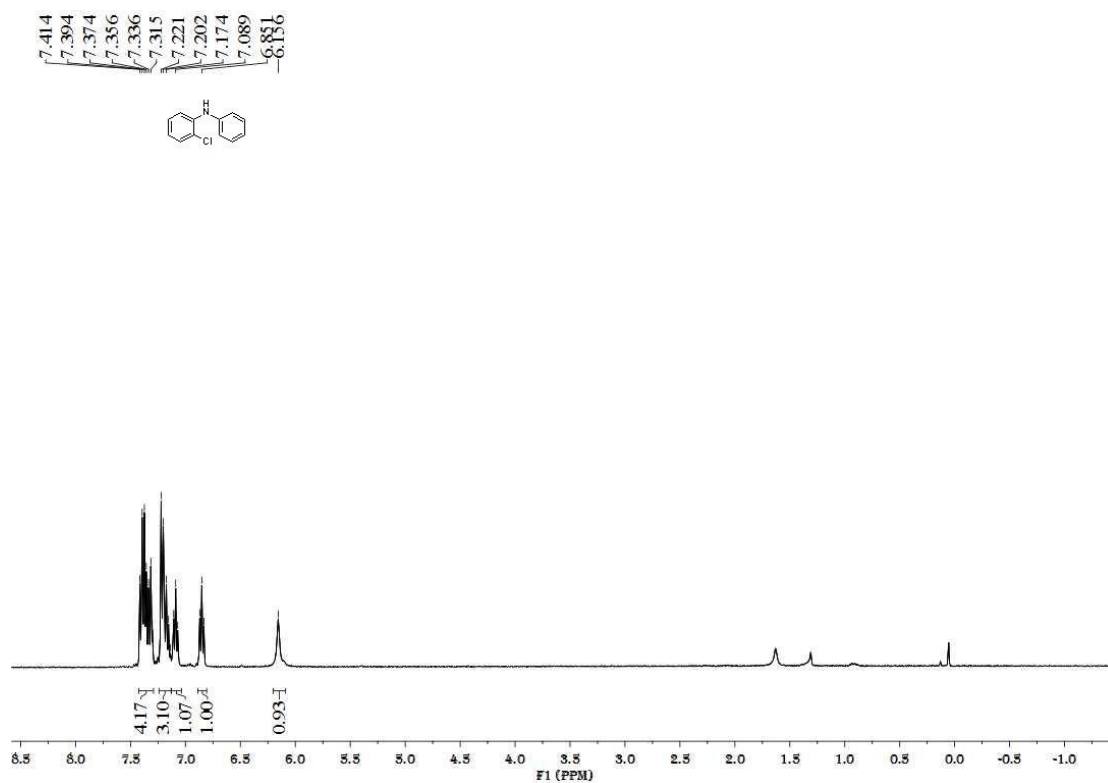**Figure S89**. ¹H NMR spectrum of **6l**, related to **Scheme 3**
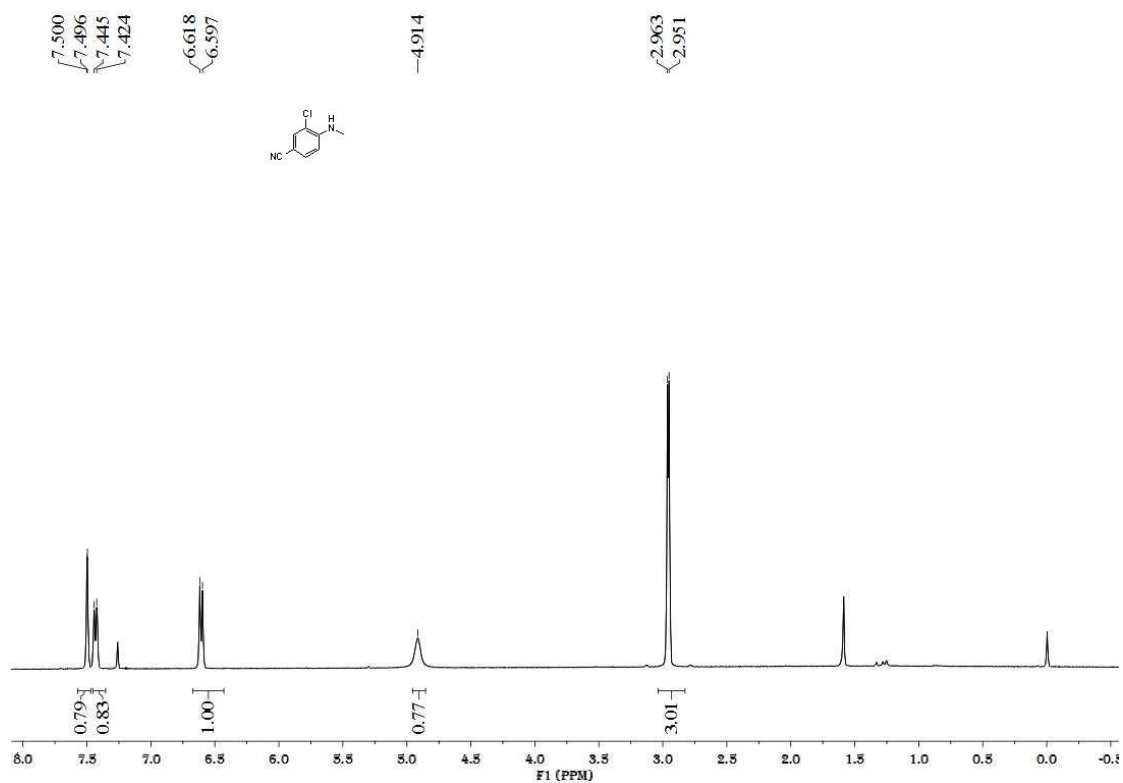
Figure S90. ¹³C NMR spectrum of **6l**, related to **Scheme 3**
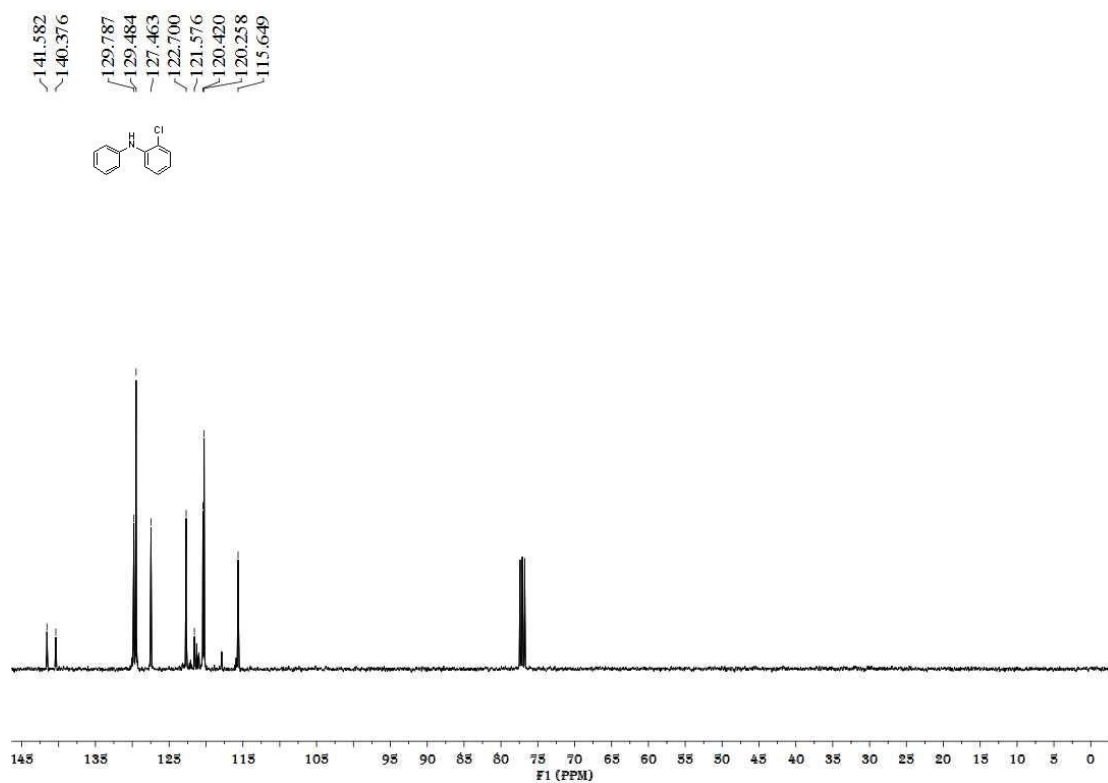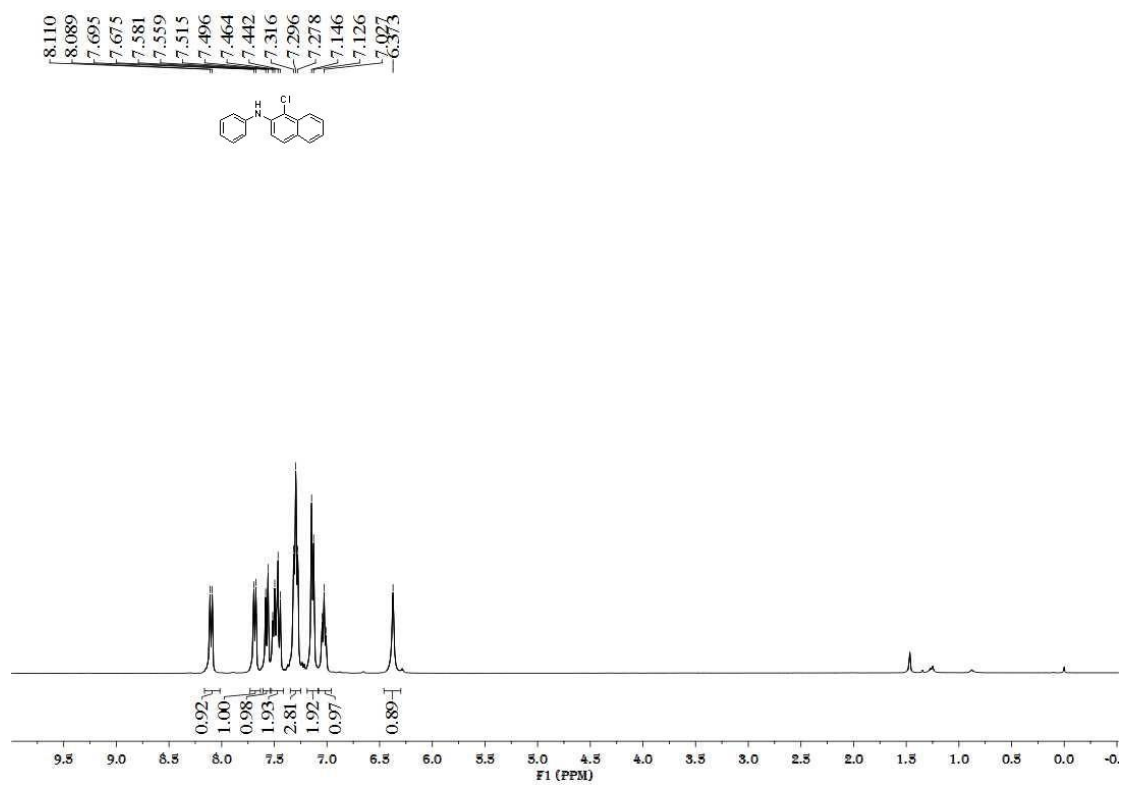
7.312
7.292
7.139
7.121
7.104
7.101
6.824
6.821
6.804
6.801
6.770
6.766
6.748
6.732
6.728

4.087

1.00
0.97
0.96
0.98

2.05

8.0 7.5 7.0 6.5 6.0 5.5 5.0 4.5 4.0 3.5 3.0 2.5 2.0 1.5 1.0 0.5 0.0
F1 (PPM)
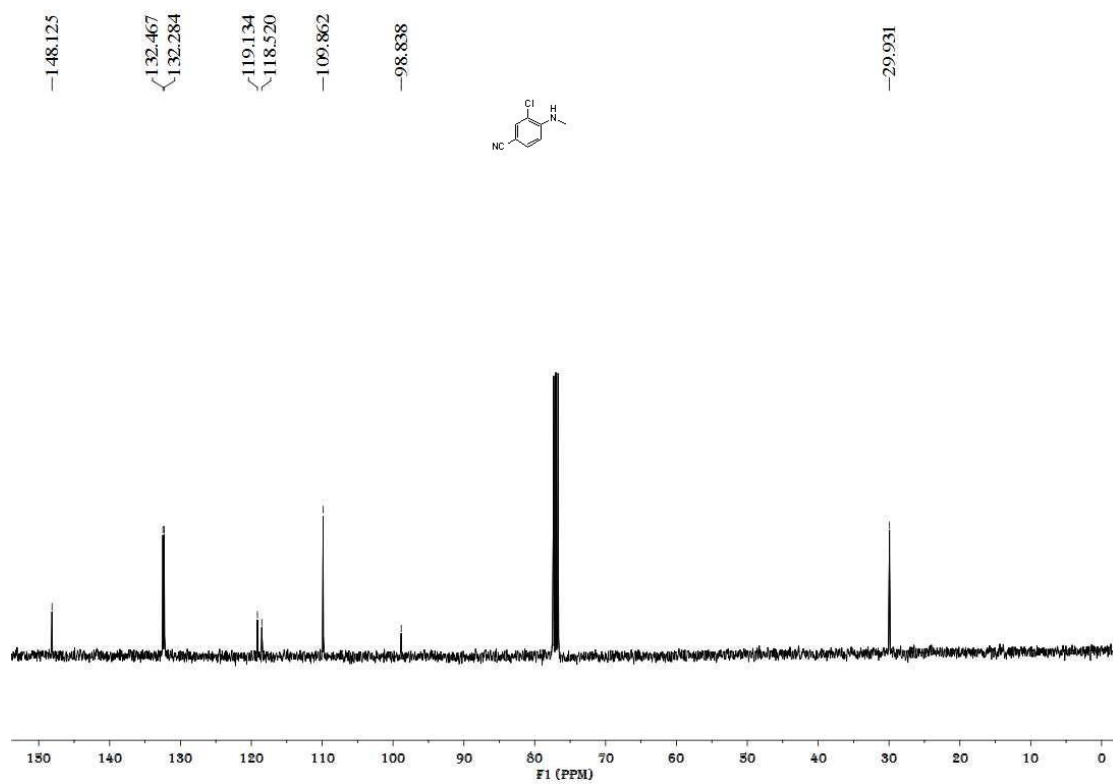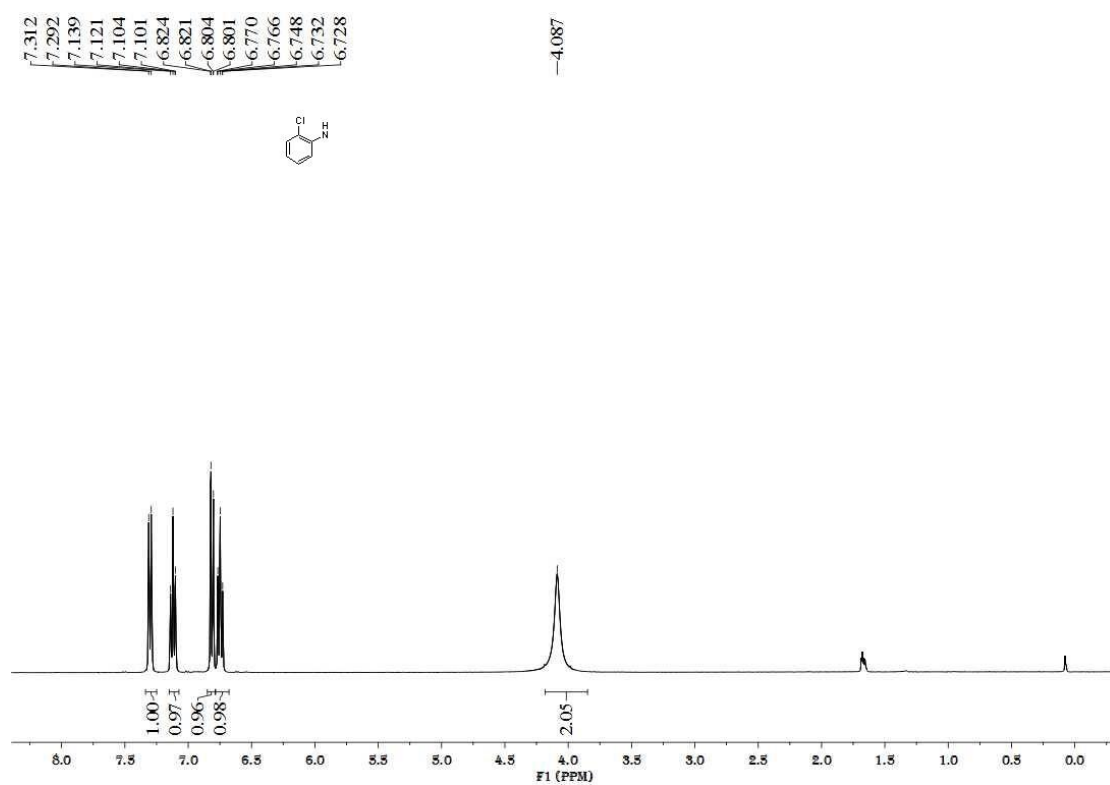
Figure S91. ^{1}H NMR spectrum of **6m**, related to **Scheme 3**

142.935

129.423
127.634
119.303
119.029
115.885

145 135 125 115 105 95 90 85 80 75 70 65 60 55 50 45 40 35 30 25 20 15 10 5 0 -5
F1 (PPM)
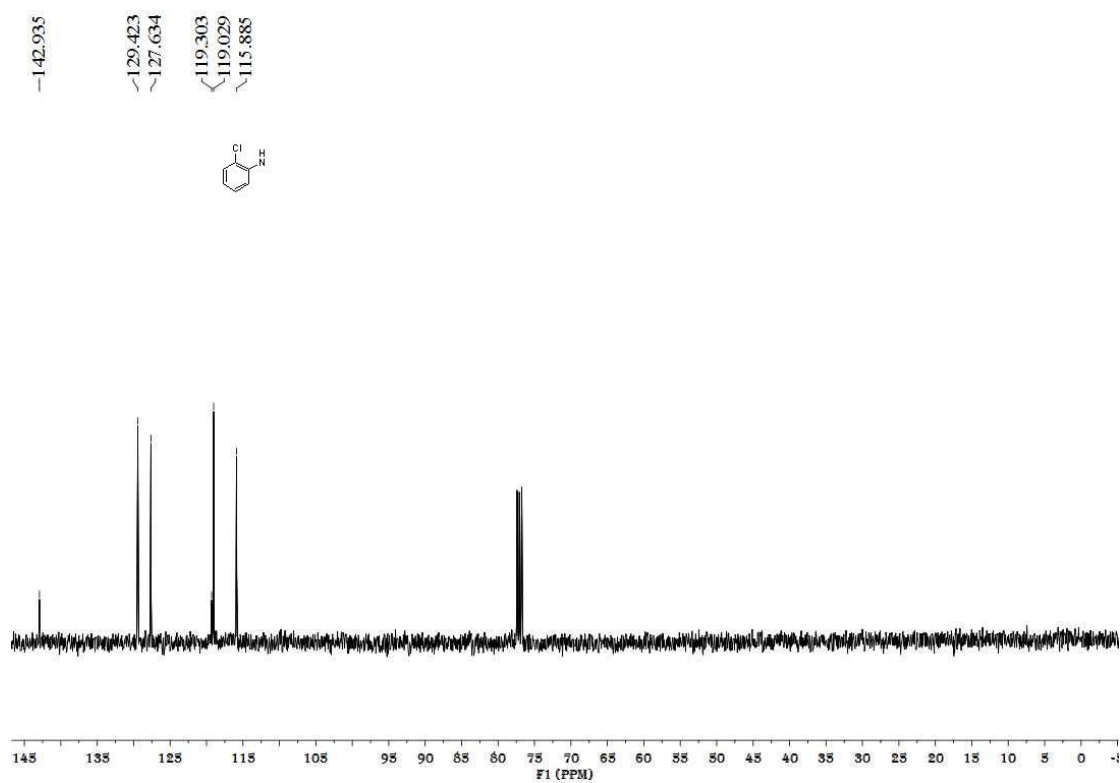
Figure S92. ^{13}C NMR spectrum of **6m**, related to **Scheme 3**

Figure S93. ^{1}H NMR spectrum of **6n**, related to **Scheme 6**

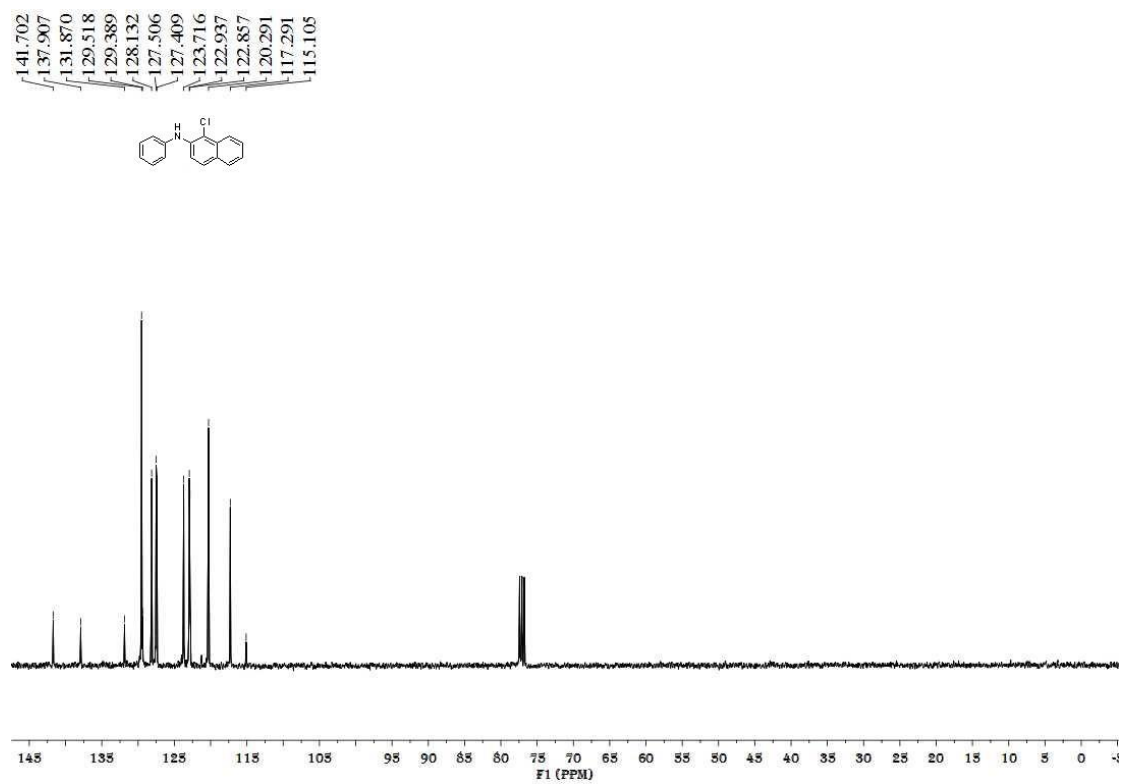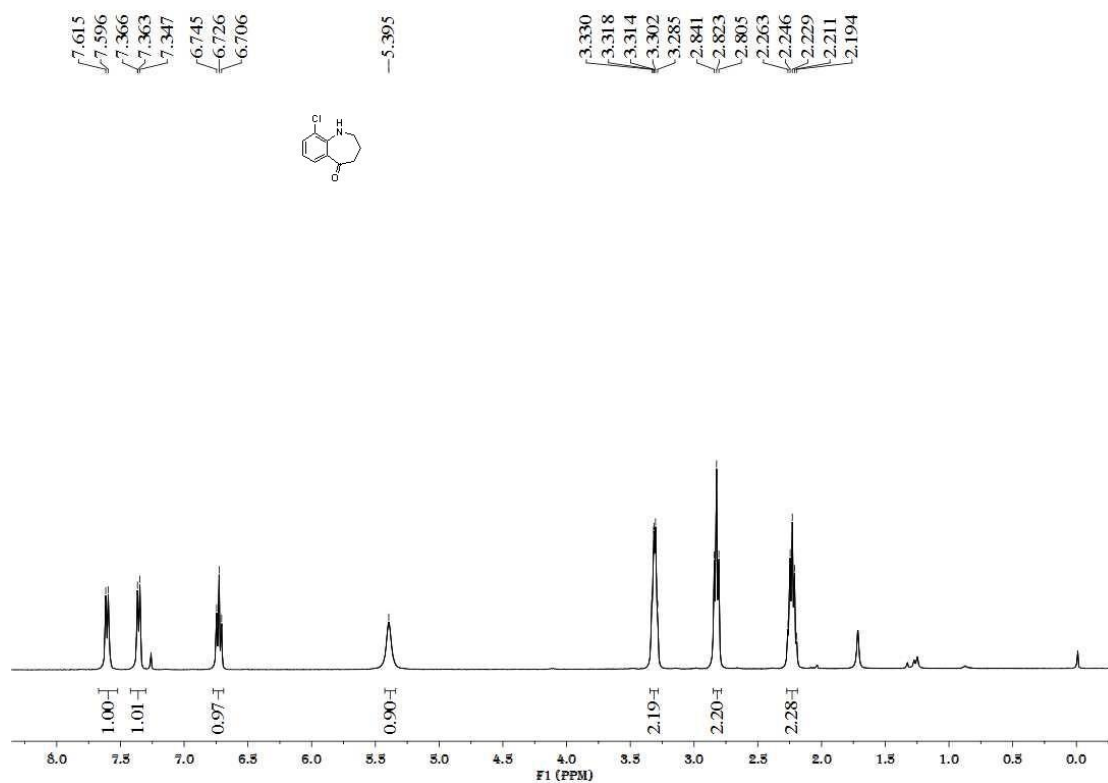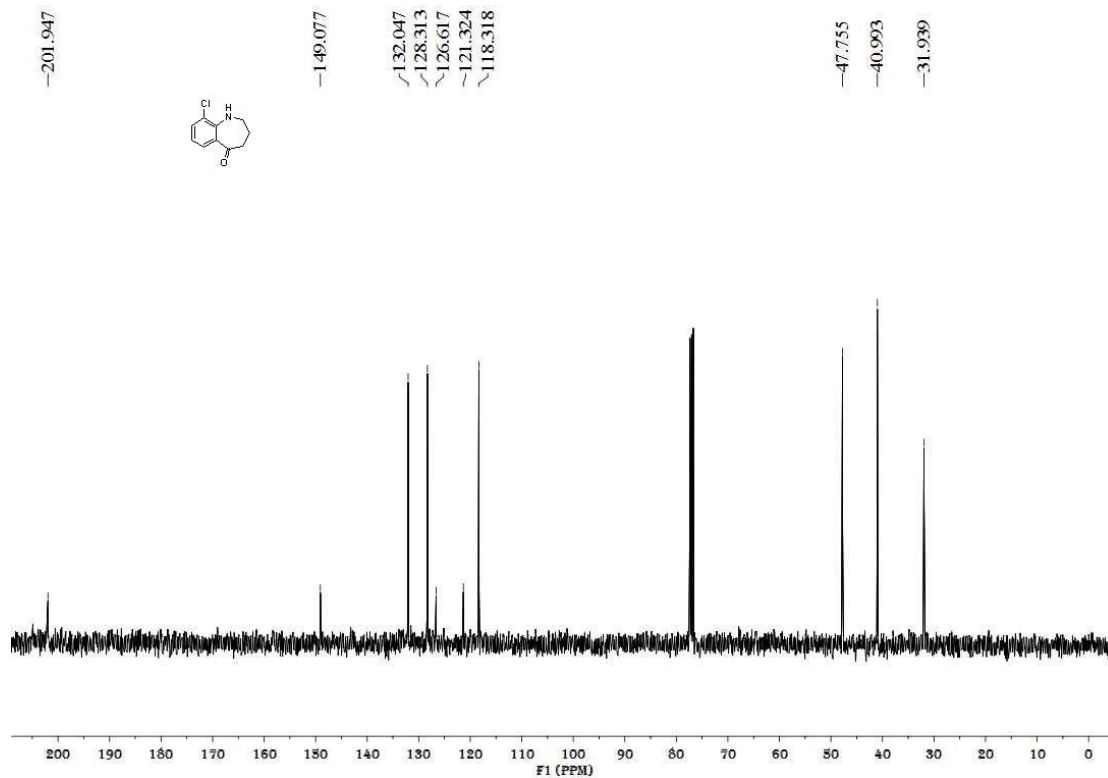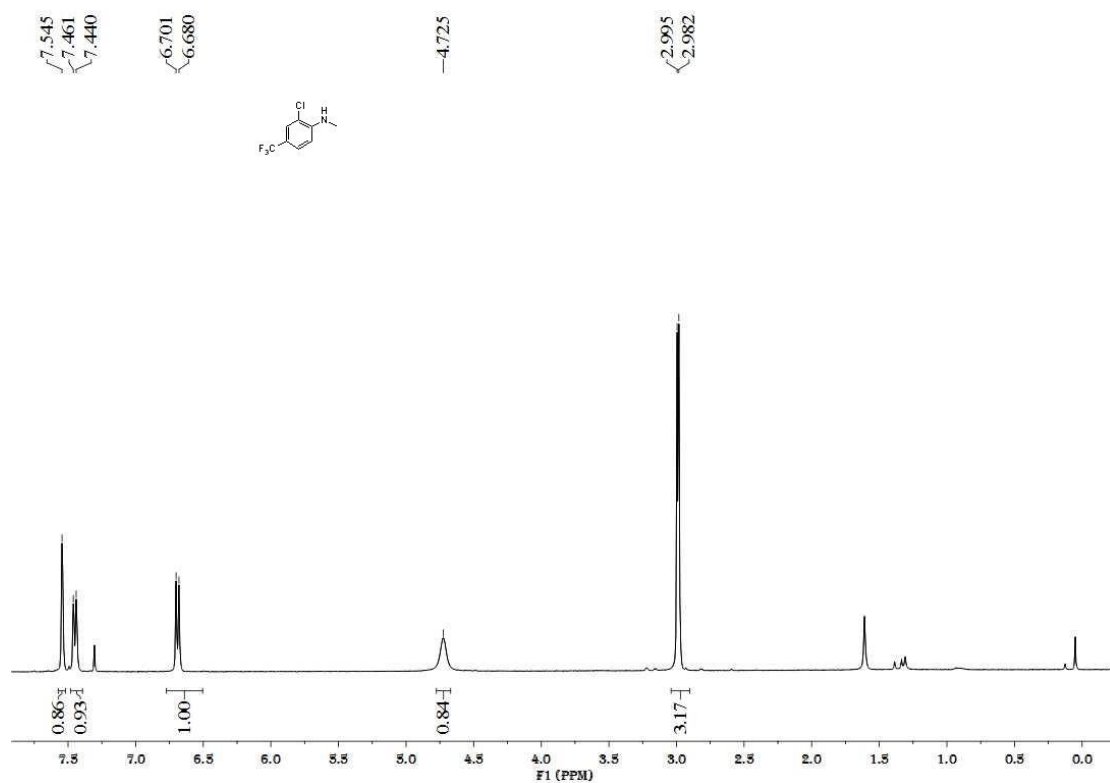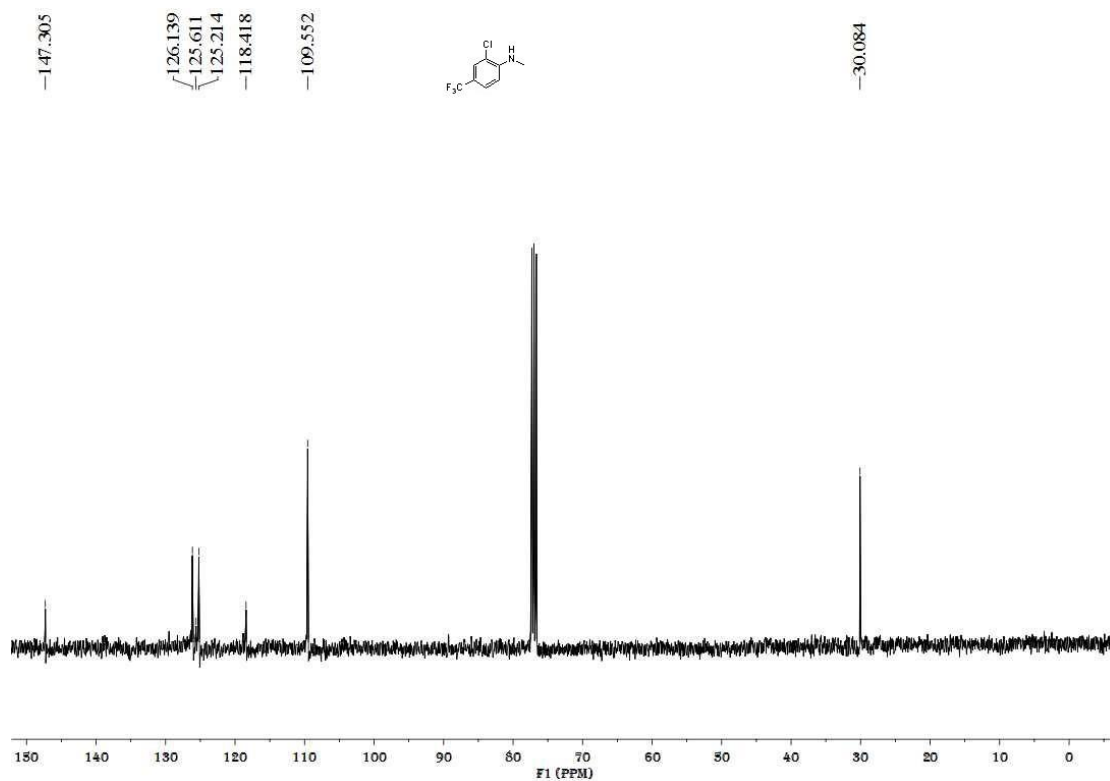**Figure S94**. ^{13}C NMR spectrum of **6n**, related to **Scheme 6**

Figure S95. ^{1}H NMR spectrum of **7**, related to **Scheme 5**

8.364
8.192
8.172
8.158
8.139
7.772
7.753
7.642
7.624
7.607
7.523
7.506
7.487
7.470
7.453
7.414
7.396
7.381
7.339
7.324
7.303

1.00
2.00
2.02
2.07
4.09
1.05
1.17

Figure S96. ^{13}C NMR spectrum of **7**, related to **Scheme 5**

139.482
139.089
137.276
129.295
128.411
127.584
125.981
120.497
119.577
118.708
118.712

Figure S97. ^{1}H NMR spectrum of **8**, related to **Scheme 5**

10.275
10.175
8.308
8.288
8.107
8.087
7.812
7.793
7.552
7.532
7.516
7.499
7.479
7.350
7.332
7.318
7.315
7.301
7.299

0.89
0.99
1.00
1.00
1.01
2.03
2.03

.1.0 10.5 10.0 9.5 9.0 8.5 8.0 7.5 7.0 6.5 6.0 5.5 5.0 4.5 4.0 3.5 3.0 2.5 2.0 1.5 1.0 0.5 0.0 -0.5
F1 (PPM)
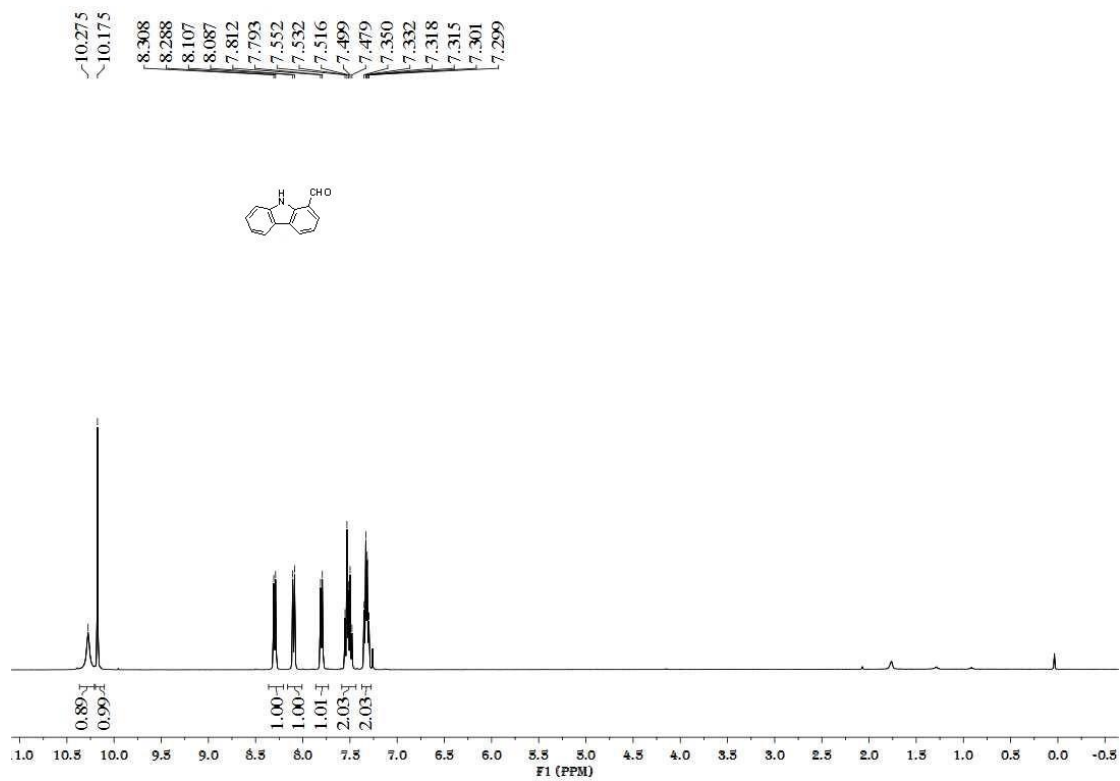
Figure S98. ^{13}C NMR spectrum of **8**, related to **Scheme 5**

193.474

140.033
138.070
131.255
126.920
126.779
124.694
121.947
120.483
119.499
118.790
111.492

200 190 180 170 160 150 140 130 120 110 100 90 80 70 60 50 40 30 20 10 0
F1 (PPM)

Figure S99. ^{1}H NMR spectrum of **9**, related to **Scheme 5**

Figure S100. ^{13}C NMR spectrum of **9**, related to **Scheme 5**

Figure S101. ^{1}H NMR spectrum of **10**, related to **Scheme 5**

Figure S102. ^{13}C NMR spectrum of **10**, related to **Scheme 5**
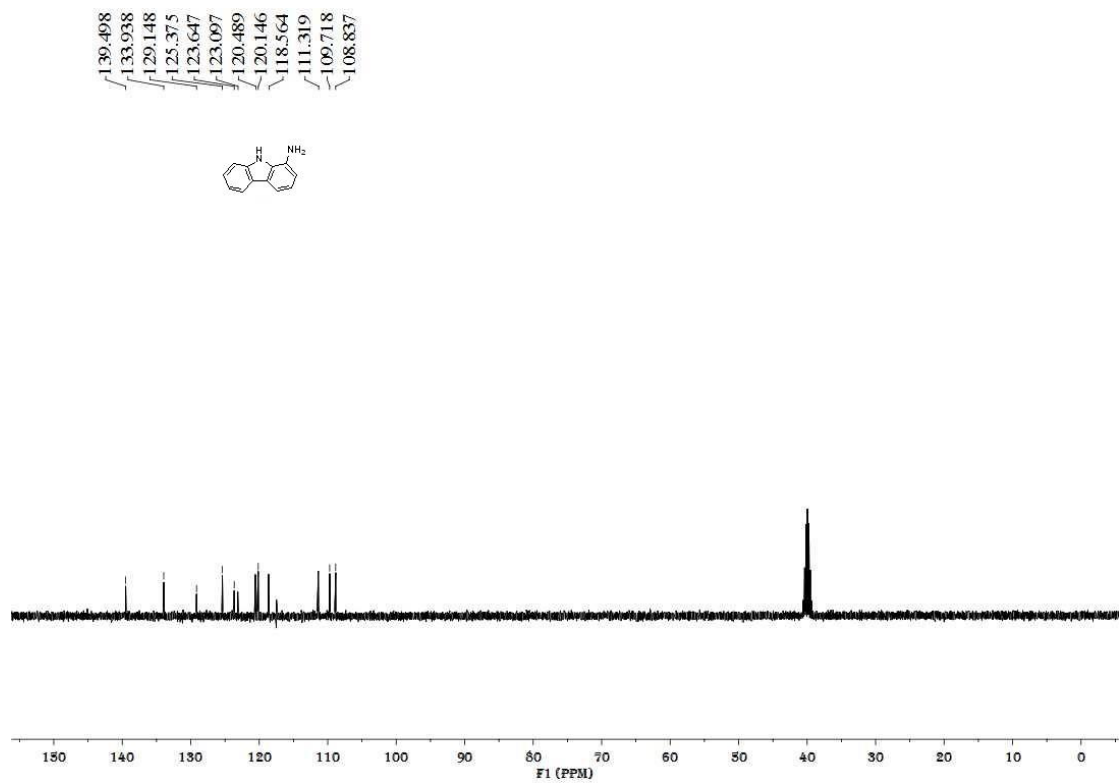
Figure S103. ^{1}H NMR spectrum of **11**, related to **Scheme 6**
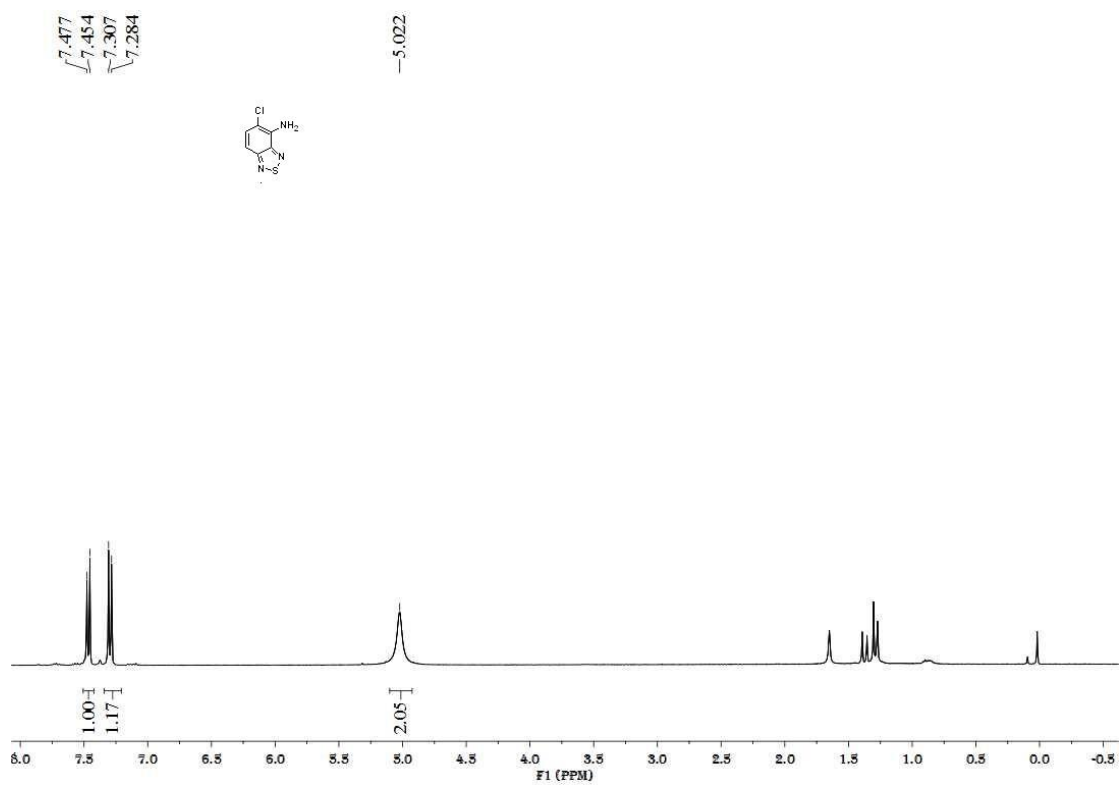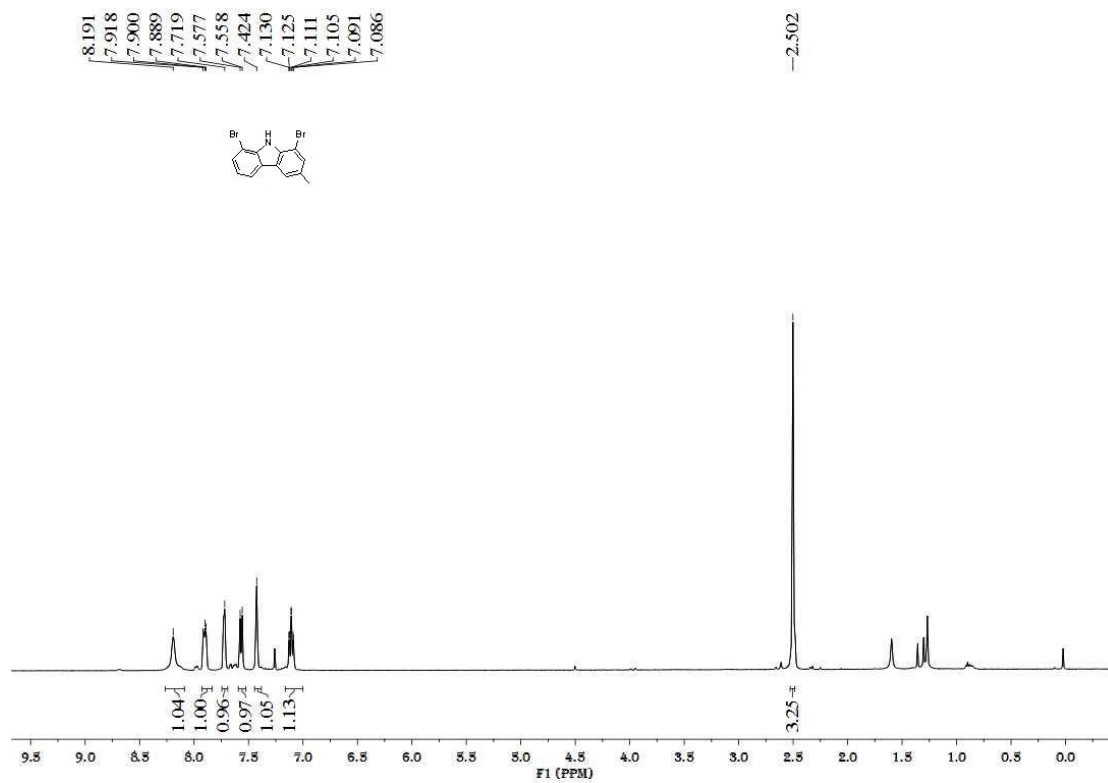

Figure S104. ^{13}C NMR spectrum of **11**, related to **Scheme 6**
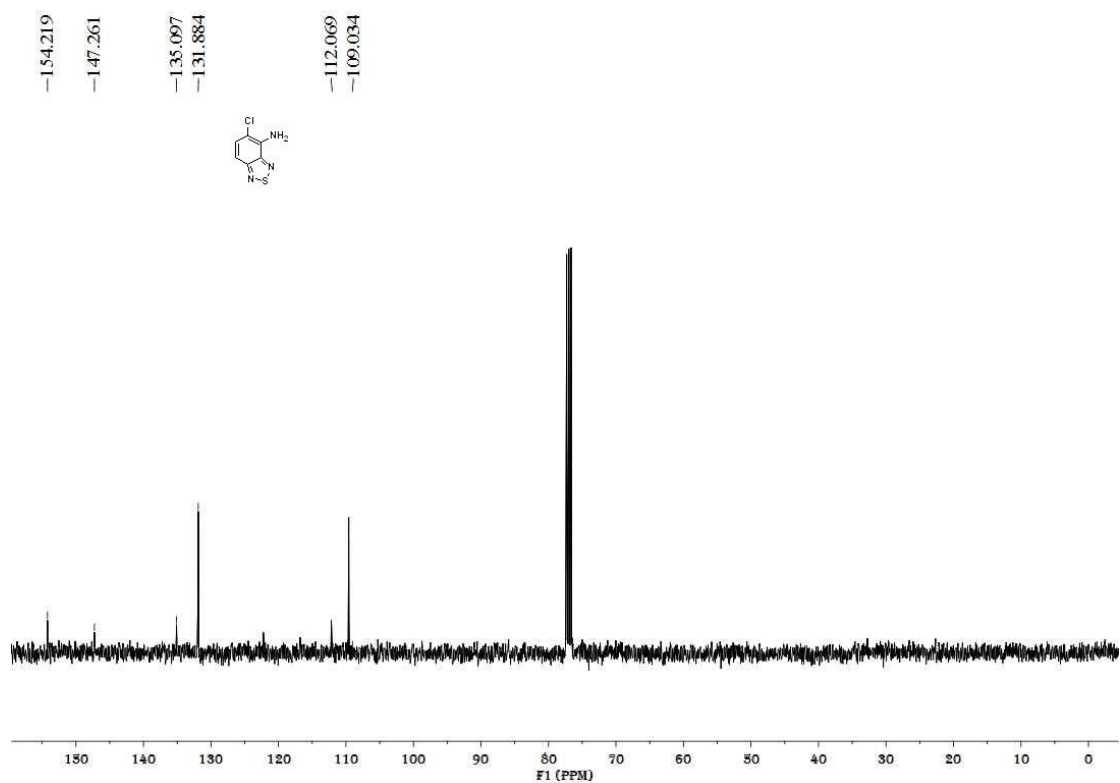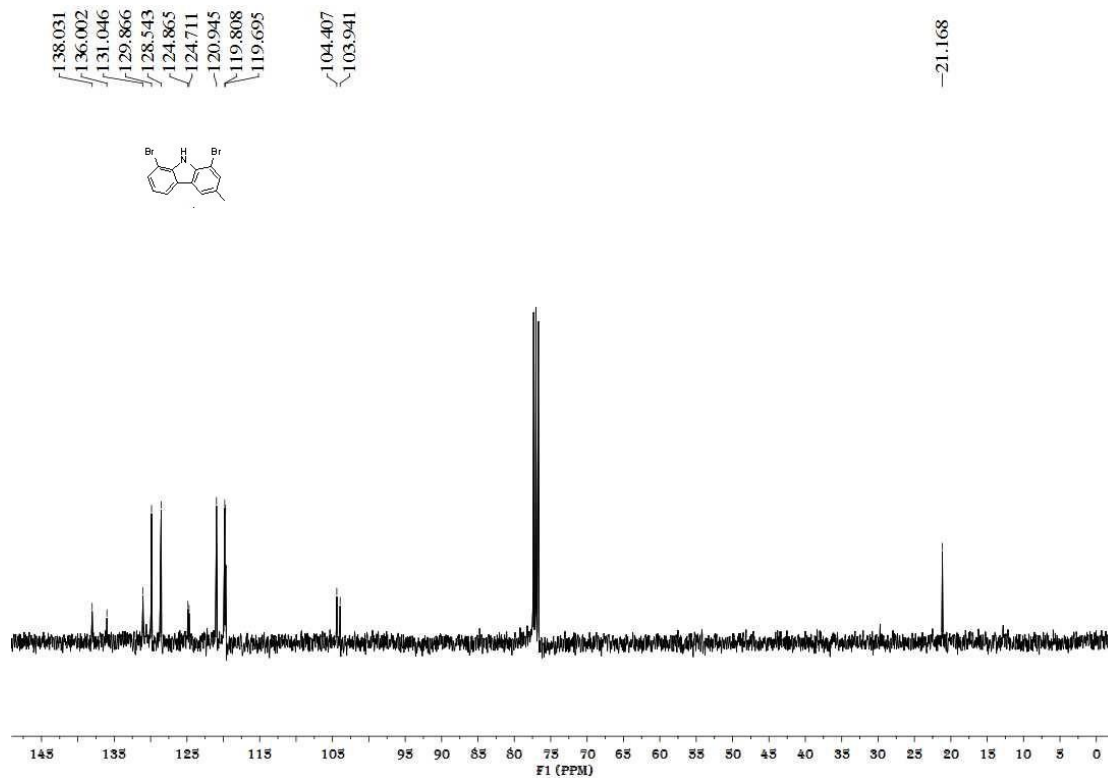
Figure S105. ^{1}H NMR spectrum of **12**, related to **Scheme 6**
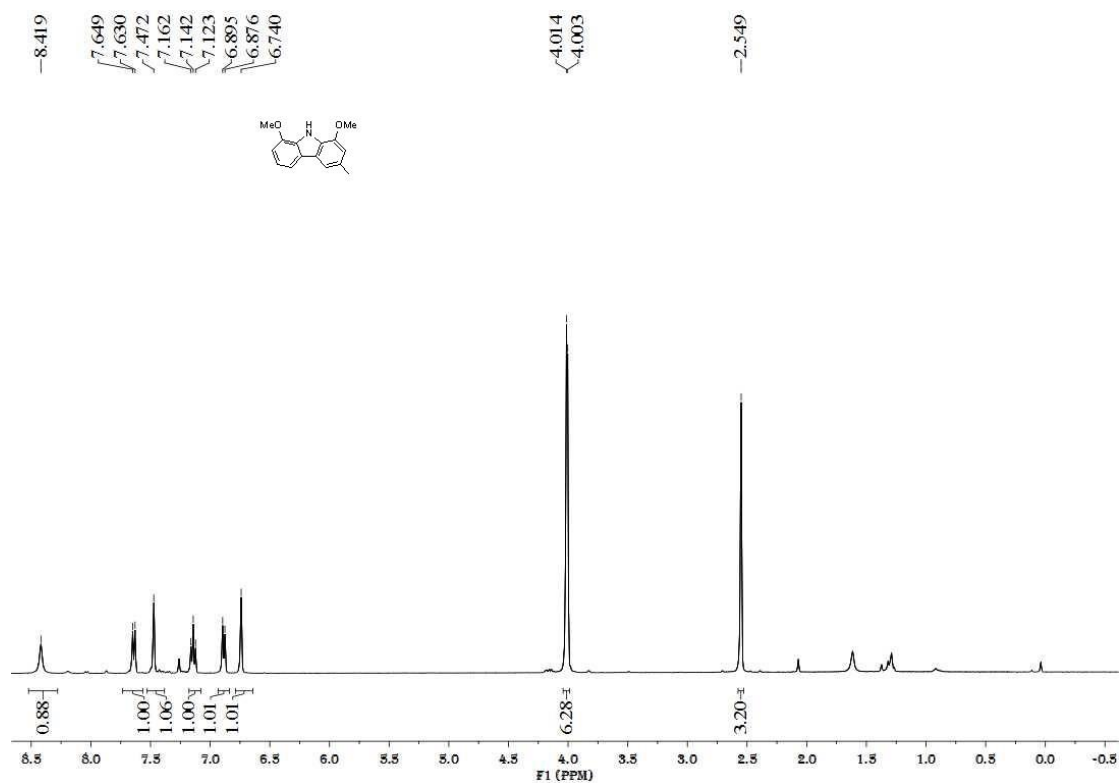
Figure S106. ^{13}C NMR spectrum of **12**, related to **Scheme 6**
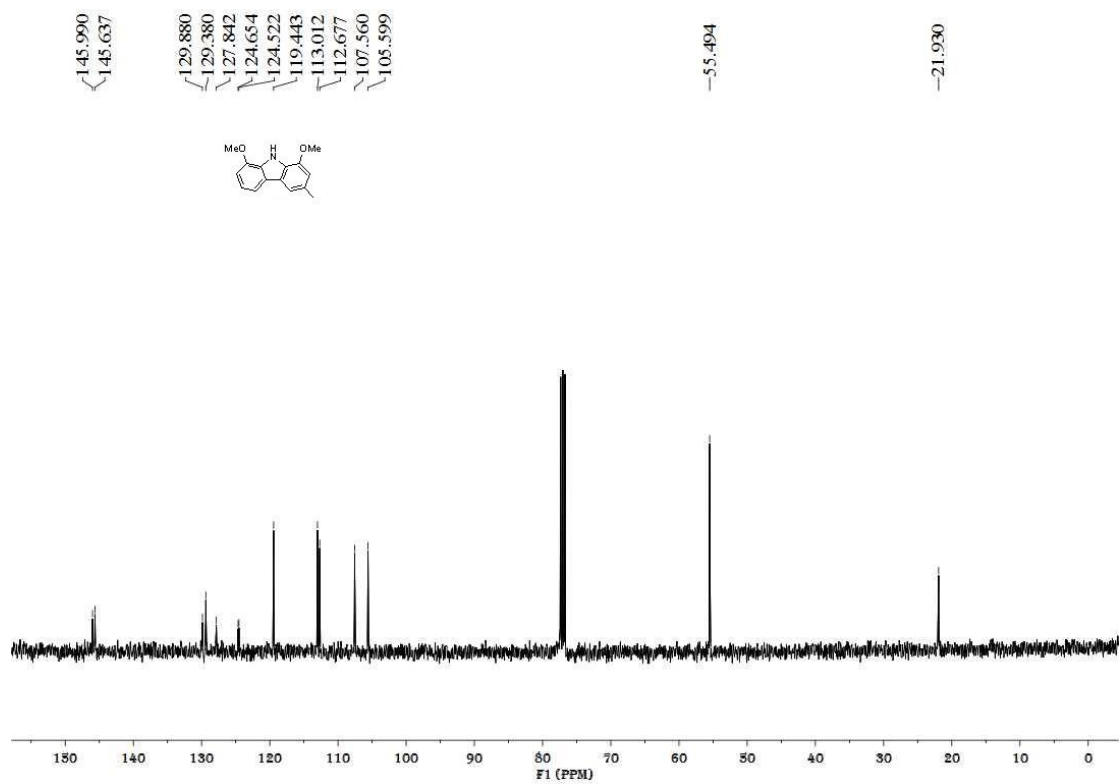
Figure S107. ^{1}H NMR spectrum of **13**, related to **Scheme 6**
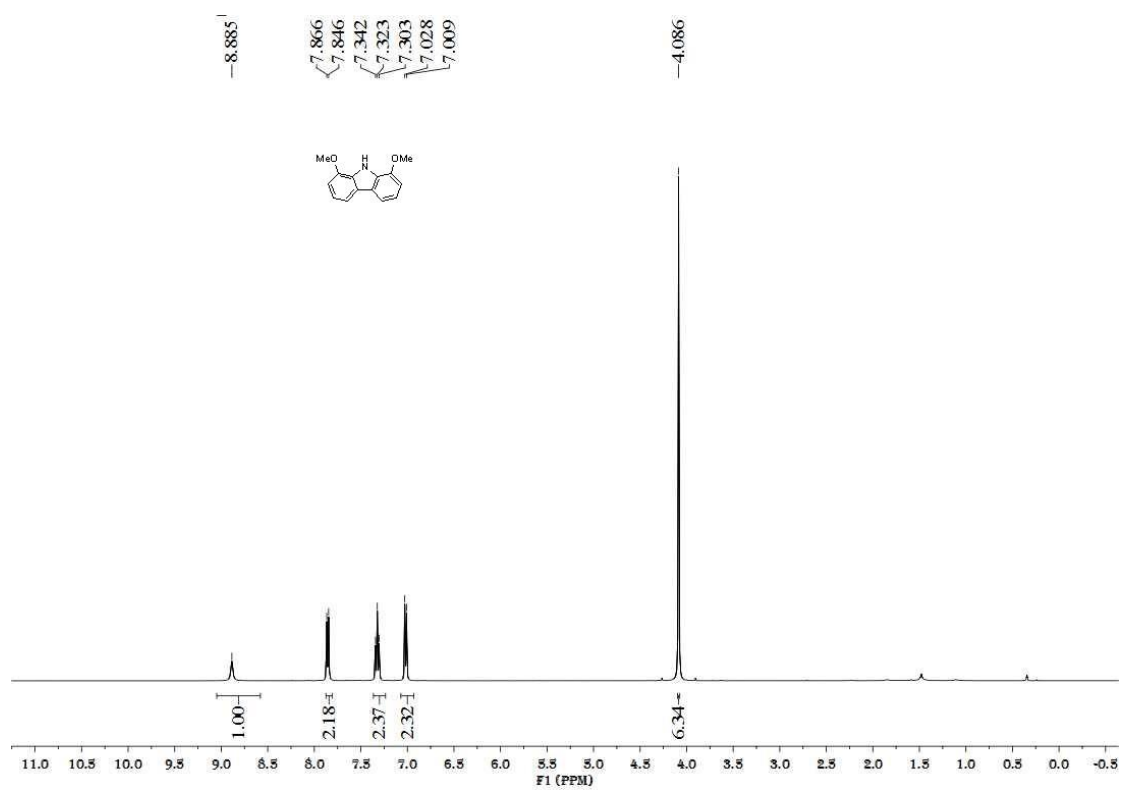
Figure S108. ^{13}C NMR spectrum of **13**, related to **Scheme 6**
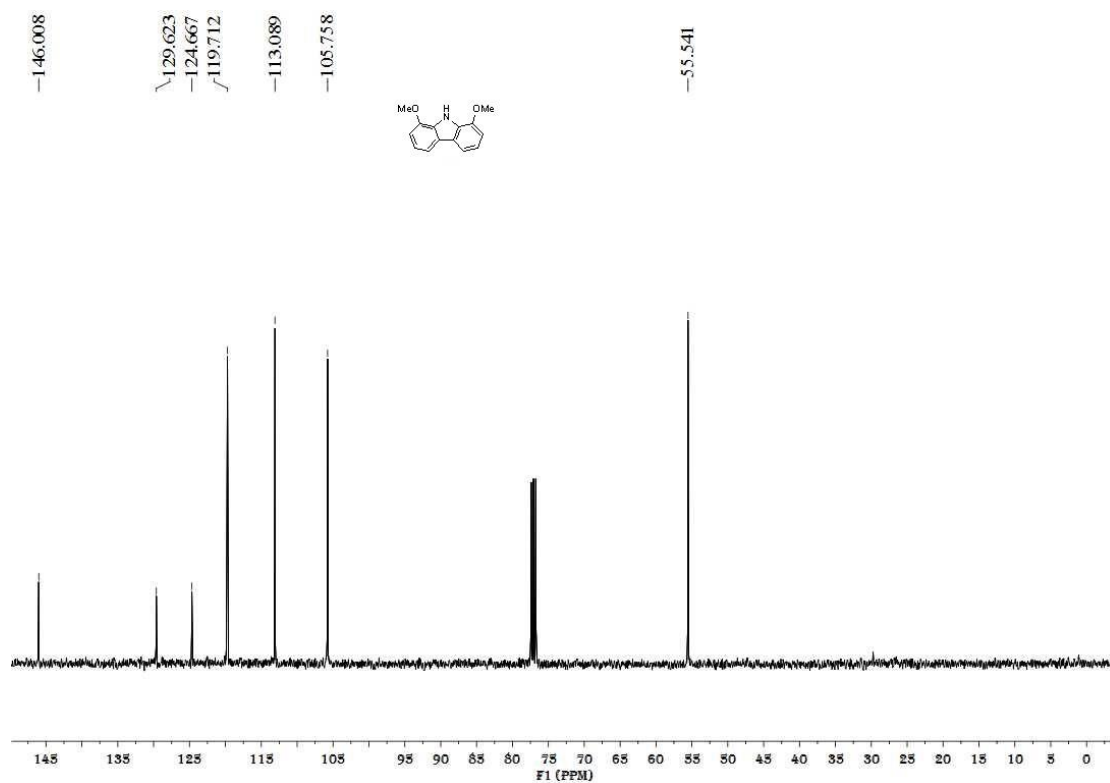
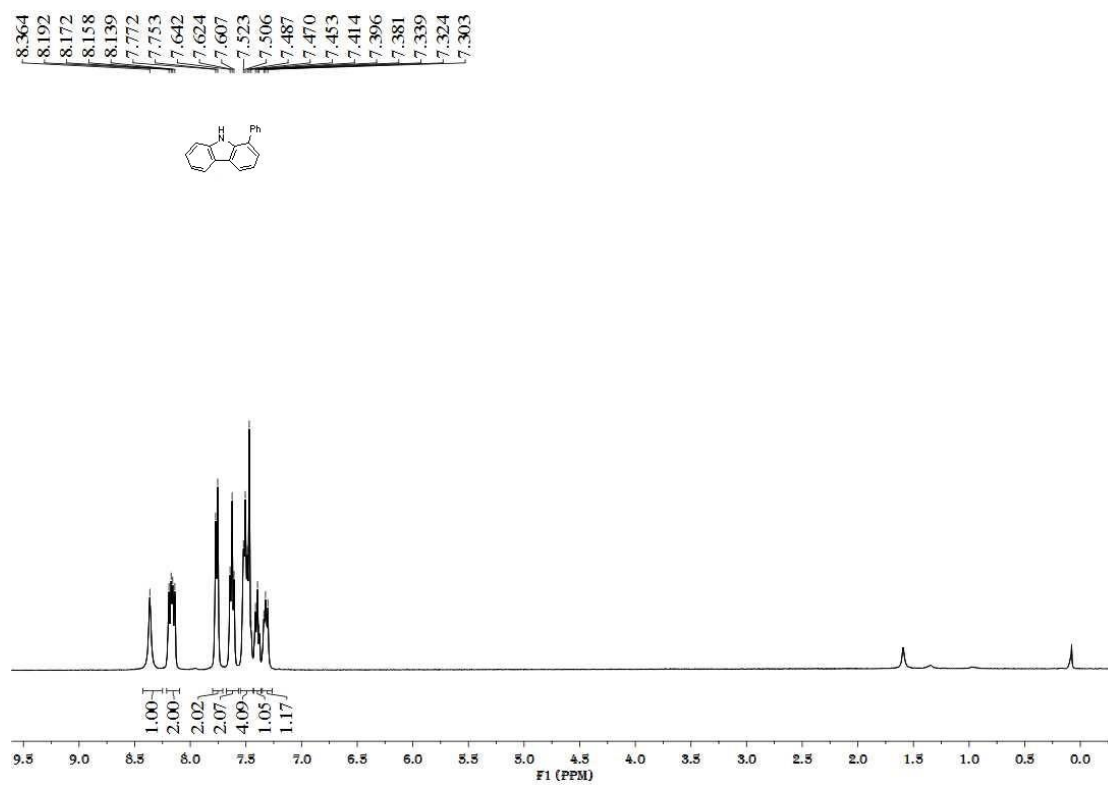**Figure S109**. ^{1}H NMR spectrum of **14**, related to **Scheme 6**
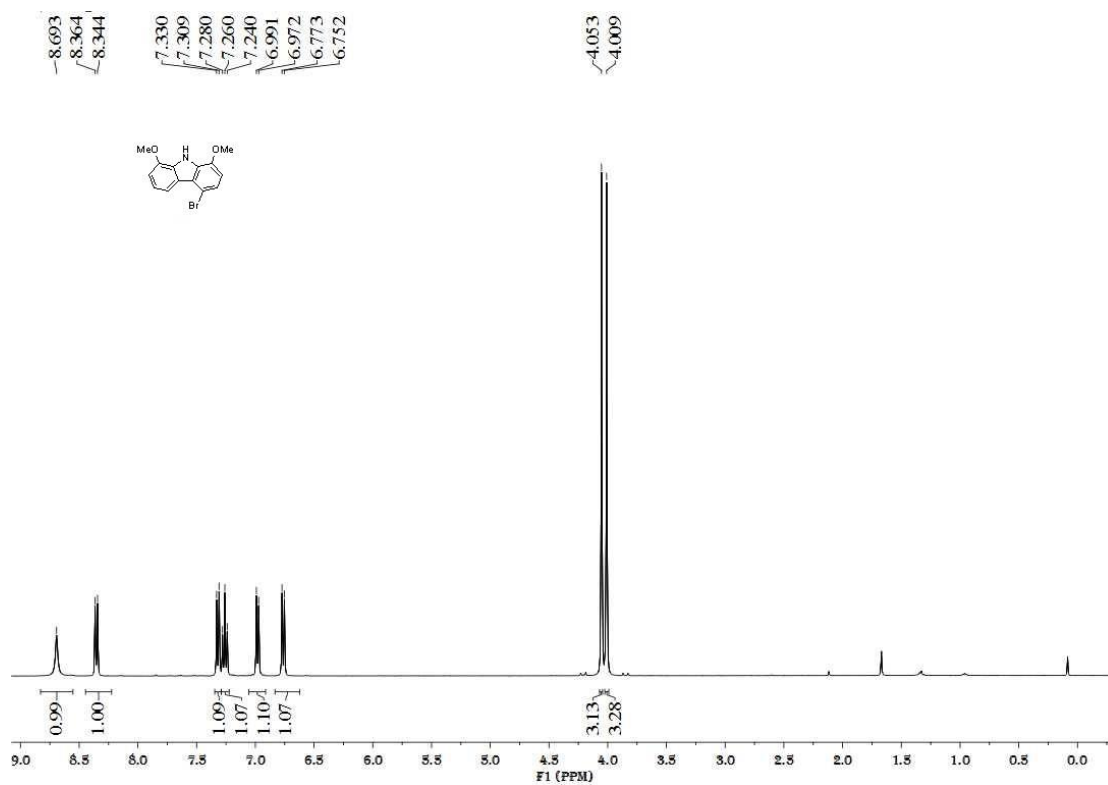
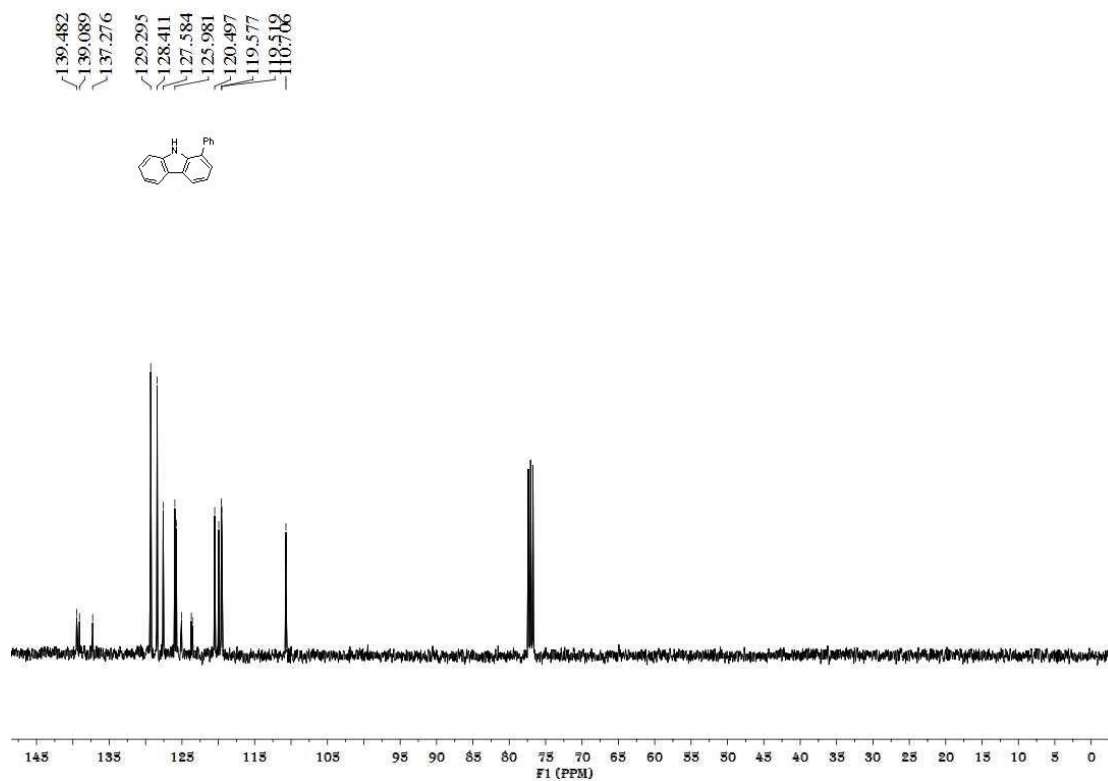**Figure S110**. ^{13}C NMR spectrum of **14**, related to **Scheme 6**
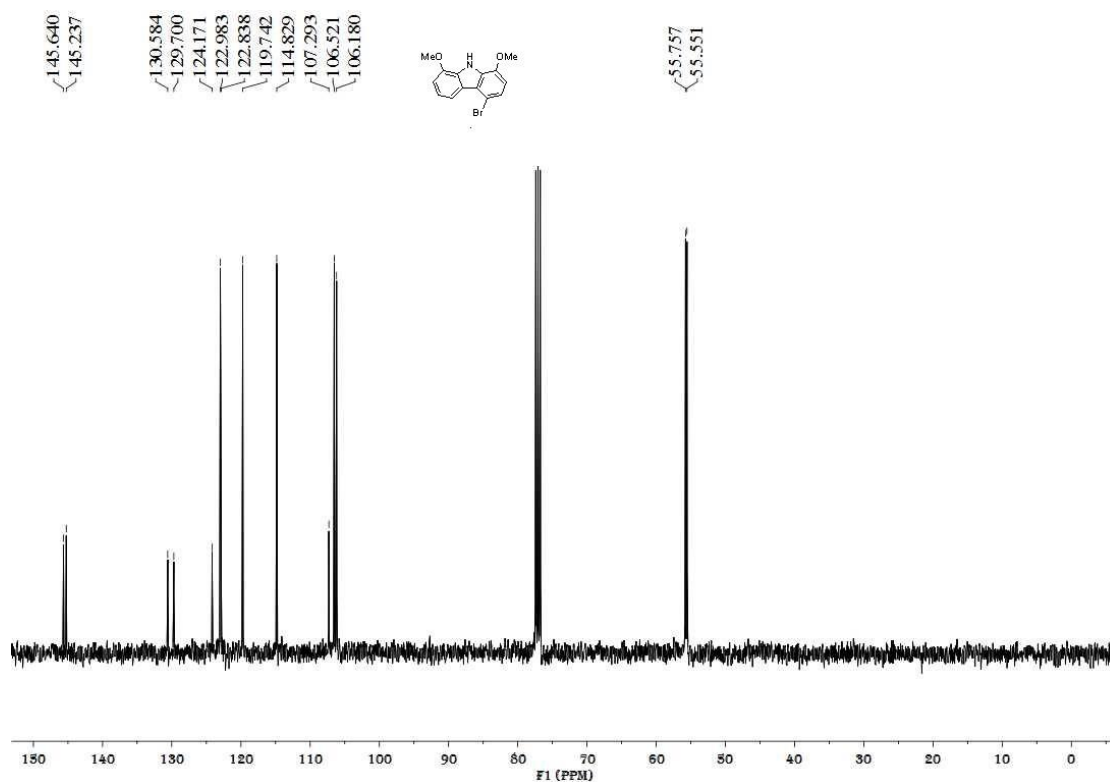
Figure S111. ^{1}H NMR spectrum of **15**, related to **Scheme 6**
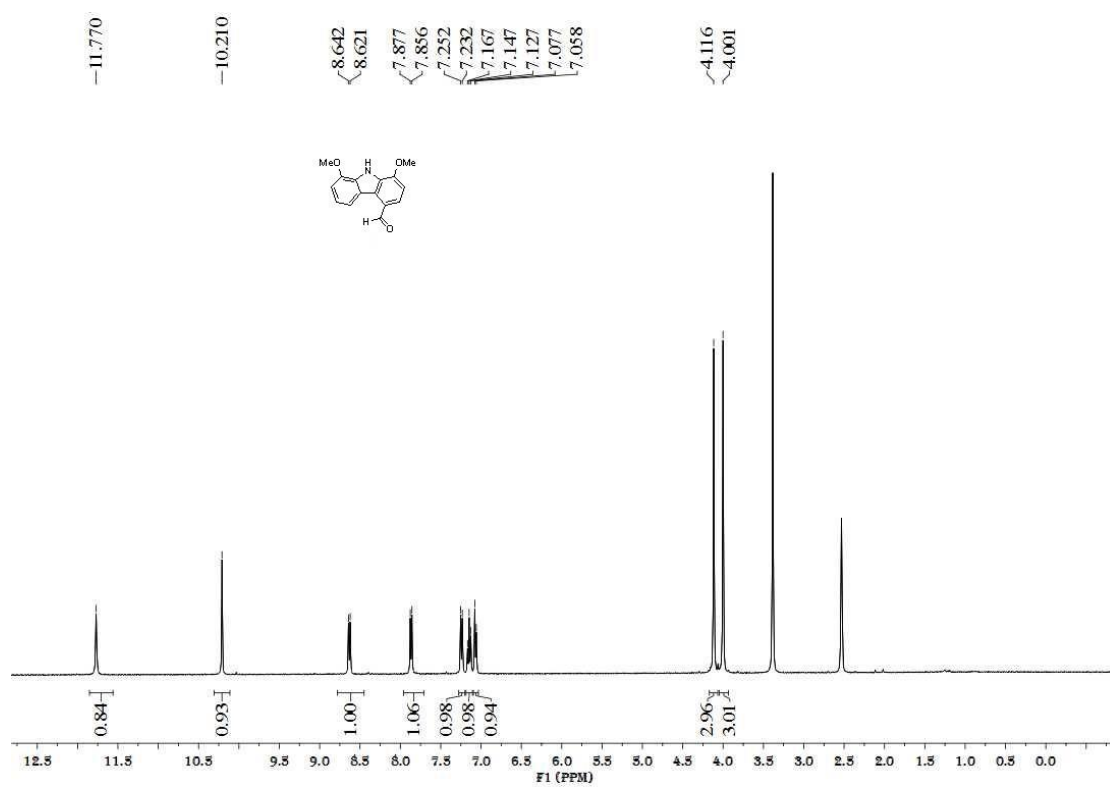
Figure S112. ^{13}C NMR spectrum of **15**, related to **Scheme 6**

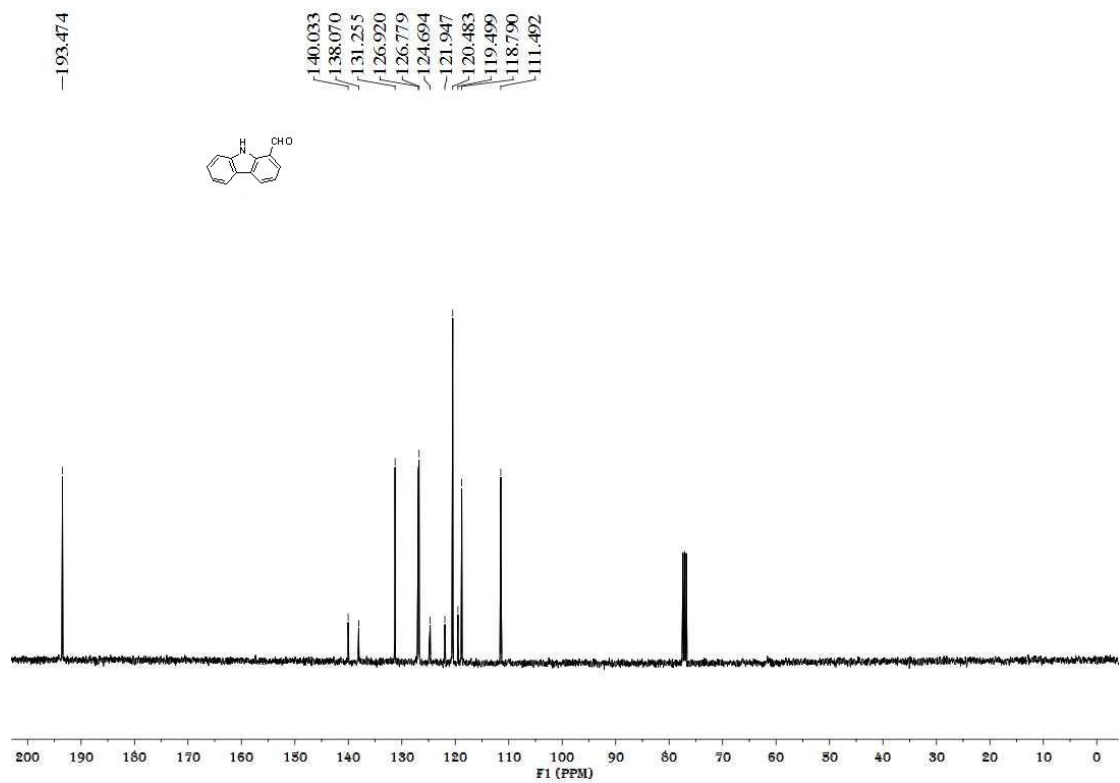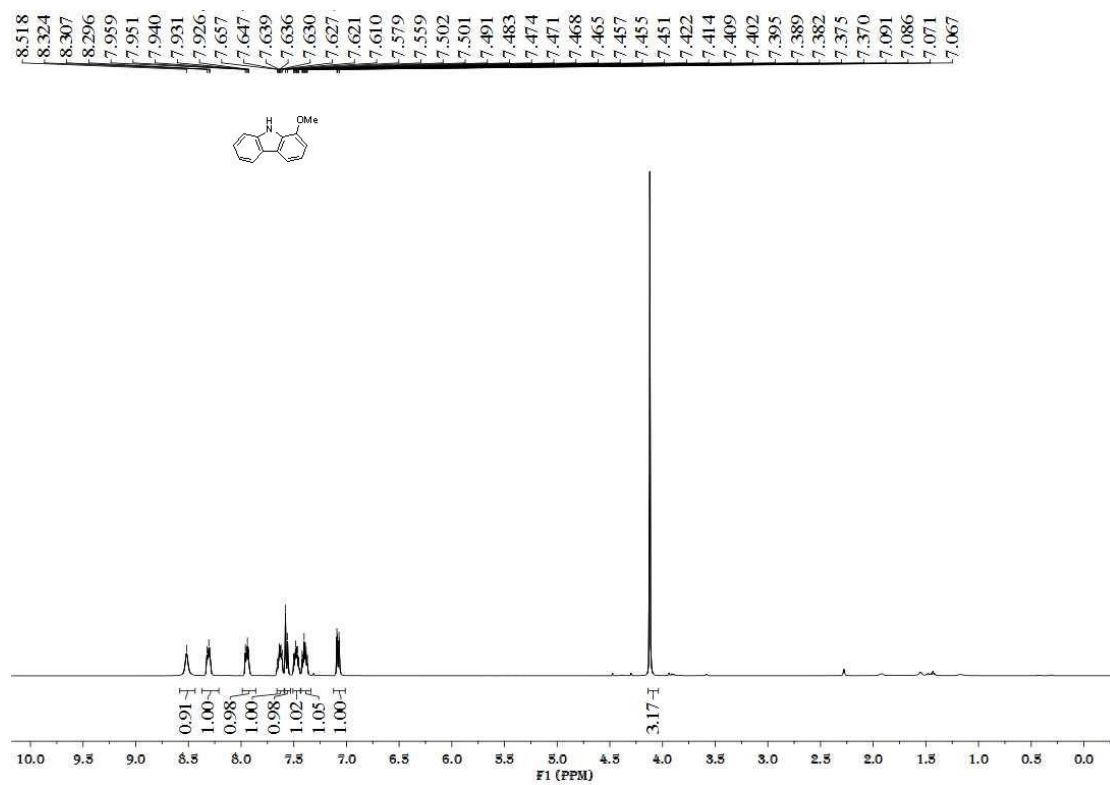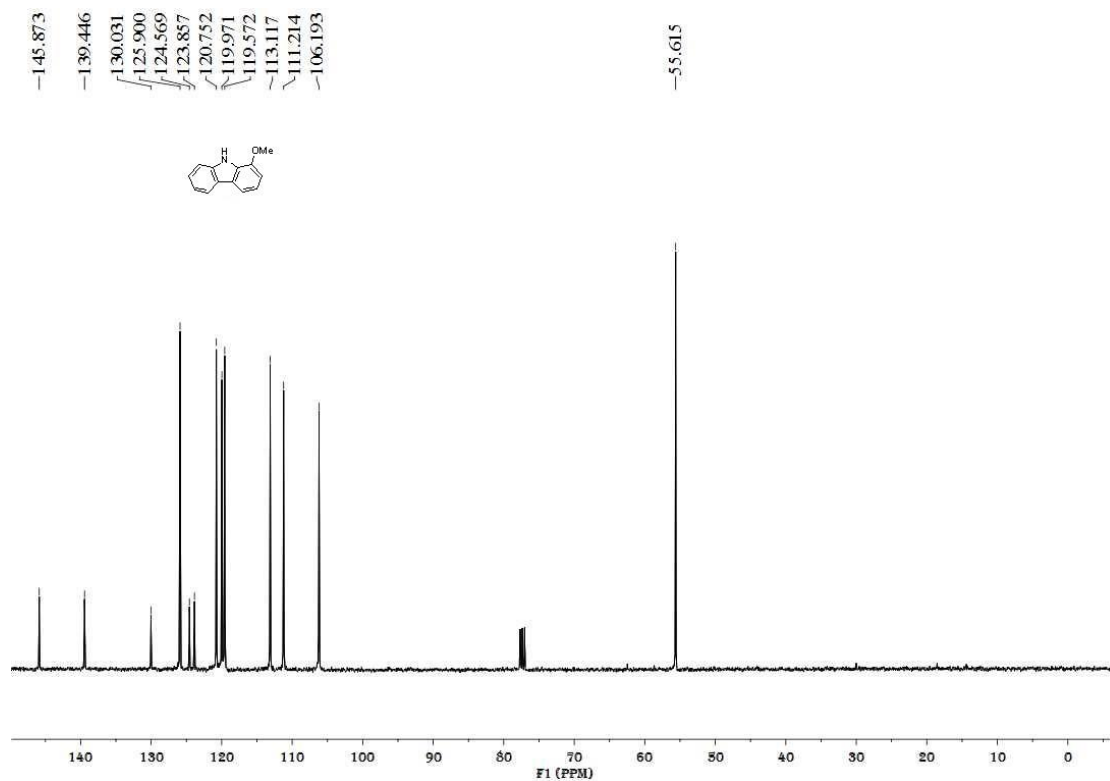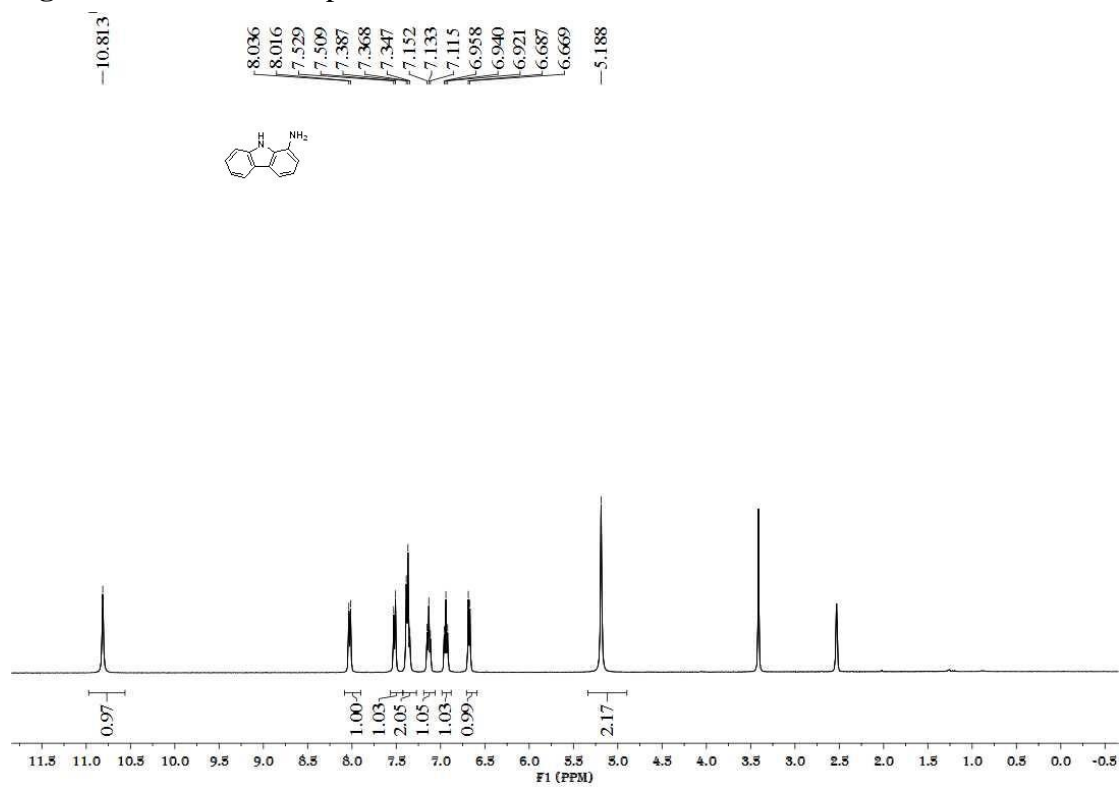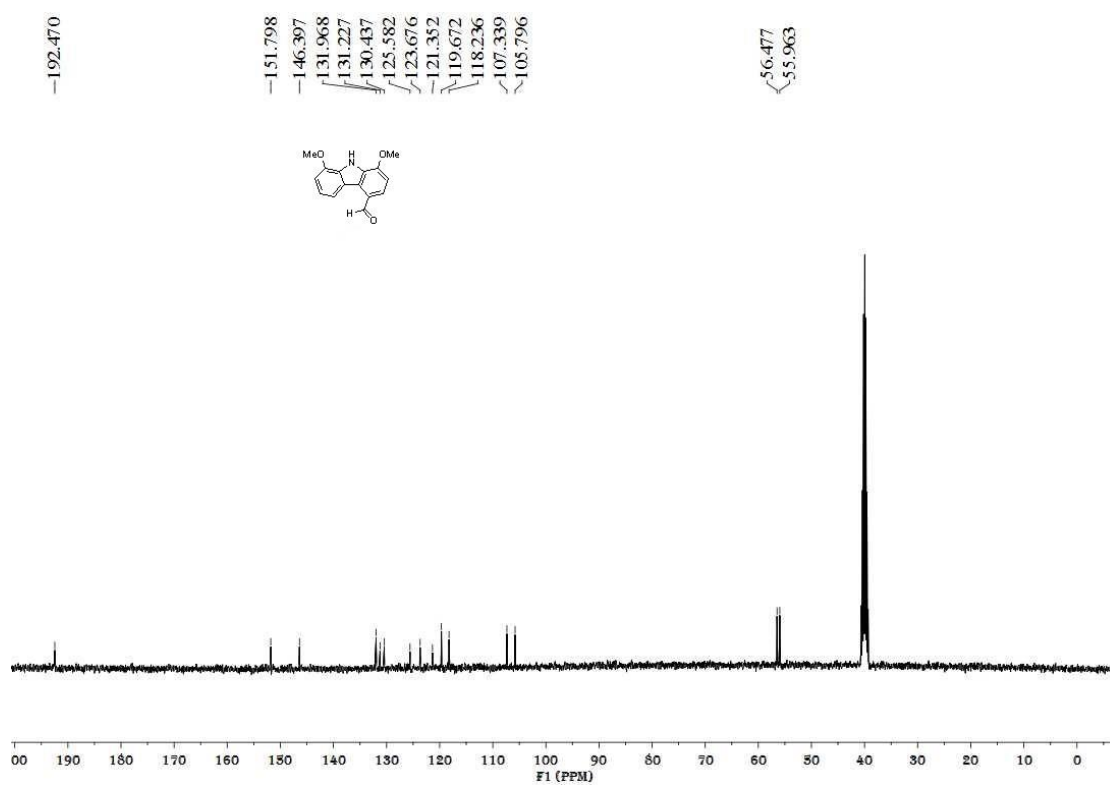**Figure S113**. ^{1}H NMR spectrum of **16**, related to **Scheme 6**
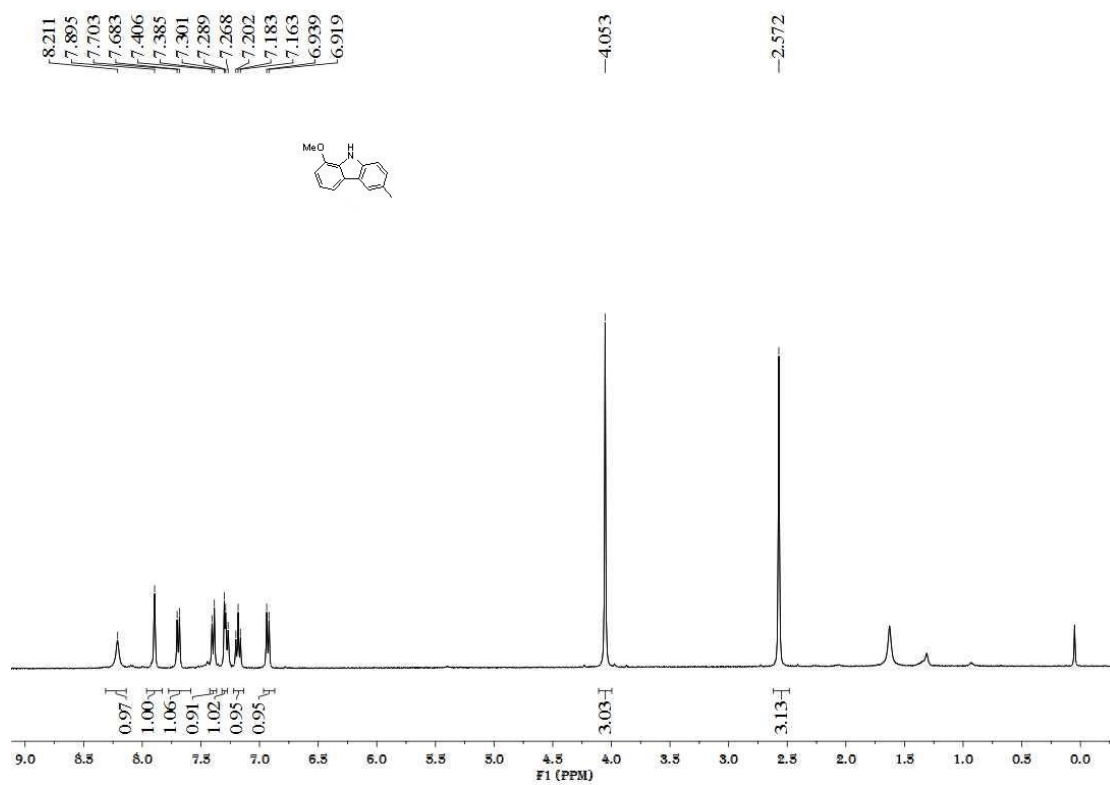
Figure S114. ^{13}C NMR spectrum of **16**, related to **Scheme 6**
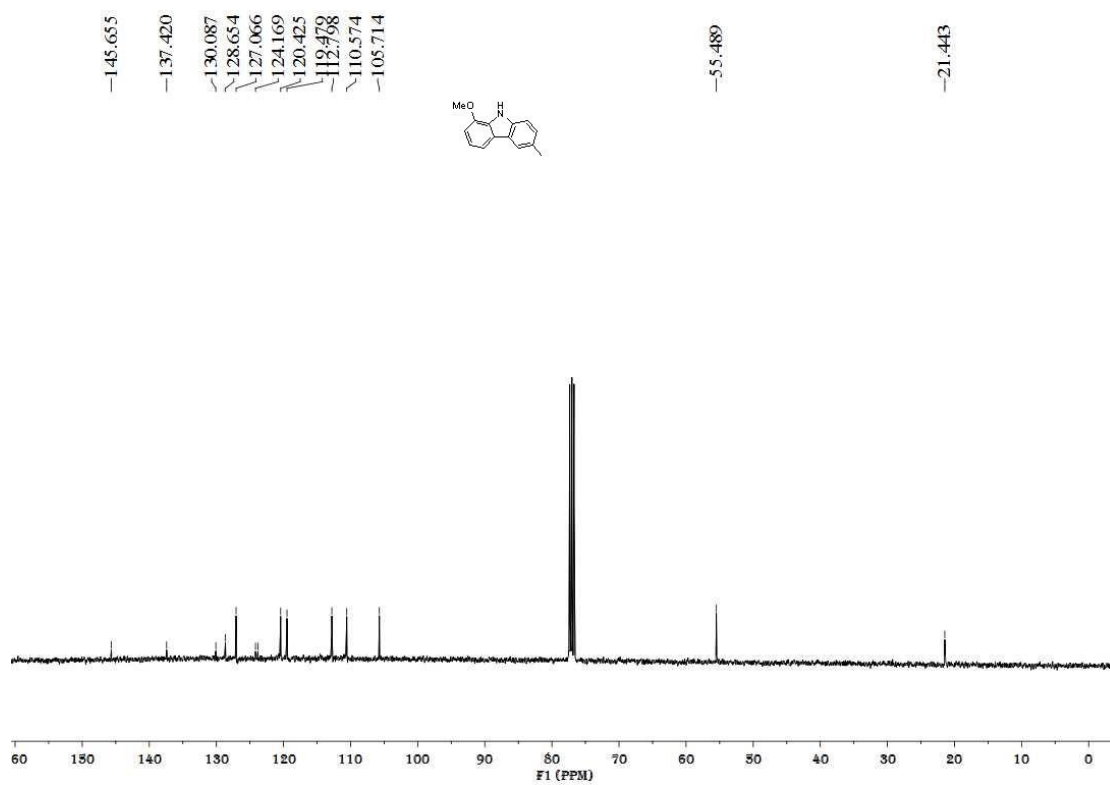
Figure S115. ^{1}H NMR spectrum of **8D-2a**, related to **Scheme 2**

8.263
8.073
8.054
8.026
8.007
7.585
7.566
7.495
7.471
7.300
7.281
7.260
7.150
7.130
7.111

0.91
1.00
0.98
1.02
1.20
1.09
1.07

8.5 8.0 7.5 7.0 6.5 6.0 5.5 5.0 4.5 4.0 3.5 3.0 2.5 2.0 1.5 1.0 0.5 0.0
F1 (PPM)
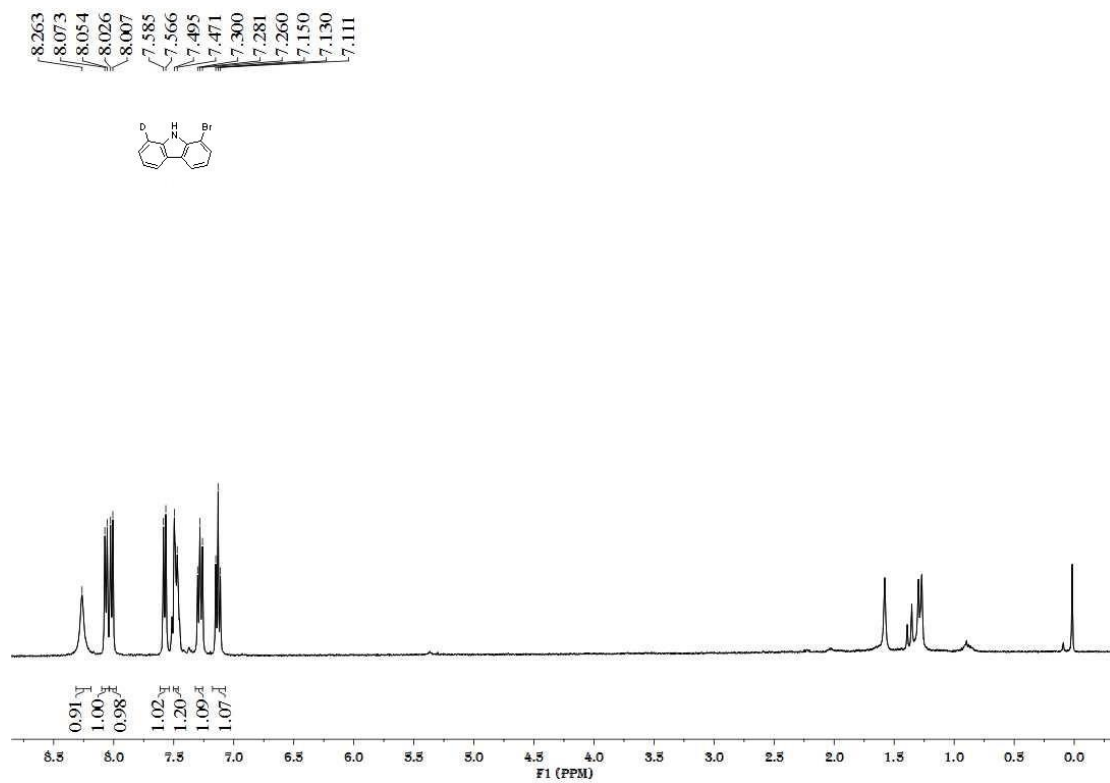
Figure S116. ^{13}C NMR spectrum of **8D-2a**, related to **Scheme 2**

139.106
127.978
126.566
126.458
124.636
120.855
120.571
120.106
119.342
117.051
104.124

45 135 125 115 105 95 90 85 80 75 70 65 60 55 50 45 40 35 30 25 20 15 10 5 0 -5
F1 (PPM)
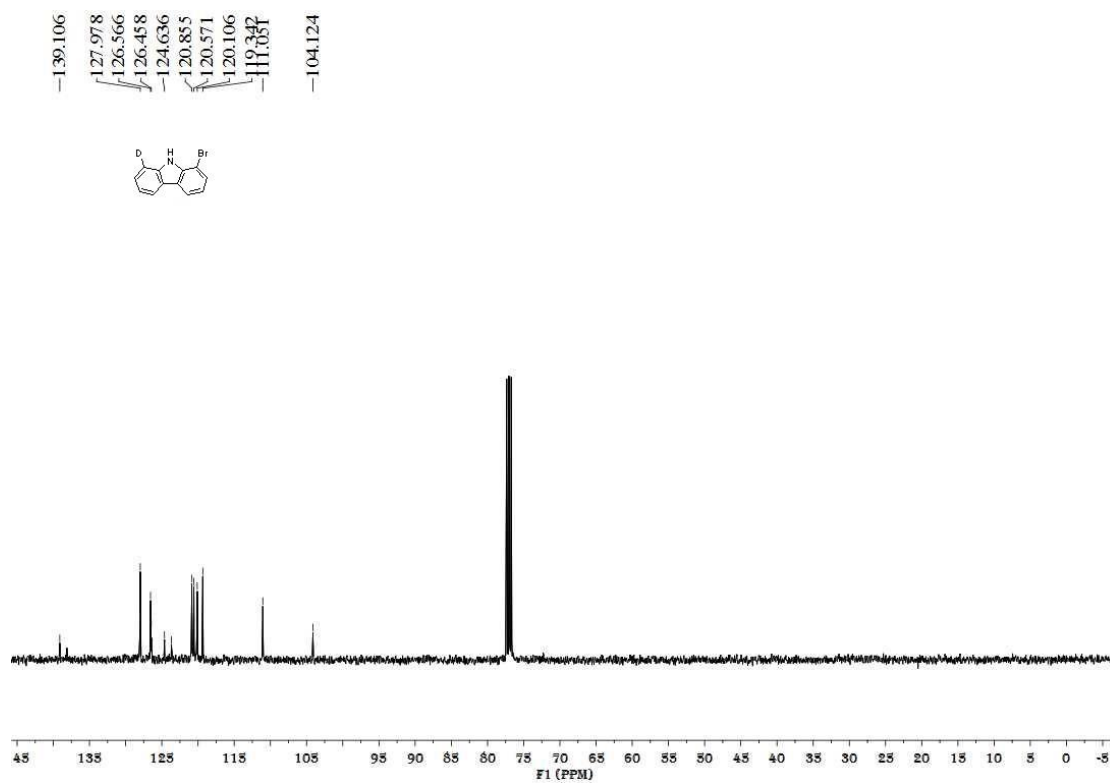
Transparent Methods

General information

Air- and moisture-sensitive syntheses were performed under argon atmosphere. Fe(OTf)$_3$ was purchased from Alfa, and Fe(OTs)$_3$ was purchased from Energy Chemical. Other chemicals were purchased from Adamas, Aldrich, TCI, Alfa etc. Unless otherwise noted, all commercial reagents were used without further purification. And the NMR spectroscopy was in full accordance with the data in the literature. The products of halogenation were characterized by ^{1}H NMR, ^{13}C NMR, MS and HRMS spectroscopy. ^{1}H and ^{13}C NMR spectra were recorded on Zhongke Niujin WNMR-I 400 (400 MHz). Chemical shift δ (ppm) was given relative to solvent: references for CDCl$_3$ were 7.26 ppm (^{1}H NMR) and 77.0 ppm (^{13}C NMR), and for d-DMSO were 2.50 ppm (^{1}H NMR) and 39.60 ppm (^{13}C NMR), and for d-toluene were 2.08, 6.97, 7.01, 7.09 ppm (^{1}H NMR), and for d-benzene were 7.16 ppm (^{1}H NMR), ^{13}C NMR spectra were acquired on a broad band decoupled mode. And for the ^{13}C NMR spectra of the ^{13}C-labelled compounds, the coupling was not analyzed due to complexity. Multiplets were assigned as s (singlet), d (doublet), dd (doublet doublet), and m (multiplet) etc. EI (Electron impact) mass spectra were recorded on a GCMS-QP2010 SE spectrometer (70 eV). ESI (electrospray ionization) high resolution mass spectra were recorded on an Agilent Technologies 6530 TOF LC/MS. UV-vis spectra were recorded on an Agilent 8454 spectrophotometer. All measurements were carried out at room temperature unless otherwise stated.

Computational methods （Fox et al., 2013）

All calculations were performed by Gaussian 09 D.01 using the range-separated hybrid WB97XD functional including dispersion correction. The dispersion correction has been proved to be critical in describing the regioselectivity of Fe-catalyzed reactions. For geometry optimizations, we used double-zeta polarized basis set 6-31g(d) for H, C, N, O, F atoms and Lanl2dz for Fe and S atom (WB97XD/B1). Frequency calculations at the same level were calculated to verify either local minima or transition states and to estimate the thermal corrections Gibbs free energy at 298K. Then, single-point energies of the optimized structures was calculated with a larger triple-zeta basis set 6-311+G(d,p) (WB97XD/B2) for non-metallic atoms and Lanl2dz for Fe and S.

Screening of the reaction conditions
Table S1: Investigation of different catalysts for *ortho*-bromination of 1a, related to Table 1ᵃ
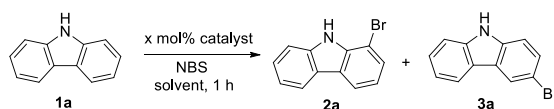
Entry	Catalyst	x	T (°C)	Yield (2a, %)	Sel. (2a, %)[b]
1	Pd(CH₃CN)₄(OTf)₂	10	90	59	76
2	FeBr₃	10	90	12	14
3	FeBr₂	10	90	13	16
4	Fe(OAc)₃	10	90	13	15
5	Fe(acac)₂	10	90	9	9
6	Fe(BF₄)₂	10	90	18	19
7	Fe(OTf)₂	10	90	9	10

[a]Reaction conditions: **1a** (0.20 mmol), NBS (1.1 equiv.), toluene (2.0 mL), in the absence of light at 90°C. Yields and o/p ratios determined by GC using n-hexadecane as an internal standard. [b]**2a**/(**2a**+**3a**).

Table S2: Investigation of different solvents for *ortho*-bromination of 1a, related to Table 1[a]
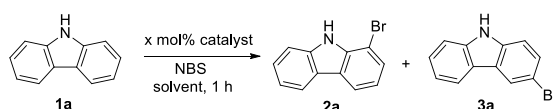
Entry	Catalyst	x	solvent	Yield (2a, %)	Sel. (2a, %)[b]
1	Fe(OTf)₃	10	toluene	69	81
2	Fe(OTf)₃	10	DCE	20	28
3	Fe(OTf)₃	10	CH₃CN	4	4
4	Fe(OTf)₃	10	1,4-Dioxane	9	11
5	Fe(OTf)₃	10	DMF	1	1
6	Fe(OTf)₃	10	THF	7	8

[a]Reaction conditions: **1a** (0.20 mmol), NBS (1.1 equiv.), solvent (2.0 mL), in the absence of light at 90°C. Yields and o/p ratios determined by GC using n-hexadecane as an internal standard. [b]**2a**/(**2a**+**3a**).

Scheme S1: *Ortho*-halogenation Reaction of Carbazoles, related to Scheme 4
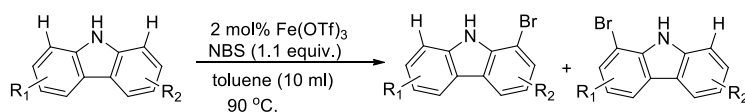
To a solution of the carbazole (0.2 mmol), catalyst Fe(OTf)₃ (0.004 mmol, 2 mol%) in toluene (10 mL) was added NBS (0.22 mmol, 1.1 equiv) at 90 °C in the absence of light. The mixture was stirred at 90 °C for 1h - 6 h. The solution was diluted with water (10 mL) and extracted with CH₂Cl₂ (3 × 10 mL). The combined organic extracts were washed with brine, dried with anhydrous Na₂SO₄, filtered and concentrated under vacuum. The residue was purified by column chromatography on silica gel (eluted with ethyl acetate/ hexane 1:20 to 1:2) to yield the corresponding *ortho*-bromination product.
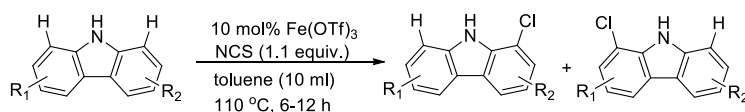
To a solution of the carbazole (0.2 mmol, 1.0 equiv.), catalyst Fe(OTf)₃ (0.02 mmol, 0.1 equiv.) in

toluene (10 mL) was added NCS (0.22 mmol, 1.1 equiv.) at 110 °C in the absence of light. The mixture was stirred at 110 °C for 6 - 12 h. The solution was diluted with water (10 mL) and extracted with CH$_2$Cl$_2$ (3 × 10 mL). The combined organic extracts were washed with brine, dried with anhydrous Na$_2$SO$_4$, filtered and concentrated under vacuum. The residue was purified by column chromatography on silica gel (eluted with ethyl acetate/ hexane 1:20 to 1:2) to yield the corresponding *ortho*-chlorination product.

Scheme S2: *Ortho*-chlorination Reaction of *N*-Methylaniline, related to Scheme 3
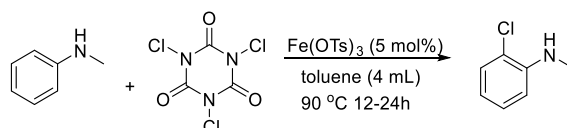
To a solution of the *N*-Methylaniline (0.2 mmol, 1.0 equiv.), catalyst Fe(OTs)$_3$ (0.01 mmol, 0.05 equiv.) in toluene (4 mL) was added TCCA (0.07 mmol, 0.35 equiv.) at 90 °C in the absence of light. The mixture was stirred at 90 °C for 12 - 24 h. The solution was diluted with water (10 mL) and extracted with CH$_2$Cl$_2$ (3 × 10 mL). The combined organic extracts were washed with brine, dried with anhydrous Na$_2$SO$_4$, filtered and concentrated under vacuum. The residue was purified by column chromatography on silica gel (eluted with ethyl acetate/ hexane 1:20 to 1:2) to yield the corresponding ortho-chlorination product.

Table S3: Optimization of *Ortho*-bromination Reaction of Phenol, related to Scheme 7
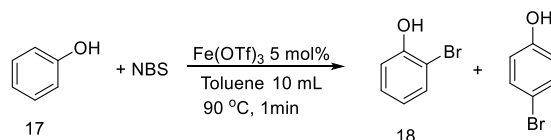
Entry	Catalyst	T (°C)	Conv(17, %)	Yield (18, %)	o / p
1	/	90	52	16	62 / 38
2	Fe(OTf)$_3$	90	99	85	96 / 4

[a]Reaction conditions: **17** (0.20 mmol), NBS (1.1 equiv.), toluene (10.0 mL), in the absence of light at 90 °C. Yields and *o/p* ratios determined by GC using *n*-hexadecane as an internal standard.

## Scheme S3: *Ortho*-bromination Reaction of Phenol, related to Scheme 7
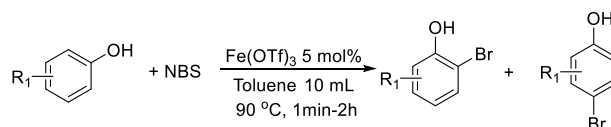
To a solution of the Phenol (0.2 mmol), catalyst Fe(OTf)$_3$ (0.01 mmol, 5 mol%) in toluene (10 mL) was added NBS (0.22 mmol, 1.1 equiv) at 90 °C in the absence of light. The mixture was stirred at 90 °C for 1min - 2 h. The solution was diluted with water (10 mL) and extracted with CH$_2$Cl$_2$ (3 × 10 mL). The combined organic extracts were washed with brine, dried with anhydrous Na$_2$SO$_4$, filtered and concentrated under vacuum. The residue was purified by column chromatography on silica gel (eluted with ethyl acetate/ hexane 1:20 to 1:2) to yield the corresponding *ortho*-bromination product.

Preparations of target product 7-10

To a dry 25 mL round bottom flask equipped with a stir bar were added **2a** (0.5 mmol, 1.0 equiv.), 4-chlorophenylboronic acid (0.55 mmol, 1.1 equiv.), K_2CO_3 (2.0 mmol, 4.0 equiv.), and $PdCl_2(PPh_3)_2$ (0.025 mmol, 0.05 equiv.). Toluene (6 mL), 4 mL of H_2O, and 2 mL of EtOH were added, and the resulting mixture was heated to 95 ˚C. After 16 hours, the reaction mixture was cooled, and the mixture was diluted with 25 mL of saturated aqueous NH_4Cl and 25 mL of CH_2Cl_2. The resulting biphasic solution was separated. The organic phase was washed 1 $\times$ 25 mL of water and 1 $\times$ 25 mL of saturated aqueous $NaHCO_3$. The organic phase was dried over Na_2SO_4 and decanted. The filtrate was concentrated in vacuo to afford an oil.

To a suspension of sodium hydride (1.3 mmol) in dry THF (8 mL), compound **2a** (0.5 mmol) was added and stirred at 0 °C under nitrogen for 40 min before the temperature was lowered to -78 °C. To the mixture a solution of n-butyl lithium (4 mL of a 1.7 M solution in hexane, 6.8 mmol) was added dropwise by a syringe over 3 min. The mixture was then allowed to reach rt over 1 h before being cooled again to -78 °C. Dry DMF (1 mL, 13 mmol) was introduced into the reaction mixture via a syringe and the mixture was allowed to reach rt. The mixture was stirred for additional 1.5 h at rt before it was poured into a 1 M H_3PO_4 solution (40 mL) which afforded a fine precipitate. The precipitate was filtered through a bed of celite and the product was extracted in hot pyridine (20 mL). The solution was diluted with water (20 mL) to induce precipitation which was then suction filtered. The solid material was repeatedly washed with diethyl ether and the yellowish impurity was completely removed.

DMF (6 mL), CuI (95%, 0.48 mmol), and **2a** (0.5 mmol) were added to a solution of metallic sodium (9.3 mmol) in absolute MeOH (1.5 mL). The reaction mixture was refluxed (oil bath temperature) 120 °C) for 3 h under an argon atmosphere. After the reaction, EtOAc (20 mL) was added to the reaction mixture and the insoluble materials were filtered through Celite and washed with EtOAc. The filtrate was washed with brine, dried over Na_2SO_4, filtered, and concentrated. The residue was chromatographed on a column of silica gel using 10:1 *n*-hexane/EtOAc to give 1-methoxy-9*H*-carbazole.

2a (0.5 mmol), aqueous ammonia (0.15 mL, 2.5 mmol), CuI (0.1 mmol), 2-carboxylic acid-quinoline-*N*-oxide (0.2 mmol), and K_2CO_3 (1.3 mmol) in 1 mL of DMSO was heated at 80 °C for 23 h. Then the cooled mixture was partitioned between water and ethyl acetate. The organic layer was separated, and the aqueous layer was extracted with ethyl acetate (3 x 10 mL). The combined organic layers were washed with brine, dried over Na_2SO_4, and concentrated under vacuum. The residue was purified by chromatography on silicon gel with petroleum ether and ethyl acetate as eluent to provide the primary aryl amine.

Catalyst recycling

Initially, to a solution of the carbazole (0.2 mmol, 1.0 equiv.), catalyst $Fe(OTf)_3$ (0.004 mmol, 0.02 equiv.) in toluene (10 mL) was added NBS (0.22 mmol, 1.1 equiv.) at 90 ºC in the absence of light. The mixture was stirred at 90 ºC for 1 h affording *ortho*-brominated product 83% yield and 90% selectivity. The first round recycling was performed by allowing reaction mixture to cool to room temperature and additional carbazole (0.2 mmol, 1.0 equiv.), NBS (0.22 mmol, 1.1 equiv.) were added to the reaction and stirred at 90 ºC for 1 h providing product in 80% yield 89% selectivity. The second and third rounds were performed in a similar fashion giving product yields in 79% and 75%, and selectivities in 79% and 75%, respectively.

Table S4 : Catalyst recycling, related to Scheme 4
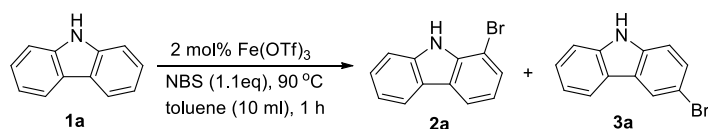
Catalyst recycling	Yield, (2a %)	2a /(2a+ 3a)
0 round	83	90%
First round	80	89%
Second round	79	87%
Third round	75	80%

Schenme S4 :Reaction scale-up, related to Scheme 4

To a solution of the **1a** (300 mmol, 1.0 equiv.), catalyst Fe(OTf)$_3$ (6.0 mmol, 0.02 equiv.) in toluene (200 mL) was added 330 mmol NBS (divided into five portions, once of addition every 60 minutes) at 90 °C in the absence of light. The mixture was stirred at 90 °C for 1 h. 42.6 g of **2a** was obtained through recrystallization.

Schenme S5 : The total synthesis of natural compounds., related to Scheme 6

2l
78% yield (Table 2)

16

Mukolidine
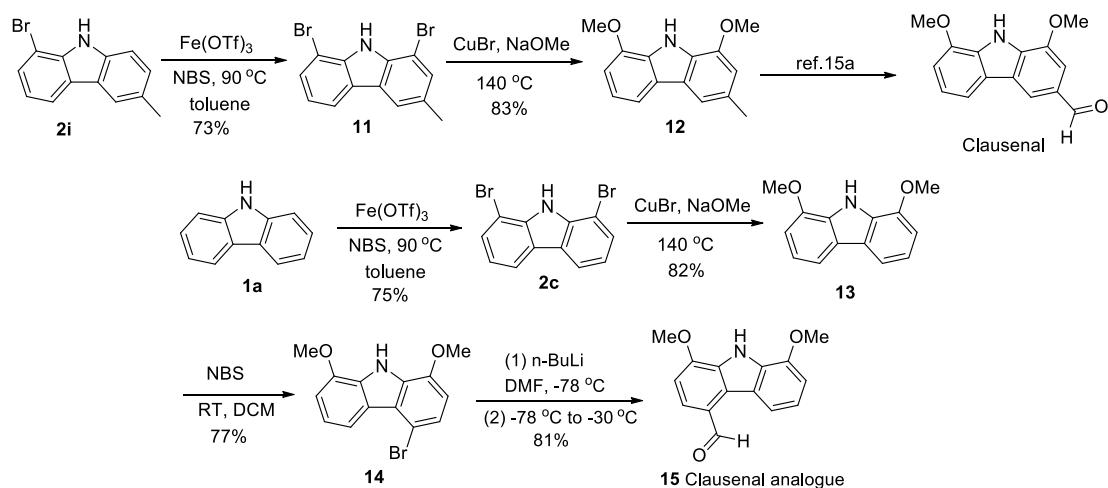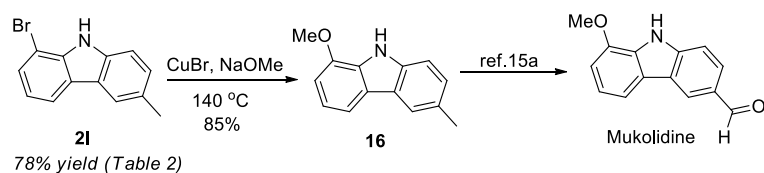
Preparations of target product 11-16

1,8-dibromo-3-methyl-9*H*-carbazole (11)
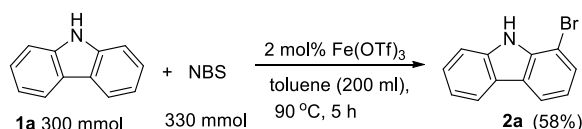
To a solution of **2i** (0.2 mmol, 1.0 equiv.), catalyst Fe(OTf)$_3$ (0.004 mmol, 0.02 equiv.) in toluene (10 mL) was added NBS (0.22 mmol, 1.1 equiv.) at 90 ºC in the absence of light. The mixture was stirred at 90 ºC for 2 h. The solution was diluted with water (10 mL) and extracted with CH$_2$Cl$_2$ (3 × 10 mL). The combined organic extracts were washed with brine, dried with anhydrous Na$_2$SO$_4$, filtered and concentrated under vacuum. The residue was purified by column chromatography on silica gel (eluted with ethyl acetate/ hexane 1:20 to 1:2) to yield the corresponding *ortho*-bromination product.

1,8-dimethoxy-3-methyl-9*H*-carbazole (12) (Tamariz et al., 2017)

DMF (8 mL), CuI (95%, 1.0 mmol), and **11** (0.5 mmol) were added to mixture of metallic sodium (18.6 mmol) in absolute MeOH (3.0 mL). The reaction mixture was refluxed (oil bath temperature) 120 °C) for 3 h under an argon atmosphere. After the reaction, EtOAc (40 mL) was added to the reaction mixture and the insoluble materials were filtered through Celite and washed with EtOAc. The filtrate was washed with brine, dried over Na$_2$SO$_4$, filtered, and concentrated. The residue was chromatographed on a column of silica gel using 10:1 *n*-hexane/EtOAc to give 1,8-dimethoxy-3-methyl-9*H*-carbazole.

1,8-dimethoxy-9H-carbazole (13) (Sperry et al., 2017)

DMF (8 mL), CuI (95%, 1.0 mmol), and **2c** (0.5 mmol) were added to the mixture of metallic sodium (18.6 mmol) in absolute MeOH (3.0 mL). The reaction mixture was refluxed (oil bath temperature) 120 °C) for 3 h under an argon atmosphere. After the reaction, EtOAc (40 mL) was added to the reaction mixture and the insoluble materials were filtered through Celite and washed with EtOAc. The filtrate was washed with brine, dried over Na$_2$SO$_4$, filtered, and concentrated. The residue was chromatographed on a column of silica gel using 10:1 *n*-hexane/EtOAc to give **13**.

4-bromo-1,8-dimethoxy-9*H*-carbazole (14)

To a solution of the **13** (0.5 mmol, 1.0 equiv.), NBS (0.55 mmol, 1.1 equiv.) in DMF (10 mL) (0.22 mmol, 1.1 equiv.) at 25 ºC in the absence of light. The mixture was stirred at 25 ºC for 10 h. The solution was diluted with water (10 mL) and extracted with CH$_2$Cl$_2$ (3 × 10 mL). The combined organic extracts were washed with brine, dried with anhydrous Na$_2$SO$_4$, filtered and concentrated under vacuum. The residue was purified by column chromatography on silica gel (eluted with ethyl acetate/ hexane 1:20 to 1:2) to yield the corresponding **14**.

### 1,8-dimethoxy-9*H*-carbazole-4-carbaldehyde (15)

To a suspension of sodium hydride (1.3 mmol) in dry THF (8 mL), compound **14** (0.5 mmol) was added and stirred at 0 °C under nitrogen for 40 min before the temperature was lowered to -78 °C. To the mixture a solution of *n*-butyl lithium (4 mL of a 1.7 M solution in hexane, 6.8 mmol) was added dropwise by a syringe over 3 min. The mixture was then allowed to reach rt over 1 h before being cooled again to -78 °C. Dry DMF (1 mL, 13 mmol) was introduced into the reaction mixture via a syringe and the mixture was allowed to reach rt. The mixture was stirred for additional 1.5 h at rt before it was poured into a 1 M H$_3$PO$_4$ solution (40 mL) which afforded a fine precipitate. The precipitate was filtered through a bed of celite and the product was extracted in hot pyridine (20 mL).

The solution was diluted with water (20 mL) to induce precipitation which was then suction filtered. The solid material was repeatedly washed with diethyl ether and the yellowish impurity was completely removed.

1-methoxy-6-methyl-9*H*-carbazole (16) (Tamariz et al., 2011)

DMF (6 mL), CuI (95%, 0.48 mmol), and **2l** (0.5 mmol) were added to a solution of metallic sodium (9.3 mmol) in absolute MeOH (1.5 mL). The reaction mixture was refluxed (oil bath temperature) 120 °C) for 3 h under an argon atmosphere. After the reaction, EtOAc (20 mL) was added to the reaction mixture and the insoluble materials were filtered through Celite and washed with EtOAc. The filtrate was washed with brine, dried over Na_2SO_4, filtered, and concentrated. The residue was chromatographed on a column of silica gel using 10:1 *n*-hexane/EtOAc to give **16**.

Schenme S5 : Control experiments, related to Table 1
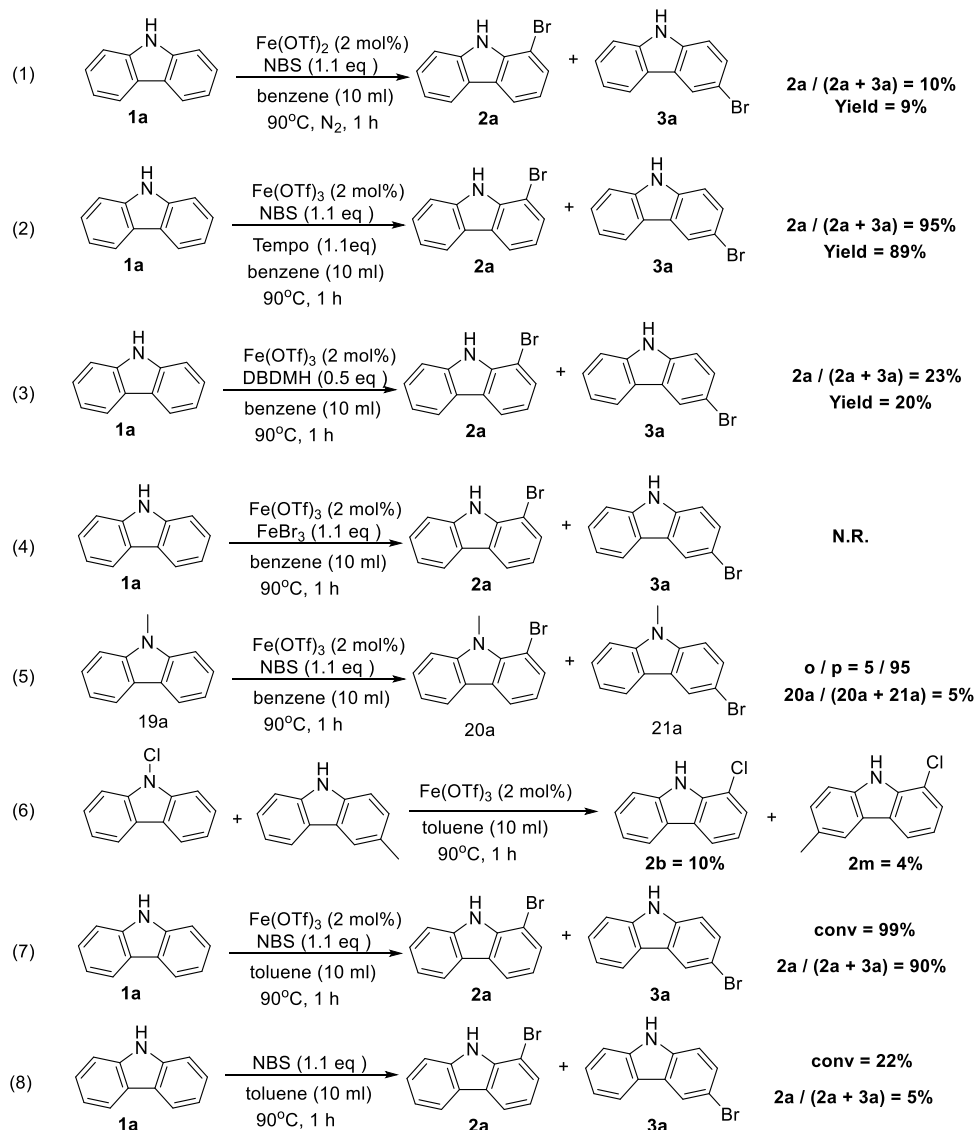
## Schenme S6 : KIE study, related to Scheme 2
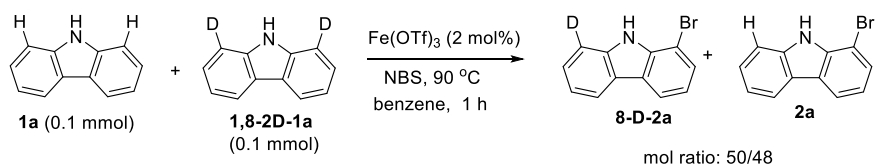
Preparations of target product 18

1-bromo-8-deuterium-9*H*-carbazole (18)

To a solution of the **1,8-2D-1a** (0.2 mmol, 1.0 equiv.), catalyst Fe(OTf)$_3$ (0.004 mmol, 0.02 equiv.) in benzene (10 mL) was added NBS (0.22 mmol, 1.1 equiv.) in the absence of light at 90 °C. The mixture was stirred at 90 °C for 1 h. The solution was diluted with water (10 mL) and extracted with CH$_2$Cl$_2$ (3 × 10 mL). The combined organic extracts were washed with brine, dried with anhydrous Na$_2$SO$_4$, filtered and concentrated under vacuum. The residue was purified by column chromatography on silica gel to yield the corresponding *ortho*-bromination product.

UV-Vis for Carbazole study

Figure S117: UV-vis spectra of 1a; Both spectra were measured in toluene, related to Figure 1, 2, 3, 4,
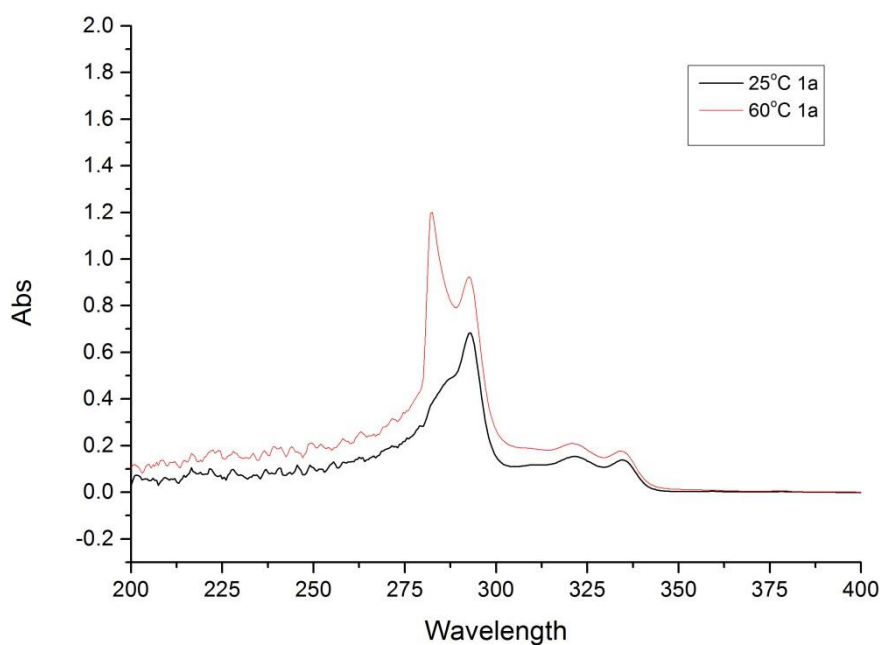
Control NMR experiment

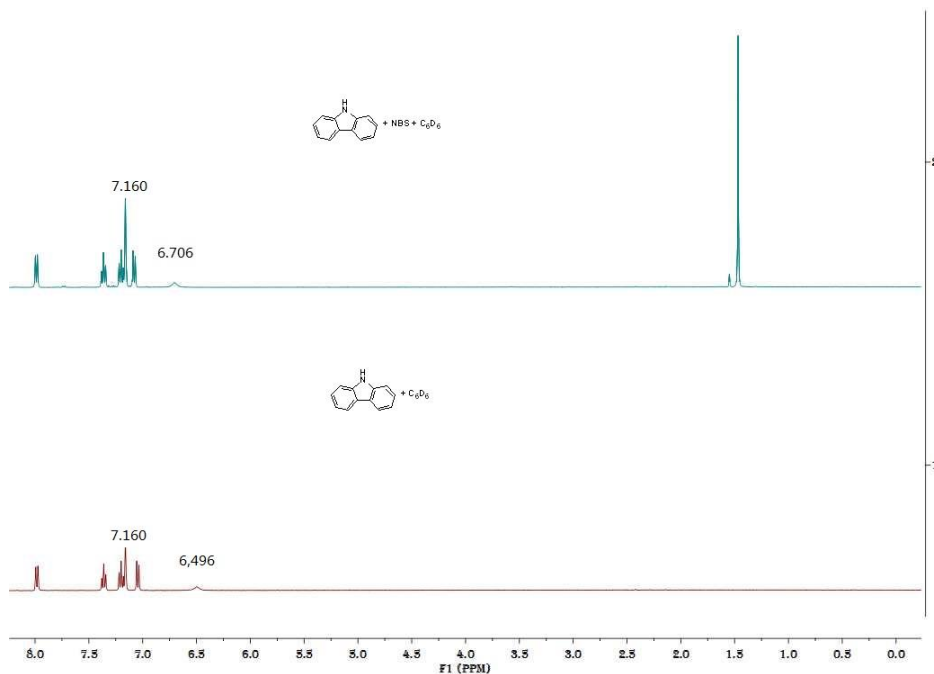**Figure S118: Carbazole in d-benzene and Carbazole + NBS in d-benzene, related to Figure 1, 2, 3, 4,**

Figure S119: NBS + Al(OTf)₃ in d-toluene 25 ºC and NBS + Al(OTf)₃ in d-toluene 60 ºC, related to Figure 1, 2, 3, 4
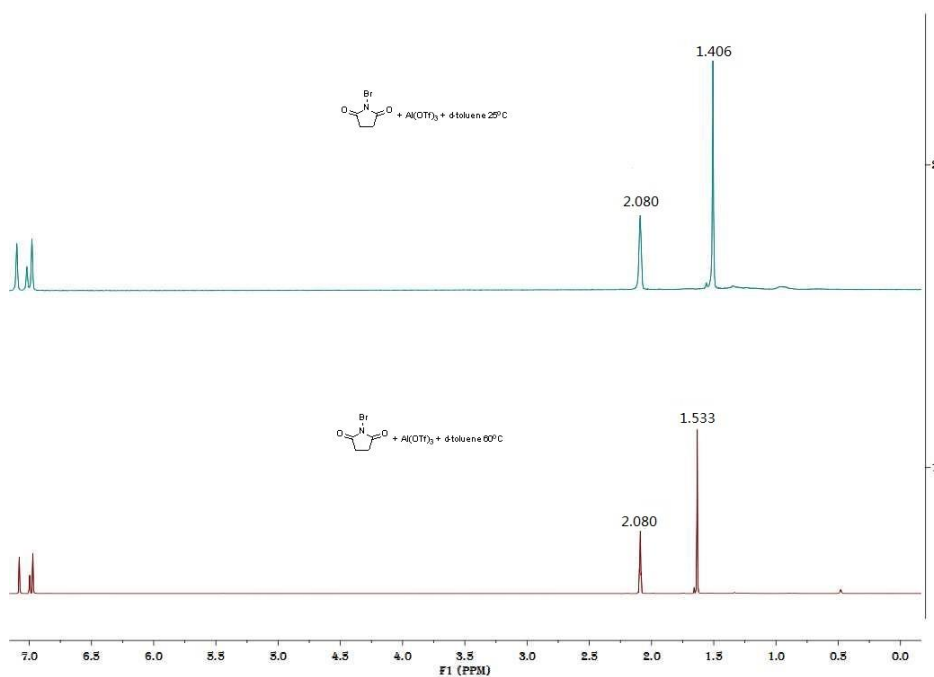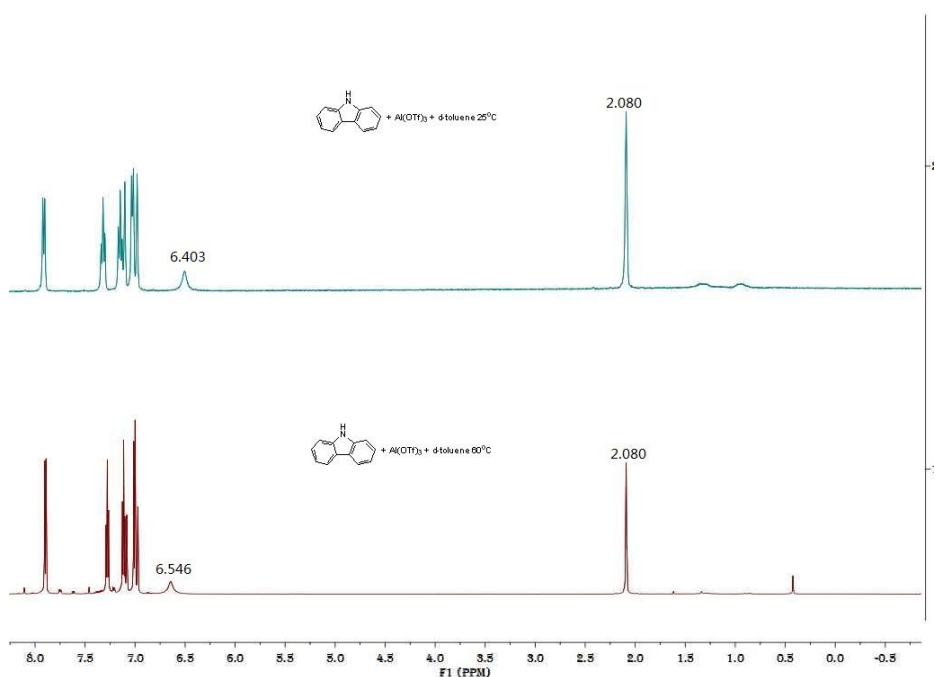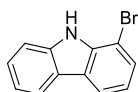
Figure S120: NBS + Al(OTf)₃ in d-toluene 25 °C and NBS + Al(OTf)₃ in d-toluene 60 °C, related to Figure 1, 2, 3, 4
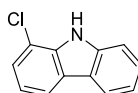

Characterization data for products

1-bromo-9H-carbazole (2a) (Cho et al., 2017)

White solid; Yield = 75%, o/p = 90/10; ¹H NMR (400 MHz, d-DMSO) δ 11.49 (s, 1H), 8.15 (d, J = 7.6 Hz, 2H), 7.63 (d, J = 7.6 Hz, 2H), 7.49 - 7.43 (m, 1H), 7.24 (t, J = 7.5 Hz, 1H), 7.16 - 7.12 (m, 1H). ¹³C NMR (101 MHz, d-DMSO) δ 140.3, 138.6, 128.3, 126.8, 124.7, 123.0, 121.1, 120.4, 120.0, 119.8, 112.1, 104.0.

1-chloro-9H-carbazole (2b) (Kronberg et al., 2011)

White solid; Yield = 57%, o/p = 75/25 ; ¹H NMR (400 MHz, CDCl₃) δ 8.30 (s, 1H), 8.08 (d, J = 7.8 Hz, 1H), 7.98 (d, J = 7.8 Hz, 1H), 7.54 - 7.39 (m, 3H), 7.30 - 7.26 (m, 1H), 7.19 (t, J = 7.8 Hz, 1H). ¹³C NMR (101 MHz, CDCl₃) δ 139.3, 136.7, 126.6, 125.1, 124.8, 123.5, 120.8, 120.2, 120.1, 118.8, 116.0, 111.1.
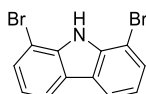

1,8-dibromo-9H-carbazole (2c) (Thummel et al., 2008)

White solid; Yield = 75%, *o/p* = 89/11; ^{1}H NMR (400 MHz, *d*-DMSO) δ 11.19 (s, 1H), 8.23-8.20 (m, 2H), 7.84 - 7.56 (m, 2H), 7.33 - 7.07 (m, 2H). ^{13}C NMR (101 MHz, *d*-DMSO) δ 138.8, 129.8, 125.2, 121.6, 120.5, 104.6.
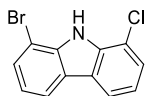

1-bromo-8-chloro-9*H*-carbazole (2d)

White solid; Yield = 74%, *o/p* = 88/12; ^{1}H NMR (400 MHz, CDCl$_3$) δ 8.37 (s, 1H), 7.97 (d, *J* = 7.8 Hz, 1H), 7.92 (d, *J* = 7.8 Hz, 1H), 7.60 (d, *J* = 7.7 Hz, 1H), 7.45 (d, *J* = 7.7 Hz, 1H), 7.12 - 7.13 (m, 2H). ^{13}C NMR (101 MHz, CDCl$_3$) δ 137.9, 136.3, 128.7, 125.8, 125.1, 124.7, 121.2, 120.9, 119.8, 119.3, 116.5, 104.5. HRMS (ESI) calcd for C$_{12}$H$_7$BrClNH m/z [M + H]$^+$: 279.9523; found: 279.9521.
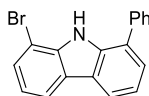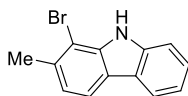

1-bromo-8-phenyl-9*H*-carbazole (2e)

White solid; Yield = 70%, *o/p* = 85/15; ^{1}H NMR (400 MHz, CDCl$_3$) δ 8.46 (s, 1H), 8.08 - 8.06 (m, 2H), 7.75 (d, *J* = 7.3 Hz, 2H), 7.67 - 7.57 (m, 3H), 7.52 (d, *J* = 7.4 Hz, 2H), 7.40 (d, *J* = 7.6 Hz, 1H), 7.19 - 7.14 (m, 1H). ^{13}C NMR (101 MHz, CDCl$_3$) δ 138.7, 138.1, 136.9, 129.5, 128.3, 128.2, 127.8, 126.6, 125.6, 124. 9, 124.1, 120.8, 120.7, 120.0, 119.5, 104.3. HRMS (ESI) calcd for C$_{18}$H$_{12}$BrNH m/z [M + H]$^+$: 322.0226; found: 322.0231.
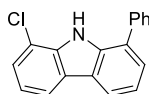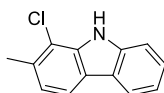

1-chloro-8-phenyl-9*H*-carbazole (2f)

White solid; Yield = 67%, *o/p* = 80/20; ^{1}H NMR (400 MHz, CDCl$_3$) δ 8.46 (s, 1H), 8.08 (d, *J* = 7.8 Hz, 1H), 8.02 (d, *J* = 7.7 Hz, 1H), 7.74 (d, *J* = 7.6 Hz, 2H), 7.61 (t, *J* = 7.1 Hz, 2H), 7.52 - 7.48 (m, 2H), 7.44 (d, *J* = 7.6 Hz, 1H), 7.38 (t, *J* = 7.5 Hz, 1H), 7.21 (t, *J* = 7.7 Hz, 1H). ^{13}C NMR (101 MHz, CDCl$_3$) δ 138.7, 137.1, 136.7, 129.5, 128.3, 127.8, 126.6, 125.6, 125.2, 125.1, 124.0, 120.7, 120.4, 119.9, 118.9, 116.1. HRMS (ESI) calcd for C$_{18}$H$_{12}$ClNH m/z [M + H]$^+$: 278.0731; found: 278.0737.

1-bromo-2-methyl-9*H*-carbazole (2g) (Bumwoo et al., 2016)

White solid; Yield = 83%, *o/p* = 92/8; ^{1}H NMR (400 MHz, CDCl$_3$) δ 8.26 (s, 1H), 8.05 (d, *J* = 8.0 Hz, 1H), 7.91 (d, *J* = 7.9 Hz, 1H), 7.55 - 7.40 (m, 2H), 7.34 - 7.23 (m, 1H), 7.15 (d, *J* = 7.7 Hz, 1H), 2.61 (s, 3H). ^{13}C NMR (101 MHz, CDCl$_3$) δ 139.1, 138.8, 134.7, 126.0, 124.0, 122.3, 122.1, 120.5, 119.9, 118.8, 110.9, 106.2, 22.4.

1-chloro-2-methyl-9*H*-carbazole (2h)

White solid; Yield = 75%, *o/p* = 88/12 ; ^{1}H NMR (400 MHz, CDCl$_3$) δ 8.18 (s, 1H), 8.02 (d, *J* = 7.8 Hz, 1H), 7.83 (d, *J* = 7.9 Hz, 1H), 7.44 (s, 2H), 7.10 (d, *J* = 7.8 Hz, 1H), 2.56 (s, 3H). ^{13}C NMR (101 MHz,

CDCl$_3$) δ 139.3, 137.3, 132.9, 125.9, 123.9, 122.8, 122.2, 120.5, 120.0, 118.2, 115.9, 111.0, 19.1. HRMS (ESI) calcd for C$_{13}$H$_{10}$ClNH m/z [M + H]$^+$: 216.0575; found: 216.0576.
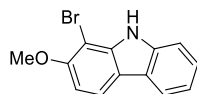
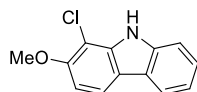**1-bromo-2-methoxy-9*H*-carbazole (2i)**

White solid; Yield = 73%, *o/p* = 85/15; ^{1}H NMR (400 MHz, CDCl$_3$) δ 8.15 (s, 1H), 7.95 (d, *J* = 7.7 Hz, 1H), 7.89 (d, *J* = 8.5 Hz, 1H), 7.45 - 7.33 (m, 2H), 7.28 - 7.17 (m, 1H), 6.84 (d, *J* = 8.5 Hz, 1H), 3.98 (s, 3H). ^{13}C NMR (101 MHz, CDCl$_3$) δ 154.5, 139.9, 139.4, 125.4, 123.9, 120.1, 120.1, 119.6, 118.6, 110.8, 104.9, 92.7, 57.0. HRMS (ESI) calcd for C$_{13}$H$_{10}$BrNOH m/z [M + H]$^+$: 276.0019; found: 276.0029.


1-chloro-2-methoxy-9*H*-carbazole (2j)

White solid; Yield = 75%, *o/p* = 87/13 ; ^{1}H NMR (400 MHz, *d*-DMSO) δ 11.41 (s, 1H), 8.05 - 7.98 (m, 2H), 7.56 (d, *J* = 6.1 Hz, 1H), 7.42 - 7.38 (m, 1H), 7.21 - 7.18 (m, 1H), 7.02 - 6.96 (m, 1H), 3.95 (s, 3H). ^{13}C NMR (101 MHz, CDCl$_3$) δ 153.6, 139.7, 138.5, 125.4, 123.7, 120.0, 119.9, 118.8, 118.7, 110.9, 105.1, 103.7, 56.9. HRMS (ESI) calcd for C$_{13}$H$_{10}$ClNOH m/z [M + H]$^+$: 232.0524; found: 232.0527.
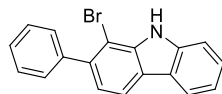

1-bromo-2-phenyl-9*H*-carbazole (2k)

Gray solid; Yield = 75%, *o/p* = 88/12; ^{1}H NMR (400 MHz, CDCl$_3$) δ 8.39 (s, 1H), 8.11 (d, *J* = 8 Hz, 1H), 8.05 (t, *J* = 8 Hz, 1H), 7.62 - 7.57 (m, 2H), 7.52 - 7.46 (m, 5H), 7.35 - 7.32 (m, 1H), 7.28 (s, 1H). ^{13}C NMR (101 MHz, CDCl$_3$) δ 141.1, 139.4, 139.3, 138.8, 129.8, 128.8, 127.9, 127.4, 126.4, 123.7, 123.3, 122.5, 120.8, 120.1, 119.0, 111.0. HRMS (ESI) calcd for C$_{18}$H$_{12}$BrNH m/z [M + H]$^+$: 322.0226; found: 322.0231.
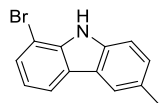
**1-bromo-6-methyl-9*H*-carbazole (2l) (Driver et al., 2009)**

White solid; Yield = 78%, *o/p* = 91/9; ^{1}H NMR (400 MHz, CDCl$_3$) δ 8.17 (s, 1H), 7.97 (d, *J* = 7.8 Hz, 1H), 7.85 (s, 1H), 7.55 (d, *J* = 7.7 Hz, 1H), 7.39 (d, *J* = 8.2 Hz, 1H), 7.28 (d, *J* = 8.2 Hz, 1H), 7.10 (t, *J* = 7.7 Hz, 1H), 2.54 (s, 3H). ^{13}C NMR (101 MHz, CDCl$_3$) δ 138.4, 137.3, 129.5, 127.9, 127.8, 124.50, 123.8, 120.7, 120.3, 119.2, 110.7, 104.1, 21.5.
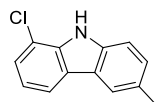

1-chloro-6-methyl-9*H*-carbazole (2m)

White solid; Yield = 70%, *o/p* = 82/18; ^{1}H NMR (400 MHz, *d*-DMSO) δ 11.40 (s, 1H), 8.06 - 7.99 (m, 2H), 7.57 (d, *J* = 6.6 Hz, 1H), 7.41 - 7.37 (m, 1H), 7.21 - 7.16 (m, 1H), 7.02 - 6.99 (m, 1H), 3.96 (s, 3H). ^{13}C NMR (101 MHz, *d*-DMSO) δ 153.6, 140.8, 138.8, 125.6, 123.3, 120.3, 119.7, 119.6, 118.6,

111.7, 105.2, 103.1, 57.1. HRMS (ESI) calcd for $C_{13}H_{10}ClNH$ m/z $[M + H]^+$: 216.0575; found: 216.0579.
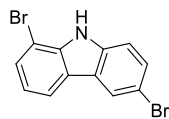

1,6-dibromo-9*H*-carbazole (2n)

Yellow solid; Yield = 63%, *o/p* = 75/25; ^{1}H NMR (400 MHz, *d*-DMSO) δ 11.64 (s, 1H), 8.41 (s, 2H), 8.21 (dd, *J* = 7.8 Hz, 1H), 7.66 (dd, *J* = 7.7 Hz, 1H), 7.54 - 7.59 (m, 2H), 7.33 - 7.01 (m, 2H). ^{13}C NMR (101 MHz, *d*-DMSO) δ 139.0, 138. 9, 129.2, 129.1, 125.0, 123.8, 123.6, 120.9, 120.6, 114.1, 111. 9, 104.1. HRMS (ESI) calcd for $C_{12}H_7Br_2NH$ m/z $[M + H]^+$: 323.9018; found: 323.9016.
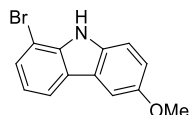

1-bromo-6-methoxy-9*H*-carbazole (2o)

White solid; Yield = 70%, *o/p* = 81/19; ^{1}H NMR (400 MHz, CDCl₃) δ 8.09 (d, *J* = 8.0 Hz, 1H), 7.85 (s, 1H), 7.63 - 7.62 (m, 1H), 7.47 - 7.43 (m, 1H), 7.35 (d, *J* = 8.1 Hz, 1H), 7.28 - 7.26 (m, 1H), 7.14 - 7.11 (m, 1H), 3.98 (s, 3H).^{13}C NMR (101 MHz, CDCl₃) δ 144.9, 139.1, 130.8, 126.3, 123.3, 123.1, 122.4, 119.5, 110.8, 107.3, 106.7, 55.8. HRMS (ESI) calcd for $C_{13}H_{10}BrNOH$ m/z $[M + H]^+$: 276.0019; found: 276.0029.
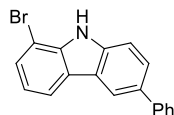

1-bromo-6-phenyl-9*H*-carbazole (2p)

White solid; Yield = 73%, *o/p* = 86/14; ^{1}H NMR (400 MHz, CDCl₃) δ 8.28 (s, 1H), 8.26 (s, 1H), 8.05 (d, *J* = 7.7 Hz, 1H), 7.70 - 7.72 (m, 3H), 7.61 - 7.45 (m, 4H), 7.37 (t, *J* = 7.4 Hz, 1H), 7.15 (t, *J* = 7.8 Hz, 1H). ^{13}C NMR (101 MHz, CDCl₃) δ 141.8, 138.5, 133.7, 128.8, 128.2, 127.3, 126.7, 126.2, 124.7, 124.2, 122.2, 120.7, 119.4, 119.3, 111.3, 104.2. HRMS (ESI) calcd for $C_{18}H_{12}BrNH$ m/z $[M + H]^+$: 322.0226; found: 322.0231.
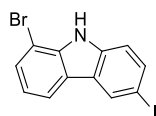

1-bromo-6-iodo-9*H*-carbazole (2q)

White solid; Yield = 66%, *o/p* = 80/20; ^{1}H NMR (400 MHz, CDCl₃) δ 8.36 (s, 1H), 8.26 (s, 1H), 7.94 (d, *J* = 7.4 Hz, 1H), 7.72 (d, *J* = 6.9 Hz, 1H), 7.61 (d, *J* = 7.3 Hz, 1H), 7.28 (d, *J* = 8.3 Hz, 1H), 7.16 (t, *J* = 7.6 Hz, 1H). ^{13}C NMR (101 MHz, CDCl₃) δ 138.1, 134.8, 129.7, 128.7, 127.2, 126.1, 123.2, 121.0, 119.5, 113.0, 104.2, 82.7. HRMS (ESI) calcd for $C_{12}H_7BrINH$ m/z $[M + H]^+$: 371.8879; found: 371.8872.
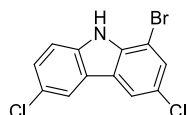
**1-bromo-3,6-dichloro-9*H*-carbazole (2r)**

White solid; Yield = 78%; ^{1}H NMR (400 MHz, CDCl₃) δ 8.25 (s, 1H), 7.94 (s, 1H), 7.89 (s, 1H), 7.59 (s, 1H), 7.47 - 7.40 (m, 2H). ^{13}C NMR (101 MHz, CDCl₃) δ 137.8, 137.1, 128.3, 127.4, 125.9, 125.5, 124.0, 123.9, 120.7, 119.3, 112.3, 104.3. HRMS (ESI) calcd for $C_{12}H_7BrCl_2NH$ m/z $[M + H]^+$:

313.9133; found: 313.9136.
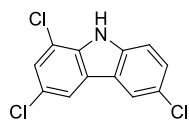
1,3,6-trichloro-9H-carbazole (2s) (Pielichowski et al., 2004)

White solid; Yield = 78%; ^{1}H NMR (400 MHz, *d*-DMSO) δ 11.93 (s, 1H), 8.45 (d, *J* = 11.8 Hz, 2H), 7.68 (s, 1H), 7.62 - 7.52 (m, 2H). ^{13}C NMR (101 MHz, *d*-DMSO) δ 139.5, 136.4, 130.0, 127.8, 125.1, 124.2, 123.9, 122.9, 116.9, 114.2, 112.3, 110.9.
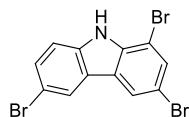
1,3,6-tribromo-9H-carbazole (2t) (Pielichowski et al., 2004)

Gray solid; Yield = 80%; ^{1}H NMR (400 MHz, *d*-DMSO) δ 11.84 (s, 1H), 8.50 (s, 2H), 7.83 (s, 1H), 7.60 - 7.55 (m, 2H). ^{13}C NMR (101 MHz, *d*-DMSO) δ 139.4, 138.0, 130.5, 130.0, 124.9, 124.3, 124.0, 123.3, 114.3, 112.3, 111.3, 105.0. HRMS (ESI) calcd for $C_{12}H_7Br_3NH$ m/z [M + H]$^+$: 401.8123; found: 401.8129.
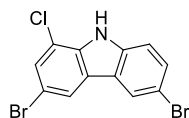
3,6-dibromo-1-chloro-9H-carbazole (2u)

White solid; Yield = 80% ; ^{1}H NMR (400 MHz, *d*-DMSO) δ 11.91 (s, 1H), 8.30 (d, *J* = 9.1 Hz, 2H), 7.60 - 7.55 (m, 2H), 7.49 (d, *J* = 8.6 Hz, 1H). ^{13}C NMR (101 MHz, *d*-DMSO) δ 139.4, 136.3, 127.4, 125.4, 124.6, 124.5, 123.7, 123.4, 121.2, 119.9, 116.6, 113.7. HRMS (ESI) calcd for $C_{12}H_6Br_2ClNH$ m/z [M + H]$^+$: 357.8628; found: 357.8630.
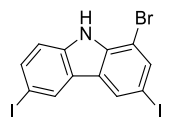
1-bromo-3,6-diiodo-9H-carbazole (2v)

White solid; Yield = 80%; ^{1}H NMR (400 MHz, *d*-DMSO) δ 11.78 (s, 1H), 8.62 (s, 2H), 7.91 (s, 1H), 7.74 (d, *J* = 6.9 Hz, 1H), 7.42 (d, *J* = 8.3 Hz, 1H). ^{13}C NMR (101 MHz, *d*-DMSO) δ 139.5, 138.0, 135.6, 135.4, 130.2, 129.1, 125.5, 124.5, 114.6, 105.2, 83.4, 82.2. HRMS (ESI) calcd for $C_{12}H_7BrI_2NH$ m/z [M + H]$^+$: 497.7846; found: 497.7851.
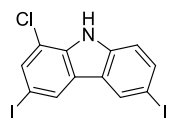
1-chloro-3,6-diiodo-9H-carbazole (2w)

Brown solid; Yield = 83%; ^{1}H NMR (400 MHz, CDCl$_3$) δ 8.29 (s, 1H), 8.24 (s, 1H), 8.13 (s, 1H), 7.73 - 7.63 (m, 2H), 7.23 (d, *J* = 8.5 Hz, 1H). ^{13}C NMR (101 MHz, CDCl$_3$) δ 138.3, 136.0, 135.5, 133.3, 129.8, 127.8, 125.7, 125.3, 124.6, 118.8, 117.0, 113.1. HRMS (ESI) calcd for $C_{12}H_6ClI_2NH$ m/z [M + H]$^+$: 453.8351; found: 453.8355.
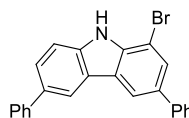
**1-bromo-3,6-diphenyl-9H-carbazole (2x)**

Yellow solid; Yield = 75%; ^{1}H NMR (400 MHz, CDCl$_3$) δ 8.30 (s, 1H), 8.25 (s, 2H), 7.84 (s, 1H), 7.74 - 7.69 (m, 5H), 7.55 - 7.48 (m, 5H), 7.39 (d, J = 7.2 Hz, 2H). ^{13}C NMR (101 MHz, CDCl$_3$) δ141.7, 140.9, 139.0, 138.0, 134.7, 133.6, 128.9, 128.9, 127.6, 127.3, 127.0, 126.7, 126.3, 125.1, 124.4, 119.5, 118.0, 111.3, 104.5. HRMS (ESI) calcd for C$_{24}$H$_{16}$BrNH m/z [M + H]$^+$: 398.0539; found: 398.0543.
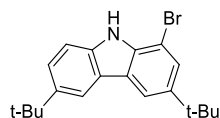

1-bromo-3,6-di-tert-butyl-9*H*-carbazole (2y) (Ema et al., 2016)

White solid; Yield = 67%; ^{1}H NMR (400 MHz, CDCl$_3$) δ 8.07 (s, 2H), 8.03 (s, 1H), 7.61 (s, 1H), 7.52 (d, J = 8.5 Hz, 1H), 7.40 (d, J = 8.6 Hz, 1H), 1.47 (s, 9H), 1.46 (s, 9H). ^{13}C NMR (101 MHz, CDCl$_3$) δ 144.0, 142.9, 137.7, 136.7, 125.7, 124.6, 124.3, 123.6, 116.6, 115.5, 110.5, 103.7, 32.0
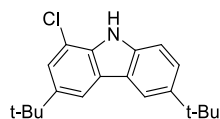

3,6-di-tert-butyl-1-chloro-9*H*-carbazole (2z)

Brown solid; Yield = 85%; ^{1}H NMR (400 MHz, CDCl$_3$) δ 8.07 (s, 2H), 7.99 (s, 1H), 7.52 (d, J = 8.1 Hz, 1H), 7.47 (s, 1H), 7.40 (d, J = 8.4 Hz, 1H), 1.47 (s, 18H). 13C NMR (101 MHz, CDCl$_3$) δ 143.7, 142.9, 137.8, 135.2, 124.8, 124.4, 123.5, 122.9, 116.6, 115.4, 114.9, 110.5, 31.9. HRMS (ESI) calcd for C$_{20}$H$_{24}$ClNH m/z [M + H]$^+$: 314.1670; found: 314.1672.
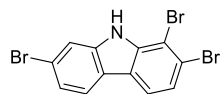

1,2,7-tribromo-9*H*-carbazole (2aa)

White solid; Yield = 68%, *o/p* = 82/18; ^{1}H NMR (400 MHz, CDCl$_3$) δ 8.29 (s, 1H), 7.87 (d, J = 8.3 Hz, 1H), 7.82 (d, J = 8.2 Hz, 1H), 7.65 (s, 1H), 7.49 (d, J = 8.2 Hz, 1H), 7.41 (d, J = 8.3 Hz, 1H). ^{13}C NMR (101 MHz, CDCl$_3$) δ 139.9, 139.3, 124.7, 123.8, 122.5, 122.4, 121.9, 121.4, 120.3, 120.0, 114.2, 106.9.
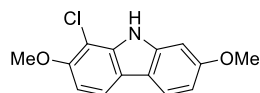
1-chloro-2,7-dimethoxy-9*H*-carbazole (2ab)

White solid; Yield = 55%, *o/p* = 71/29; ^{1}H NMR (400 MHz, *d*-DMSO) δ 11.24 (s, 1H), 7.90 (t, J = 7.9 Hz, 2H), 7.02 (s, 1H), 6.97 (d, J = 8.5 Hz, 1H), 6.81 (d, J = 8.5 Hz, 1H), 3.93 (s, 3H), 3.85 (s, 3H). ^{13}C NMR (101 MHz, *d*-DMSO) δ 158.6, 152.7, 142.1, 138.7, 121.1, 118.8, 118.6, 117.0, 108.5, 105.2, 103.1, 95.7, 57.1, 55.7. HRMS (ESI) calcd for C$_{14}$H$_{12}$ClNO$_2$H m/z [M + H]$^+$: 262.0629; found: 262.0631.

.
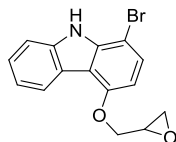
1-bromo-4-(oxiran-2-ylmethoxy)-9*H*-carbazole (2ac)

White solid; Yield = 66%, *o/p* = 78/22; ^{1}H NMR (400 MHz, CDCl$_3$) δ 8.36 (s, 1H), 8.34 (s, 1H), 7.55 - 7.41 (m, 3H), 7.35 - 7.31 (m 1H), 6.57 (d, J = 8.5 Hz, 1H), 4.50 - 4.47 (m, 1H), 4.23 - 4.19 (m 1H), 3.59 (s, 1H), 3.06 - 3.04 (m 1H), 2.94 - 2.92 (m 1H). ^{13}C NMR (101 MHz, CDCl$_3$) δ 154.2, 139.0,

138.3, 128.2, 125.8, 123.5, 123.0, 120.4, 113.9, 110.6, 102.8, 95.8, 69.0, 50.3, 44.8. HRMS (ESI) calcd for C$_{15}$H$_{12}$BrNO$_2$H m/z [M + H]$^+$: 318.0124; found: 318.0125.
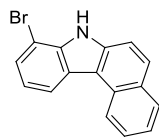
8-bromo-7*H*-benzo[c]carbazole (2ad) (Lee et al., 2015)
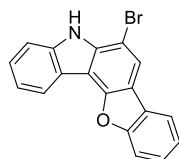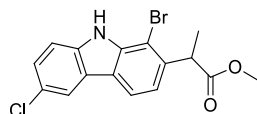
White solid; Yield = 58%, *o/p* = 71/29; ^{1}H NMR (400 MHz, CDCl$_3$) δ 8.71 (d, *J* = 8.3 Hz, 1H), 8.59 (s, 1H), 8.47 (d, *J* = 8.0 Hz, 1H), 8.01 (d, *J* = 8.0 Hz, 1H), 7.88 (d, *J* = 8.7 Hz, 1H), 7.75 - 7.70 (m, 1H), 7.65 - 7.56 (m, 2H), 7.54 - 7.50 (m, 1H), 7.28 - 7.24 (m, 1H). ^{13}C NMR (101 MHz, CDCl$_3$) δ 137.0, 136.9 129.9, 129.4, 129.3, 128.2, 127.1, 126.5, 125.2, 123.4, 123.1, 121.3, 121.1, 116.0, 112.6, 104.7.

6-bromo-5*H*-benzofuro[3,2-c]carbazole (2ae)

White solid; Yield = 65%, *o/p* = 77/23; ^{1}H NMR (400 MHz, *d*-DMSO) δ 11.89 (s, 1H), 8.47 (s, 1H), 8.35 (d, *J* = 7.8 Hz, 1H), 8.20 (d, *J* = 7.7 Hz, 1H), 7.85 (d, *J* = 7.8 Hz, 1H), 7.74 (d, *J* = 8.1 Hz, 1H), 7.59 - 7.38 (m, 4H). ^{13}C NMR (101 MHz, *d*-DMSO) δ 155.91, 149.91, 139.91, 138.50, 126.75, 126.45, 124.33, 123.88, 122.34, 120.84, 120.75, 120.47, 116.76, 112.54, 112.11, 108.94, 99.36. HRMS (ESI) calcd for C$_{18}$H$_{10}$BrNOH m/z [M + H]$^+$: 336.0019; found: 336.0020.

methyl 2-(1-bromo-6-chloro-9*H*-carbazol-2-yl)propanoate (2af)

White solid; Yield = 75%, *o/p* = 90/10; ^{1}H NMR (400 MHz, CDCl$_3$) δ 8.33 (s, 1H), 7.90 (s, 1H), 7.82 (d, *J* = 7.2 Hz, 1H), 7.35 (s, 2H), 7.15 (d, *J* = 7.2 Hz, 1H), 4.38 - 4.33 (m, 1H), 3.69 (s, 3H), 1.57 (s, 3H). ^{13}C NMR (101 MHz, CDCl$_3$) δ 174.43, 139.13, 139.03, 137.52, 126.41, 125.51, 124.65, 122.24, 120.33, 119.60, 119.37, 111.95, 105.97, 52.21, 44.29, 18.12. HRMS (ESI) calcd for C$_{16}$H$_{13}$BrClNO$_2$H m/z [M + H]$^+$: 365.9891; found: 365.9897.
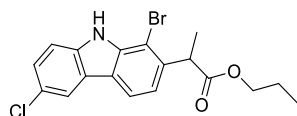
propyl 2-(1-bromo-6-chloro-9*H*-carbazol-2-yl)propanoate (2ag)

White solid; Yield = 74%, *o/p* = 90/10; ^{1}H NMR (400 MHz, CDCl$_3$) δ 8.32 (s, 1H), 7.97 (s, 1H), 7.89 (d, *J* = 8.4 Hz, 1H), 7.40 (s, 2H), 7.20 (d, *J* = 8.4 Hz, 1H), 4.40 - 4.35 (m, 1H), 4.07 (t, *J* = 6.6 Hz, 2H), 1.58 (d, *J* = 6.4 Hz, 5H), 0.85 (t, *J* = 7.2 Hz, 3H). ^{13}C NMR (101 MHz, CDCl$_3$) δ 174.05, 139.21, 137.88, 137.58, 126.47, 125.65, 124.84, 122.26, 120.43, 119.59, 119.54, 111.98, 106.12, 66.57, 44.45, 21.90, 18.12, 10.26. HRMS (ESI) calcd for C$_{18}$H$_{17}$BrClNO$_2$Na m/z [M + Na]$^+$: 416.0023; found: 416.0028

2-chloro-*N*-methylaniline (6a) (Zhu et al., 2015)

Colorless oil; Yield = 78%, *o/p* = 85/15; ^{1}H NMR (400 MHz, CDCl$_3$) δ 7.32 (d, *J* = 8.3 Hz, 1H), 7.27 - 7.18 (m, 1H), 6.72 - 6.68 (m, 2H), 4.40 (br, 1H), 2.96 (d, *J* = 5.0 Hz, 3H). ^{13}C NMR (101 MHz, CDCl$_3$) δ 145.0, 129.0, 127.9, 119.1, 117.0, 110.6, 30.4.
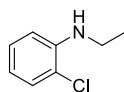
2-chloro-*N*-ethylaniline (6b) (Zh0u et al., 2016)

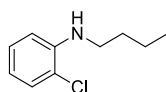Colorless oil; Yield = 77%, *o/p* = 85/15; ^{1}H NMR (400 MHz, CDCl$_3$) δ 7.26 - 7.24 (m, 1H), 7.16 - 7.09 (m, 1H), 6.67 - 6.54 (m, 2H), 4.19 (br, 1H), 3.23 - 3.18 (m, 2H), 1.33 - 1.22 (m, 3H). ^{13}C NMR (101 MHz, CDCl$_3$) δ 144.2, 129.1, 127.8, 118.9, 116.9, 111.1, 38.2, 14.7.

### *N*-butyl-2-chloroaniline (6c) (Shankarling et al., 2013)

Colorless oil; Yield = 75%, *o/p* = 84/16; ^{1}H NMR (400 MHz, CDCl$_3$) δ 7.20 (d, *J* = 6.4 Hz, 1H), 7.11 - 7.07 (m, 1H), 6.62 - 6.50 (m, 2H), 4.21 (br, 1H), 3.11 (t, *J* = 6.4 Hz, 2H), 1.65 - 1.58 (m, 2H), 1.44 - 1.39 (m, 2H), 0.93 (t, *J* = 7.5 Hz, 3H). ^{13}C NMR (101 MHz, CDCl$_3$) δ 144.3, 129.1, 127.7, 119.0, 116.8, 111.1, 43.4, 31.4, 20.3, 13.9.
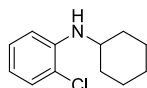
2-chloro-*N*-cyclohexylaniline (6d) (Cai et al., 2017)

Light yellow oil; Yield = 82%, *o/p* = 88/12; ^{1}H NMR (400 MHz, CDCl$_3$) δ 7.23 - 7.20 (m, 1H), 7.11 - 7.06 (m, 1H), 6.65 (d, *J* = 8.4 Hz, 1H), 6.58 - 6.53 (m, 1H), 4.20 (br, 1H), 3.28 (s, 1H), 2.03 (d, *J* = 10.8 Hz, 2H), 1.77 - 1.74(m, 2H), 1.65 - 1.62m, 1H), 1.41 - 1.32(m 2H), 1.26 - 1,18(m 3H). ^{13}C NMR (101 MHz, CDCl$_3$) δ 143.2, 129.3, 127.7, 119.0, 116.5, 111.7, 51.4, 33.2, 25.9, 24.9.
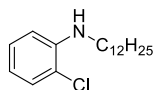
2-chloro-*N*-dodecylaniline (6e)

Light yellow oil; Yield = 65%, *o/p* = 75/25; ^{1}H NMR (400 MHz, CDCl$_3$) δ 7.31 - 7.26 (m, 1H), 7.21 - 7.17(m, 1H), 6.72 - 6.60(m, 2H), 4.31 (br, 1H), 3.23 - 3.20 (m, 2H), 1.72 - 1.33 (m, 20H), 0.95 (t, *J* = 6.4Hz, 3H). ^{13}C NMR (101 MHz, CDCl$_3$) δ 144.2, 129.0, 127.7, 118.9, 116.8, 111.1, 43.7, 31.9, 29.7, 29.6, 29.4, 29.4, 29.2, 27.1, 22.7, 14.1. HRMS (ESI) calcd for C$_{18}$H$_{30}$ClNH m/z [M + H]$^+$: 296.2140; found: 296.2144.
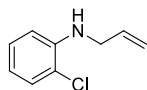
N-allyl-2-chloroaniline (6f) (Wang et al., 2016)

Colorless oil; Yield = 85%, *o/p* = 91/9; ^{1}H NMR (400 MHz, CDCl$_3$) δ 7.37 - 7.29 (m, 4H), 7.12 - 7.02 (m, 1H), 6.66 - 6.63 (m, 2H), 4.75 (br, 1H), 4.43 - 4.40 (m, 2H). ^{13}C NMR (101 MHz, CDCl$_3$) δ 143.9, 138.8, 129.1, 128.8, 127.8, 127.3, 117.5, 111.5, 47.9.
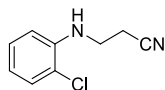
3-((2-chlorophenyl)amino)propanenitrile (6g) (Zargarian et al., 2016)

White solid; Yield = 75%, *o/p* = 86/14; ^{1}H NMR (400 MHz, CDCl$_3$) δ 7.38 - 7.31 (m, 1H), 7.22 (t, *J* = 7.6 Hz, 1H), 6.78 - 6.68 (m, 2H), 4.68 (br, 1H), 3.67 - 3.61 (m, 2H), 2.75 - 2.69 (m, 2H). ^{13}C NMR (101 MHz, CDCl$_3$) δ 142.2, 129.65, 127.9, 119.8, 118.5, 117.8, 110.9, 39.5, 18.1.

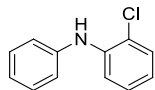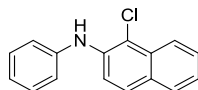**2-chloro-*N*-phenylaniline (6j) (Rossi et al., 2009)**

Light yellow oil; Yield = 70%, *o/p* = 83/17; ^{1}H NMR (400 MHz, CDCl$_3$) δ 7.41 - 7.30 (m, 4H), 7.22 - 7.14 (m, 3H), 7.09 (t, *J* = 7.3 Hz, 1H), 6.85 (t, *J* = 7.6 Hz, 1H), 6.16 (br, 1H). ^{13}C NMR (101 MHz, CDCl$_3$) δ 141.6, 140.4, 129.8, 129.5, 127.5, 122.7, 121.6, 120.4, 120.3, 115.7.


1-chloro-*N*-phenylnaphthalen-2-amine (6i) (Falvey et al., 2005)

Brown oil; Yield = 90%, *o/p* = 95/5; ^{1}H NMR (400 MHz, CDCl$_3$) δ 8.10 (d, *J* = 8.4 Hz, 1H), 7.68 (d, *J* = 8.0 Hz, 1H), 7.57 (d, *J* = 8.8 Hz, 1H), 7.52 - 7.44 (m, 2H), 7.30 (t, *J* = 7.6 Hz, 3H), 7.14 (d, *J* = 8.0 Hz, 2H), 7.03 (t, *J* = 7.1 Hz, 1H), 6.37 (br, 1H). ^{13}C NMR (101 MHz, CDCl$_3$) δ 141.7, 137.9, 131.9, 129.5, 129.4, 128.1, 127.5, 127.4, 123.7, 122.9, 122.9, 120.3, 117.3, 115.1.
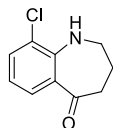
9-chloro-3,4-dihydro-1*H*-benzo[b]azepin-5(2H)-one (6h) (Mori et al., 1997)

White solid; Yield = 76%, *o/p* = 88/12; ^{1}H NMR (400 MHz, CDCl$_3$) δ 7.61 (d, *J* = 7.6 Hz, 1H), 7.37 - 7.35 (m, 1H), 6.73 (t, *J* = 7.9 Hz, 1H), 5.40 (s, 1H), 3.33 - 3.29 (m, 2H), 2.82 (t, *J* = 7.2 Hz, 2H), 2.26 - 2.19 (m, 2H). ^{13}C NMR (101 MHz, CDCl$_3$) δ 201.9, 149.1, 132.1, 128.3, 126.6, 121.3, 118.3, 47.7, 41.0, 31.9.
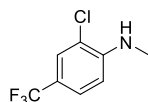
2-chloro-*N*-methyl-4-(trifluoromethyl)aniline (6k) (Roth et al., 2003)

Light yellow oil; Yield = 90%; ^{1}H NMR (400 MHz, CDCl$_3$) δ 7.54 (s, 1H), 7.45 (d, *J* = 8.4 Hz, 1H), 6.69 (d, *J* = 8.4 Hz, 1H), 4.72 (s, 1H), 2.99 (d, *J* = 5.2 Hz, 2H). ^{13}C NMR (101 MHz, CDCl$_3$) δ 147.3, 126.1, 125.6, 125.2, 118.4, 109.5, 30.1.
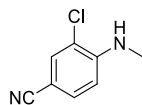
3-chloro-4-(methylamino)benzonitrile (6l) (Jeganmohan et al., 2013)

Light yellow oil; Yield = 88%; Yield = 88%; ^{1}H NMR (400 MHz, CDCl$_3$) δ 7.50 (d, *J* = 1.6 Hz, 1H), 7.43 (d, *J* = 8.4 Hz, 1H), 6.61 (d, *J* = 8.4 Hz, 1H), 4.91 (br, 1H), 2.96 (s, 3H). ^{13}C NMR (101 MHz, CDCl$_3$) δ 148.1, 132.5, 132.3, 119.1, 118.5, 109.9, 98.8, 29.9.
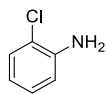
2-chloroaniline (6m) (Sun et al., 2018)

Light yellow oil; Yield = 58%, *o/p* = 70/30; ^{1}H NMR (400 MHz, CDCl$_3$) δ 7.30 (d, *J* = 7.9 Hz, 1H), 7.14 - 7.10 (m, 1H), 6.82 - 6.80 (m, 1H), 6.77 - 6.73 (m, 1H), 4.09 (s, 2H). ^{13}C NMR (101 MHz, CDCl$_3$) δ 142.9, 129.4, 127.6, 119.3, 119.0, 115.9.
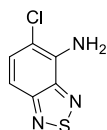
5-chlorobenzo[c][1,2,5]thiadiazol-4-amine (6n) (Deng et al., 2005)

Light yellow oil; Yield = 80%, *o/p* = 95/5; ^{1}H NMR (400 MHz, CDCl$_3$) δ 7.47 (d, *J* = 9.2 Hz, 1H), 7.30 (d, *J* = 9.2 Hz, 1H), 5.02 (br, 2H). ^{13}C NMR (101 MHz, CDCl$_3$) δ 154.2, 147.3, 135.1, 131.9, 112.1, 109.0.

1-phenyl-9*H*-carbazole (7) (Unsworth et al., 2015)

White solid; ^{1}H NMR (400 MHz, CDCl$_3$) δ 8.36 (s, 1H), 8.19 - 8.14 (m, 2H), 7.76 (d, *J* = 7.6 Hz, 2H), 7.62 (t, *J* = 7.2 Hz, 2H), 7.52 - 7.45 (m, 4H), 7.41 - 7.38 (m, 1H), 7.34 - 7.30 (m, 1H). ^{13}C NMR (101 MHz, CDCl$_3$) δ 139.5, 139.1, 137.3, 129.3, 128.4, 127.6, 126.0, 125.8, 125.1, 123.7, 123.6, 120.5, 119.9, 119.6, 119.5, 110.7.
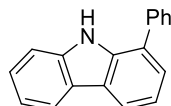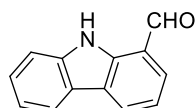

9*H*-carbazole-1-carbaldehyde (8) (Brimble et al., 2016)

Red solid; ^{1}H NMR (400 MHz, CDCl$_3$) δ 10.28 (s, 1H), 10.18 (s, 1H), 8.30 (d, *J* = 7.7 Hz, 1H), 8.10 (d, *J* = 7.8 Hz, 1H), 7.80 (d, *J* = 7.4 Hz, 1H), 7.55 - 7.48(m, 2H), 7.35 - 7.30(m, 2H). ^{13}C NMR (101 MHz, CDCl$_3$) δ 193.5, 140.0, 138.1, 131.3, 126.9, 126.8, 124.7, 121.9, 120.5, 119.5, 118.8, 111.5.
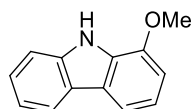
1-methoxy-9*H*-carbazole (9) (Vranken et al., 2017)

White solid; ^{1}H NMR (400 MHz, CDCl$_3$) δ 8.52 (s, 1H), 8.32-8.30 (m, 1H), 8.00 - 7.93 (m, 1H), 7.66 - 7.61 (m, 1H), 7.57 (d, *J* = 8.0 Hz, 1H), 7.50 - 7.47 (m, 1H), 7.42 - 7.37 (m, 1H), 7.09 - 7.07 (m, 1H), 4.12 (s, 3H). ^{13}C NMR (101 MHz, CDCl$_3$) δ 145.9, 139.5, 130.0, 125.9, 124.6, 123.9, 120.8, 119.9, 119.6, 113.1, 111.2, 106.2, 55.6.
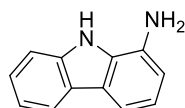
9*H*-carbazol-1-amine (10) (Gale et al., 2009)

White solid; ¹H NMR (400 MHz, *d*-DMSO) δ 10.81 (s, 1H), 8.03 (d, *J* = 8.0 Hz, 1H), 7.52 (d, *J* = 8.0 Hz, 1H), 7.37 (t, *J* = 8.0 Hz, 2H), 7.13 (t, *J* = 7.4 Hz, 1H), 6.94 (t, *J* = 7.6 Hz, 1H), 6.68 (d, *J* = 7.5 Hz, 1H), 5.19 (s, 2H). ¹³C NMR (101 MHz, *d*-DMSO) δ 139.5, 133.9, 129.2, 125.4, 123.7, 123.1, 120.6, 120.2, 118.7 111.4, 109.7, 108.8.

1,8-dibromo-3-methyl-9*H*-carbazole (11)

White solid; ¹H NMR (400 MHz, CDCl₃) δ 8.19 (s, 1H), 7.92 - 7.89 (m, 1H), 7.72 (s, 1H), 7.57 (d, *J* = 7.6 Hz, 1H), 7.42 (s, 1H), 7.13 - 7.09 (m, 1H), 2.50 (s, 3H). ¹³C NMR (101 MHz, CDCl₃) δ 138.0, 136.0, 131.1, 129.9, 128.5, 124.9, 124.7, 120.9, 119.8, 119.7, 104.4, 103.9, 21.2. HRMS (ESI) calcd for C₁₃H₉Br₂NH m/z [M + H]⁺: 337.9175; found: 337.9178.

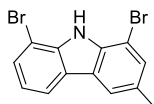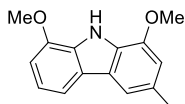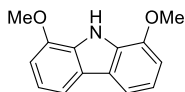**1,8-dimethoxy-3-methyl-9*H*-carbazole (12) (Tamariz et al., 2017)**

White solid; ¹H NMR (400 MHz, CDCl₃) δ 8.42 (s, 1H), 7.64 (d, *J* = 7.8 Hz, 1H), 7.47 (s, 1H), 7.14 (t, *J* = 7.8 Hz, 1H), 6.89 (d, *J* = 7.7 Hz, 1H), 6.74 (s, 1H), 4.01 (d, *J* = 4.1 Hz, 6H), 2.55 (s, 4H). ¹³C NMR (101 MHz, CDCl₃) δ 146.0, 145.6, 129.9, 129.4, 127.8, 124.7, 124.5, 119.4, 113.0, 112.7, 107.6, 105.6, 55.5, 21.9.

1,8-dimethoxy-9*H*-carbazole (13) (Sperry et al., 2017)

White solid; ¹H NMR (400 MHz, CDCl₃) δ 8.89 (s, 1H), 7.86 (d, *J* = 7.9 Hz, 2H), 7.32 (t, *J* = 7.8 Hz, 2H), 7.02 (d, *J* = 7.8 Hz, 2H), 4.09 (s, 6H). ¹³C NMR (101 MHz, CDCl₃) δ 146.0, 129.6, 124.7, 119.7, 113.1, 105.8, 55.5.
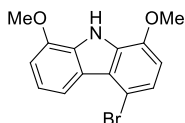
4-bromo-1,8-dimethoxy-9*H*-carbazole (14)

White solid; ¹H NMR (400 MHz, CDCl₃) δ 8.69 (s, 1H), 8.35 (d, *J* = 8.1 Hz, 1H), 7.32 (d, *J* = 8.4 Hz, 1H), 7.26 (t, *J* = 8.0 Hz, 1H), 6.98 (d, *J* = 7.8 Hz, 1H), 6.76 (d, *J* = 8.3 Hz, 1H), 4.05 (s, 3H), 4.01 (s, 3H). ¹³C NMR (101 MHz, CDCl₃) δ 145.6, 145.2, 130.6, 129.7, 124.2, 123.0, 122.8, 119.7, 114.8, 107.3, 106.5, 106.2, 55.8, 55.6. HRMS (ESI) calcd for C₁₄H₁₂BrNO₂H m/z [M + H]⁺: 306.0124; found: 306.0134.
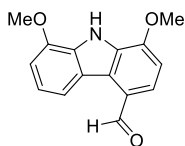
1,8-dimethoxy-9*H*-carbazole-4-carbaldehyde (15)

White solid; mp 235 - 238 °C; ^{1}H NMR (400 MHz, d-DMSO) δ 11.77 (s, 1H), 10.21 (s, 1H), 8.63 (d, J = 8.2 Hz, 1H), 7.87 (d, J = 8.1 Hz, 1H), 7.24 (d, J = 8.2 Hz, 1H), 7.15 (t, J = 7.9 Hz, 1H), 7.07 (d, J = 7.6 Hz, 1H), 4.12 (s, 3H), 4.00 (s, 3H). ^{13}C NMR (101 MHz, d-DMSO) δ 192.5, 151.8, 146.4, 131.9, 131.2, 130.4, 125.6, 123.7, 121.4, 119.7, 118.2, 107.3, 105.8, 56.5, 55.9 HRMS (ESI) calcd for $C_{14}H_{12}BrNO_2H$ m/z [M + H]$^+$: 256.0968; found: 256.0973.
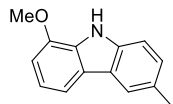
1-methoxy-6-methyl-9H-carbazole (16) (Tamariz et al., 2011)
White solid; ^{1}H NMR (400 MHz, CDCl$_3$) δ 8.21 (s, 1H), 7.90 (s, 1H), 7.69 (d, J = 7.8 Hz, 1H), 7.40 (d, J = 8.2 Hz, 1H), 7.29 (d, J = 4.8 Hz, 1H), 7.18 (t, J = 7.8 Hz, 1H), 6.93 (d, J = 7.8 Hz, 1H), 4.05 (s, 3H), 2.57 (s, 3H). ^{13}C NMR (101 MHz, CDCl$_3$) δ 145.7, 137.4, 130.1, 128.7, 127.1, 124.2, 123.8, 119.9, 119.5, 112.8, 110.6, 105.7, 55.5, 21.4.
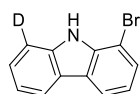

1-bromo-8-deuterium-9H-carbazole (18)
White solid; ^{1}H NMR (400 MHz, CDCl$_3$) δ 8.26 (s, 1H), 8.06 (d, J = 7.8 Hz, 1H), 8.02 (d, J = 7.7 Hz, 1H), 7.58 (d, J = 7.8 Hz, 1H), 7.50-7.45 (m, 1H), 7.31-7.24 (m, 1H), 7.13 (t, J = 7.8 Hz, 1H). ^{13}C NMR (101 MHz, CDCl$_3$) δ 139.1, 128.0, 126.6, 126.5, 124.6, 123.7, 120.9, 120.6, 120.1, 119.3, 111.1, 104.1.

References

Chatterjee, T., Roh, G. B., Shoaib, M. A., Suhl, C. H., Kim, J. S., Cho, C. G. and Cho, E. J. (2017). Visible-Light-Induced Synthesis of Carbazoles by in Situ Formation of Photosensitizing Intermediate. Organic letters, *19*, 1906 - 1909.

Svanfelt, J. and Kronberg, L. (2011). Synthesis of substituted diphenylamines and carbazoles: phototransformation products of diclofenac. Environmental Chemistry Letters, *9*, 141 - 144.

Mudadu, M. S., Singh, A. N. and Thummel, R. P. (2008). Preparation and Study of 1,8-Di(pyrid-2′-yl)carbazoles. The Journal of organic chemistry, *73*, 6513 - 6520.

Lee, S., Kwak, Y. and Bumwoo, P. A. R. K. U.S. (2016). Patent Application *No. 15/093,400.*

Stokes, B. J., Richert, K. J. and Driver, T. G. (2009). Examination of the Mechanism of Rh$_2$(II)-Catalyzed Carbazole Formation Using Intramolecular Competition Experiments**.** The Journal of organic chemistry, *74*, 6442 - 6451.

Bogdal, D.; Lukasiewicz, M. and Pielichowski, J. (2004). Halogenation of carbazole and other aromatic compounds with hydrohalic acids and hydrogen peroxide under microwave irradiation. Green Chemistry, *6*. 110 - 113.

Maeda, C., Todaka, T., Ueda, T. and Ema, T. (2016). Color-Tunable Solid-State Fluorescence Emission from Carbazole-Based BODIPY. Chemistry–A European Journal, *22*, 7508 - 7513.

Lee, B., Lee, S., Kim, D. and Lee, H. (2015) Preparation of carbazole compounds as organic electronic device materials. PCT Int. Appl., 2015108377.

Wang, D., Kuang, D., Zhang, F., Yang, C. and Zhu, X. (2015). Room-Temperature Copper-Catalyzed Arylation of Dimethylamine and Methylamine in Neat Water. Advanced Synthesis & Catalysis,

Yuan, M. L., Xie, J. H., Zhu, S. F. and Zhou, Q. L. (2016). Deoxygenative Hydrogenation of Amides

Catalyzed by a Well-Defined Iridium Pincer Complex. ACS Catalysis, *6*, 3665 - 3669.

Lobo, H. R., Singh, B. S., Pinjari, D. V., Pandit, A. B. and Shankarling, G. S. (2013). Ultrasound-assisted intensification of bio-catalyzed synthesis of mono-N-alkyl aromatic amines. Biochemical engineering journal, *70*, 29 - 34.

Li, Z. L. and Cai, C. (2017). Iron Catalyzed Oxidative C(sp^3)–N Cross Coupling of Amides with C(sp^3)–H via a Radical Process. ChemistrySelect, *2*, 8076 - 8079.

Du, Z., Yan, Y., Fu, Y. and Wang, K. (2016). Palladium-Catalyzed Direct Amination of Allylic Alcohols in Aqueous Media. Asian Journal of Organic Chemistry, *5*, 812 - 818.

Lapointe, S. and Zargarian, D. (2016). On the mechanism of Ni(ii)-promoted Michael-type hydroamination of acrylonitrile and its substituted derivatives. Dalton Transactions, *45*, 15800 - 15810.

Buden, M. E., Vaillard, V. A., Martin, S. E. and Rossi, R. A. (2009). Synthesis of Carbazoles by Intramolecular Arylation of Diarylamide Anions. The Journal of organic chemistry, *74*, 4490 - 4498.

Kung, A. C. and Falvey, D. E. (2005). Photogenerated N-Methyl-N-1-naphthylnitrenium Ion: Laser Flash Photolysis, Trapping Rates, and Product Study. The Journal of organic chemistry, *70*, 3127 - 3132.

Kondo, K., Ogawa, H., Yamashita, H., Miyamoto, H., Tanaka, M., Nakaya, K. and Mori, T. (1997). 7-Chloro-5-hydroxy-1-[2-methyl-4-(2-methylbenzoylamino)benzoyl]-2,3,4,5-tetrahydro-1H-1-benzaze pine (OPC-41061): A potent, orally active nonpeptide arginine vasopressin V2 receptor antagonist. Bioorganic & Medicinal Chemistry, *7*, 1743 - 1754.

Stenkamp, D., Mueller, S. G. and Roth, G. J.(2003). Preparation of arylamides as melanin concentrating hormone (MCH) receptor antagonists.

Chinnagolla, R. K., Pimparkar, S. and Jeganmohan, M. (2013). Ruthenium-catalyzed intramolecular selective halogenation of *O*-methylbenzohydroximoyl halides: a new route to halogenated aromatic nitriles. Chemical Communications, *49*, 3146 - 3148.

Jiang, H. Y., Zhang, S. S. and Sun, B. (2018). Highly Selective Hydrogenation with Ionic Liquid Stabilized Nickel Nanoparticles. Catalysis Letters, *148*, 1336 - 1344.

Xu, J.; Shen, Y.; Xiang, L. and Deng, Y. (2005). Chin. J. Pharm. *36*, 593 - 595.

James, M. J., Clubley, R. E., Palate, K. Y., Procter, T. J., Wyton, A. C., O'Brien, P. and Unsworth, W. P. (2015). Silver(I)-Catalyzed Dearomatization of Alkyne-Tethered Indoles: Divergent Synthesis of Spirocyclic Indolenines and Carbazoles. Organic letters, *17*, 4372 - 4375.

Rennison, D., Gueret, S. M., Laita, O., Bland, R. J., Sutherland, I. A., Boddy, I. K. and Brimble, M. A. (2016). Substituted Carbazoles – A New Class of Anthelmintic Agent. Australian Journal of Chemistry, *69*, 1268 - 1276.

Arredondo, V., Hiew, S. C., Gutman, E. S., Premachandra, I. D. U. A. and Van Vranken, D. L. (2017). Enantioselective Palladium-Catalyzed Carbene Insertion into the N−H Bonds of Aromatic Heterocycles. Angewandte Chemie International Edition, *56*, 4156 - 4159.

Hiscock, J. R., Caltagirone, C., Light, M. E., Hursthouse, M. B. and Gale, P. A. (2009). Fluorescent carbazolylurea anion receptors. Organic & biomolecular chemistry, *7*, 1781 - 1783.

Hernández-Benitez, R. I., Zarate-Zarate, D., Delgado, F. and Tamariz, J. (2017). Palladium-Catalyzed Synthesis of Diarylamines and 1- and 2-Oxygenated Carbazoles: Total Syntheses of Natural Alkaloids Clauraila A, Clausenal, Clausine P, and 7-Methoxy-O-methylmukonal. Synthesis, *49*, 4357 - 4371.

Liyu, J. and Sperry, J. (2017). Synthesis of putative clausenal from carbazole using sequential C–H borylations. Tetrahedron letters, *58*, 1699 - 1701.

Bautista, R., Bernal, P., Montiel, L. E., Delgado, F. and Tamariz, J. (2011). Total Synthesis of the Natural Carbazoles Glycozolicine, Mukoline, and Mukolidine, Starting from

4,5-Dimethyleneoxazolidin-2-ones. Synthesis, *06*, 929 - 933.

Frisch, M. J., Trucks, G. W., Schlegel, H. B., Scuseria, Cheeseman, G. E., M. A. Robb, J. R., Scalmani, G., Barone, V., Mennucc,i B., Petersson, G. A., Nakatsuji, H., Caricato, M., Li, X., Hratchian, H. P., Izmaylov, A. F., Bloino, J., Zheng, G., J. Sonnenberg, L., Hada, M., Ehara, M., Toyota, K., Fukuda, Hasegawa, R., Ishida, J., Nakajima, M., Honda, T., Y., Kitao, O., Nakai, H., Vreven, T., Montgomery, J. A., Jr. Peralta, J. E., Ogliaro, F., Bearpark, M., Heyd, J. J., Brothers, E., Kudin, K. N., Staroverov, V. N., Keith, T., Kobayashi, R., Normand, J., Raghavachari, K., Rendell, A., J. Burant, C., Iyengar, S. S., Tomasi, J., Cossi, M., Rega, N., Millam, J. M., Klene, M., Knox, J. E., Cross, J. B., Bakken, V., Adamo, C., Jaramillo, J., Gomperts, R., Stratmann, R. E., Yazyev, O., Austin, A. J., Cammi, R., Pomelli, C., Ochterski, J. W., Martin, R. L., Morokuma, K., Zakrzewski, V. G., Voth, G. A., Salvador, P., Dannenberg, J. J., Dapprich, S., Daniels, A. D., Farkas, O., Foresman, J. B., Ortiz, J. V., Cioslowski, J., and Fox, D. J., Gaussian, Inc., (2013). Wallingford CT.